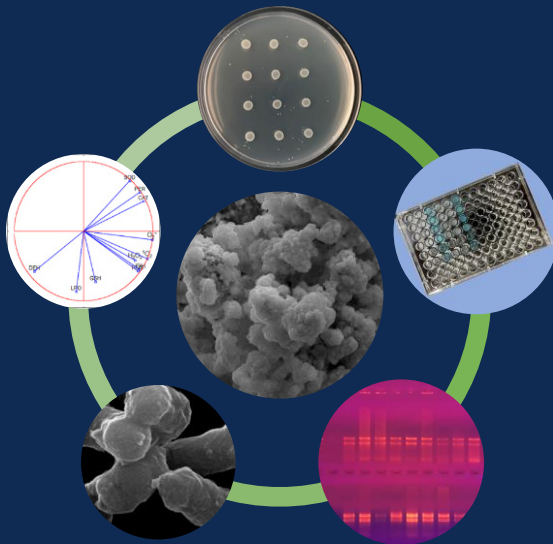




# Indukcja stresu oksydacyjnego w komórkach bakterii przez wybrane nanocząstki metaliczne oraz jego związek z aktywnością przeciwdrobnoustrojową



Oliwia Metryka

Uniwersytet Śląski w Katowicach  
Szkoła Doktorska w Uniwersytecie Śląskim  
Wydział Nauk Przyrodniczych

OLIWIA METRYKA

**Indukcja stresu oksydacyjnego w komórkach bakterii przez wybrane  
nanocząstki metaliczne oraz jego związek z aktywnością  
przeciwdrobnoustrojową**

Praca doktorska

Promotor:  
prof. dr hab. Agnieszka Mrozik  
Uniwersytet Śląski w Katowicach

Promotor pomocniczy:  
dr Daniel Wasilkowski  
Uniwersytet Śląski w Katowicach

Praca została sfinansowana ze środków Narodowego Centrum Nauki, przyznanych w ramach grantu  
PRELUDIUM 20 nr 2021/41/N/NZ9/02506.

Katowice 2023

## **Podziękowania**

*Pragnę złożyć najserdeczniejsze podziękowania Pani prof. dr hab. Agnieszce Mrozik za opiekę merytoryczną i nieocenioną pomoc w trakcie realizowania niniejszej pracy. Dziękuję za wszystkie cenne wskazówki, inspirację, przekazaną wiedzę, życzliwość, wyrozumiałość, cierpliwość, nieograniczone wsparcie, dobroć i motywację w realizacji badań naukowych.*

*Chciałabym również serdecznie podziękować Panu dr Danielowi Wasilkowskiemu za nieocenioną pomoc merytoryczną i praktyczną. Dziękuję za pomoc w analizach statystycznych, wszystkie rady, życzliwość, pogodę ducha, wsparcie w trudnych chwilach i poświęcony czas.*

*Specjalne podziękowania składam współautorce artykułu Pani dr hab. Małgorzacie Adamczyk-Habrajskiej z Instytutu Inżynierii Materiałowej, Wydziału Nauk Ścisłych i Technicznych Uniwersytetu Śląskiego za pomoc i poświęcony czas w obrazowaniu materiału biologicznego z wykorzystaniem skaningowej mikroskopii elektronowej.*

*Dziękuję także wszystkim Pracownikom byłej Katedry Biochemii, Instytutu Biologii, Biotechnologii i Ochrony Środowiska, Wydziału Nauk Przyrodniczych Uniwersytetu Śląskiego za rady, pomoc, owocne dyskusje naukowe, życzliwość, wsparcie i spędzony wspólnie mile czas.*

*Chciałabym również podziękować Moim kochanym Dziadkom, Rodzicom i Siostrze za nieustające wsparcie i pomoc, bezgraniczną cierpliwość, troskę, motywację, niegasnącą wiarę we mnie oraz za niewyczerpującą się otuchę w chwilach zwątpienia. Bez wsparcia Bliskich nie osiągnęłabym tak wiele, dlatego pragnę dedykować tę pracę Mojemu drogiemu Dziadkowi.*

## Spis treści

I. Autoreferat rozprawy.....	5
I.1. Wprowadzenie.....	5
I.2. Cel pracy doktorskiej.....	9
I.3. Materiały i metody.....	11
I.3.1. Materiały do badań i warunki hodowli bakterii.....	11
I.3.2. Wyznaczanie wskaźników toksyczności.....	11
I.3.3. Pomiary stężenia wolnych rodników tlenowych.....	12
I.3.4. Pomiary aktywności enzymów antyoksydacyjnych oraz poziomu glutationu.....	13
I.3.5. Utlenianie białek i peroksydacja lipidów.....	13
I.3.6. Badanie genotoksyczności NPs.....	14
I.3.7. Pomiary aktywności oddechowej bakterii.....	15
I.3.8. Interakcje NPs z osłonami komórkowymi bakterii.....	15
I.3.9. Mapowanie komórek bakterii.....	15
I.3.10. Analiza statystyczna wyników.....	15
I.4. Wyniki i dyskusja wyników.....	17
I.4.1. Ocena indukcji stresu oksydacyjnego oraz funkcjonowania układu antyoksydacyjnego w komórkach bakterii traktowanych NPs.....	17
I.4.2. Ocena zmian w profilach transkrypcyjnych i antyoksydacyjnych komórek bakterii traktowanych NPs.....	20
I.4.3. Ocena zmian w strukturze i właściwościach osłon komórkowych oraz metabolizmie oddechowym bakterii traktowanych NPs.....	22
I.5. Literatura.....	27
I.6. Źródła internetowe.....	35
II. Publikacje wchodzące w skład rozprawy.....	36
II.1.....	37
Metryka O., Wasilkowski D., Mrozik A. 2021. Insight into the antibacterial activity of selected metal nanoparticles and alterations within the antioxidant defence system in <i>Escherichia coli</i> , <i>Bacillus cereus</i> and <i>Staphylococcus epidermidis</i> . International Journal of Molecular Sciences 22(21): 11811	
II.2.....	60
Metryka O., Wasilkowski D., Mrozik A. 2022. Evaluation of the effects of Ag, Cu, ZnO and TiO <sub>2</sub> nanoparticles on the expression level of oxidative stress-related genes and the activity of antioxidant enzymes in <i>Escherichia coli</i> , <i>Bacillus cereus</i> and <i>Staphylococcus epidermidis</i> . International Journal of Molecular Sciences 23(9): 4966	
II.3.....	81
Metryka O., Wasilkowski D., Adamczyk-Habrajska M., Mrozik A. 2023. Undesirable consequences of the metallic nanoparticles action on the properties and functioning of <i>Escherichia coli</i> , <i>Bacillus cereus</i> and <i>Staphylococcus epidermidis</i> membranes. Journal of Hazardous Materials 446: 130728	
III. Wnioski.....	97
IV. Streszczenie.....	98
V. Summary.....	101

VI. Oświadczenia doktoranta i współautorów.....104

## I. Autoreferat rozprawy

### I.1. Wprowadzenie

Nanotechnologia na przestrzeni ostatnich kilkudziesięciu lat stała się jednym z wiodących i najbardziej obiecujących odkryć naukowych, oferującym niezwykle postęp w badaniach, produkcji i praktycznym zastosowaniu nanomateriałów. Za pioniera i wizjonera nanotechnologii uznaje się Richarda Feynmana, który w czasie wykładu „There’s plenty of room at the bottom – an invitation to enter a new field of physics” w 1959 roku przedstawił koncepcję manipulacji materii na poziomie pojedynczych atomów. Było to znaczącym osiągnięciem naukowym, zapoczątkowującym złotą erę nanowszechświata (Hulla i in., 2015; Bayda i in., 2020). Współczesny postęp w nanotechnologii dotyczy głównie produkcji nowych nanomateriałów i opracowywania procesów w nanoskali, wykorzystywanych w różnych dziedzinach/branżach/gałęziach przemysłu począwszy od artykułów gospodarstwa domowego, produkcji żywności, nanoinformatyki, elektroniki, motoryzacji, pozyskiwania energii, medycyny, farmakologii, diagnostyki czy też ochrony środowiska (Khan i in., 2019; Ali, 2020; Bayda i in., 2020). W raporcie analitycznym Europejskiej Agencji Chemikaliów (ECHA, ang. European Chemicals Agency) z maja 2022 roku i dotyczącym wdrażania nanomateriałów, ich produkcji, eksploatacji i przeznaczonych nakładów finansowych na rynku w Unii Europejskiej (w tym krajów Europejskiego Obszaru Gospodarczego i Szwajcarii) oszacowano, że budżet w roku 2020 wyniósł 5 200 mln EUR i dotyczył produkcji 140 000 ton produktów. Szacuje się również, że w ciągu najbliższych 5 lat ilość wprowadzanych na rynek produktów nanotechnologicznych będzie rosła na poziomie 13,9% skumulowanego rocznego wskaźnika wzrostu (CAGR, ang. compound annual growth rate). Liderem rynku nanotechnologicznego w Unii Europejskiej są Niemcy. W Polsce według danych statystycznych wytworzonych zostało w latach 2016 - 2022 około 4 kiloton produktów z dodatkiem nanomateriałów o łącznej wartości 200 milionów EUR. Europejski rynek nanotechnologiczny niezaprzeczalnie zdominowany jest przez nanomateriały nieorganiczne na bazie tlenków metali, stanowiące 75,7% udziału w rynku, natomiast ich odpowiedniki metaliczne stanowią jedynie 8,3% (<https://euon.echa.europa.eu>). Globalny nakład przemysłu nanotechnologicznego na nieorganiczne nanomateriały oszacowano na 2,4 miliarda USD w 2021 roku i prognozuje się, że do 2030 roku będzie on eskalować z CAGR na poziomie 11,66% (<https://www.polarismarketresearch.com>).

Wykładniczy wzrost produkcji i zastosowań nanomateriałów związany jest z ich unikalnymi i cennymi właściwościami, głównie efektami kwantowymi i powierzchniowymi, które odróżniają je od odpowiedników w większej skali. Nanomateriały charakteryzują się dużym stosunkiem powierzchni do objętości, co zwiększa ich reaktywność ze względu na zwiększoną powierzchnię reakcji, liczbę cząstek na jednostkę masy oraz udział atomów na powierzchni materiału (Joudeh i Linke, 2022; Vineeth Kumar i in., 2022). Szczególną cechą nanomateriałów, w szczególności nanocząstek (NPs, ang. nanoparticles) na bazie metali, jest ich aktywność przeciwdrobnoustrojowa, polegająca na wielopłaszczyznowym i niespecyficznym sposobie działania na różne biomolekuły i procesy metaboliczne (Sánchez-López i in., 2020). Chociaż takie właściwości są pożądane w walce z mikroorganizmami patogennymi, to ich niezamierzone uwalnianie do środowiska może stanowić zagrożenie dla mikroorganizmów niebędących celem ich działania. Dodatkowo ich wysoka trwałość, stabilność, reaktywność, niska biodegradowalność oraz możliwość bioakumulacji i biomagnifikacji

zwiększają ryzyko ich toksycznego działania na organizmy żywe. Inżynieryjne NPs dostają się do środowiska (atmosfery, wód powierzchniowych, gleby) w wyniku zamierzonych lub niezamierzonych działań, w tym pośrednio i bezpośrednio jako odpady z zakładów produkcyjnych, transportu, ogólnego użytkowania i utylizacji (Bundschuh i in., 2018; Vineeth Kumar i in., 2022). Szacuje się, że zintensyfikowane stosowanie i wytwarzanie nanoproduktów prowadzi do niekontrolowanego uwalniania ich do środowiska, z czego 63 - 91% trafia na składowiska odpadów, a 8 - 28% do gleby (Bundschuh i in., 2018; Ameen i in., 2021). Dane szacunkowe z 2014 roku wskazują, że w Unii Europejskiej nanomateriały zawierające w swoim składzie  $\text{TiO}_2$  i  $\text{ZnO}$  uległy kumulacji w glebie (odpowiednio 45 000 i 1400 ton), osadach (odpowiednio 44 000 i 7000 ton) i na składowiskach odpadów (odpowiednio 40 000 i 1000 ton). Podobnie nanomateriały z dodatkiem  $\text{Ag}$  trafiają na składowiska odpadów (40 ton) i do osadów (30 ton) (Sun i in., 2016). Pomimo znacznego postępu w rozwoju metod analitycznych, nadal nie ma dostępnych narzędzi, które umożliwiłyby kontrolę stężeń nanomateriałów w różnych ekosystemach oraz ocenę zagrożenia wynikającego z pojawienia się ich w środowisku. Wynika to głównie z trudności w odróżnieniu nanomateriałów naturalnych od inżynieryjnych, braku wystandaryzowanych metod analitycznych i skali do oceny ich potencjalnego zagrożenia. Ponadto nanomateriały mogą ulegać różnym biotransformacjom i wchodzić w złożone reakcje z innymi składnikami ekosystemu, znacznie utrudniając ich ilościowy pomiar w matrycach biologicznych (Bundschuh i in., 2018; Abdolaphur Monikh i in., 2022). Pomimo licznych doniesień naukowych dotyczących toksycznego działania nanocząstek na mikroorganizmy i zaawansowanych badań w tym zakresie, wiedza na temat mechanizmów interakcji NPs z komórkami bakterii jest wciąż fragmentaryczna i nie odzwierciedla w pełni ich negatywnego działania na poziomie komórkowym.

Odnosząc się do najnowszych wyników prac naukowych w literaturze, nieorganiczne NPs wyróżniają się wszechstronnym i wielokierunkowym działaniem przeciwdrobnoustrojowym. Do głównych mechanizmów bakteriobójczego działania metalicznych NPs należą: naruszenie integralności i ciągłości osłon komórkowych, generowanie reaktywnych form tlenu (RFT), genotoksyczność, uszkodzenia struktur wewnątrzkomórkowych, rozprzęganie procesów metabolicznych, inicjujących w ostateczności kaskadę sygnalizacyjną procesów apoptotycznych (Slavin i in., 2017; Parra-Ortiz i Malmsten, 2022). Podstawowymi mechanizmami działania nieorganicznych NPs na komórki bakterii są zewnątrzkomórkowe i wewnątrzkomórkowe generowanie produkcji RFT oraz indukcja stresu oksydacyjnego (Slavin i in., 2017; Shaikh i in., 2019; Yeh i in., 2020). Do głównych RFT należą: anionorodnik ponadtlenkowy ( $\text{O}_2^{\cdot-}$ ), rodnik hydroksylowy ( $\cdot\text{OH}$ ), rodnik wodoronadtlenkowy ( $\text{HO}_2^{\cdot-}$ ), nadtlenek wodoru ( $\text{H}_2\text{O}_2$ ), tlen singletowy ( $^1\text{O}_2$ ) oraz rodniki organiczne, takie jak rodnik nadtlenkowy ( $\text{ROO}\cdot$ ) czy alkoksylowy ( $\text{RO}\cdot$ ) (Dayem i in., 2017; Slavin i in., 2017; Canaparo i in., 2020). Metaliczne NPs z rdzeniem zbudowanym z metali przejściowych, jako nietrwałe związki redoks, mogą generować RFT w wyniku reakcji redukcji-utleniania zachodzących na powierzchni NPs, ich bezpośredniego oddziaływania z obecnymi w środowisku utleniaczami/rodnikami oraz katalitycznej dysocjacji tlenu cząsteczkowego na atomy tlenu (Li i in., 2012; Canaparo i in., 2020; Gao i in., 2021). Elektrony wtórne uwolnione z sieci napromieniowanych NPs mogą reagować z akceptorami obecnymi w otoczeniu, takimi jak woda czy cząsteczki biologiczne, promując produkcję różnych RFT (Hubenko i in., 2018). Ponadto dodatkowym atrybutem zwiększającym bakteriobójcze działanie NPs jest uwalnianie jonów metali z powierzchni, co może przyczynić się do zwiększenia poziomu RFT w wyniku zaburzeń komórkowych

cykli redoks, destabilizacji łańcucha transportu elektronów, zaburzeń ekspresji wybranych genów oraz wzmożonej reakcji Fentona, typu Fentona i Habera-Weissa (Manke i in., 2013; Canaparo i in., 2020; Yu i in., 2020). Uwolnione jony metali ciężkich mogą również reagować z białkami, zawierającymi klastry żelazowo-siarkowe, skutkując nadmiernym uwalnianiem jonów żelaza i jednocześnie inicjując wytwarzanie RFT (Makabenta i in., 2021). Ponadto wolne jony metali, takie jak  $\text{Cu}^{2+}$  mogą przyłączać się do określonych miejsc w cząsteczce DNA i w wyniku przejściowych reakcji redoks generować  $\cdot\text{OH}$  w pobliżu miejsc przyłączenia (Shkodenko i in., 2020). Doniesienia literaturowe wskazują również na możliwość wzmożonej generacji RFT przez NPs po uprzedniej fotoaktywacji (napromieniowaniu), indukując powstawanie dziur elektronowych w paśmie walencyjnym ( $E_v$ ). Wzbudzone elektrony w paśmie przewodnictwa ( $e^-$ ) i dziury w paśmie walencyjnym ( $h^+$ ) posiadają potencjał redoks, co czyni je wysoce reaktywnymi czynnikami redukującymi i utleniającymi (Li i in., 2012; Hubenko i in., 2018).

Warto podkreślić, że RFT powstają także w komórkach bakterii niepoddanych stresowi i pełnią istotne funkcje w ich metabolizmie (Cheeseman i in., 2020; Li i in., 2021). Jednym z najczęstszych mechanizmów syntezy RFT w komórkach drobnoustrojów jest fosforylacja oksydacyjna. Podczas przenoszenia elektronów przez łańcuch transportu elektronów może dochodzić do ich przypadkowego wycieku i wykorzystania w reakcjach wtórnych indukujących produkcję  $\text{O}_2^{\cdot-}$  oraz  $\text{H}_2\text{O}_2$ , będących prekursorami do syntezy innych RFT (Imlay, 2003; McBee i in., 2017; Collin, 2019). Ponadto  $\text{O}_2^{\cdot-}$  oraz  $\text{H}_2\text{O}_2$  powstają jako produkty uboczne autoutleniania oksydoreduktaz i dehydrogenaz oddechowych oraz nieselektywnego przenoszenia elektronów przez flawonoidy (Imlay, 2003). Z kolei  $^1\text{O}_2$  może powstawać jako produkt uboczny w takich procesach, jak: peroksydacja lipidów, rozkład nadtlenków organicznych czy utlenianie  $\text{O}_2$  (Onyango, 2016; Hubenko i in., 2018). Paradoks toksyczności RFT przypisuje się obecności niesparowanego elektronu na zewnętrznej powłoce, co czyni je wysoce niestabilnymi i reaktywnymi w porównaniu z innymi cząsteczkami (Bisht i Dada, 2017). W warunkach naturalnych zachowana jest równowaga między wytwarzaniem RFT a ich usuwaniem, natomiast w warunkach stresu ta równowaga zostaje zaburzona.

Stres oksydacyjny indukowany przez NPs, uwolnione jony metali oraz RFT w komórkach drobnoustrojów może prowadzić do uszkodzeń różnych struktur komórkowych i składników budulcowych osłon zewnętrznych, inicjując kaskadę reakcji utleniania i w konsekwencji prowadząc do degradacji białek i lipidów (Muñiz Diaz i in., 2017; Behera i in., 2019). Co interesujące, każdy rodzaj RFT charakteryzuje się swoistą reaktywnością oraz poziomem toksyczności, a wybiórcze działanie wolnych rodników jest odwrotnie proporcjonalne do ich reaktywności. Na przykład anionorodnik ponadtlenkowy ( $\text{O}_2^{\cdot-}$ ) może być zarówno utleniaczem i reduktorem, jak również prekursorem innych RFT, w tym  $\text{H}_2\text{O}_2$ ,  $\cdot\text{OH}$  i  $^1\text{O}_2$  (Li i in., 2012; Collin, 2019; Canaparo i in., 2020). Przeciwnie  $\text{H}_2\text{O}_2$  jest silnym utleniaczem, ale ze względu na stabilność i brak wypadkowego ładunku stanowi substrat do syntezy  $\cdot\text{OH}$  (Li i in., 2012; Collin, 2019). W odróżnieniu od pozostałych RFT,  $\cdot\text{OH}$  ze względu na wysoki potencjał redoks jest wysoce reaktywnym i niespecyficznym utleniaczem, reagującym z każdą napotkaną makrocząsteczką (Collin, 2019; Cui i Smith, 2022). Komórki bakteryjne posiadają systemy ochronne, które zabezpieczają je przed działaniem NPs i RFT. System antyoksydacyjny składa się z enzymów antyoksydacyjnych, tj. katalazy (CAT, ang. catalase), peroksydazy (PER, ang. peroxidase) i dysmutazy ponadtlenkowej (SOD, ang. superoxide dismutase) oraz ze zredukowanego glutationu (GSH, ang. reduced glutathione) - nieenzymatycznego



przeciwutleniacza, który stanowi gotowy układ do ochrony komórek bakteryjnych przed stresem oksydacyjnym (Ezraty i in., 2017; Slavin i in., 2017; Borisov i in., 2021). Funkcją wymienionych antyoksydantów jest redukcja ogólnego poziomu RFT w komórkach. SOD obniża stężenie  $O_2^{\cdot-}$  w wyniku reakcji dysmutacji. Z kolei CAT, PER i GSH redukują poziom  $H_2O_2$  w komórce (Imlay, 2003; Fang, 2011; Ezraty i in., 2017). W warunkach stresowych wywołanych obecnością NPs i RFT skuteczne funkcjonowanie przeciwutleniaczy może zostać zaburzone w wyniku trwałego uszkodzenia białek lub upośledzenia początkowych etapów ich syntezy (Ezraty i in., 2017; Borisov i in., 2021; Mammari i in., 2022). Wykazano, że metaliczne NPs posiadają właściwości genotoksyczne i uszkadzają DNA. Hamują również replikację DNA, zaburzają ekspresję informacji genetycznej w komórce oraz stymulują horyzontalny transfer genów (Karimi i Mohseni Fard, 2017; Wang i in., 2017; Zhang i in., 2018a). Szczególnym przypadkiem ich działania jest wpływ na ekspresję informacji genetycznej komórki, prowadzący do zmian w syntezie przeciwutleniaczy. Warto podkreślić, że RNA jest bardziej podatny na szkodliwe działanie RFT niż DNA, co prowadzi do upośledzenia procesu transkrypcji (Seixas i in., 2022). Wybrane przykłady genotoksycznego działania NPs przedstawiono w pracy Metryka i in. (2022), stanowiącej rozdział II.2 niniejszej rozprawy doktorskiej. Ze względu na bardzo ograniczoną liczbę prac dotyczących generowania różnorodnych form RFT, ekspresji genów stresu oksydacyjnego i funkcjonowania układu antyoksydacyjnego komórek bakteryjnych traktowanych NPs jako powiązanych ze sobą mechanizmów toksyczności, przedstawione we wspomnianej pracy wyniki można uznać za nowatorskie.

Ciekawym i tylko fragmentarycznie wyjaśnionym mechanizmem działania NPs jest ich wpływ na ścianę i błonę komórkową bakterii. Wykazano, że bezpośrednie oraz pośrednie oddziaływanie NPs z osłonami zewnętrznymi bakterii może prowadzić do trwałych uszkodzeń barier ochronnych, destabilizacji potencjału błonowego, zmian strukturalnych, zwiększenia przepuszczalności błony, nasilenia peroksydacji lipidów, zakłócenia aktywności transportowej, rozprężnięcia fosforylacji oksydacyjnej i wycieku zawartości wewnątrzkomórkowej (Baptista i in., 2018; Yeh i in., 2020; Staroń i Długosz, 2021). Modyfikacjom tym towarzyszy między innymi zmiana aktywności enzymów metabolizmu oddechowego, w tym dehydrogenaz (DEH) i ATPazy (Vardanyan i in., 2015; Gómez-Núñez i in., 2020; Lange i in., 2022). Ze względu na odmienną budowę ściany komórkowej bakterii Gram-ujemnych i Gram-dodatnich, mechanizmy interakcji bakterii z tych grup mikrobiologicznych a NPs są odmienne i przeważnie specyficzne gatunkowo (Yeh i in., 2020; Linklater i in., 2021). Przedstawione w artykule Metryki i in. (2023) wyniki dotyczące funkcjonowania błony komórkowej i aktywności oddechowej komórek dostarczają nowej wiedzy na temat różnic w odpowiedzi różnych bakterii na stres NPs i stanowią cenny wkład w wyjaśnienie mechanizmów ich działania.

## I.2. Cel pracy doktorskiej

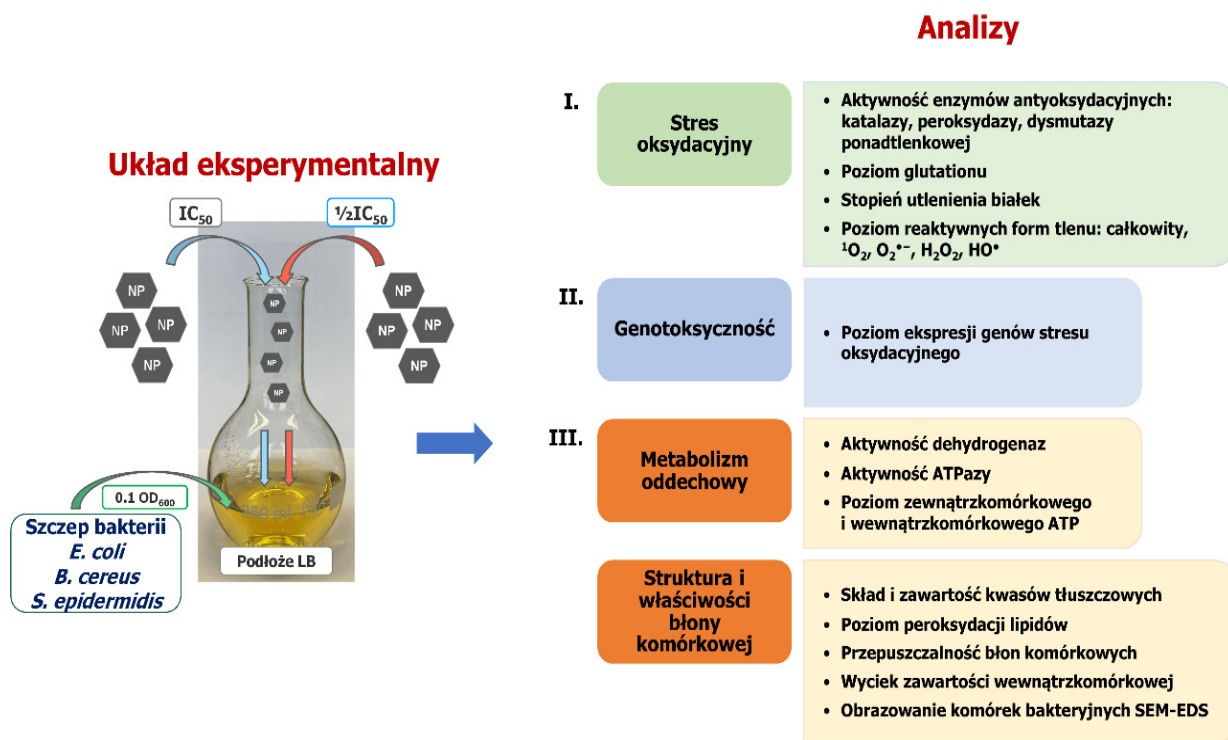
Celem rozprawy doktorskiej jest wieloaspektowa analiza mechanizmów indukcji stresu oksydacyjnego w komórkach bakterii: *Escherichia coli* (ATCC® 25922™), *Bacillus cereus* (ATCC® 11778™) i *Staphylococcus epidermidis* (ATCC® 12228™), eksponowanych na działanie nanocząstek metalicznych: Ag-NPs, Cu-NPs, TiO<sub>2</sub>-NPs i ZnO-NPs.

W pracy zweryfikowano następujące hipotezy badawcze: (1) NPs wpływają na działanie bakteryjnych antyoksydantów; (2) NPs wpływają na poziom ekspresji genów stresu oksydacyjnego; (3) NPs modyfikują aktywność oddechową komórek bakteryjnych oraz (4) NPs oddziałują z osłonami zewnętrznymi bakterii i powodują zmiany morfologiczne komórek.

Aby osiągnąć powyższy cel oraz zweryfikować słuszność hipotez badawczych, zrealizowano następujące zadania badawcze:

1. Wyznaczono wskaźniki toksyczności NPs względem badanych szczepów bakterii,
2. Zbadano rolę NPs w indukcji stresu oksydacyjnego w komórkach bakterii,
3. Przeprowadzono analizę genotoksyczności NPs,
4. Określono zmiany w metabolizmie oddechowym bakterii oraz w strukturze i właściwościach błony komórkowej,
5. Zobrazowano komórki bakterii eksponowane na NPs z wykorzystaniem skaningowej mikroskopii elektronowej (SEM-EDS).

Zadania badawcze wykonywano w trzech etapach. Pierwszy etap obejmował ocenę toksyczności NPs oraz analizę wskaźników stresu oksydacyjnego, w drugim etapie zbadano genotoksyczność NPs, a na trzeci etap składały się badania metabolizmu oddechowego komórek bakterii oraz zmian w strukturze i właściwościach zewnętrznych osłon komórkowych. Schemat obrazujący układ eksperymentalny z uwzględnieniem wszystkich wykonanych analiz ilustruje rys. 1.



Rys. 1. Schemat układu eksperymentalnego z uwzględnieniem etapów realizacji i zadań badawczych.

### I.3. Materiały i metody

#### I.3.1. Materiały do badań i warunki hodowli bakterii

W badaniach wykorzystano trzy referencyjne szczepy bakterii pochodzące z American Type Culture Collection (ATCC): *Escherichia coli* (ATCC® 25922™), *Bacillus cereus* (ATCC® 11778™) i *Staphylococcus epidermidis* (ATCC® 12228™). Bakterie przechowywano i pasażowano na podłożu agarowo-bulionowym rekomendowanym przez ATCC® (BD Difco™ Nutrient Broth BD 234000, BD Bacto™ Tryptic Soy Broth BD 211825). Wyjściowym punktem do badań było wyznaczenie krzywych wzrostu bakterii oraz określenie czasu, w którym komórki bakterii osiągały połowę fazy logarytmicznego wzrostu. Krzywe wzrostu bakterii wyznaczano tradycyjną metodą hodowli komórek w bulionie lizogenicznym Luria-Bertani (LB; pepton K 10 g L<sup>-1</sup>, ekstrakt drożdżowy 5 g L<sup>-1</sup>, chlorek sodu 10 g L<sup>-1</sup>) i oznaczenia ich liczebności metodą posiewu powierzchniowego na podłożu LB zestalone agarem (Monod, 1949; Pepper i Gerba, 2005; Maier, 2009).

W kolejnym etapie komórki bakterii pochodzące z połowy fazy logarytmicznego wzrostu poddawano 24-godzinnej ekspozycji na działanie czterech rodzajów NPs: Ag-NPs (<100 nm, Sigma-Aldrich nr. kat. 576832), Cu-NPs (25 nm, Sigma Aldrich nr. kat. 774081), ZnO-NPs (<50 nm, Sigma-Aldrich nr. kat. 677450) i TiO<sub>2</sub>-NPs (20 nm, US Research Nanomaterials Inc. nr. kat. US1019F). Doboru NPs do badań dokonano na podstawie danych literaturowych oraz sondaży statystycznych uwzględniających produkcję i eksploatację nanomateriałów nieorganicznych. Wszystkie NPs charakteryzowały się wysoką czystością, w granicach 97 - 99,5%. Roztwory podstawowe NPs przygotowywano w sterylnej wodzie Millipore i każdorazowo przed użyciem poddawano sonikacji przez 10 - 20 minut z wykorzystaniem dezintegratora ultradźwiękowego Vibra Cell™ (20 kHz), aby zapobiec aglomeracji/agregacji NPs (Nowak i in., 2016). Szczegółowe warunki prowadzenia hodowli bakteryjnych opisano w pracy Metryka i in. (2021), stanowiącej rozdział II.1 niniejszej rozprawy doktorskiej.

#### I.3.2. Wyznaczenie wskaźników toksyczności

Potencjalną toksyczność Ag-NPs, Cu-NPs, ZnO-NPs i TiO<sub>2</sub>-NPs względem bakterii *E. coli*, *B. cereus* i *S. epidermidis* badano w podłożu LB z dodatkiem różnych stężeń NPs (Wiegand i in., 2008; Bagchi i in., 2013). W tym celu podłożu zaszczepiano zawiesiną bakteryjną w 0,85% NaCl do uzyskania gęstości optycznej hodowli OD<sub>600</sub> = 0,1 (~10<sup>7</sup> jtk mL<sup>-1</sup>). Kolejno do hodowli bakteryjnych dodawano NPs w stężeniach od 0,1 do 1500 mg L<sup>-1</sup> i inkubowano w temperaturze 37 °C z wytrząsaniem (140 obr./min). Próby kontrolne stanowiły hodowle bakterii nietraktowane NPs. Po 24-godzinnej inkubacji przygotowywano serię rozcieńczeń każdej hodowli w 0,85% NaCl, wysiewano na podłożu stałe LB i inkubowano przez 24 godziny w temperaturze 37 °C. Liczebność komórek wyrażano jako log jtk mL<sup>-1</sup>. Na podstawie zebranych danych wyznaczono następujące wskaźniki toksyczności: minimalne stężenie hamujące (MIC, ang. minimal inhibitory concentration), minimalne stężenie bakteriobójcze (MBC, ang. minimal bactericidal concentration) oraz stężenie hamujące w 50% wzrost bakterii (IC<sub>50</sub>, ang. half-maximal inhibitory concentration). Wartości MIC i MBC wyznaczano za pomocą wskaźnika śmiertelności, przyjmując odpowiednio 99% i 100% zahamowania wzrostu bakterii jako wartości równoznaczne (Wiegand i in., 2008; Bagchi i in., 2013). Natomiast stężenie IC<sub>50</sub> wyznaczano za pomocą kalkulatora AAT Bioquest (<https://www.aatbio.com/tools/ic50->

calculator), które weryfikowano z wykorzystaniem oprogramowania GraphPad Prism 5 (GraphPad Software, USA). Wyznaczenie wartości tych wskaźników stanowiło kluczowy etap do kolejnych badań, w których używano komórek bakterii eksponowanych na NPs w stężeniu  $IC_{50}$  oraz  $\frac{1}{2}IC_{50}$ .

### ***1.3.3. Pomiary stężenia wolnych rodników tlenowych***

W celu zbadania rodzaju generowanych RFT przez Ag-NPs, Cu-NPs, ZnO-NPs i TiO<sub>2</sub>-NPs w komórkach *E. coli*, *B. cereus* i *S. epidermidis* wykonywano pomiary ogólnego stężenia RFT oraz poszczególnych form RFT, w tym O<sub>2</sub><sup>•-</sup>, <sup>1</sup>O<sub>2</sub>, H<sub>2</sub>O<sub>2</sub> i •OH metodami spektroskopowymi. Ze względu na wysoką reaktywność oraz niski okres półtrwania różnych form RFT, w tej części badań zastąpiono podłoże LB buforowaną fosforanem solą fizjologiczną (PBS) w celu zapobiegnięcia niespecyficznym reakcjom RFT ze związkami obecnymi w podłożu. Co więcej, czas ekspozycji komórek bakterii na NPs został dostosowany do pomiaru wybranych RFT. Pomiary RFT prowadzono w próbach biotycznych zawierających komórki bakteryjne i NPs oraz w próbach abiotycznych zawierających PBS i NPs. Prowadzenie pomiarów w próbach abiotycznych miało na celu zbadanie zdolności NPs do spontanicznego generowania RFT w roztworach niezawierających komórek bakteryjnych. Otrzymane wartości dla prób abiotycznych wykorzystywano jako tło do skorygowania danych otrzymanych dla prób biotycznych. Wewnątrzkomórkowe stężenie RFT oznaczano za pomocą barwnika diocyanu 2',7'-dichlorodihydrofluoresceiny (H<sub>2</sub>DCFDA, ang. 2',7'-dichlorodihydrofluorescein diacetate), który jest utleniany przez RFT w cytozolu do związku fluorescencyjnego 2',7'-dichlorofluoresceiny (DCF, ang. 2',7'-dichlorofluorescein) (Yang i in., 2013). Pomiary fluorescencji powstałego DCF wykonywano przy długości fali wzbudzenia  $\lambda = 485$  nm i długości fali emisji  $\lambda = 530$  nm. W międzyczasie z badanych prób pobierano zawiesinę bakterii w celu wykonania posiewów powierzchniowych na podłożu stałym i oznaczenia liczebności bakterii. Z kolei stężenie O<sub>2</sub><sup>•-</sup> mierzono metodą polegającą na redukcji soli tetrazoliowej XTT do barwnego formazanu (Horst i in., 2013). Równolegle określano poziom <sup>1</sup>O<sub>2</sub> na podstawie wygaszania fluorescencji 1,3-difenyloizobenzofuranu (DPBF, ang. 1,3-diphenylisobenzofuran) przy  $\lambda = 410$  nm (Zhang i in., 2018b). Stężenie H<sub>2</sub>O<sub>2</sub> w komórkach bakterii mierzono z użyciem odczynnika Amplex Red (AR) i peroksydazy chrzanowej, która przekształca AR w rezorufinę fluorescencyjną w obecności H<sub>2</sub>O<sub>2</sub> (Seaver i Imlay, 2001). Stężenie H<sub>2</sub>O<sub>2</sub> ( $\mu$ M) w badanych próbach obliczano korzystając ze współczynnika kierunkowego krzywej kalibracyjnej ( $y = 1592,9x$ ) wyznaczonej dla roztworu wzorcowego H<sub>2</sub>O<sub>2</sub> (100  $\mu$ M) w zakresie stężeń od 0,024  $\mu$ M do 50  $\mu$ M. Natomiast tworzenie •OH w komórkach bakterii badano metodą pośrednią opartą na degradacji dezoksyrybozy do produktów łatwo reagujących z kwasem tiobarbiturowym (TBA, ang. thiobarbituric acid) i mierzonych spektrofotometrycznie przy  $\lambda = 532$  nm (Rice-Evans i in., 1991a; Meghana i in., 2015). Stężenie •OH obliczano korzystając ze współczynnika kierunkowego krzywej kalibracyjnej ( $y = 8,832x$ ) wykonanej dla różnych stężeń dialdehydu malonowego (MDA, ang. malondialdehyde) w zakresie stężeń od 0 do 0,1  $\mu$ M. Szczegółowe warunki oznaczeń ogólnego poziomu RFT oraz poszczególnych rodzajów RFT w komórkach bakteryjnych traktowanych NPs opisano w pracy Metryka i in. (2021), stanowiącej rozdział II.1 niniejszej rozprawy doktorskiej.

### ***1.3.4. Pomiary aktywności enzymów antyoksydacyjnych oraz poziomu glutationu***

W celu poznania odpowiedzi komórek bakterii na stres wywołany obecnością NPs i generacją RFT, badano funkcjonowanie bakteryjnego systemu antyoksydacyjnego i towarzyszących zmian patologicznych. Ze względu na to, że enzymy antyoksydacyjne, tj. CAT, PER i SOD stanowią pierwszą linię obrony komórki przed szkodliwym działaniem RFT, pomiary ich aktywności były kluczowe w celu oceny działania systemu ochrony komórek bakteryjnych przed stresem. Aktywność enzymów antyoksydacyjnych mierzono w surowych frakcjach enzymatycznych otrzymanych metodą Hegeman'a (1966), z uwzględnieniem ogólnego stężenia białka oznaczanego metodą Bradford'a (1976). Metoda pomiaru aktywności CAT polegała na degradacji  $H_2O_2$  w obecności aktywnego enzymu (Banerjee i in., 2015; David i in., 2016). Aktywność PER mierzono metodą kolorymetryczną z pirogalem jako donorem elektronów i  $H_2O_2$  jako akceptorem elektronów. Natomiast aktywność SOD mierzono z wykorzystaniem gotowego zestawu odczynników zawierających oksydazę ksantynową i sól tetrazoliową. W metodzie tej  $O_2^{\cdot-}$  powstający w wyniku reakcji katalizowanej przez oksydazę ksantynową redukuje sól tetrazolu do czerwonego formazanu. W obecności aktywnego enzymu SOD stężenie  $O_2^{\cdot-}$  spada, ograniczając redukcję soli tetrazolowej. Dodatkowo w celu zidentyfikowania wpływu NPs na układ antyoksydacyjny bakterii mierzono poziom zredukowanego GSH, który jest ważnym nieenzymatycznym składnikiem układu antyoksydacyjnego. Zasada oznaczania GSH opierała się na reakcji grupy sulfhydrylowej z kwasem 5,5'-ditiobis(2-nitrobenzoesowym) (DTNB, ang. 5,5'-dithiobis(2-nitrobenzoic acid)), znanym jako odczynnik Ellman'a, w wyniku czego powstaje barwny kwas 5-tio-2-nitrobenzoesowy (TNB, ang. 5-thio-2-nitrobenzoic acid) (Kumar i in., 2011). Metody i warunki oznaczenia stężeń CAT, PER i SOD oraz poziomu zredukowanego GSH w komórkach bakteryjnych traktowanych NPs przedstawiono w pracy Metryki i in. (2021), stanowiącej rozdział II.1 niniejszej rozprawy doktorskiej.

### ***1.3.5. Utlenianie białek i peroksydacja lipidów***

W oddzielnych eksperymentach zbadano wpływ NPs na utlenianie białek poprzez pomiar zawartości grup karbonylowych ( $>C=O$ ) i aminowych ( $-NH_2$ ) oraz indukcję peroksydacji lipidów w komórkach bakterii traktowanych NPs. Zasada oznaczenia zawartości  $>C=O$  opierała się na reakcji grup karbonylowych białek z 2,4-dinitrofenylohydrazyną (DNPH, ang. 2,4-dinitrophenylhydrazine), w wyniku której powstają 2,4-dinitrofenylohydrazony, mierzone kolorymetrycznie (Levine i in., 1990; Rice-Evans i in., 1991b; Chatterjee i in., 2014). Pomiar zawartości  $-NH_2$  opierał się natomiast na reakcji fluoresceiny z grupami aminowymi, w wyniku której powstaje produkt fluorescencyjny proporcjonalnie do zawartości aminy w próbce, podczas gdy niezwiązana fluorescamina hydrolyzuje do produktów niefluorescencyjnych (Rice-Evans i in., 1991b; Wang i in., 2021). W procesie peroksydacji lipidów jednym z najbardziej powszechnych produktów jest aldehyd malonowy MDA, który reaguje z TBA tworząc chromofor, mierzony spektrofotometrycznie (Rice-Evans i in., 1991c; Chatterjee i in., 2014). Szczegółowe opisy powyższych analiz przedstawiono w pracy Metryki i in. (2021), stanowiącej rozdział II.1 niniejszej rozprawy doktorskiej.

### 1.3.6. Badanie genotoksyczności NPs

Istotnym i bardzo ważnym etapem badań była analiza właściwości genotoksycznych NPs, polegająca na ocenie zmian w ekspresji wybranych genów kodujących białka o aktywności podobnej do CAT, PER i SOD. Pozyskane informacje umożliwiły porównanie zmian w tworzeniu produktu na poziomie ekspresji wybranych genów oraz aktywności ich drugorzędowych odpowiedników molekularnych. W ramach tej serii eksperymentów przeprowadzono: (1) izolacje i oczyszczanie całkowitego RNA, (2) syntezę cDNA na matrycy RNA, (3) analizę poziomu transkrypcji genów z użyciem cDNA (jako matrycy) oraz wybranych genów stresu oksydacyjnego metodą RT-qPCR (Żur i in., 2020). U bakterii *E. coli* były to następujące geny: *katE* (kodujący katalazę HPII), *katG* (kodujący enzym dwufunkcyjny o działaniu katalazy i peroksydazy), *sodA* (kodujący dysmutazę ponadtlenkową zawierającą Mn w centrum aktywnym), *sodB* (kodujący dysmutazę ponadtlenkową zawierającą Fe w centrum aktywnym), *sodC* (kodujący dysmutazę ponadtlenkową zawierającą Cu-Zn w centrum aktywnym) oraz *ycdB* (kodujący podjednostkę peroksydazy). Z kolei do genów stresu oksydacyjnego bakterii *B. cereus* należały: *katA* (kodujący katalazę), *katE* (kodujący katalazę HPII), *sodA1* (kodujący dysmutazę ponadtlenkową zawierającą Mn w centrum aktywnym), *sodA2* (kodujący dysmutazę ponadtlenkową zawierającą Mn w centrum aktywnym), *tpx* (kodujący peroksydazę tiolową) i *yoyM* (kodujący enzym o charakterze dysmutazy ponadtlenkowej zawierającej w centrum aktywnym Zn). Natomiast u bakterii *S. epidermidis* analizie poddano geny: *bsaA* (kodujący homolog peroksydazy glutationowej), *katA* (kodujący katalazę), *npr* (kodujący peroksydazę NADH), *sodA* (kodujący dysmutazę ponadtlenkową zawierającą w centrum aktywnym Mn/Fe) oraz *tpx* (kodujący peroksydazę tiolową). Aby określić poziom ekspresji badanych genów, wykorzystano metodę opracowaną przez Livak i Schmittgen (2001). Geny metabolizmu podstawowego wykorzystano jako geny referencyjne do normalizacji poziomu ekspresji genów docelowych ze względu na podobny poziom ich ekspresji zarówno w komórkach traktowanych NPs, jak i w komórkach kontrolnych (Sohm i in., 2015; Moore i in., 2017). Genami referencyjnymi stosowanymi jako kontrola wewnętrzna w komórkach *E. coli* były: *gyrA* (kodujący podjednostkę A gyrazy DNA), *gyrB* (kodujący podjednostkę B gyrazy DNA) i *rpoE* (kodujący czynnik sigma-E polimerazy RNA) (Hou i in., 2012; Osonga i in., 2018). Podobny zestaw genów metabolizmu podstawowego wybrano dla szczepu *B. cereus*, z wyjątkiem *rpoE*, który zastąpiono genem *rpoB* (kodującym podjednostkę  $\beta$  polimerazy RNA) (Ko i in., 2004). Natomiast jako geny metabolizmu podstawowego *S. epidermidis* wybrano *gyrB*, *rpoB* i *pyk* (kodujący kinazę pirogronianową) (Sihto i in., 2014). Startery dla każdego wybranego genu zaprojektowano przy użyciu Primer-BLAST (<https://www.ncbi.nlm.nih.gov/tools/primer-blast/>) oraz sekwencji genomów szczepów referencyjnych dostępnych na stronie internetowej ATCC (<https://genomes.atcc.org/genomes/>). Specyficzność zaprojektowanych starterów przetestowano wstępnie za pomocą reakcji kontrolnej z Color Taq PCR Master Mix (2x) (EURx, nr. kat. E2525) w celu wyeliminowania nieprawidłowo dobranych starterów do wygenerowanej matrycy cDNA. Dodatkowo w celu analizy fragmentacji/degradacji RNA przeprowadzono elektroforezę uzyskanych produktów w żelu agarozowym (Chatterjee i in., 2014). Szczegółowy opis analizy poziomu transkrypcji wybranych genów bakteryjnych oraz zastosowaną w tym celu metodologię opisano w pracy Metryki i in. (2022), stanowiącej rozdział II.2 niniejszej rozprawy doktorskiej.

### ***1.3.7. Pomiary aktywności oddechowej bakterii***

Interakcje NPs z powierzchnią komórek bakteryjnych oraz potencjalne uszkodzenia osłon komórkowych mogą prowadzić do zaburzeń w metabolizmie oddechowym mikroorganizmów. W związku z tym zbadano wpływ Ag-NPs, Cu-NPs, ZnO-NPs i TiO<sub>2</sub>-NPs na aktywność DEH bakterii metodą kolorymetryczną z bezbarwnym chlorkiem 2,3,5-trifenylolektrozolowym jako akceptorem elektronów i protonów, który jest enzymatycznie redukowany do barwnego 1,3,5-trifenyloformazanu (Nweke i in., 2007). Szczegółowy opis tej metody uwzględniono w pracy Metryki i in. (2021), stanowiącej rozdział II.1 niniejszej rozprawy doktorskiej. Dodatkowo przeprowadzono pomiary aktywności ATPazy oraz stężenia wewnątrzkomórkowego i zewnątrzkomórkowego ATP w komórkach bakterii traktowanych NPs. Pomiary aktywności ATPazy oraz stężenia ATP wykonywano z wykorzystaniem komercyjnie dostępnych zestawów odczynników odpowiednio z firmy Sigma Aldrich (nr. kat. MAK113) i ThermoFisher Scientific (nr. kat. A22066).

### ***1.3.8. Interakcje NPs z osłonami komórkowymi bakterii***

Wyjaśnienie interakcji NPs z osłonami komórkowymi bakterii było fundamentalne, ponieważ stanowią one pierwszą barierę ochronną komórek przed szkodliwym działaniem tych nanostruktur. Jest to szczególnie istotne w przypadku NPs o rozmiarach większych niż 10 nm, gdyż nie są one swobodnie transportowane do wnętrza komórki. Dlatego też w celu zbadania bezpośredniego i pośredniego działania NPs na osłony komórkowe, wykonywano pomiary przepuszczalności błony komórkowej oraz wycieku zawartości wewnątrzkomórkowej metodami spektrofotometrycznymi (Devi i in., 2013; Halder i in., 2015; Kora i Sashidhar, 2015). Dodatkowo przeprowadzono izolacje kwasów tłuszczowych z komórek bakterii metodą MIDI-FAME (Sasser, 1990), aby ocenić zmiany w składach i zawartościach poszczególnych grup kwasów tłuszczowych (nasyconych cyklopropanowych, hydroksyloowych i rozgałęzionych oraz nienasyconych). Rozdziały metyloowych estrów kwasów tłuszczowych (FAMES, ang. fatty acid methyl esters) przeprowadzono metodą chromatografii gazowej, natomiast ich identyfikacji dokonywano z wykorzystaniem specjalistycznego oprogramowania MIDI Microbial Identification System Sherlock (wersja 6.2B) i biblioteki TSBA 6 firmy MIDI Inc. Szczegółowy opis tej części badań przedstawiono w pracy Metryki i in. (2023), stanowiącej rozdział II.3 niniejszej rozprawy doktorskiej.

### ***1.3.9. Mapowanie komórek bakterii***

W celu analizy zmian w morfologii komórek bakterii po ekspozycji na NPs oraz ich dystrybucji na powierzchni komórek, przeprowadzono obrazowanie komórek za pomocą skaningowej mikroskopii elektronowej (SEM-EDS). Etapy przygotowywania materiału biologicznego do analizy SEM-EDS opisano w pracy Metryki i in. (2023), stanowiącej rozdział II.3 niniejszej rozprawy doktorskiej.

### ***1.3.10. Analiza statystyczna wyników***

W celu określenia istotnych różnic między analizowanymi układami badawczymi, wszystkie otrzymane wyniki poddawano analizie statystycznej przy użyciu oprogramowania Statistica® (wersja



13.1, TIBCO Software Inc., USA). Różnice statystyczne między wynikami uzyskanymi dla prób poddanych działaniu NPs i prób kontrolnych wyznaczano za pomocą jednokierunkowej analizy wariancji (ANOVA, ang. analysis of variance), a następnie testu post-hoc Tukey'a dla  $p < 0,05$ . Szczegółowy opis stosowanych analiz statystycznych do poszczególnych zbiorów wyników opisano w pracach Metryki i in. (2021; 2022; 2023), stanowiących rozdziały II.1, II.2 i II.3 niniejszej rozprawy doktorskiej.

## I.4. Wyniki i dyskusja wyników

### I.4.1. Ocena indukcji stresu oksydacyjnego oraz funkcjonowania układu antyoksydacyjnego w komórkach bakterii traktowanych NPs

Istotną kwestią w badaniach toksyczności nowych środków przeciwdrobnoustrojowych jest precyzyjne zdefiniowanie ich bakteriobójczego i bakteriostatycznego działania na mikroorganizmy. Dlatego też ocenę potencjalnego działania antybakteryjnego badanych NPs przeprowadzono na podstawie wyznaczenia podstawowych wskaźników toksykologicznych: MIC, MBC i IC<sub>50</sub>. Uzyskane wartości tych parametrów potwierdziły przeciwbakteryjne działanie wszystkich NPs względem *E. coli*, *B. cereus* i *S. epidermidis*. Jednocześnie stwierdzono zróżnicowaną wrażliwość badanych szczepów na stres wywołany ich ekspozycją na poszczególne rodzaje NPs. Biorąc pod uwagę stężenia MIC wyznaczone dla *E. coli*, wzrastające działanie bakteriobójcze poszczególnych NPs można uszeregować następująco: TiO<sub>2</sub>-NPs < ZnO-NPs < Cu-NPs < Ag-NPs. Z kolei przeciwdrobnoustrojowe działanie NPs względem *B. cereus* i *S. epidermidis* odzwierciedlają odpowiednio następujące szeregi: Ag-NPs < ZnO-NPs < TiO<sub>2</sub>-NPs < Cu-NPs oraz TiO<sub>2</sub>-NPs < ZnO-NPs < Ag-NPs < Cu-NPs. Odnosząc się do tych szeregów można wnioskować, że badane szczepy były bardziej wrażliwe na toksyczne działanie nanocząstek metali niż tlenków metali. Przyczyną tego zjawiska może być szybsze uwalnianie jonów metali ciężkich z powierzchni NPs zbudowanych wyłącznie z pojedynczych pierwiastków niż z powierzchni tlenków, co powoduje gromadzenie się ich w nadmiarze i w konsekwencji wywołuje efekt cytotoksyczny (Odzak i in., 2014; Wang i in., 2016; Ghorbani i in., 2020). Właściwość ta przypisywana nanomateriałom nieorganicznym określana jest często „efektem konia trojańskiego” (Gutiérrez i in., 2017). Co więcej, podobny wpływ Ag-NPs i Cu-NPs na przeżywalność komórek bakteryjnych może wynikać ze zbliżonej konfiguracji elektronowej i składu chemicznego Ag (I) i Cu (I) (Eckhardt i in., 2013; Slavin i in., 2017). Warto jednak zaznaczyć, że spośród badanych szczepów szczególnie wrażliwe na obecność Cu-NPs były bakterie Gram-dodatnie *B. cereus* i *S. epidermidis*. Większa podatność tych szczepów na bakteriobójcze działanie Cu-NPs niż Gram-ujemnej bakterii *E. coli* może być powiązana ze zwiększonym powinowactwem jonów Cu<sup>2+</sup> do grup karboksylowych i aminowych na powierzchni komórek (Azam i in., 2012; Bagchi i in., 2013; Wang i in., 2017). Z doniesień literaturowych wynika, że bakterie Gram-dodatnie i Gram-ujemne w różnym stopniu są wrażliwe lub odporne na działanie NPs, co można przypisać istotnym różnicom w budowie ich ściany komórkowej. Ściana komórkowa bakterii Gram-ujemnych ma cienką warstwę peptydoglikanu, co czyni ją bardziej przepuszczalną dla uwolnionych z NPs jonów metali i ułatwia ich transport do wnętrza komórki w porównaniu do grubej warstwy gęsto usieciowanego peptydoglikanu w ścianie komórkowej bakterii Gram-dodatnich, gdzie jony metali mogą być unieruchamiane przez grupy funkcyjne kwasów teichojowych i teichuronowych (Slavin i in., 2017). Na przykład wiązanie jonów Ag<sup>+</sup> w warstwach peptydoglikanu ściany komórkowej bakterii Gram-dodatnich zwiększało istotnie ich oporność na działanie Ag-NPs w porównaniu do *E. coli* (Peszke i in., 2017). Wyniki otrzymane w ramach niniejszej pracy potwierdziły wysoki stopień śmiertelności komórek *E. coli* po traktowaniu Ag-NPs, ZnO-NPs i TiO<sub>2</sub>-NPs w porównaniu do *B. cereus* i *S. epidermidis*.

Kolejnym etapem podjętych badań była ocena zdolności Ag-NPs, Cu-NPs, ZnO-NPs i TiO<sub>2</sub>-NPs do generowania RFT w komórkach *E. coli*, *B. cereus* i *S. epidermidis* jako potencjalnego

mechanizmu przeciwdrobnoustrojowego. Na podstawie uzyskanych wyników stwierdzono istotne zmiany w poziomie oznaczanych rodzajów RFT w komórkach traktowanych NPs w porównaniu do ich poziomu w komórkach kontrolnych. Co interesujące, każdy rodzaj NPs powodował niespecyficzną indukcję wybranych rodzajów RFT w komórkach bakterii, co utrudniło wyciągnięcie ogólnych wniosków. W związku z tym obserwowane zmiany w całkowitym stężeniu RFT i stężeniach indywidualnych RFT analizowano oddzielnie dla każdego szczepu. Analiza statystyczna wyników uzyskanych dla każdego szczepu wykazała, że badane NPs w najmniejszym stopniu generowały tworzenie  $^1\text{O}_2$ . Można sądzić, że ograniczona indukcja powstawania  $^1\text{O}_2$  w komórkach bakterii przez Ag-NPs, Cu-NPs, ZnO-NPs i  $\text{TiO}_2$ -NPs mogła wynikać z prowadzenia układów eksperymentalnych bez dostępu światła. Dane literaturowe wskazują bowiem, że zdolności nieorganicznych NPs do generowania RFT, łącznie z  $^1\text{O}_2$ , wzrastają w wyniku procesu fotoaktywacji poprzez indukcję powierzchniowego rezonansu plazmonowego oraz reakcji pośrednich anionorodnika ponadtlenkowego  $\text{O}_2^{\cdot-}$  (Li i in., 2012; Zhang i in., 2013; Hubenko i in., 2018). W odniesieniu do otrzymanych wyników, największy wzrost całkowitego stężenia RFT w komórkach *E. coli* i *B. cereus* nastąpił po ekspozycji na Cu-NPs. Z kolei ZnO-NPs i  $\text{TiO}_2$ -NPs miały znaczący wpływ na produkcję RFT w komórkach *S. epidermidis*. Ustalono, że NPs w największym stopniu indukowały tworzenie RFT w komórkach *B. cereus* i *S. epidermidis*, natomiast w mniejszym stopniu w komórkach *E. coli*. Odnosząc się do poziomu poszczególnych form RFT, zasadniczy udział w całkowitym stężeniu RFT w komórkach *E. coli* traktowanych Cu-NPs miały  $\text{O}_2^{\cdot-}$ ,  $\text{H}_2\text{O}_2$  i  $\cdot\text{OH}$ , w komórkach *S. epidermidis* traktowanych  $\text{TiO}_2$ -NPs -  $\text{O}_2^{\cdot-}$  i  $\cdot\text{OH}$ , a w komórkach *B. cereus* eksponowanych na Cu-NPs i ZnO-NPs -  $\text{O}_2^{\cdot-}$  i  $\text{H}_2\text{O}_2$ . Stężenia  $\text{O}_2^{\cdot-}$ ,  $\text{H}_2\text{O}_2$  i  $\cdot\text{OH}$  w komórkach są dodatnio sprzężone, gdyż istnienie oraz poziom tych form RFT w układach biologicznych są współzależne. Redukcja  $\text{O}_2^{\cdot-}$  zwiększa poziom  $\text{H}_2\text{O}_2$ , który następnie w wyniku klasycznej reakcji Fentona i jej modyfikacjom prowadzi do wytworzenia  $\cdot\text{OH}$  (Imlay, 2003; McBee i in., 2017; Collin, 2019).

Brak równowagi między generacją RFT a funkcjonowaniem układu antyoksydacyjnego prowadzi do stresu oksydacyjnego i zmian patologicznych w komórkach drobnoustrojów. Jednym z biomarkerów stresu oksydacyjnego jest GSH zawierający grupy sulfhydrylowe, które jako donory wodoru umożliwiają detoksykację RFT, w szczególności  $\text{H}_2\text{O}_2$ . GSH, należący do niskocząsteczkowych tioli, jako nieenzymatyczny związek o wysokim potencjale redoks stanowi pierwszą linię obrony komórek bakterii przed stresem oksydacyjnym (Masip i in., 2006; Lemire i in., 2017; Stewart i in., 2020). Wyniki przedstawione w niniejszej rozprawie potwierdziły fundamentalne znaczenie GSH w ochronie komórek *E. coli* i *S. epidermidis* przed stresem oksydacyjnym. Dowodem na to był spadek stężenia GSH w komórkach *E. coli* eksponowanych na ZnO-NPs i Ag-NPs oraz w komórkach *S. epidermidis* traktowanych ZnO-NPs w odniesieniu do jego stężenia w komórkach kontrolnych. Dla porównania stężenie GSH w komórkach *B. cereus* nie zmieniło się istotnie, co wskazuje na niewielki jego udział w ochronie tego szczepu przed stresem oksydacyjnym. Warto podkreślić, że każdy mikroorganizm posiada unikalny i swoisty mechanizm obrony, charakteryzujący się odmienną zawartością i udziałem przeciwutleniaczy w mechanizmach ochronnych. Udokumentowano, że GSH występuje w większej ilości u bakterii Gram-ujemnych (w stężeniach rzędu milimoli) niż u bakterii Gram-dodatnich (Smirnova i Oktyabrsky, 2005; Ku i Gan, 2021). Niemniej jednak bakterie Gram-dodatnie produkują inne niskocząsteczkowe tiole jako bufory redoks, na przykład bacillithiol (BAC) o funkcji i budowie analogicznej do GSH (Sharma i in., 2013; Ku i

Gan, 2021). Można zatem wnioskować, że nieznaczne zmiany w stężeniu GSH w komórkach *B. cereus* i *S. epidermidis* w porównaniu do jego stężenia w komórkach *E. coli* mogą świadczyć o wykorzystaniu przez te komórki odmiennych mechanizmów ochronnych przed akumulacją RFT niż niekatalityczny system antyoksydacyjny. Wniosek ten potwierdzają badania Yuan i in. (2017), którzy stwierdzili większy spadek poziomu GSH w komórkach *P. aeruginosa* niż *S. aureus* traktowanych Ag-NPs. Oceniając zdolność GSH do obrony komórek bakteryjnych przed nadmiernym wytwarzaniem i akumulacją RFT należy mieć również na uwadze to, że zarówno NPs i uwolnione jony metali mogą oddziaływać z grupami tiolowymi GSH, prowadząc do wzrostu stężenia jego formy utlenionej (GSSG, ang. glutathione disulfide) (Slavin i in., 2017; Stewart i in., 2020).

Produkcja RFT w komórkach bakterii wiąże się nierozdzielnie z utlenianiem różnych biomolekuł, w tym przede wszystkim lipidów i białek. Proces utleniania lipidów jest specyficzny gatunkowo i zależy od rodzaju lipidów wchodzących w skład błony komórkowej (Lemire i in., 2017; Dimova i in., 2022). Do oceny stopnia peroksydacji lipidów u badanych bakterii wybrano biopskaźnik stanu redoks, czyli poziom MDA, będącego produktem ubocznym utleniania lipidów (Dimova i in., 2022). Stwierdzono, że traktowanie komórek *E. coli*, *B. cereus* i *S. epidermidis* Ag-NPs, Cu-NPs i TiO<sub>2</sub>-NPs skutkowało istotnym wzrostem poziomu peroksydacji lipidów, natomiast w obecności ZnO-NPs nie obserwowano tego zjawiska. Największy wzrost poziomu peroksydacji lipidów, o 160,95 i 194,49% w odniesieniu do kontroli, nastąpił odpowiednio w komórkach *B. cereus* i *S. epidermidis* traktowanych Cu-NPs. Dla porównania w komórkach *E. coli* wzrost ten był największy w obecności TiO<sub>2</sub>-NPs i wynosił 43,23%. Przyczyną różnego stopnia peroksydacji lipidów może być odmienna zawartość nienasyconych kwasów tłuszczowych w badanych szczepach, gdyż to głównie ta grupa kwasów ulega utlenieniu (Lemire i in., 2017; Dimova i in., 2022). Analiza FAME przeprowadzona w ramach pracy Metryki i in. (2023), stanowiącej rozdział II.3 niniejszej rozprawy, potwierdziła znacznie wyższy udział nienasyconych kwasów tłuszczowych w komórkach bakterii Gram-dodatnich, zarówno nietraktowanych, jak i traktowanych NPs w porównaniu do ich zawartości w komórkach *E. coli*. Ponadto stwierdzono pozytywną korelację pomiędzy poziomem peroksydacji lipidów a udziałem nienasyconych kwasów tłuszczowych w komórkach *S. epidermidis* traktowanych Cu-NPs. Z kolei mniejsza produkcja MDA w komórkach *E. coli* niż u pozostałych szczepów może być przyczyną dodatkowej ochrony komórek przez większe stężenie GSH oraz stymulację aktywności enzymatycznego układu antyoksydacyjnego. Warto podkreślić, że spośród oznaczanych RFT, <sup>•</sup>OH i <sup>1</sup>O<sub>2</sub> mogą inicjować proces peroksydacji lipidów prowadząc do poważnych zmian strukturalnych w osłonach komórkowych bakterii (Grotto i in., 2009; Chatterjee i in., 2014; Bhattacharya i in., 2021). Na przykład znaczny wzrost stężenia <sup>•</sup>OH w komórkach *B. cereus* i *S. epidermidis* był dodatnio skorelowany ze wzrostem poziomu MDA. Natomiast wysoki poziom <sup>1</sup>O<sub>2</sub> w komórkach *E. coli* traktowanych TiO<sub>2</sub>-NPs może wyjaśniać wpływ tej formy RFT na poziom peroksydacji lipidów. Zależność pomiędzy większym poziomem RFT i wzrostem poziomu MDA w komórkach *E. coli* w obecności Cu-NPs oraz Ag-NPs obserwowali także w swoich badaniach Chatterjee i in. (2014), Korshed i in. (2016) oraz Quinteros i in. (2016).

NPs, uwolnione jony metali ciężkich oraz RFT mogą wchodzić także w interakcje z grupami funkcyjnymi białek, prowadząc do zmian w ich strukturze i utraty aktywności biologicznej (Wang i in., 2017; Seixas i in., 2022). Jedną z konsekwencji utleniania białek jest zmiana zawartości grup karbonylowych oraz aminowych (Chatterjee i in., 2014; Xiong i Guo, 2021). Najczęściej

przypisywaną modyfikacją białek indukowaną przez RFT jest karbonylacja białek. Analiza zawartości grup karbonylowych potwierdziła znaczny ich wzrost w strukturze białek szczepów *E. coli*, *B. cereus* i *S. epidermidis* eksponowanych na wszystkie rodzaje NPs. Największy i porównywalny wzrost zawartości grup karbonylowych białek o 10 - 12% nastąpił u bakterii *E. coli* traktowanych Ag-NPs, ZnO-NPs i TiO<sub>2</sub>-NPs. Z kolei u bakterii *B. cereus* i *S. epidermidis* największy wzrost zawartości tych grup o 25 - 31% wywołał kontakt komórek z tlenkami metali. W przypadku grup aminowych, największy wzrost ich zawartości u wszystkich szczepów stwierdzono po ekspozycji na ZnO-NPs. Wyniki tej części badań opublikowano w pracy Metryki i in. (2021), która stanowi rozdział II.1 prezentowanej rozprawy.

#### **I.4.2. Ocena zmian w profilach transkrypcyjnych i antyoksydacyjnych komórek bakterii traktowanych NPs**

Kolejnym etapem badań była analiza zmian w profilach transkrypcyjnych i antyoksydacyjnych komórek *E. coli*, *B. cereus* i *S. epidermidis* traktowanych NPs. Wyniki tej serii badań można uznać za nowatorskie, gdyż wiedza w tym zakresie jest bardzo ograniczona. Niewiele jest prac eksperymentalnych łączących wpływ NPs na ekspresję genów i syntezę enzymów systemu obrony antyoksydacyjnej. Uzyskane wyniki wskazały, że Ag-NPs, Cu-NPs, ZnO-NPs i TiO<sub>2</sub>-NPs istotnie wpływały na ekspresję wybranych genów stresu oksydacyjnego oraz aktywność enzymów antyoksydacyjnych u badanych szczepów bakterii. Wpływ NPs na ekspresję genów był unikalny dla każdej bakterii i zależał od zastosowanego stężenia NPs.

Przeprowadzone analizy potwierdziły zróżnicowany wpływ poszczególnych NPs w stężeniach IC<sub>50</sub> i ½IC<sub>50</sub> na względny poziom ekspresji genów *katE*, *katG*, *ycdB*, *sodA*, *sodB* i *sodC* w komórkach *E. coli*. Ekspozycja bakterii na Ag-NPs, Cu-NPs i TiO<sub>2</sub>-NPs spowodowała spadek względnego poziomu ekspresji analizowanych genów, natomiast obecność ZnO-NPs wywołała efekt przeciwny. Zmiany w odpowiedzi transkrypcyjnej *E. coli* zależały nie tylko od rodzaju NPs, ale również od ich stężenia. Chociaż względny poziom ekspresji wielu genów uległ obniżeniu, nie miało to wpływu na negatywne funkcjonowanie układu oksydacyjnego, gdyż wszystkie NPs stymulowały aktywność badanych enzymów. Mając na uwadze plejotropowe działanie NPs, obniżony względny poziom ekspresji analizowanych genów kodujących białka o aktywności podobnej do enzymów antyoksydacyjnych mógł być przyczyną regulacji innych genów, związanych na przykład z naprawą uszkodzeń w osłonach komórkowych lub strukturze kwasów nukleinowych. Dodatkowo zawartość mRNA w komórce w określonym czasie nie zawsze jest komplementarna do ilości występującego w niej białka (Sohm i in., 2015).

W równoległym prowadzonym eksperymencie, traktowanie komórek *B. cereus* poszczególnymi rodzajami NPs wywołało wzrost względnego poziomu ekspresji genów *katA*, *katE*, *tpx*, *yojM*, *sodA1* i *sodA2*. Najwyższy, bo około 159-krotny i 165-krotny wzrost względnego poziomu ekspresji genu *katE* nastąpił w komórkach traktowanych odpowiednio Cu-NPs i TiO<sub>2</sub>-NPs w stężeniu IC<sub>50</sub> oraz Ag-NPs w stężeniu ½IC<sub>50</sub>. Warto podkreślić, że gen *katE*, kodujący katalazę zależną od obecności alternatywnego czynnika sigma B ( $\sigma^B$ ), ulega ekspresji w warunkach stresowych (van Schaik i in., 2005; Ceragioli i in., 2010). Czynnikiem stresowym mającym bezpośredni wpływ na wzmożoną ekspresji genu *katE* u *B. cereus* mogły być jony uwolnionych metali lub RFT, wygenerowane przez NPs. Słuszność takiego wniosku potwierdzają badania Ganesh Babu i in. (2011), którzy wykazali, że

ekspresja genu *katE* w komórkach *B. cereus* poddanych działaniu  $\text{AgNO}_3$  była bezpośrednio indukowana przez jony  $\text{Ag}^+$ . Biorąc ten wynik pod uwagę, wzrost względnego poziomu ekspresji genu *katE* w komórkach *B. cereus* mógł być wywołany przez jony  $\text{Ag}^+$  uwolnione z Ag-NPs. Istotnym wnioskiem z tej części badań jest również stwierdzenie dodatniej korelacji pomiędzy ekspresją genu *sodA2* a poziomem rodnika  $\text{O}_2^{\cdot-}$  w komórkach bakterii traktowanych Ag-NPs i ZnO-NPs w stężeniu  $\text{IC}_{50}$ .

Odpowiedź komórek *S. epidermidis* na działanie NPs również znalazła odzwierciedlenie w różnym poziomie ekspresji badanych genów. Stwierdzono, że Ag-NPs i Cu-NPs obniżały względny poziom ekspresji genów: *bsaA*, *katA*, *npr*, *tpx* i *sodA*, natomiast przeciwny efekt powodowały ZnO-NPs i  $\text{TiO}_2$ -NPs. W komórkach traktowanych ZnO-NPs w stężeniu  $\text{IC}_{50}$  nastąpił największy wzrost względnego poziomu ekspresji genów *bsaA*, *npr* i *sodA*. Na podstawie analizy statystycznej stwierdzono u tego szczepu istotne różnice w ekspresji genu *sodA*, który jak wynika z literatury podlega regulacji przez  $\text{O}_2^{\cdot-}$  (Karavolos i in., 2003). Ponadto stwierdzono dodatnią korelację pomiędzy ekspresją genu *sodA*, aktywnością SOD i poziomem  $\text{O}_2^{\cdot-}$  w komórkach *S. epidermidis* eksponowanych na  $\text{TiO}_2$ -NPs w stężeniu  $\text{IC}_{50}$ . Wyniki tej części badań genetycznych zawiera artykuł Metryki i in. (2022), stanowiący rozdział II.2 prezentowanej rozprawy.

Ochrona komórek bakterii przed stresem oksydacyjnym wymaga prawidłowego funkcjonowania katalitycznego układu antyoksydacyjnego. Aktywność podstawowych enzymów antyoksydacyjnych, tj. CAT, PER i SOD jest powszechnie wykorzystywana jako biomarker stresu oksydacyjnego. W niniejszej pracy stwierdzono zasadnicze zmiany w profilach antyoksydacyjnych *E. coli*, *B. cereus* i *S. epidermidis* w następstwie traktowania NPs. Szczegółowe wyniki tej części badań opublikowano w pracach Metryki i in. (2021; 2022), stanowiących rozdziały II.1 i II.2 prezentowanej rozprawy. Stwierdzono, że w komórkach *E. coli* wszystkie NPs stymulowały aktywność CAT, PER i SOD, przy czym największy wzrost aktywności dotyczył CAT i PER. Największy wpływ na aktywność enzymów antyoksydacyjnych *E. coli* wykazały Cu-NPs i ZnO-NPs. Znaczący wpływ na aktywność enzymów antyoksydacyjnych miały także różne stężenia NPs, szczególnie na aktywność CAT. Zmiany aktywności transkrypcyjnej genów kodujących białka o aktywności CAT i PER były wprost proporcjonalne do ogólnej aktywności enzymów CAT i PER. Ponadto indukcja tworzenia  $\text{H}_2\text{O}_2$  przez Cu-NPs była dodatnio skorelowana ze stymulacją aktywności CAT. Dla porównania aktywność SOD w komórkach *E. coli* eksponowanych na działanie Cu-NPs i ZnO-NPs była znacznie wyższa w porównaniu do jej aktywności w innych układach badawczych ze względu na wyższy poziom wewnątrzkomórkowego i zewnątrzkomórkowego  $\text{O}_2^{\cdot-}$ . Świadczy to o aktywnej odpowiedzi antyoksydantów na generację RFT przez te NPs. Należy podkreślić, że aktywność CAT w komórkach *E. coli* wyróżniała się wyższą aktywnością właściwą niż PER. Uzasadnieniem tego zjawiska jest występowanie dwóch rodzajów CAT, do których należą hydroperoksydaza typu I (HPI, ang. hydroperoxidase I) o aktywności bifunkcyjnej CAT-PER i hydrokuperoksydaza typu II (HPH, ang. hydroperoxidase II) o aktywności podobnej do CAT (Schellhorn, 1995; Loewen, 1996).

Wszystkie NPs miały również stymulujący wpływ na funkcjonowanie systemu antyoksydacyjnego bakterii *B. cereus*. Podobnie jak u *E. coli*, największe zmiany stwierdzono w aktywności CAT i PER. Analiza statystyczna potwierdziła zależność aktywności CAT i SOD *B. cereus* od stężeń  $\text{IC}_{50}$  i  $\frac{1}{2}\text{IC}_{50}$  poszczególnych NPs. Aktywność CAT, PER i SOD w komórkach *B. cereus*

była w największym stopniu stymulowana przez Cu-NPs i ZnO-NPs. Wyniki uzyskane z pomiarów  $H_2O_2$  i  $O_2^{\cdot-}$  w komórkach tych bakterii dodatkowo potwierdzają zależność pomiędzy aktywnością przeciwutleniaczy a ekspozycją na Cu-NPs i ZnO-NPs. Stwierdzono także dodatnią korelację pomiędzy aktywnością CAT i SOD a profilami transkrypcyjnymi genów kodujących białka o aktywności podobnej do analizowanych enzymów w komórkach traktowanych Cu-NPs i ZnO-NPs. Interesującym wynikiem była wyższa aktywność właściwa CAT, PER i SOD komórkach *B. cereus* eksponowanych na ZnO-NPs w stężeniu  $\frac{1}{2}IC_{50}$  niż w komórkach traktowanych ZnO-NPs w stężeniu  $IC_{50}$ . Można sądzić, że przyczyną tego zjawiska była agregacja/aglomeracja ZnO-NPs w wyższym stężeniu, ograniczająca reaktywność NPs. Sposób dystrybucji ZnO-NPs i tworzenie agregatów na powierzchni komórek *B. cereus* obserwowane podczas obrazowania techniką SEM może wskazywać na taką możliwość.

Zmiany aktywności CAT, PER i SOD w komórkach *S. epidermidis* traktowanych NPs były trudne do interpretacji, ponieważ każdy rodzaj NPs w odmienny i często przeciwstawny sposób wpływał na profil katalityczny tych enzymów. W wyniku ekspozycji bakterii na wszystkie NPs stwierdzono wzrost aktywności SOD i spadek aktywności PER. Największy wzrost aktywności SOD w porównaniu z aktywnością tego enzymu w komórkach kontrolnych nastąpił po traktowaniu komórek  $TiO_2$ -NPs ( $IC_{50}$ ). Natomiast największy spadek aktywności CAT i PER ustalono odpowiednio w komórkach eksponowanych na działanie Cu-NPs ( $IC_{50}$ ) i ZnO-NPs ( $\frac{1}{2}IC_{50}$ ). Zmiany aktywności antyoksydantów w komórkach *S. epidermidis* były w większości przypadków dodatnio skorelowane z wysokim poziomem  $H_2O_2$  i  $O_2^{\cdot-}$ . W przeciwieństwie do wyników uzyskanych dla *E. coli* i *B. cereus*, w komórkach *S. epidermidis* wystąpiły istotne rozbieżności między poziomem ekspresji badanych genów, a aktywnością ich molekularnych odpowiedników. Mimo jednak tych różnic, analizy statystyczne wykazały dodatnią korelację między ekspresją badanych genów a aktywnością oznaczanych enzymów przeciwutleniających. Dane literaturowe wskazują, że spadek aktywności enzymów antyoksydacyjnych może być związany z uwalnianiem jonów metali z powierzchni NPs i ich oddziaływaniem z białkami bakteryjnymi, prowadzącymi w efekcie do ich inaktywacji lub denaturacji (Slavin i in., 2017; Huang i in., 2018; Liao i in., 2019). Jako przykład mogą posłużyć kationy  $Zn^{2+}$  i  $Cu^{2+}$ , które tworzą bardzo stabilne kompleksy z białkami w wyniku oddziaływania z grupami -SH, -NH<sub>2</sub>, -COOH i wiążą się w miejscach niebędących ich miejscem wiązania, takim jak klastry Fe-S (Hassan i in., 2017; Raghunath i Perumal, 2017; Wang i in., 2017). Dodatkowo zaburzenia homeostazy metali i detoksykacji  $H_2O_2$  mogą prowadzić do inaktywacji enzymów Fe-zależnych poprzez utlenienie  $Fe^{2+}$  do  $Fe^{3+}$ , co skutkuje ich dysocjacją z miejsca wiązania i pozostawieniem wolnego miejsca do przyłączenia  $Zn^{2+}$  (Chandrangsu i in., 2017).

#### **I.4.3. Ocena zmian w strukturze i właściwościach osłon komórkowych oraz metabolizmie oddechowym bakterii traktowanych NPs**

Ostatnim etapem badań było wyjaśnienie interakcji NPs z osłonami komórkowymi bakterii oraz towarzyszących im zmian patologicznych. Jedną z konsekwencji oddziaływania NPs z powierzchnią komórek bakterii były zmiany w metabolizmie oddechowym. Użytecznym biomarkerem w tej analizie były DEH, odgrywające istotną rolę w aktywności metabolicznej drobnoustrojów i obiegu elektronów (Heikal i in., 2014; Billenkamp i in., 2015). W komórkach *E. coli*, *B. cereus* i *S. epidermidis* traktowanych NPs stwierdzono zróżnicowaną aktywność DEH.

Uzyskane wyniki potwierdziły stymulujący wpływ Ag-NPs i TiO<sub>2</sub>-NPs na aktywność DEH w komórkach *E. coli*, natomiast odwrotny efekt wywołały Cu-NPs i ZnO-NPs. Z kolei Cu-NPs, ZnO-NPs i TiO<sub>2</sub>-NPs dodane do hodowli *B. cereus* powodowały spadek aktywności DEH. W przypadku *S. epidermidis*, Ag-NPs i Cu-NPs stymulowały aktywność DEH, podczas gdy pozostałe NPs zmniejszały aktywność tych enzymów. Warto podkreślić, że większe zmiany w aktywności DEH obserwowano u *B. cereus* i *S. epidermidis* niż u *E. coli*. Przyczyną zwiększonej wrażliwości DEH bakterii Gram-dodatnich na nanocząstki tlenków metali mogło być wzmożone uwalnianie jonów metali i ich nasilona interakcja z powierzchnią komórek bakterii (Korshed i in., 2016; Slavin i in., 2017; Yuan i in., 2017). Wyniki tej części badań opublikowano w pracy Metryki i in. (2021), stanowiącej rozdział II.1 prezentowanej rozprawy.

Adenozynotrifosforan (ATP) jako uniwersalny nośnik energii biologicznie użytecznej może być przydatnym biomarkerem stresu wywołanego w komórce przez różne związki chemiczne, w tym NPs. Uzyskane w tej pracy wyniki potwierdziły istotne różnice w całkowitym stężeniu ATP (wewnątrz- i zewnątrzkomórkowym) w komórkach *E. coli*, *B. cereus* i *S. epidermidis* eksponowanych na poszczególne NPs. Warto podkreślić, że zasadnicze zmiany dotyczyły głównie stężenia wewnątrzkomórkowego ATP. Stwierdzono, że traktowanie *E. coli* ZnO-NPs i TiO<sub>2</sub>-NPs powodowało spadek wewnątrzkomórkowej i zewnątrzkomórkowej zawartości ATP, natomiast Ag-NPs wywoływały efekt przeciwny. W większości układów eksperymentalnych z *B. cereus*, wszystkie NPs powodowały spadek wewnątrzkomórkowego i zewnątrzkomórkowego stężenia ATP. Z kolei malejący wpływ poszczególnych NPs na wewnątrzkomórkowe i zewnątrzkomórkowe stężenia ATP w komórkach *S. epidermidis* prezentuje następujący szereg: TiO<sub>2</sub>-NPs < Cu-NPs < Ag-NPs < ZnO-NPs. Zmiany ogólnego stężenia ATP w komórkach bakterii mogą wynikać z zakłóceń w prawidłowym funkcjonowaniu DEH, co potwierdzono w niniejszej pracy. Co więcej, spadek całkowitego poziomu ATP był skorelowany ze spadkiem aktywności ATPazy. Warto wyjaśnić, że pozakomórkowe stężenie ATP jako cząsteczki sygnalizacyjnej zmienia się podczas poszczególnych faz wzrostu komórek bakteryjnych, oprócz wzrostu jego stężenia wynikającego z uszkodzeń błony komórkowej (Ihssen i in., 2021). Taką koncepcję potwierdziły badania Planchon i in. (2017), którzy udokumentowali spadek wewnątrzkomórkowego stężenia ATP w komórkach *E. coli* traktowanych TiO<sub>2</sub>-NPs przy jednoczesnym zwiększeniu puli pozakomórkowej tego związku. Dodatkowo stężenie ATP zmienia się dynamicznie w warunkach stresowych, ponieważ jest on wykorzystywany w różnych procesach komórkowych, w tym syntezie białek (Deng i in., 2021). Na przykład cząsteczki ATP mogą być wykorzystane jako siła napędowa w syntezie białek redoks jako mechanizmu obronnego przed stresem wywołanym przez NPs, co wyjaśniałoby spadek wewnątrzkomórkowego poziomu ATP oraz wzmożoną aktywność enzymatycznego układu przeciwutleniaczy.

Ważnym czynnikiem wpływającym na stężenie ATP w komórce jest aktywność ATPazy, dlatego podjęto próbę zbadania całkowitego poziomu tego związku oraz zidentyfikowania korelacji pomiędzy aktywnością enzymu a poziomem ATP u badanych szczepów bakterii traktowanych NPs. W komórkach *E. coli* w większości przypadków stwierdzono znaczny spadek aktywności ATPazy po traktowaniu NPs. Wyjątek stanowiły komórki eksponowane na ZnO-NPs, w których aktywność tego enzymu była wyższa niż w komórkach kontrolnych. Spadek aktywności ATPazy nastąpił również w komórkach *B. cereus* traktowanych Ag-NPs, Cu-NPs i ZnO-NPs, natomiast TiO<sub>2</sub>-NPs miały działanie stymulujące. Podobnie pomiary aktywności ATPazy w komórkach *S. epidermidis* traktowanych Ag-



NPs, Cu-NPs, ZnO-NPs i TiO<sub>2</sub>-NPs potwierdziły spadek aktywności tego enzymu. Spadek aktywności ATPazy był dodatnio skorelowany ze spadkiem ogólnego stężenia ATP w komórkach badanych bakterii oraz zmianami w zawartości grup karbonylowych białek. Dane literaturowe wskazują, że NPs mogą wpływać na syntezę białek poprzez zmiany poziomu ekspresji odpowiednich genów oraz powodować denaturację białek rybosomu (Slavin i in., 2017). Sohm i in. (2015) stwierdzili na przykład znaczące obniżenie względnego poziomu ekspresji genów kodujących białka wchodzące w skład ATPazy *E. coli* traktowanej TiO<sub>2</sub>-NPs, co miało odzwierciedlenie w zmniejszonym stężeniu ATP i eksporcie protonów. W tej pracy, prawdopodobnie uwolnione jony metali ciężkich i generowane RFT w komórkach *E. coli*, *B. cereus* i *S. epidermidis* mogły przyczynić się do zmian aktywności transkrypcyjnej genów kodujących białka o ważnych funkcjach w oddychaniu komórkowym i wpływać dodatkowo na syntezę enzymów metabolizmu oddechowego.

Pośrednie i bezpośrednie oddziaływanie NPs z błonami komórkowymi bakterii może prowadzić do nieodwracalnych zmian w ich strukturze i funkcjonowaniu. Na podstawie analizy korelacji stwierdzono, że zmiany w przepuszczalności błony komórkowej *E. coli* traktowanych NPs były w większości przypadków skorelowane z wyciekami treści komórkowej. Największe zmiany w przepuszczalności błony komórkowej i nasilenie wycieku cytoplazmy stwierdzono u tego szczepu po ekspozycji na ZnO-NPs w stężeniach IC<sub>50</sub> i ½IC<sub>50</sub>. W przypadku szczepów *B. cereus* i *S. epidermidis*, analiza statystyczna wykazała brak istotnych różnic w przepuszczalności błony pomiędzy komórkami traktowanymi NPs a komórkami kontrolnymi. Wyjaśnieniem tych rozbieżności może być odmienna budowa ściany komórkowej badanych bakterii. Potwierdzeniem tego wniosku mogą być również badania Khater i in. (2020), którzy udokumentowali, że przepuszczalność błony i jej potencjał u *E. coli* po ekspozycji na TiO<sub>2</sub>-NPs różniły się istotnie od wartości tych parametrów u *Staphylococcus aureus*. Co więcej, z danych literaturowych wynika, że szczep *B. cereus* wytwarza siderofory, które chelatują żelazo i inne metale, zapewniając tym samym niezależne mechanizmy tolerancji metali (Zawadzka i in., 2009; Schalk i in., 2011). Istnieje możliwość, że siderofory mogą wspomagać wychwytywanie i dyfuzję uwolnionych jonów metali z NPs oraz zapewniać dodatkową ochronę procesów metabolicznych oraz błon przed uszkodzeniami. Biorąc pod uwagę różnice w przepuszczalności błony i wycieku cytoplazmy po ekspozycji badanych bakterii na NPs można przypuszczać, że mogły one w większym stopniu indukować powstawanie dziur w osłonach komórkowych *E. coli* niż u pozostałych szczepów w wyniku interakcji z powierzchnią bakterii lub akumulować się w błonie komórkowej, powodując w konsekwencji intensywny wyciek treści komórkowej.

Z przeprowadzonych analiz w ramach niniejszej pracy wynika, że Ag-NPs, Cu-NPs, ZnO-NPs i TiO<sub>2</sub>-NPs w stężeniach IC<sub>50</sub> i ½IC<sub>50</sub> w różny sposób wpływały na skład i właściwości błon komórkowych badanych szczepów. Grupami kwasów tłuszczowych najbardziej podatnymi na działanie NPs były u wszystkich bakterii cyklopropanowe oraz hydroksylowe kwasy tłuszczowe. Na przykład u bakterii *E. coli* traktowanych Ag-NPs w stężeniu IC<sub>50</sub> nastąpił znaczny spadek zawartości tych kwasów, połączony z jednoczesnym wzrostem udziału kwasów prostolącuchowych. Podobnie ekspozycja *E. coli* na Cu-NPs w stężeniu ½IC<sub>50</sub> powodowała wyraźny spadek procentowej zawartości cyklopropanowych i hydroksylowanych kwasów tłuszczowych oraz dodatkowo kwasów rozgałęzionych. Podobny wpływ na udział kwasów cyklopropanowych i hydroksylowanych w profilach FAME szczepu *S. epidermidis* miały Ag-NPs i Cu-NPs w stężeniu IC<sub>50</sub>. Przeprowadzone analizy wskazały, że Ag-NPs i Cu-NPs, niezależnie od zastosowanego stężenia, powodowały u *E. coli*

i *S. epidermidis* najbardziej znaczące modyfikacje składu i zawartości analizowanych grup kwasów tłuszczowych. Z kolei w komórkach *B. cereus* stwierdzono istotny wzrost zawartości procentowej cyklopropanowych kwasów tłuszczowych po ekspozycji na ZnO-NPs w stężeniu  $\frac{1}{2}IC_{50}$  i towarzyszący mu spadek zawartości rozgałęzionych i nienasyconych kwasów tłuszczowych. Największy spadek zawartości rozgałęzionych kwasów tłuszczowych w profilach tych bakterii udokumentowano po ekspozycji na Cu-NPs i ZnO-NPs w stężeniu  $\frac{1}{2}IC_{50}$ . Podsumowując, analiza FAME ujawniła zależny od stężenia wpływ badanych NPs na udział procentowy analizowanych grup kwasów tłuszczowych u *E. coli*, *B. cereus* i *S. epidermidis*. Bakterie Gram-dodatnie okazały się bardziej wrażliwe na działanie NPs niż *E. coli*. Rola analizowanych grup kwasów tłuszczowych w funkcjonowaniu błony komórkowej jest różna. Według Poger i Mark (2015) cyklopropanowe kwasy tłuszczowe stabilizują błony komórkowe, zwiększając stopień uporządkowania lipidów w porównaniu z ich nienasyconymi prekursorami oraz ograniczają rotację wiązań otaczających pierścień cyklopropanu. Ich obecność sprzyja również występowaniu zmian konformacyjnych typu „gauche” w łańcuchach węglowodorowych lipidów, zwiększając poprzeczną dyfuzję cząsteczek lipidów oraz płynność błony komórkowej. Natomiast hydroksylowe i rozgałęzione kwasy tłuszczowe odpowiadają w głównej mierze za sztywność dwuwarstwy lipidowej (Kumariya i in., 2015). Wyniki tych badań mają dużą wartość poznawczą, gdyż dotychczasowa wiedza w tym zakresie jest bardzo ograniczona. Podjęcie się wyjaśnienia wpływu NPs na skład kwasów tłuszczowych u badanych szczepów było ważnym zadaniem, ponieważ ich skład i zawartość determinują dynamiczny charakter błony, co dodatkowo chroni komórkę przed czynnikami toksycznymi, w tym przed NPs.

Analizę SEM przeprowadzono w celu zbadania rozmieszczenia i interakcji poszczególnych NPs z powierzchnią bakterii oraz określenia potencjalnych uszkodzeń w ich osłonach zewnętrznych. Stwierdzono, że poszczególne NPs charakteryzowały się różnym stopniem powinowactwa do powierzchni badanych szczepów. Na przykład ZnO-NPs wykazywały najsilniejsze powinowactwo do powierzchni *E. coli* i były równomiernie rozproszone na całej powierzchni komórek. Z kolei Cu-NPs gromadziły się miejscach peryferyjnych komórek *E. coli*. Przyczyną tego zjawiska może być większa ilość miejsc wiązania NPs w tych częściach komórki, jak również oddziaływanie ze składnikami lipopolisacharydów, które uczestniczą w tworzeniu wiązań wodorowych i oddziaływań hydrofobowych z NPs (Poh i in., 2018). Analiza SEM potwierdziła także silne powinowactwo ZnO-NPs do całej powierzchni komórek *B. cereus*. Na powierzchni komórek widoczne były duże i warstwowe skupiska ZnO-NPs, które dodatkowo tworzyły aglomeraty i agregaty o różnych kształtach. Uzasadnieniem tych obserwacji może być silne wyłapywanie ZnO-NPs i wiązanie ich przez warstwy peptydoglikanu i kwasy teichojowe. W szczególności jony metali dwuwartościowych wiązane są przez grupy fosforanowe kwasów teichojowych (Thomas i Rice, 2015), co może potwierdzać adhezję Cu-NPs ( $Cu^{2+}$ ) i ZnO-NPs ( $Zn^{2+}$ ) do powierzchni komórek *B. cereus*. Interesujące wyniki uzyskano podczas obrazowania komórek *S. epidermidis* traktowanych Cu-NPs i  $TiO_2$ -NPs. Cu-NPs tworzyły duże aglomeraty o nieregularnej dystrybucji na powierzchni komórek, co spowodowało niewielkie zmiany morfologiczne komórek. Natomiast  $TiO_2$ -NPs tworzyły jednolitą monowarstwę na powierzchni komórek, w której okazjonalnie pojawiały się większe skupiska NPs. Z danych literaturowych wynika, że  $TiO_2$ -NPs silnie oddziałują z grupami  $-COO^-$  w błonie komórkowej (Huang i in., 2017). Warto podkreślić, że Ag-NPs w najmniejszym stopniu ulegały adhezji do powierzchni *E. coli*, *B. cereus* i *S. epidermidis* w porównaniu z pozostałymi NPs. Może to

wynikać z potencjalnie niższego dodatniego ładunku wypadkowego Ag-NPs, a tym samym mniejszego przyciągania tych NPs do ujemnie naładowanych zewnętrznych warstw komórek drobnoustrojów. Wyniki tej części badań opublikowano w pracy Metryki i in. (2023), stanowiących rozdział II.3 prezentowanej rozprawy.

Uzupełnieniem zaprezentowanych w pracy doktorskiej wyników będzie nowa wiedza na temat specyficznych interakcji komórek bakterii z NPs, obejmujących zmiany strukturalne w fosfolipidach, lipidach, kwasach tłuszczowych oraz drugorzędowej i trzeciorzędowej strukturze białek błonowych z wykorzystaniem spektroskopii w podczerwieni (ATR-FTIR). Podjęta zostanie również próba analizy powierzchni komórek bakteryjnych oraz ustalenia charakterystycznego rozkładu powierzchniowego pierwiastków wchodzących w skład NPs metodą SEM-EDS. Zagadnienie wpływu działania NPs na komórki bakterii będzie dodatkowo poszerzone o pomiary potencjału zeta NPs, relatywnego potencjału błony komórkowej oraz hydrofobowości. Takie zaawansowane badania są obecnie na etapie realizacji lub zaplanowane do wykonania w ramach projektu Preludium 20.

## I.5. Literatura

1. Abdolapur Monikh F., Guo Z., Zhang P., Vijver M.G., Lynch I., Valsami-Jones E., Peijnenburg W.J.G.M. 2022. An analytical workflow for dynamic characterization and quantification of metal-bearing nanomaterials in biological matrices. *Nat Protoc* 17: 1926-1952
2. Ali A.S. 2020. Application of nanomaterials in environmental improvement. In: Sen M. (ed.), *Nanotechnology and the Environment*. IntechOpen, pp. 1-20
3. Ameen F., Alsamhary K., Alabdullatif J.A., ALNadhari S. 2021. A review on metal-based nanoparticles and their toxicity to beneficial soil bacteria and fungi. *Ecotoxicol Environ Saf* 213: 112027
4. Azam A., Ahmed A.S., Oves M., Khan M.S., Memic A. 2012. Size-dependent antimicrobial properties of CuO nanoparticles against Gram-positive and -negative bacterial strains. *Int J Nanomedicine* 7: 3527-3535
5. Bagchi B., Kar S., Dey S.K., Bhandary S., Roy D., Mukhopadhyay T.K., Das S., Nandy P. 2013. In situ synthesis and antibacterial activity of copper nanoparticle loaded natural montmorillonite clay based on contact inhibition and ion release. *Colloids Surf B Biointerfaces* 108: 358-365
6. Banerjee G., Pandey S., Ray A.K., Kumar R. 2015. Bioremediation of heavy metals by a novel bacterial strain *Enterobacter cloacae* and its antioxidant enzyme activity, flocculant production, and protein expression in presence of lead, cadmium, and nickel. *Water Air Soil Pollut* 226: 91
7. Baptista P.V., McCusker M.P., Carvalho A., Ferreira D.A., Mohan N.M., Martins M., Fernandes A.R. 2018. Nano-strategies to fight multidrug resistant bacteria – “A battle of the titans”. *Front Microbiol* 9: 1441
8. Bayda S., Adeel M., Tuccinardi T., Cordani M., Rizzolio F. 2020. The history of nanoscience and nanotechnology from chemical-physical applications to nanomedicine. *Molecules* 25(1): 112
9. Behera N., Arakha M., Priyadarshinee M., Pattanayak B.S., Soren S., Jha S., Mallick B.C. 2019. Oxidative stress generated at nickel oxide nanoparticle interface results in bacterial membrane damage leading to cell death. *RSC Adv* 9: 24888-24894
10. Bhattacharya P., Dey A., Neogi S. 2021. An insight into the mechanism of antibacterial activity by magnesium oxide nanoparticles. *J Mater Chem B* 9: 5329-5339
11. Billenkamp F., Peng T., Berghoff B.A., Klug G. 2015. A cluster of four homologous small RNAs modulates C1 metabolism and the pyruvate dehydrogenase complex in *Rhodobacter sphaeroides* under various stress conditions. *J Bacteriol* 197(10): 1839-1852
12. Bisht S., Dada R. 2017. Oxidative stress: major executioner in disease pathology, role in sperm DNA damage and preventive strategies. *Front Biosci (Schol Ed)* 9(3): 420-447
13. Borisov V.B., Siletsky S.A., Nastasi M.R., Forte E. 2021. ROS defense systems and terminal oxidases in bacteria. *Antioxidants (Basel)* 10(6): 839
14. Bradford M.M. 1976. A rapid and sensitive method for the quantitation of microgram quantities of proteins utilizing the principle of protein-dye binding. *Anal Biochem* 72(7): 248-254
15. Bundschuh M., Filser J., Lüderwald S., McKee M.S., Metreveli G., Schaumann G.E., Schulz R., Wagner S. 2018. Nanoparticles in the environment: where do we come from, where do we go to? *Environ Sci Eur* 30(1): 6
16. Canaparo R., Foglietta F., Limongi T., Serpe L. 2020. Biomedical applications of reactive oxygen species generation by metal nanoparticles. *Materials* 14(1): 53

17. Ceragioli M., Mols M., Moezelaar R., Ghelardi E., Senesi S., Abee T. 2010. Comparative transcriptomic and phenotypic analysis of the responses of *Bacillus cereus* to various disinfectant treatments. *Appl Environ Microbiol* 76(10): 3352-3360
18. Chandransu P., Rensing C., Helmann J.D. 2017. Metal homeostasis and resistance in bacteria. *Nat Rev Microbiol* 15(6): 338-350
19. Chatterjee A.K., Chakraborty R., Basu T. 2014. Mechanism of antibacterial activity of copper nanoparticles. *Nanotechnology* 25(13): 135101
20. Cheeseman S., Christofferson A.J., Kariuki R., Cozzolino D., Daeneke T., Crawford R.J., Truong V.K., Chapman J., Elbourne A. 2020. Antimicrobial metal nanomaterials: from passive to stimuli-activated applications. *Adv Sci (Weinh)* 7(10): 1902913
21. Collin F. 2019. Chemical basis of reactive oxygen species reactivity and involvement in neurodegenerative diseases. *Int J Mol Sci* 20(10): 2407
22. Cui H., Smith A.L. 2022. Impact of engineered nanoparticles on the fate of antibiotic resistance genes in wastewater and receiving environments: a comprehensive review. *Environ Res* 204(Pt D): 112373
23. David M., Krishna P.M., Sangeetha J. 2016. Elucidation of impact of heavy metal pollution on soil bacterial growth and extracellular polymeric substances flexibility. *3 Biotech* 6: 172
24. Dayem A.A., Hossain M.K., Lee S.B., Kim K., Saha S.K., Yang G.M., Choi H.Y., Cho S.G. 2017. The role of reactive oxygen species (ROS) in the biological activities of metallic nanoparticles. *Int J Mol Sci* 18(1): 120
25. Deng Y., Beahm D.R., Ionov S., Sarpeshkar R. 2021. Measuring and modeling energy and power consumption in living microbial cells with a synthetic ATP reporter. *BMC Biol* 19(1): 101
26. Devi K.P., Sakthivel R., Nisha S.A., Suganthi N., Pandian S.K. 2013. Eugenol alters the integrity of cell membrane and acts against the nosocomial pathogen *Proteus mirabilis*. *Arch Pharm Res* 36(3): 282-292
27. Dimova M., Tugai A., Tugai T., Iutynska G., Dordevic D., Kushkevych I. 2022. Molecular research of lipid peroxidation and antioxidant enzyme activity of *Comamonas testosteroni* bacterial cells under the hexachlorobenzene impact. *Int J Mol Sci* 23(19): 11415
28. Eckhardt S., Brunetto P.S., Gagnon J., Priebe M., Giese B., Fromm K.M. 2013. Nanobio silver: its interactions with peptides and bacteria, and its uses in medicine. *Chem Rev* 113(7): 4708-4754
29. Ezraty B., Gennaris A., Barras F., Collet J.F. 2017. Oxidative stress, protein damage and repair in bacteria. *Nat Rev Microbiol* 15(7): 385-396
30. Fang F.C. 2011. Antimicrobial actions of reactive oxygen species. *mBio* 2(5): e00141-11
31. Ganesh Babu M.M., Sridhar J., Gunasekaran P. 2011. Global transcriptome analysis of *Bacillus cereus* ATCC 14579 in response to silver nitrate stress. *J Nanobiotechnology* 9: 49
32. Gao F., Shao T., Yu Y., Xiong Y., Yang L. 2021. Surface-bound reactive oxygen species generating nanozymes for selective antibacterial action. *Nat Commun* 12(1): 745
33. Ghorbani R., Biparva P., Moradian F. 2020. Assessment of antibacterial activity and the effect of copper and iron zerovalent nanoparticles on gene expression *DnaK* in *Pseudomonas aeruginosa*. *BioNanoScience* 10: 204-211

34. Gómez-Núñez M.F., Castillo-López M., Sevilla-Castillo F., Roque-Reyes O.J., Romero-Lechuga F., Medina-Santos D.I., Martínez-Daniel R., Peón A.N. 2020. Nanoparticle-based devices in the control of antibiotic resistant bacteria. *Front Microbiol* 11: 563821
35. Grotto D., Santa Maria L., Valentini J., Paniz C., Schmitt G., Garcia S.C., Pomblum V.J., Rocha J.B.T., Farina M. 2009. Importance of the lipid peroxidation biomarkers and methodological aspects for malondialdehyde quantification. *Quim Nova* 32: 169-174
36. Gutiérrez M.F., Malaquias P., Hass V., Matos T.P., Lourenço L., Reis A., Loguercio A.D., Farago P.V. 2017. The role of copper nanoparticles in an etch-and-rinse adhesive on antimicrobial activity, mechanical properties and the durability of resin-dentine interfaces. *J Dent* 61: 12-20
37. Halder S., Yadav K.K., Sarkar R., Mukherjee S., Saha P., Haldar S., Karmakar S., Sen T. 2015. Alteration of Zeta potential and membrane permeability in bacteria: a study with cationic agents. *Springerplus* 4: 672
38. Hassan K.A., Pederick V.G., Elbourne L.D., Paulsen I.T., Paton J.C., McDevitt C.A., Eijkelkamp B.A. 2017. Zinc stress induces copper depletion in *Acinetobacter baumannii*. *BMC Microbiol* 17(1): 59
39. Hegeman G.D. 1966. Synthesis of the enzymes of the mandelate pathway by *Pseudomonas putida* I. Synthesis of enzymes by the wild type. *J Bacteriol* 91(3): 1140-1154
40. Heikal A., Nakatani Y., Dunn E., Weimar M.R., Day C.L., Baker E.N., Lott J.S., Sazanov L.A., Cook G.M. 2014. Structure of the bacterial type II NADH dehydrogenase: a monotopic membrane protein with an essential role in energy generation. *Mol Microbiol* 91(5): 950-964
41. Horst A.M., Vukanti R., Priester J.H., Holden P.A. 2013. An assessment of fluorescence- and absorbance-based assays to study metal-oxide nanoparticle ROS production and effects on bacterial membranes. *Small* 9(9-10): 1753-1764
42. Hou Z., Fink R.C., Black E.P., Sugawara M., Zhang Z., Diez-Gonzalez F., Sadowsky M.J. 2012. Gene expression profiling of *Escherichia coli* in response to interactions with the lettuce rhizosphere. *J Appl Microbiol* 113(5): 1076-1086
43. Huang G., Ng T.W., An T., Li G., Wang B., Wu D., Yip H.Y., Zhao H., Wong P.K. 2017. Interaction between bacterial cell membranes and nano-TiO<sub>2</sub> revealed by two-dimensional FTIR correlation spectroscopy using bacterial ghost as a model cell envelope. *Water Res* 118: 104-113
44. Huang Z., He K., Song Z., Zeng G., Chen A., Yuan L., Li H., Hu L., Guo Z., Chen G. 2018. Antioxidative response of *Phanerochaete chrysosporium* against silver nanoparticle-induced toxicity and its potential mechanism. *Chemosphere* 211: 573-583.
45. Hubenko K., Yefimova S., Tkacheva T., Maksimchuk P., Borovoy I., Klochkov V., Kavok N., Opolonin O., Malyukin Y. 2018. Reactive oxygen species generation in aqueous solutions containing GdVO<sub>4</sub>:Eu<sup>3+</sup> nanoparticles and their complexes with methylene blue. *Nanoscale Res Lett* 13(1): 100
46. Hulla J.E., Sahu S.C., Hayes A.W. 2015. Nanotechnology: history and future. *Hum Exp Toxicol* 34(12): 1318-1321
47. Ihssen J., Jovanovic N., Sirec T., Spitz U. 2021. Real-time monitoring of extracellular ATP in bacterial cultures using thermostable luciferase. *PLoS One* 16(1): e0244200
48. Imlay J.A. 2003. Pathways of oxidative damage. *Annu Rev Microbiol* 57: 395-418

49. Joudeh N., Linke D. 2022. Nanoparticle classification, physicochemical properties, characterization, and applications: a comprehensive review for biologists. *J Nanobiotechnology* 20(11): 262
50. Karavolos M.H., Horsburgh M.J., Ingham E., Foster S.J. 2003. Role and regulation of the superoxide dismutases of *Staphylococcus aureus*. *Microbiology (Reading)* 149(Pt 10): 2749-2758
51. Karimi E., Mohseni Fard E. 2017. Nanomaterial effects on soil microorganisms. In: Ghorbanpour M., Khanuja M., Varma A. (eds.), *Nanoscience and plant-soil systems*. Springer International Publishing, pp. 137-200
52. Khan I., Saeed K., Khan I. 2019. Nanoparticles: properties, applications and toxicities. *Arab J Chem* 12(7): 908-931
53. Khater M.S., Kulkarni G.R., Khater S.S., Gholap H., Patil R. 2020. Study to elucidate effect of titanium dioxide nanoparticles on bacterial membrane potential and membrane permeability. *Mater Res Express* 7(3): 035005
54. Ko K.S., Kim J.W., Kim J.M., Kim W., Chung S.I., Kim I.J., Kook Y.H. 2004. Population structure of the *Bacillus cereus* group as determined by sequence analysis of six housekeeping genes and the *plcR* gene. *Infect Immun* 72(9): 5253-5261
55. Kora A.J., Sashidhar R.B. 2015. Antibacterial activity of biogenic silver nanoparticles synthesized with gum ghatti and gum olibanum: a comparative study. *J Antibiot (Tokyo)* 68(2): 88-97
56. Korshed P., Li L., Liu Z., Wang T. 2016. The molecular mechanisms of the antibacterial effect of picosecond laser generated silver nanoparticles and their toxicity to human cells. *PLoS One* 11(8): e0160078
57. Ku J.W.K., Gan Y.H. 2021. New roles for glutathione: modulators of bacterial virulence and pathogenesis. *Redox Biol* 44: 102012
58. Kumar A., Pandey A.K., Singh S.S., Shanker R., Dhawan A. 2011. Engineered ZnO and TiO<sub>2</sub> nanoparticles induce oxidative stress and DNA damage leading to reduced viability of *Escherichia coli*. *Free Radic Biol Med* 51(10): 1872-1881
59. Kumariya R., Sood S.K., Rajput Y.S., Saini N., Garsa A.K. 2015. Increased membrane surface positive charge and altered membrane fluidity leads to cationic antimicrobial peptide resistance in *Enterococcus faecalis*. *Biochim Biophys Acta Biomembr* 1848(6): 1367-1375
60. Lange A., Sawosz E., Daniluk K., Wierzbicki M., Małolepszy A., Gołębiowski M., Jaworski S. 2022. Bacterial surface disturbances affecting cell function during exposure to three-compound nanocomposites based on graphene materials. *Nanomaterials (Basel)* 12(17): 3058
61. Lemire J., Alhasawi A., Appanna V.P., Tharmalingam S., Appanna V.D. 2017. Metabolic defence against oxidative stress: the road less travelled so far. *J Appl Microbiol* 123(4): 798-809
62. Levine R.L., Garland D., Oliver C.N., Amici A., Climent I., Lenz A.G., Ahn B.W., Shaltiel S., Stadtman E.R. 1990. Determination of carbonyl content in oxidatively modified proteins. *Methods Enzymol* 186: 464-478
63. Li H., Zhou X., Huang Y., Liao B., Cheng L., Ren B. 2021. Reactive oxygen species in pathogen clearance: the killing mechanisms, the adaption response, and the side effects. *Front Microbiol* 11: 622534

64. Li Y., Zhang W., Niu J., Chen Y. 2012. Mechanism of photogenerated reactive oxygen species and correlation with the antibacterial properties of engineered metal-oxide nanoparticles. *ACS Nano* 6(6): 5164-5173
65. Liao S., Zhang Y., Pan X., Zhu F., Jiang C., Liu Q., Cheng Z., Dai G., Wu G., Wang L., Chen L. 2019. Antibacterial activity and mechanism of silver nanoparticles against multidrug-resistant *Pseudomonas aeruginosa*. *Int J Nanomedicine* 14: 1469-1487
66. Linklater D.P., Baulin V.A., Juodkazis S., Crawford R.J., Stoodley P., Ivanova E.P. 2021. Mechano-bactericidal actions of nanostructured surfaces. *Nat Rev Microbiol* 19(1): 8-22
67. Livak K.J., Schmittgen T.D. 2001. Analysis of relative gene expression data using real-time quantitative PCR and the  $2^{-\Delta\Delta CT}$  method. *Methods* 25(4): 402-408
68. Loewen P. 1996. Probing the structure of catalase HPII of *Escherichia coli* - a review. *Gene* 179(1): 39-44
69. Maier R.M. 2009. Bacterial growth. In: Maier R.M., Pepper I.L., Gerba C.P. (eds.), *Environmental Microbiology*. Elsevier Academic Press, pp. 37-54
70. Makabenta J.M.V., Nabawy A., Li C.H., Schmidt-Malan S., Patel R., Rotelio V.M. 2021. Nanomaterial-based therapeutics for antibiotic-resistant bacterial infections. *Nat Rev Microbiol* 19: 23-36
71. Mammari N., Lamouroux E., Boudier A., Duval R.E. 2022. Current knowledge on the oxidative-stress-mediated antimicrobial properties of metal-based nanoparticles. *Microorganisms* 10(2): 437
72. Manke A., Wang L., Rojanasakul Y. 2013. Mechanisms of nanoparticle-induced oxidative stress and toxicity. *Biomed Res Int* 2013: 942916
73. Masip L., Veeravalli K., Georgiou G. 2006. The many faces of glutathione in bacteria. *Antioxid Redox Signal* 8(5-6): 753-762
74. McBee M.E., Chionh Y.H., Sharaf M.L., Ho P., Cai M.W., Dedon P.C. 2017. Production of superoxide in bacteria is stress- and cell state-dependent: a gating-optimized flow cytometry method that minimizes ROS measurement artifacts with fluorescent dyes. *Front Microbiol* 8: 459
75. Meghana S., Kabra P., Chakraborty S., Padmavathy N. 2015. Understanding the pathway of antibacterial activity of copper oxide nanoparticles. *RSC Adv* 5: 12293-12299
76. Metryka O., Wasilkowski D., Mroziak A. 2021. Insight into the antibacterial activity of selected metal nanoparticles and alterations within the antioxidant defence system in *Escherichia coli*, *Bacillus cereus* and *Staphylococcus epidermidis*. *Int J Mol Sci* 22(21): 11811
77. Metryka O., Wasilkowski D., Mroziak A. 2022. Evaluation of the effects of Ag, Cu, ZnO and TiO<sub>2</sub> nanoparticles on the expression level of oxidative stress-related genes and the activity of antioxidant enzymes in *Escherichia coli*, *Bacillus cereus* and *Staphylococcus epidermidis*. *Int J Mol Sci* 23(9): 4966
78. Metryka O., Wasilkowski D., Adamczyk-Habrajska M., Mroziak A. 2023. Undesirable consequences of the metallic nanoparticles action on the properties and functioning of *Escherichia coli*, *Bacillus cereus* and *Staphylococcus epidermidis* membranes. *J Hazard Mater* 446: 130728
79. Monod J. 1949. The growth of bacterial cultures. *Annu Rev Microbiol* 3: 371-394
80. Moore J.D., Avellan A., Noack C.W., Guo Y., Lowry G.V., Gregory K.B. 2017. Time-dependent bacterial transcriptional response to CuO nanoparticles differs from that of Cu<sup>2+</sup> and provides insights into CuO nanoparticle toxicity mechanisms. *Environ Sci Nano* 4: 2321-2335



81. Muñiz Diaz R., Cardoso-Avila P.E., Pérez Tavares J.A., Patakfalvi R., Villa Cruz V., Pérez Ladrón de Guevara H., Gutiérrez Coronado O., Arteaga Garibay R.I., Saavedra Arroyo Q.E., Marañón-Ruiz V.F., Castañeda Contreras J. 2021. Two-step triethylamine-based synthesis of MgO nanoparticles and their antibacterial effect against pathogenic bacteria. *Nanomaterials (Basel)* 11(2): 410
82. Nowak A., Szade J., Talik E., Zubko M., Wasilkowski D., Dulski M., Balin K., Mroziak A., Peszke J. 2016. Physicochemical and antibacterial characterization of ionocyt Ag/Cu powder nanoparticles. *Matter Charact* 117: 9-16
83. Nweke C.O., Alisi C.S., Okolo J.C., Nwanyanwu C.E. 2007. Toxicity of zinc to heterotrophic bacteria from a tropical river sediment. *Appl Ecol Env Res* 5 (1): 123-132
84. Odzak N., Kistler D., Behra R., Sigg L. 2014. Dissolution of metal and metal oxide nanoparticles in aqueous media. *Environ Pollut* 191: 132-138
85. Onyango A.N. 2016. Endogenous generation of singlet oxygen and ozone in human and animal tissues: mechanisms, biological significance, and influence of dietary components. *Oxidant Med Cell Longev* 2016: 2398573
86. Osonga F.J., Akgul A., Yazgan I., Akgul A., Ontman R., Kariuki V.M., Eshun G.B., Sadik O.A. 2018. Flavonoid-derived anisotropic silver nanoparticles inhibit growth and change the expression of virulence genes in *Escherichia coli* SM10. *RSC Adv* 8: 4649-4661
87. Parra-Ortiz E., Malmsten M. 2022. Photocatalytic nanoparticles - from membrane interactions to antimicrobial and antiviral effects. *Adv Colloid Interface Sci* 299: 102526
88. Pepper I.L., Gerba C.P. 2005. *Environmental Microbiology. A Laboratory Manual*. Elsevier Academic Press, pp. 3-10
89. Peszke J., Dulski M., Nowak A., Balin K., Zubko M., Sułowicz S., Nowak B., Piotrowska-Seget Z., Talik E., Wojtyniak M., Mrozek-Wilczkiewicz A., Malarz K., Szade J. 2017. Unique properties of silver and copper silica-based nanocomposites as antimicrobial agents. *RSC Adv* 7(45): 28092-28104
90. Planchon M., Léger T., Spalla O., Huber G., Ferrari R. 2017. Metabolomic and proteomic investigations of impacts of titanium dioxide nanoparticles on *Escherichia coli*. *PLoS One* 12: e0178437
91. Poger D., Mark A.E. 2015. A ring to rule them all: the effect of cyclopropane fatty acids on the fluidity of lipid bilayers. *J Phys Chem B* 119(17): 5487-5495
92. Poh T.Y., Ali N.A.B.M., Mac Aogáin M., Kathawala M.H., Setyawati M.I., Ng K.W., Chotirmall S.H. 2018. Inhaled nanomaterials and the respiratory microbiome: clinical, immunological and toxicological perspectives. *Part Fibre Toxicol* 15(1): 46
93. Quinteros M.A., Cano Aristizábal V., Dalmasso P.R., Paraje M.G., Páez P.L. 2016. Oxidative stress generation of silver nanoparticles in three bacterial genera and its relationship with the antimicrobial activity. *Toxicol In Vitro* 36: 216-223
94. Raghunath A., Perumal E. 2017. Metal oxide nanoparticles as antimicrobial agents: a promise for the future. *Int J Antimicrob Agents* 49(2): 137-152
95. Rice-Evans C.A., Diplock A.T., Symons M.C.R. 1991a. The detection and characterization of free radical species. In: Rice-Evans C.A., Diplock A.T., Symons M.C.R. (eds.), *Laboratory Techniques*

- in Biochemistry and Molecular Biology, Techniques in Free Radical Research, Elsevier, Amsterdam, The Netherlands, vol. 22, pp. 51-100
96. Rice-Evans C.A., Diplock A.T., Symons M.C.R. 1991b. Detection of protein structural modifications induced by free radicals. In: Rice-Evans C.A., Diplock A.T., Symons M.C.R. (eds.), Laboratory Techniques in Biochemistry and Molecular Biology, Techniques in Free Radical Research, Elsevier, Amsterdam, The Netherlands, vol. 22, pp. 207-235
  97. Rice-Evans C.A., Diplock A.T., Symons M.C.R. 1991c. Investigation of the consequences of free radical attack on lipids. In: Rice-Evans C.A., Diplock A.T., Symons M.C.R. (eds.), Laboratory Techniques in Biochemistry and Molecular Biology, Techniques in Free Radical Research, Elsevier, Amsterdam, The Netherlands, vol. 22, pp. 125-184
  98. Sánchez-López E., Gomes D., Esteruelas G., Bonilla L., Lopez-Machado A.L., Galindo R., Cano A., Espina M., Ettcheto M., Camins A., Silva A.M., Durazzo A., Santini A., Garcia M.L., Souto E.B. 2020. Metal-based nanoparticles as antimicrobial agents: an overview. *Nanomaterials (Basel)* 10(2): 292
  99. Sasser M. 1990. Bacterial identification by gas chromatographic analysis of fatty acid methyl esters (GC-FAME); Technical Note #101; MIDI: Newark, DE, USA, revised 2006
  100. Schalk I.J., Hannauer M., Braud A. 2011. New roles for bacterial siderophores in metal transport and tolerance. *Environ Microbiol* 13(11): 2844-2854
  101. Schellhorn H.E. 1995. Regulation of hydroperoxidase (catalase) expression in *Escherichia coli*. *FEMS Microbiol Lett* 131(2): 113-119
  102. Seaver L.C., Imlay J.A. 2001. Alkyl hydroperoxide reductase is the primary scavenger of endogenous hydrogen peroxide in *Escherichia coli*. *J Bacteriol* 183(24): 7173-7181
  103. Seixas A.F., Quendera A.P., Sousa J.P., Silva A.F.Q., Arraiano C.M., Andrade J.M. 2022. Bacterial response to oxidative stress and RNA oxidation. *Front Genet* 12: 821535
  104. Shaikh S., Nazam N., Rizvi S.M.D., Ahmad K., Baig M.H., Lee E.J., Choi I. 2019. Mechanistic insights into the antimicrobial actions of metallic nanoparticles and their implications for multidrug resistance. *Int J Mol Sci* 20(10): 2468
  105. Sharma S.V., Arbach M., Roberts A.A., Macdonald C.J., Groom M., Hamilton C.J. 2013. Biophysical features of bacillithiol, the glutathione surrogate of *Bacillus subtilis* and other firmicutes. *Chembiochem* 14(16): 2160-2168
  106. Shkodenko L., Kassirov I., Koshel E. 2020. Metal oxide nanoparticles against bacterial biofilms: perspectives and limitations. *Microorganisms* 8(10): 1545
  107. Sihto H.M., Tasara T., Stephan R., Johler S. 2014. Validation of reference genes for normalization of qPCR mRNA expression levels in *Staphylococcus aureus* exposed to osmotic and lactic acid stress conditions encountered during food production and preservation. *FEMS Microbiol Lett* 356(1): 134-140
  108. Slavin Y.N., Asnis J., Häfeli U.O., Bach H. 2017. Metal nanoparticles: understanding the mechanisms behind antibacterial activity. *J Nanobiotechnol* 15(1): 65
  109. Smirnova G.V., Oktyabrsky O.N. 2005. Glutathione in bacteria. *Biochemistry (Mosc)* 70(11): 1199-1211
  110. Sohm B., Immel F., Bauda P., Pagnout C. 2015. Insight into primary mode of action of TiO<sub>2</sub> nanoparticles on *Escherichia coli* in the dark. *Proteomics* 15(1): 98-113

111. Staroń A., Długosz O. 2021. Antimicrobial properties of nanoparticles in the context of advantages and potential risks of their use. *J Environ Sci Health A* 56(6): 680-693
112. Stewart L.J., Ong C.L.Y., Zhang M.M., Brouwer S., McIntyre L., Davies M.R., Walker M.J., McEwan A.G., Waldron K.J., Djoko K.Y. 2020. A role for glutathione in buffering excess intracellular copper in *Streptococcus pyogenes*. *mBio* 11(6): e02804-20
113. Sun T.Y., Bornhöft N.A., Hungerbühler K., Nowack B. 2016. Dynamic probabilistic modeling of environmental emissions of engineered nanomaterials. *Environ Sci Technol* 50(9): 4701-4711
114. Thomas K.J. 3rd, Rice C.V. 2015. Equilibrium binding behavior of magnesium to wall teichoic acid. *Biochim Biophys Acta* 1848(10 Pt A): 1981-1987
115. van Schaik W., Zwietering M.H., de Vos W.M., Abee T. 2005. Deletion of the *sigB* gene in *Bacillus cereus* ATCC 14579 leads to hydrogen peroxide hyperresistance. *Appl Environ Microbiol* 71(10): 6427-6430
116. Vardanyan Z., Gevorkyan V., Ananyan M., Vardapetyan H., Trchounian A. 2015. Effects of various heavy metal nanoparticles on *Enterococcus hirae* and *Escherichia coli* growth and proton-coupled membrane transport. *J Nanobiotechnol* 13: 69
117. Vineeth Kumar C.M., Karthick V., Kumar V.G., Inbakandan D., Rene E.R., Suganya K.S.U., Embrandiri A., Dhas T.S., Ravi M., Sowmiya P. 2022. The impact of engineered nanomaterials on the environment: release mechanism, toxicity, transformation, and remediation. *Environ Res* 212(Pt B): 113202
118. Wang D., Lin Z., Wang T., Yao Z., Qin M., Zheng S., Lu W. 2016. Where does the toxicity of metal oxide nanoparticles come from: the nanoparticles, the ions, or a combination of both? *J Hazard Mater* 308: 328-334
119. Wang L., Hu C., Shao L. 2017. The antimicrobial activity of nanoparticles: present situation and prospects for the future. *Int J Nanomed* 12: 1227-1249
120. Wang S., Zhou Q., Chen X., Luo R.H., Li Y., Liu X., Yang L.M., Zheng Y.T., Wang P. 2021. Modification of *N*-terminal  $\alpha$ -amine of proteins via biomimetic *ortho*-quinone-mediated oxidation. *Nat Commun* 12(1): 2257
121. Wiegand I., Hilpert K., Hancock R.E.W. 2008. Agar and broth dilution methods to determine the minimal inhibitory concentration (MIC) of antimicrobial substance. *Nat Protoc* 3(2): 163-175
122. Xiong Y.L., Guo A. 2021. Animal and plant protein oxidation: chemical and functional property significance. *Foods* 10(1): 40
123. Yang Y., Wang J., Xiu Z., Alvarez P.J. 2013. Impacts of silver nanoparticles on cellular and transcriptional activity of nitrogen-cycling bacteria. *Environ Toxicol Chem* 32(7): 1488-1494
124. Yeh Y.C., Huang T.H., Yang S.C., Chen C.C., Fang J.Y. 2020. Nano-based drug delivery or targeting to eradicate bacteria for infection mitigation: a review of recent advances. *Front Chem* 8: 286
125. Yu Z., Li Q., Wang J., Yu Y., Wang Y., Zhou Q., Li P. 2020. Reactive oxygen species-related nanoparticle toxicity in the biomedical field. *Nanoscale Res Lett* 15(1): 115
126. Yuan Y.G., Peng Q.L., Gurunathan S. 2017. Effects of silver nanoparticles on multiple drug-resistant strains of *Staphylococcus aureus* and *Pseudomonas aeruginosa* from mastitis-infected goats: an alternative approach for antimicrobial therapy. *Int J Mol Sci* 18(3): 569

127. Zawadzka A.M., Abergel R.J., Nichiporuk R., Andersen U.N., Raymond K.N. 2009. Siderophore-mediated iron acquisition systems in *Bacillus cereus*: identification of receptors for anthrax virulence-associated petrobactin. *Biochemistry* 48(16): 3645-3657
128. Zhang W., Li Y., Niu J., Chen Y. 2013. Photogeneration of reactive oxygen species on uncoated silver, gold, nickel, and silicon nanoparticles and their antibacterial effects. *Langumir* 29(15): 4647-4651
129. Zhang Y., Gu A.Z., Xie S., Li X., Cen T., Li D., Chen J. 2018a. Nano-metal oxides induce antimicrobial resistance *via* radical-mediated mutagenesis. *Environ Int* 121(Pt 2): 1162-1171
130. Zhang Y., Huang P., Wang D., Chen J., Liu W., Hu P., Huang M., Chen X., Chen Z. 2018b. Near-infrared-triggered antibacterial and antifungal photodynamic therapy based on lanthanide-doped upconversion nanoparticles. *Nanoscale* 10: 15485-15495
131. Żur J., Piński A., Wojcieszynska D., Smulek W., Guzik U. 2020. Diclofenac degradation-enzymes, genetic background and cellular alterations triggered in diclofenac-metabolizing strain *Pseudomonas moorei* KB4. *Int J Mol Sci* 21(18): 6786

## I.6. Źródła internetowe

<https://euon.echa.europa.eu/documents/2435000/3268573/eumarketstudy.pdf/3a9daabf-eef9-9294-1e1a-2273bd219dc4?t=1667820390467> (05.2023)

<https://www.polarismarketresearch.com/industry-analysis/metal-nanoparticles-market> (05.2023)

<https://www.aatbio.com/tools/ic50-calculator> (05.2023)

<https://www.ncbi.nlm.nih.gov/tools/primer-blast/> (05.2023)

<https://genomes.atcc.org/genomes> (05.2023)

## **II. Publikacje wchodzące w skład rozprawy**

## II.1

Metryka O., Wasilkowski D., Mroziak A. 2021. Insight into the antibacterial activity of selected metal nanoparticles and alterations within the antioxidant defence system in *Escherichia coli*, *Bacillus cereus* and *Staphylococcus epidermidis*. *International Journal of Molecular Sciences* 22(21): 11811



Article

# Insight into the Antibacterial Activity of Selected Metal Nanoparticles and Alterations within the Antioxidant Defence System in *Escherichia coli*, *Bacillus cereus* and *Staphylococcus epidermidis*

Oliwia Metryka <sup>1,\*</sup> , Daniel Wasilkowski <sup>2</sup> and Agnieszka Mrozik <sup>2,\*</sup>

<sup>1</sup> Doctoral School, University of Silesia, Bankowa 14, 40-032 Katowice, Poland

<sup>2</sup> Institute of Biology, Biotechnology and Environmental Protection, Faculty of Natural Sciences, University of Silesia, Jagiellońska 28, 40-032 Katowice, Poland; daniel.wasilkowski@us.edu.pl

\* Correspondence: oliwia.metryka@us.edu.pl (O.M.); agnieszka.mrozik@us.edu.pl (A.M.)

**Abstract:** The antimicrobial activity of nanoparticles (NPs) is a desirable feature of various products but can become problematic when NPs are released into different ecosystems, potentially endangering living microorganisms. Although there is an abundance of advanced studies on the toxicity and biological activity of NPs on microorganisms, the information regarding their detailed interactions with microbial cells and the induction of oxidative stress remains incomplete. Therefore, this work aimed to develop accurate oxidation stress profiles of *Escherichia coli*, *Bacillus cereus* and *Staphylococcus epidermidis* strains treated with commercial Ag-NPs, Cu-NPs, ZnO-NPs and TiO<sub>2</sub>-NPs. The methodology used included the following determinations: toxicological parameters, reactive oxygen species (ROS), antioxidant enzymes and dehydrogenases, reduced glutathione, oxidatively modified proteins and lipid peroxidation. The toxicological studies revealed that *E. coli* was most sensitive to NPs than *B. cereus* and *S. epidermidis*. Moreover, NPs induced the generation of specific ROS in bacterial cells, causing an increase in their concentration, which further resulted in alterations in the activity of the antioxidant defence system and protein oxidation. Significant changes in dehydrogenases activity and elevated lipid peroxidation indicated a negative effect of NPs on bacterial outer layers and respiratory activity. In general, NPs were characterised by very specific nano-bio effects, depending on their physicochemical properties and the species of microorganism.

**Keywords:** bacteria; nanoparticles; toxicological parameters; reactive oxygen species; antioxidant enzymes; protein and lipid oxidation



**Citation:** Metryka, O.; Wasilkowski, D.; Mrozik, A. Insight into the Antibacterial Activity of Selected Metal Nanoparticles and Alterations within the Antioxidant Defence System in *Escherichia coli*, *Bacillus cereus* and *Staphylococcus epidermidis*. *Int. J. Mol. Sci.* **2021**, *22*, 11811. <https://doi.org/10.3390/ijms222111811>

Academic Editor: Lorenzo Corsi

Received: 26 September 2021

Accepted: 29 October 2021

Published: 30 October 2021

**Publisher's Note:** MDPI stays neutral with regard to jurisdictional claims in published maps and institutional affiliations.



**Copyright:** © 2021 by the authors. Licensee MDPI, Basel, Switzerland. This article is an open access article distributed under the terms and conditions of the Creative Commons Attribution (CC BY) license (<https://creativecommons.org/licenses/by/4.0/>).

## 1. Introduction

The dynamic development of education, technology, and market economy worldwide requires high advancement in the research of new materials that may resolve current global problems. Nanotechnology and its microscopic universe offer unlimited possibilities for contemporary science and various branches of industry. One of the benefits of modern nanotechnology is the production of nanomaterials (NMs) with antimicrobial activity and implementing them into different commercial processes and products as a defence against multidrug resistant infectious microorganisms [1–3]. Direct manipulation of synthesised NMs and adequate alteration of their properties can create broad-spectrum and long-term antimicrobials, which is a substantial trait, especially in the medical field. For instance, inorganic NMs based on metal and metal oxides have been utilised in biomedical implant materials, such as dental implants, through their application on the implant surfaces as nanocoatings or as an integral part of the material. Consecutively, this could prevent the origin and further development of infections in the place of implant insertion, increasing the chance of successful surgeries [4–6]. On the other hand, the release of such NMs into the environment is a potential threat to microbial populations that are not a target of their

action. According to Bundschuh et al. [7], approximate global estimates of the accumulation of NMs in the environment indicate that the main accumulators of such structures are landfills (63–91%) and soil (8–28%). Despite significant advances in analytical methods, it is still impossible to measure the concentrations of NMs in various ecosystems and assess their environmental risk [7]. Therefore, it is urgent to fully evaluate the impact of NMs on different microbial strains to determine their safe use and prevent possible risks of their presence in ecological sinks.

Nanomaterials, including nanoparticles (NPs), have attracted much attention in the last decade due to their antimicrobial properties and non-specific targeting of treated microorganisms. The mode of action of NPs involves, among others, the disruption of the integrity of bacterial outer layers, increase in the permeabilisation of the bacterial cell membrane, destruction of intracellular structures, or decrease in bacterial viability [8,9]. However, one of the most attributed and principal mechanisms of NPs toxicity is the induction of oxidative stress in microbial cells. Metallic NPs can induce the generation of reactive oxygen species (ROS) inside cells, including superoxide radical anion ( $O_2^{\bullet-}$ ), hydroxyl radical ( $\bullet OH$ ), hydroperoxyl radical ( $HO_2^{\bullet-}$ ), hydrogen peroxide ( $H_2O_2$ ), singlet oxygen ( $^1O_2$ ) and organic radicals such as peroxy radical ( $ROO^{\bullet}$ ) or alkoxy ( $RO^{\bullet}$ ) [9–11]. However, it is worth emphasising that various ROS are produced naturally in biological systems as part of redox cycling, for example,  $O_2^{\bullet-}$  and  $H_2O_2$  can be produced by the accidental release of electrons in the respiratory chain and auto-oxidation of dehydrogenases [12,13]. Similarly,  $^1O_2$  can be produced as a by-product in processes like lipid peroxidation, decomposition of organic peroxides or oxidation of  $O_2$  [14,15]. However, exposure of microorganisms to inorganic NPs can result in the greater formation of ROS, causing severe changes in their concentrations, engendering a synergistic unfavourable effect. It has been documented that metallic NPs as redox labile compounds can produce ROS, especially after prior irradiation, due to the formation of holes ( $h^+$ ) and electrons ( $e^-$ ) in conducting and valence bands, with strong redox properties [15–17]. NPs can also generate ROS without prior illumination due to oxidation-redox reactions on the surface of NPs, nanoparticle-bacterial cells and nanoparticle-oxidant/radical interactions [11,18]. Furthermore, the presence of transition metals on the surface of NPs provides additional generation of ROS through the catalysis of Fenton, Fenton-like and Haber-Weiss reactions [11,18–20].

ROS-induced stress in microbial cells can damage cellular structures and outer layers, including oxidative degradation of proteins and lipids [2,17]. Interestingly, each type of ROS is characterised by its specific reactivity. For example, induction of  $^1O_2$  can impair membrane integrity through the oxidation of cell membrane components and initiation of lipid peroxidation [16,18]. Contrarily,  $O_2^{\bullet-}$  may not be a strong oxidant; however, it is a substrate for  $H_2O_2$ ,  $\bullet OH$  and  $^1O_2$  formation [10,13,18]. The high redox potential of  $\bullet OH$  makes it a very strong oxidant, which is nonselective as it can react with any macromolecules present in cells, including proteins, nucleic acids, carbohydrates, and lipids [13,18]. It has been stated previously that  $\bullet OH$ ,  $O_2^{\bullet-}$  and  $^1O_2$  play a significant role in inducing oxidative stress in bacterial cells [16,18]. Although  $H_2O_2$  is a long-lasting ROS, it is a very stable molecule, which contributes to the generation of oxidative stress through the synthesis of  $\bullet OH$  [13]. Microbial defence system against the harmful effect of NPs and ROS consists of catalase (CAT), peroxidase (PER) and superoxide dismutase (SOD) together with non-catalytic antioxidant reduced glutathione (GSH) [10,21–23]. CAT, PER and GSH neutralise  $H_2O_2$ , while SOD reduces  $O_2^{\bullet-}$  levels [10,12]. However, an excess of ROS in bacterial cells can lead to inactivation and permanent damage of proteins, including antioxidants, through their interactions with amino acid residues [12,22]. Therefore, it is important to monitor whether the microbial defence system can withstand cellular changes in response to NPs and ROS.

To date, comprehensive knowledge regarding the impact of NPs on the antioxidant defence system in bacteria has been obtained through many studies. Despite this, there is still limited information about the particular forms of radicals induced by redox labile Ag-NPs, Cu-NPs, ZnO-NPs and  $TiO_2$ -NPs in bacterial cells. The research has mainly



focused on oxidative stress and ROS generation by selected NPs after prior irradiation and has only considered the selected effects of NPs on antioxidant enzymes activity and cellular damages. Thus, it is crucial to also measure the cycling of ROS in bacterial cells without light-assisted conditions as well as to determine the activity of as many components as possible along with specific oxidation biomarkers. Therefore, this study aimed to create detailed oxidative stress profiles for *Escherichia coli*, *Bacillus cereus* and *Staphylococcus epidermidis* under Ag-NPs, Cu-NPs, ZnO-NPs and TiO<sub>2</sub>-NPs exposure. Particular research tasks included: (1) determining the toxicological parameters of NPs towards tested bacteria, (2) measuring the general and singular ROS concentration, (3) evaluating the activity of antioxidant enzymes and dehydrogenases, (4) measuring the reduced glutathione concentration, (5) assessing the protein and lipid peroxidation level and (6) establishing the relationships between measured parameters.

## 2. Results

### 2.1. Effects of the Tested NPs on Bacteria Viability

The determined minimum bactericidal concentration (MBC), minimum inhibitory concentration (MIC), and the half-maximal inhibitory concentration (IC<sub>50</sub>) indicated varied sensitivity of all tested strains to the presence of individual NPs (Table 1). For example, based on MIC and MBC values, *E. coli* was most sensitive to pure metal NPs than metal oxide materials. By comparison, *B. cereus* exhibited a different sensitivity to the tested NPs. The NPs with a similar bactericidal effect and the highest toxicity against this strain were Cu-NPs and TiO<sub>2</sub>-NPs, while Ag-NPs and ZnO-NPs had the lowest impact on cell viability. Subsequently, *S. epidermidis* was characterised by a similar trend in the sensitivity to metal NPs and metal oxide NPs as *E. coli*; however, based on IC<sub>50</sub>, it was more resistant to Ag-NPs, TiO<sub>2</sub>-NPs and ZnO-NPs. Comparing results obtained for gram-positive strains, it can be concluded that they reacted similarly to Ag-NPs, Cu-NPs and ZnO-NPs; however, TiO<sub>2</sub>-NPs aroused significant interest, with the IC<sub>50</sub> being 14-times lower for *B. cereus* than *S. epidermidis*. Conclusively, the decreasing bactericidal properties of the tested NPs based on MIC values towards *E. coli* and *B. cereus* cells could be ordered as follows: TiO<sub>2</sub>-NPs < ZnO-NPs < Cu-NPs < Ag-NPs, and Ag-NPs < ZnO-NPs < TiO<sub>2</sub>-NPs < Cu-NPs, respectively. Unlike, the following order: TiO<sub>2</sub>-NPs < ZnO-NPs < Ag-NPs < Cu-NPs which presents the antibacterial effect of NPs towards *S. epidermidis*.

**Table 1.** The values of MBC, MIC and IC<sub>50</sub> (mg L<sup>-1</sup>) of NPs against *E. coli*, *B. cereus* and *S. epidermidis*.

Type of NPs	MBC	MIC	IC <sub>50</sub>
<i>Escherichia coli</i> ATCC 25922			
Ag-NPs	15	10	7.84
Cu-NPs	250	200	180.80
ZnO-NPs	500	425	176.10
TiO <sub>2</sub> -NPs	750	500	43.40
<i>Bacillus cereus</i> ATCC 11778			
Ag-NPs	1000	850	480.10
Cu-NPs	150	75	52.15
ZnO-NPs	1000	800	319.10
TiO <sub>2</sub> -NPs	150	100	50.30
<i>Staphylococcus epidermidis</i> ATCC 12228			
Ag-NPs	600	500	442.20
Cu-NPs	300	200	112.00
ZnO-NPs	800	750	201.70
TiO <sub>2</sub> -NPs	>1200	1050	703.40

## 2.2. Generation of ROS in Bacterial Cells by NPs

One of the studied ROS was  $H_2O_2$ , which is a common by-product of cell metabolic activity. It was found that the addition of Cu-NPs, ZnO-NPs, and  $TiO_2$ -NPs into *E. coli* culture caused a negligible increase in the level of  $H_2O_2$  ( $p > 0.05$ ) (Figure 1A). In turn, the treatment of *B. cereus* with Cu-NPs and ZnO-NPs generated a considerable ( $p < 0.05$ ) amount of  $H_2O_2$ , greater by about 11- and 2.7-fold compared to its content in the control sample, respectively. By comparison, Ag-NPs, Cu-NPs, and  $TiO_2$ -NPs caused significant, for  $p < 0.05$ , changes in the level of  $H_2O_2$  in *S. epidermidis* culture. The highest increase in this ROS concentration, about 5.5- and 3.2-fold, was recorded for Cu-NPs and  $TiO_2$ -NPs, respectively. Overall, the treatment of bacterial cells with NPs had a more stimulating effect on the generation of  $H_2O_2$  in both *B. cereus* and *S. epidermidis* than in *E. coli*.

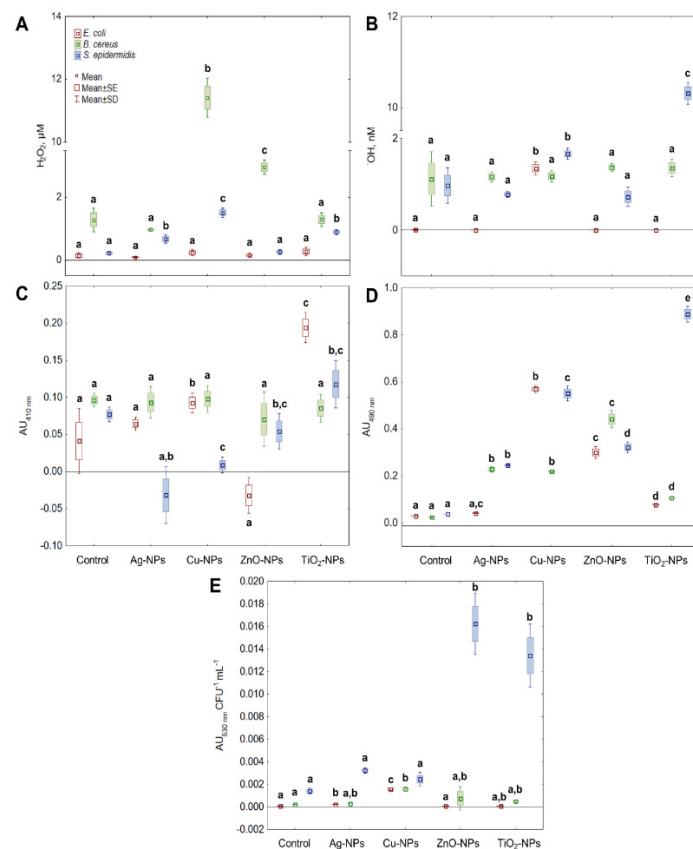


**Figure 1.** The levels of  $H_2O_2$  (A),  $\bullet OH$  (B),  $^1O_2$  (C),  $O_2^{\bullet -}$  (D) and total ROS concentration (E) in *E. coli*, *B. cereus* and *S. epidermidis* exposed to NPs at an  $IC_{50}$  value (mean  $\pm$  SD/SE;  $n = 3$ ). Means with the same letter(s) are not significant at  $p < 0.05$  within each ROS between the control and NPs-treated samples.

Due to its reactivity,  $\bullet OH$  radical is considered one of the most lethal types of ROS. It is responsible for most of the damage during oxidative stress, so it was crucial to determine its level in the cells treated with NPs. It was established that the exposure of *E. coli* to Cu-NPs resulted in a vast increase in  $\bullet OH$  level compared to the control sample (Figure 1B). However, Ag-NPs, ZnO-NPs and  $TiO_2$ -NPs did not induce substantial changes in the level of  $\bullet OH$  in these bacteria. By comparison, results obtained for *B. cereus* showed no significant differences in  $\bullet OH$  concentration between the samples treated with Ag-NPs, Cu-NPs, ZnO-NPs and  $TiO_2$ -NPs, and the control sample. In the case of *S. epidermidis* cultures exposed to Ag-NPs and ZnO-NPs, no increase in  $\bullet OH$  levels was documented. Despite that, substantial intensification of  $\bullet OH$  generation was found in *S. epidermidis* cultures treated with Cu-NPs and  $TiO_2$ -NPs, resulting in a 2.2- and 13.7-fold increase in its

content compared to the control sample. To conclude, the generation of  $\bullet\text{OH}$  was more affected by NPs in *S. epidermidis* cells than in *E. coli* and *B. cereus*.

Although  $^1\text{O}_2$  is one of the commonly studied ROS during photooxidative stress studies, it was important to distinguish whether  $^1\text{O}_2$  can be generated as a result of NPs action and modifications in redox reactions without prior irradiation. The results obtained for *E. coli* showed that only ZnO-NPs generated  $^1\text{O}_2$  in bacterial cells, causing about a 6-fold increase in its content compared to unstressed cells. Whilst treatment of *B. cereus* cells with Ag-NPs, Cu-NPs, ZnO-NPs and  $\text{TiO}_2$ -NPs did not influence any significant ( $p > 0.05$ ) alternations in  $^1\text{O}_2$  concentration. By contrast, the application of Ag-NPs and Cu-NPs to *S. epidermidis* cultures resulted in a greater, about 13.5- and 4.15-fold generation of  $^1\text{O}_2$  compared to the control sample, respectively (Figure 1C).

In parallel experiments, the ability of NPs to generate the  $\text{O}_2^{\bullet-}$  was evaluated (Figure 1D). The  $\text{O}_2^{\bullet-}$  is one of the crucial types of ROS to be widely examined because it is the first product of single-electron reduction of molecular oxygen and the substrate for SOD reaction, consequently increasing the content of  $\text{H}_2\text{O}_2$ . The obtained results revealed that Cu-NPs and ZnO-NPs had the greatest impact on the  $\text{O}_2^{\bullet-}$  production by *E. coli* compared to the non-treated cells. Interestingly, treatment of *E. coli* cells with Ag-NPs did not have a stimulating effect on the generation of  $\text{O}_2^{\bullet-}$ . Exposure of *B. cereus* to ZnO-NPs resulted in an 18.4-fold higher level of  $\text{O}_2^{\bullet-}$  in the cells compared to the control sample. Intriguingly, both Ag-NPs and Cu-NPs resulted in a similar generation level of  $\text{O}_2^{\bullet-}$  in *B. cereus*. The obtained data for *S. epidermidis* showed that all tested NPs had a stimulating effect on the generation of  $\text{O}_2^{\bullet-}$ , with the greatest ability shown by Cu-NPs and  $\text{TiO}_2$ -NPs (14.5- and 23.4-fold increase, respectively). In general, the increase in  $\text{O}_2^{\bullet-}$  level in *S. epidermidis* was affected by the NPs in the following order Ag-NPs < ZnO-NPs < Cu-NPs <  $\text{TiO}_2$ -NPs. In conclusion, the tested NPs generated the highest amount of  $\text{O}_2^{\bullet-}$  in *S. epidermidis*, while this process was less intense in *E. coli* and *B. cereus*. Additionally, based on the total concentration of ROS in bacterial cells (Figure 1E), it can be concluded that Cu-NPs generated the major quantity of different types of ROS in *E. coli* and *B. cereus* cells. In turn, the metal oxides  $\text{TiO}_2$ -NPs and ZnO-NPs had the greatest impact on ROS production in *S. epidermidis* cells (9.5- and 11.5-fold increase, respectively).

### 2.3. Activity of Antioxidant Enzymes and Dehydrogenases under NPs Stress

The ability of NPs to generate various types of ROS leads to oxidative stress in microbial cells and creates potential hazards for the survival of microorganisms. To assess the performance of the catalytic antioxidant defence system operating in NPs-treated bacterial cells, CAT, PER and SOD activities were measured. Additionally, the activity of DEH belonging to oxidoreductases was calculated to define the effect of NPs on microbial respiratory activity and their potential co-dependence in ROS generation. The obtained findings showed that all tested NPs caused an increase in the activity of CAT in *E. coli*, *B. cereus* and *S. epidermidis* (Figure 2A). Concerning *E. coli*, Ag-NPs and  $\text{TiO}_2$ -NPs manifested a weak stimulating effect on CAT activity (about a 1.5-fold increase), while Cu-NPs and ZnO-NPs showed a stronger stimulating effect (over 2-fold increase). Similarly, Cu-NPs and ZnO-NPs stimulated CAT activity in *B. cereus*, causing a 6–7 fold increase compared to CAT activity in the untreated cells. Conversely, the greatest increase in CAT activity (about 4.8-fold) in *S. epidermidis* was recorded in the presence of  $\text{TiO}_2$ -NPs. Interestingly, the exposure of *S. epidermidis* to Cu-NPs resulted in a noticeable decrease (about 1.53-fold) in the activity of CAT. Conclusively, CAT of *E. coli* and *B. cereus* was more sensitive to stress caused by tested NPs than CAT of *S. epidermidis*; however, the last bacterium was most sensitive to  $\text{TiO}_2$ -NPs.

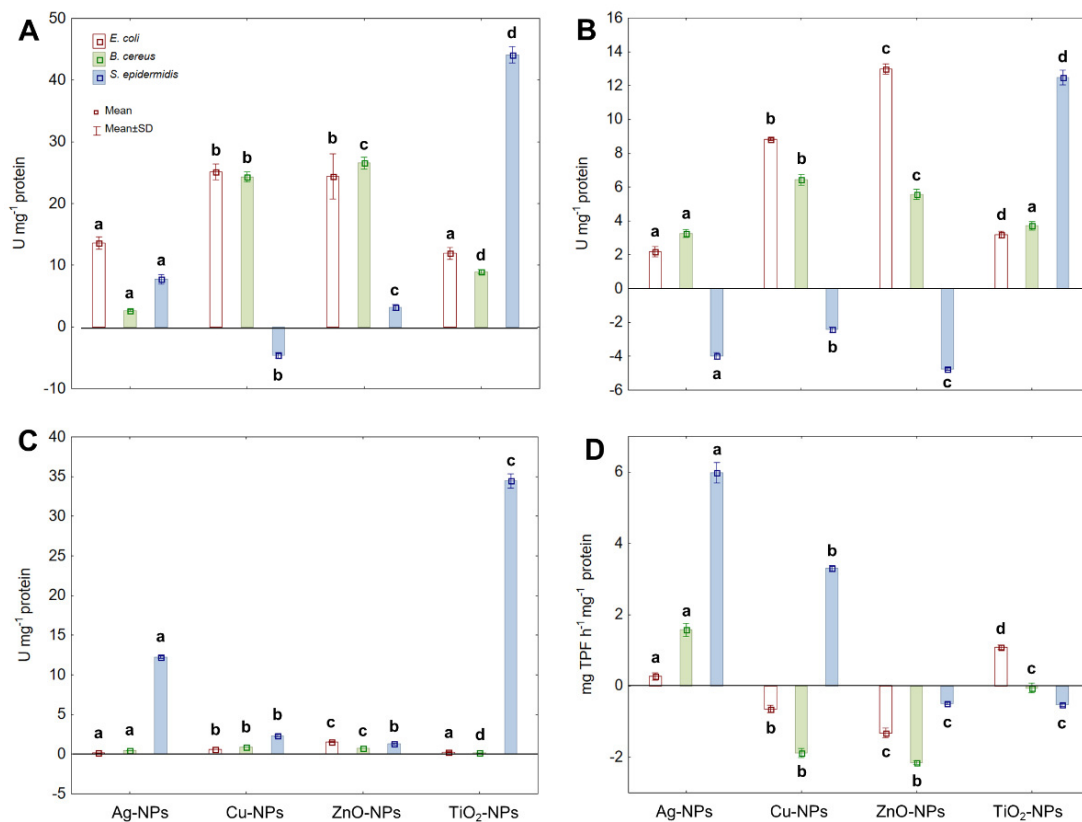


**Figure 2.** The activity of CAT (A), PER (B), SOD (C) and DEH (D) in *E. coli*, *B. cereus* and *S. epidermidis* exposed to NPs at an IC<sub>50</sub> value (mean ± SD; *n* = 3). Means with the same letter(s) are not significant at *p* < 0.05 within each enzyme between the control and NPs-treated cells.

Parallely, the activity of PER in tested bacteria under NPs-stress conditions was analysed (Figure 2B). During reactions catalysed by PER, H<sub>2</sub>O<sub>2</sub> is reduced to water contributing to its overall concentration in a cell. The addition of Cu-NPs and ZnO-NPs to *E. coli* cultures substantially enhanced PER activity (2.2- and 2.8-fold, respectively), whereas Ag-NPs and TiO<sub>2</sub>-NPs had a smaller impact on its activity (about 1.4-fold increase). The treatment of *B. cereus* with Cu-NPs and ZnO-NPs also resulted in a noticeable increase in PER activity (about 7-fold) in comparison with its activity in the control samples. Conversely, exposure of *S. epidermidis* to Ag-NPs, Cu-NPs and ZnO-NP caused a 4.3-, 1.8- and 12.9-fold decrease in PER activity, respectively. The only type of NPs that acted in the opposite way to PER activity were TiO<sub>2</sub>-NPs causing a 3.8-fold increase compared to the untreated cells. It is noteworthy that PER functioning, however different in *E. coli* and *S. epidermidis* strains, was more sensitive to NPs-stress than PER of *B. cereus*, which in turn proved to be more resistant to NPs action.

The following assayed enzyme protecting microbial cells from oxidative stress was SOD, which catalyses the dismutation of O<sub>2</sub><sup>•-</sup> to O<sub>2</sub> and H<sub>2</sub>O<sub>2</sub> further used as a substrate in catalytic protection of bacterial cells against ROS. Although exposure of tested bacteria to NPs significantly affected SOD activity, it differed significantly between individual strains (Figure 2C). Detailed analysis of data showed that the highest increase in SOD activity in *E. coli* (1.6- and 2.6-fold) was recorded in the presence of Cu-NPs and ZnO-NPs, respectively. The same NPs in the culture of *B. cereus* also had the most stimulating effect on the activity of SOD, resulting in about a 1.5-fold increase in its activity. By comparison, *S. epidermidis* exhibited the highest SOD activity under Ag-NPs and TiO<sub>2</sub>-NPs treatments, achieving a 2.7- and 5.7-fold increase in its activity compared to the control cells.

Regarding DEH, its activity was expressed in a strain-specific manner under individual NPs treatment (Figure 2D). In *E. coli*, the displayed DEH activity was about 1-fold enhanced

by Ag-NPs and TiO<sub>2</sub>-NPs; however, Cu-NPs and ZnO-NPs led to a significant decrease (1.3-fold) in its activity compared to the untreated cells. In turn, the DEH activity in *B. cereus* only increased after exposure to Ag-NPs, whereas Cu-NPs, ZnO-NPs and TiO<sub>2</sub>-NPs reduced its activity by 2.8-, 3.2- and 1.4-fold, respectively. By comparison, Ag-NPs and Cu-NPs strongly stimulated DEH activity in *S. epidermidis*, resulting in a 6.5- and 4-fold increase, respectively. Contrary, TiO<sub>2</sub>-NPs and ZnO-NPs caused a significant decrease (2.4-fold) in DEH activity in comparison with the control cells. The presented findings indicated that DEH was more affected by NPs in *B. cereus* and *S. epidermidis* than in *E. coli*.

#### 2.4. Non-Catalytic Antioxidant Defence System (GSH)

Reduced glutathione (GSH) acts as a hydrogen donor in the detoxification of H<sub>2</sub>O<sub>2</sub>; therefore, it plays an important role in a complex bacterial antioxidant defence system regulating the redox cycles. As Figure 3 indicates, the greatest reduction in the GSH level in *E. coli* was established under ZnO-NPs and Ag-NPs exposure, causing about a 1.5-fold decrease in its concentration compared to the control sample. Interestingly, no significant differences were found in the level of GSH in *B. cereus* cultured with individual NPs. Comparable to the reduction in GSH concentration in *E. coli* was the decrease (approximately 3-fold) in GSH in *S. epidermidis* treated with ZnO-NPs. Overall, ZnO-NPs were the only shared NPs for *E. coli* and *S. epidermidis*, inducing a significant reduction in their GSH levels.

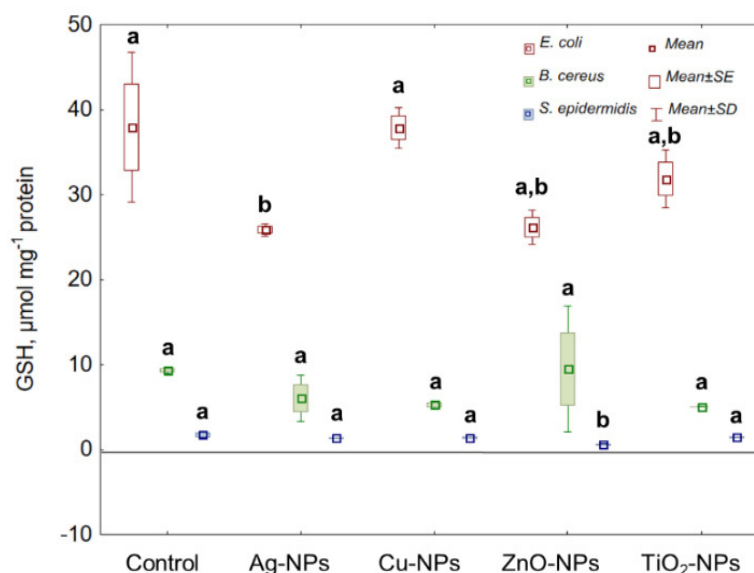


**Figure 3.** The GSH concentration in *E. coli*, *B. cereus* and *S. epidermidis* exposed to NPs at an IC<sub>50</sub> value (mean ± SD/SE; n = 3). Means with the same letter(s) are not significant at p < 0.05 between the control and NPs-treated cells.

#### 2.5. Changes in the Content of Carbonyl and Amine Groups in Proteins

Interactions of NPs and ROS with proteins can cause various structural changes resulting from their oxidation and causing the disturbance of their function. One of the consequences of protein oxidation is the increase in the level of protein carbonyls (>C=O); therefore, it is recognized as a reliable biomarker of cellular changes induced by oxidative stress. As shown in Figure 4A, the exposure of *E. coli*, *B. cereus* and *S. epidermidis* to all tested NPs increased >C=O content. In *E. coli*, the greatest and a comparable increase in >C=O by 12.43%, 11.79% and 10.29% was recorded after treatment with Ag-NPs, ZnO-NPs and TiO<sub>2</sub>-NPs, respectively. By comparison, the highest >C=O content of about 31% in *B. cereus* was confirmed under TiO<sub>2</sub>-NPs and ZnO-NPs exposure. Similar findings were obtained for *S. epidermidis* exhibiting a significant increase in >C=O by 25.53% and 26.22% after treatment with TiO<sub>2</sub>-NPs and ZnO-NPs, respectively. In general, protein oxidation was a more predominant trait of NPs in *B. cereus* and *S. epidermidis* than in *E. coli*.

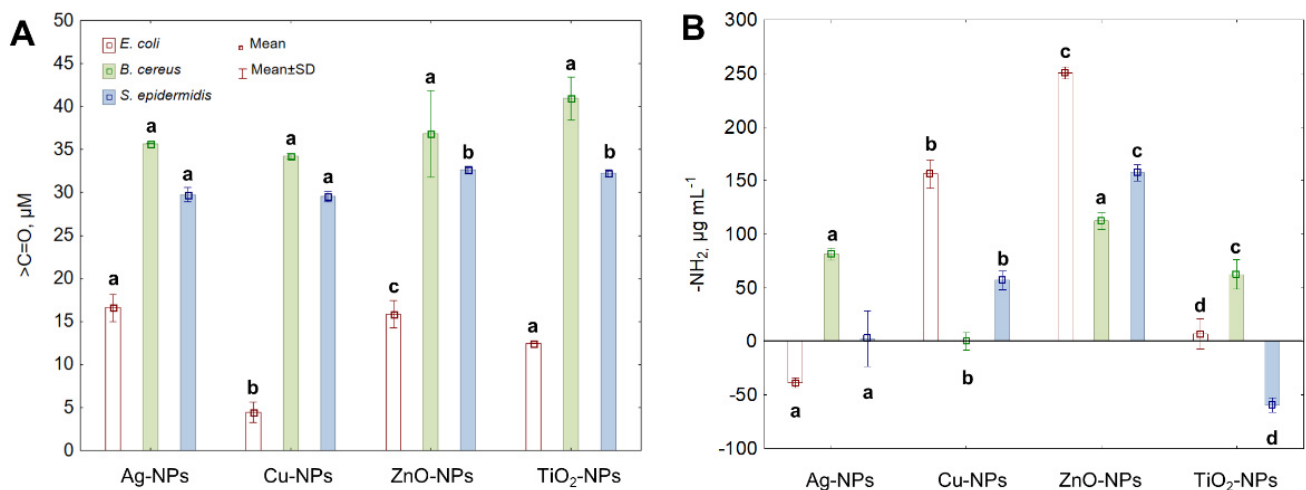


**Figure 4.** The content of >C=O (A) and -NH<sub>2</sub> (B) in *E. coli*, *B. cereus* and *S. epidermidis* cells exposed to NPs at an IC<sub>50</sub> value (mean ± SD/SE; *n* = 3). Means with the same letter(s) are not significant at *p* < 0.05 between the control and NPs-treated cells.

Protein oxidation can lead to irreversible changes in amine groups (-NH<sub>2</sub>), accompanied by protein aggregation and degradation. For this reason, it was essential also to distinguish the changes in -NH<sub>2</sub> content in bacterial cells further to explore the oxidation effect of NPs and ROS. The highest increase in -NH<sub>2</sub> by 45.08% in *E. coli* was detected in the presence of ZnO-NPs. Intriguingly, Ag-NPs caused a reduction in -NH<sub>2</sub> content in *E. coli* by 5.42%. Correspondingly, the greatest increase in -NH<sub>2</sub> by 18.52% and 23.03% in *B. cereus* and *S. epidermidis* was recorded in the presence of ZnO-NPs. Rivetingly, a decrease in -NH<sub>2</sub> concentration by 8.39% in *S. epidermidis* compared to the control cells was detected after treatment with TiO<sub>2</sub>-NPs (Figure 4B).

#### 2.6. Lipid Peroxidation in Bacterial Cells Caused by NPs

Lipid peroxidation (LPO) is one of the markers used in the analysis of oxidative stress. Therefore, this study seems necessary to distinguish the synergistic or antagonistic action between tested NPs and generated ROS. Treatment of *E. coli* cells with Ag-NPs, Cu-NPs and TiO<sub>2</sub>-NPs resulted in a significant increase in LPO level, while in the presence of ZnO-NPs the decrease in its content was observed. The highest and the lowest LPO values of 43.23% and 33.8% were obtained for the cells exposed to TiO<sub>2</sub>-NPs and ZnO-NPs, respectively. By comparison, the highest increase in the LPO values for *B. cereus* was documented at 160.95% for Cu-NPs treated cells compared to the LPO content in the untreated cells. Simultaneously, a 53.7% decrease in LPO was caused by ZnO-NPs in these cells. The obtained data also revealed the increase in LPO in *S. epidermidis* in the presence of Ag-NPs, Cu-NPs and TiO<sub>2</sub>-NPs and the decrease in the presence of ZnO-NPs. The exposure of *S. epidermidis* to Cu-NPs resulted in the highest increase in LPO values (194.49%), whereas the highest decrease (16.43%) occurred in the presence of ZnO-NPs (Figure 5).

#### 2.7. Exploratory Data Analyses

PCA and cluster analysis were carried out to analyse the variability and relationship between obtained findings and performed experiments. The results from PCA, including all NPs treatments and toxicological studies performed for *E. coli*, *B. cereus* and *S. epidermidis* explained 83.40%, 78.55% and 77.88% variability of the data, respectively (Figure 6). Coordination biplot of experiments with *E. coli* demonstrated a strong negative correlation between CAT, PER and SOD activity and >C=O content (Figure 6A). Interestingly, a negative correlation between PER and DEH was established. The O<sub>2</sub><sup>•-</sup> was most correlated with PC1; however, based on PC2, a strong negative correlation was established for GSH and LPO, and a positive correlation for -NH<sub>2</sub>. Additionally, PC1 from the correlation biplot

projection of *E. coli* distinguished three separate clusters of treated samples (Figure 6B). Based on PCA analysis, the results obtained for *E. coli* treated with Ag-NPs and TiO<sub>2</sub>-NPs were similar to the untreated samples forming one plot. In turn, coordination biplot for *B. cereus* revealed a strong negative correlation of SOD and PER, with other oxidative stress parameters being more scattered (Figure 6C). It is worth pointing out that a strong negative correlation was confirmed between ROS and GSH as well as DEH and CAT. Furthermore, based on the performed experiments, two clusters of treated samples of *B. cereus* along PC1 were distinguished: Ag-NPs with TiO<sub>2</sub>-NPs and Cu-NPs with ZnO-NPs, and an additional separate cluster consisting of the control sample (Figure 6D). Based on the PCA analysis for *S. epidermidis*, the most visible positive correlation with PC1 was observed for all parameters except for DEH, H<sub>2</sub>O<sub>2</sub>, GSH, -NH<sub>2</sub>, >C=O and ROS, which were strongly correlated with PC2. It is also worth emphasising the strong negative correlation between DEH and ROS (Figure 6E). Of all NPs tested, only TiO<sub>2</sub>-NPs were distinguished along the PC1 axis (Figure 6F).

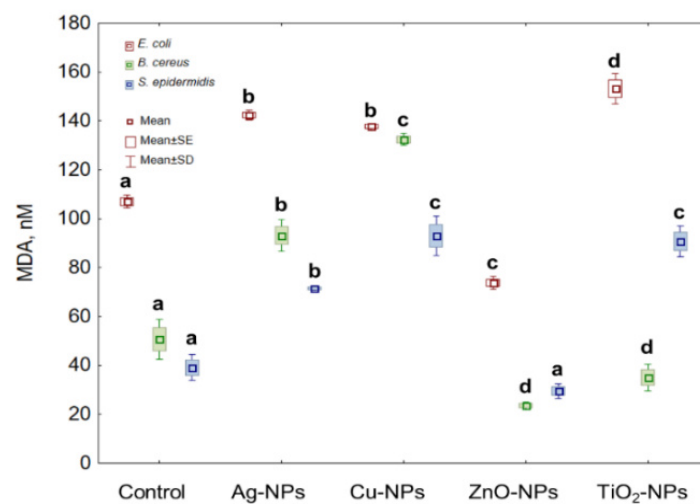


**Figure 5.** The LPO level in *E. coli*, *B. cereus* and *S. epidermidis* cells exposed to NPs at an IC<sub>50</sub> value (mean  $\pm$  SD/SE;  $n = 3$ ). Means with the same letter(s) are not significant at  $p < 0.05$  between the control and NPs-treated cells.

The cluster analysis showed characteristic relationships between particularly treated samples and conducted analysis (Figure 7). The dendrogram projection obtained for the *E. coli* strain revealed that the most differentiating analyses included measurement of LPO, DEH, GSH and protein oxidation expressed as -NH<sub>2</sub> group level (Figure 7A). By comparison, other performed analyses, formed hierarchical clusters separating into two thematically similar clusters, including antioxidant enzymes and general and specific ROS levels. It is worth underlying that according to the acquired dendrogram, the most characteristic and discriminating NPs were Cu-NPs and ZnO-NPs. However, the most similar set of results were confirmed for Ag-NPs and TiO<sub>2</sub>-NPs. The dendrogram designated for *B. cereus* revealed two separate clusters, the first consisting of control samples and the second of specific NPs treatments (Figure 7B). It is worth pointing out that the most distinguished toxicological analyses with *B. cereus* included GSH, DEH and <sup>1</sup>O<sub>2</sub>. Comparing, ROS, GSH, DEH and protein oxidation (-NH<sub>2</sub> and >C=O levels) were the most differentiating analyses for *S. epidermidis* (Figure 7C). Dendrogram made for *S. epidermidis* demonstrated a strong relationship between Ag-NPs and Cu-NPs treated samples; however, exposure of these bacteria to ZnO-NPs and TiO<sub>2</sub>-NPs had the most divergent effect on the collected results.

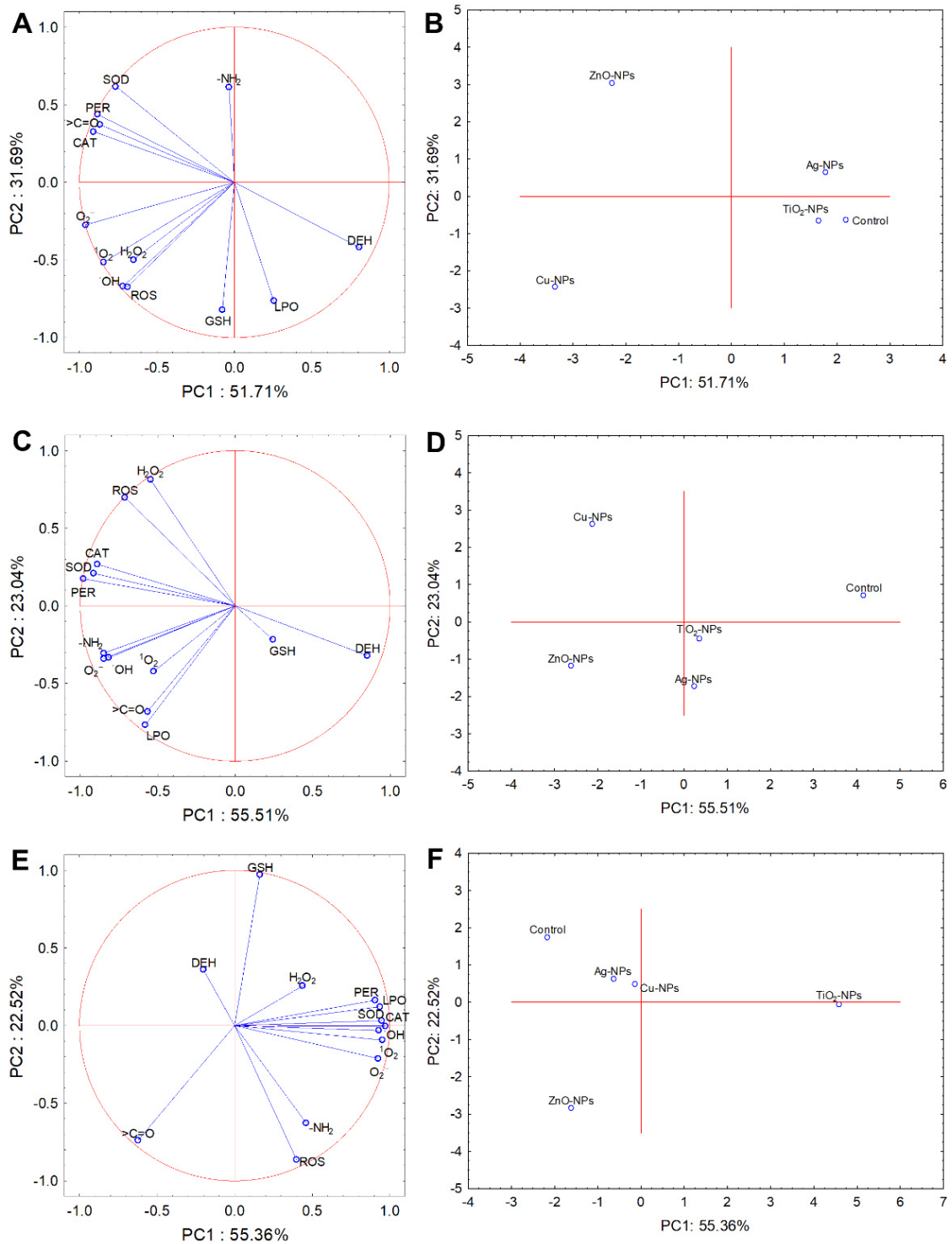


**Figure 6.** Projection of the individual plot and PCA analysis of free radicals ( $H_2O_2$ ,  $\cdot OH$ ,  $^1O_2$ ,  $O_2^{\cdot -}$ ), ROS, GSH, LPO, content of  $>C=O$  and  $-NH_2$ , and enzymes activity (CAT, PER, SOD, DEH) along PC1 and PC2 for the control and NPs-treated cells of *E. coli* (A,B), *B. cereus* (C,D) and *S. epidermidis* (E,F).



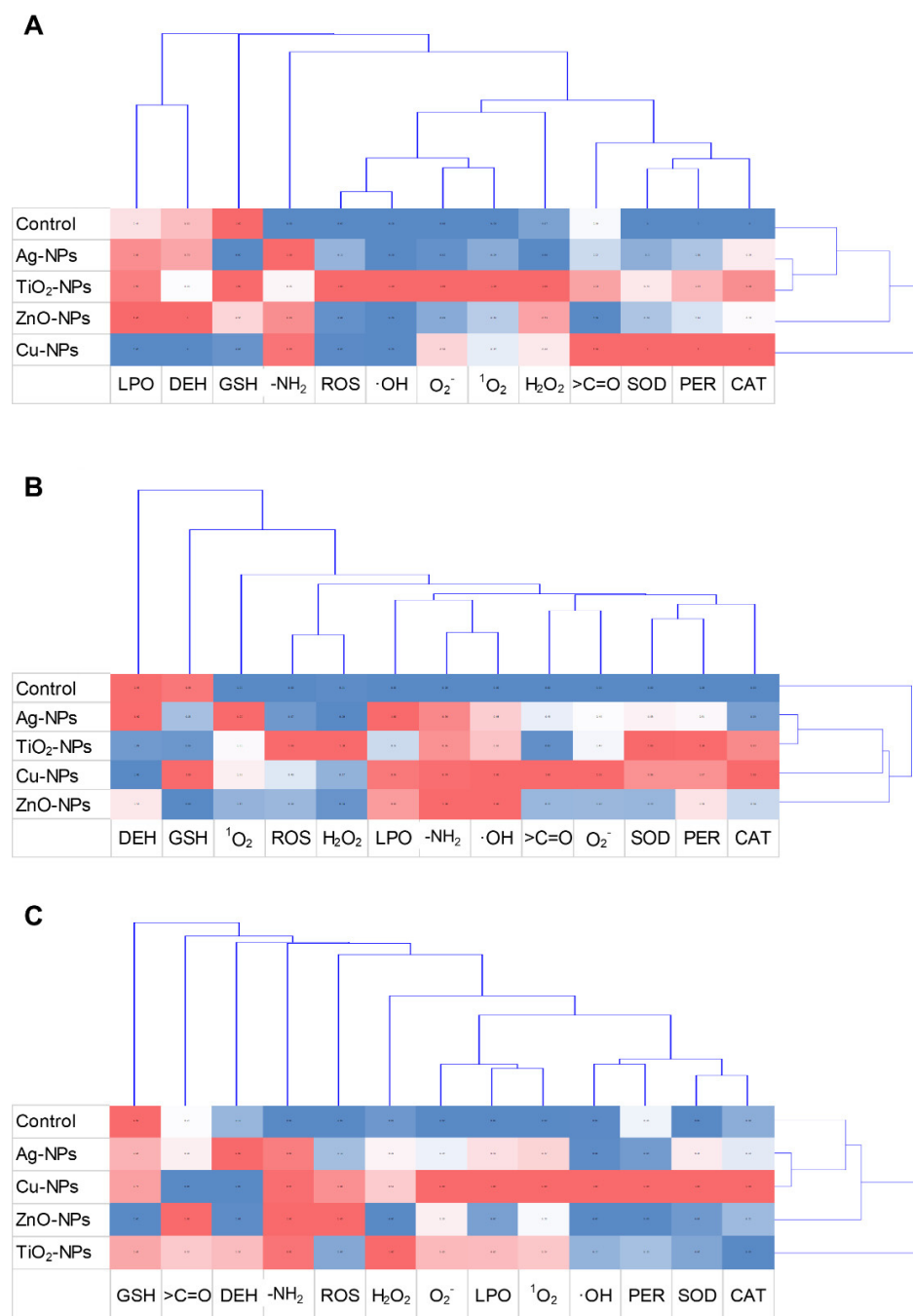


**Figure 7.** Cluster disposal of free radicals ( $\text{H}_2\text{O}_2$ ,  $\cdot\text{OH}$ ,  $^1\text{O}_2$ ,  $\text{O}_2^{\cdot-}$ ), total ROS, GSH, LPO, the content of  $>\text{C}=\text{O}$  and  $-\text{NH}_2$ , and CAT, PER, SOD, DEH activities in the control and NPs-treated cells of *E. coli* (A), *B. cereus* (B) and *S. epidermidis* (C).

### 3. Discussion

Incorporating nano-derived applications into daily use creates many solutions for the utility of different products and technological processes. Although the mathematical models based on predicted life cycles of various NPs estimate their possible unintentional targets sites and endpoints, there is still limited knowledge of how such materials will act in realistic conditions. One of the topics of the currently ongoing scientific debate on the toxicity of NPs is their potentially destructive effect on the functioning of microorganisms. Despite the huge amount of scientific data in this field, there is still controversy about the impact of NPs on microorganisms, especially these newly designed engineered NPs [7,8,24,25].

Among the several proposed mechanisms of action of metallic NPs on bacterial cells is the induction of oxidative stress by generating ROS [8,9,24,26]. Although this phenomenon has been reported in many publications, information on the individual radical forms induced by metal NPs and their combined action in disrupting cellular redox cycles remains fragmentary. Therefore, the novelty of this study is a scientific description of detailed oxidation profiles of *E. coli*, *B. cereus* and *S. epidermidis*, taking into account the accompanying pathological changes in the presence of redox unstable Ag-NPs, Cu-NPs, ZnO-NPs and TiO<sub>2</sub>-NPs.

To ensure the standardisation of nanotoxicological studies, it is important to investigate the potential toxicity of NPs by determining toxicological parameters. The conducted research confirmed the antimicrobial effect of all NPs on the tested bacterial strains, but to a different extent for individual strains. Overall, NPs were most potent against *E. coli* than *B. cereus* and *S. epidermidis*. This can be attributed to the difference in the structure of the outer layers of gram-negative and gram-positive bacteria. The cell wall of gram-negative bacteria has a thin layer of peptidoglycan, which makes it more permeable to macromolecules. Moreover, gram-negative bacteria are characterised by a higher net negative charge on the cell surface than gram-positive bacteria, which results in stronger electrostatic interactions with positively charged NPs and, therefore, the greater susceptibility of these microorganisms to the antimicrobial effect of NPs [9,24,27,28]. By comparison, *B. cereus* may be more resistant to NPs than *E. coli*, not only because of the thicker cell wall but also due to the formation of endospores that portray additional outer layers, thus providing additional protection against the negative effects of NPs [28,29]. Similar results were obtained by Ahmad et al. [28], who confirmed greater toxicity of TiO<sub>2</sub>-NPs towards *E. coli* than *B. subtilis* due to the early induction of cell death as opposed to the reduction of bacterial viability over time. Interestingly, *B. cereus* and *S. epidermidis* showed a similar response to the presence of tested NPs except for TiO<sub>2</sub>-NPs. This could be explained by the increased interaction of TiO<sub>2</sub> with the functional groups on the surface of *B. cereus* cells. It can also result from the ability of *S. epidermidis* to form a biofilm structure in the presence of TiO<sub>2</sub>-NPs and greater expression of cell wall anchored surface proteins [30]. Generally, *E. coli*, *B. cereus* and *S. epidermidis* were most susceptible to single metal NPs: Ag-NPs and Cu-NPs. This may be attributed to the faster release of heavy metal ions from their surface compared to metal oxide NPs. Furthermore, it is worth pointing out that the release of ions from NPs is dependent on their composition, physicochemical properties, culture medium and treated microorganisms; hence, there is no general rule for the dissolution of ions from different types of NPs [9,31–33]. Moreover, due to similar electron configuration and chemistry, Ag (I) and Cu (I) may exhibit similar antimicrobial properties; however, Cu plays an essential role in the physiological processes of microbial cells [9,34]. Therefore, depending on the concentration of cations released from the surface of NPs, microorganisms can or not withstand the stress caused by those ions through the activation of protective/resistance systems [9].

Treatment of *E. coli*, *B. cereus* and *S. epidermidis* with Ag-NPs, Cu-NPs, ZnO-NPs and TiO<sub>2</sub>-NPs induced ROS production in the cells. However, the total ROS concentration in *E. coli* and *B. cereus* was mostly influenced by Cu-NPs, while in *S. epidermidis* by ZnO-NPs and TiO<sub>2</sub>-NPs, which also influenced the production of particular types of ROS. The greatest contribution to the total ROS concentration in *E. coli* cells had H<sub>2</sub>O<sub>2</sub> and •OH, which levels increased in the presence of Cu-NPs. Similarly, there was a significant increase in the level of <sup>1</sup>O<sub>2</sub> in these cells after treatment with ZnO-NPs. Contrary, O<sub>2</sub><sup>•−</sup> and H<sub>2</sub>O<sub>2</sub> had the greatest effect on overall ROS concentration in *B. cereus* exposed to ZnO-NPs and Cu-NPs, respectively. By comparison, all types of individual ROS slightly contributed to the general concentration of ROS in *S. epidermidis*. The positive correlation between the H<sub>2</sub>O<sub>2</sub> and •OH generation in *E. coli* can be related to the co-dependent existence of two types of ROS in bacterial cells. This is because hydrogen peroxide, a common-by product of the metabolic activity, undergoes Fenton and Fenton-like reactions generating •OH, making its concentration in biological systems dependent on H<sub>2</sub>O<sub>2</sub> [12,13,35]. Similarly, the level of

H<sub>2</sub>O<sub>2</sub> in cells depends on the production of O<sub>2</sub><sup>•−</sup>; hence, there was a positive correlation between those two types of ROS in *B. cereus* [36]. Additionally, Ag-NPs, Cu-NPs, ZnO-NPs and TiO<sub>2</sub>-NPs can generate •OH in bacterial cells through the release of transition metals that can participate in Fenton and Fenton-like reactions [9,37]. Here, both Cu-NPs and TiO<sub>2</sub>-NPs had the most stimulating effect on ROS formation in bacterial cells. Their smaller size than Ag-NPs and ZnO-NPs may explain the above-mentioned phenomenon. Smaller NPs compared to their larger counterparts are characterised by greater surface area to volume ratio, structural and electronic modifications, which provide more reactive sites and groups on the surfaces of NPs, that could participate in the generation of ROS [9,10]. Furthermore, the induction of ROS generation by Ag-NPs, Cu-NPs, ZnO-NPs and TiO<sub>2</sub>-NPs in bacterial cells could be caused by the suppression of the activity of respiratory enzymes through their interactions with released metal ions, activation of oxidases, and interactions with cellular components [38–40]. It can be concluded that the data presented here and the literature data indicate that ROS generation by NPs is very specific and difficult to predict the effect.

The relationship between ROS generation and the functioning of the antioxidant defence system is only partially presented in the available literature. In this work, ROS generation and oxidative stress induction were confirmed by disrupting enzymatic antioxidant activity. Activities of CAT, PER and SOD in *E. coli* cells were mostly affected by ZnO-NPs and correlated with the lowest overall ROS concentration. By comparison, CAT activity in *B. cereus* was most affected by ZnO-NPs, whereas Cu-NPs were mainly impacted on PER and SOD functioning. Interestingly, the collected results for PER activity in *B. cereus* are related to a high concentration of H<sub>2</sub>O<sub>2</sub> after treatment with Cu-NPs. Activities of antioxidant enzymes in *S. epidermidis* were greatly affected by TiO<sub>2</sub>-NPs and positively correlated with high levels of H<sub>2</sub>O<sub>2</sub> and O<sub>2</sub><sup>•−</sup>. It is worth emphasising that Cu-NPs caused a significant decrease in CAT activity in this bacterium, whilst Ag-NPs, Cu-NPs and ZnO-NPs lowered the activity of PER. The observed reduction in enzyme activity may be associated with the release of ions from NPs and their interactions with bacterial proteins resulting in their suppression or denaturation [9,41,42]. Concluding, the diversified activity of the bacterial antioxidant system indicates different mechanisms of protection and adaptation of *E. coli*, *B. cereus* and *S. epidermidis* cells to stress conditions caused by particular NPs. Knowledge regarding the influence of NPs on antioxidant enzymes is limited to selected nanomaterials and microorganisms. For example, Liao et al. [42] found that exposure of *P. aeruginosa* to Ag-NPs caused an increase in the activity of CAT, PER and SOD, depending on the time and concentration of NPs. In other experiments, Yuan et al. [43] recorded a significant decrease in SOD and CAT activities in *P. aeruginosa* and *S. aureus* treated with Ag-NPs. Comparable results were obtained by Huang et al. [41], who documented an inhibitory effect of Ag-NPs on CAT, PER and SOD activities in *P. chrysosporium*, correlated with oxidative stress caused by high levels of ROS. By comparison, based on the obtained results in this study, *E. coli*, *B. cereus* and *S. epidermidis* had a more efficient response to the oxidative effects of NPs due to their stimulating effect on the activity of antioxidant enzymes.

It has been well documented that the interaction of NPs with bacterial outer layers can disrupt the cell wall and membrane integrity. Furthermore, the production of ROS, including O<sub>2</sub><sup>•−</sup> can cause additional damage through their interaction with functional groups presented on the microbial surfaces as well as their reactivity with chemical bonds in peptidoglycan layers. The damaging effect of both NPs and ROS on bacterial outer layers can lead to a disturbance in respiratory activity and ATP production [9,17,44]. Dehydrogenases play an essential role in microbial metabolic activity, especially in the respiratory metabolism of oxygen and electron cycling, during which trace amounts of different ROS may be produced [45,46]. Here, it was found that Ag-NPs, Cu-NPs, ZnO-NPs and TiO<sub>2</sub>-NPs had a specific nano-effect on DEH functioning. The investigation revealed that Cu-NPs and ZnO-NPs decreased DEH activity in *E. coli*, whilst TiO<sub>2</sub>-NPs increased their activity. In turn, Cu-NPs, ZnO-NPs and TiO<sub>2</sub>-NPs caused a significant decrease in DEH activity in *B. cereus*. In the case of *S. epidermidis*, Ag-NPs and Cu-NPs induced

DEH activity, whereas the remaining tested NPs decreased their activity. Generalising, alterations in the DEH activity in *E. coli*, *B. cereus* and *S. epidermidis* after treatment with NPs indicate damage to the cell outer layers and disturbance in their respiratory activity. Greater sensitivity of DEH to metal-oxide NPs may be attributed to the larger release of metal ions and their enhanced interactions with bacterial surfaces [9,43,47]. Nano-toxicological studies related to DEH functioning concern both their leakage from the microbial cells and their overall activity. Kumar et al. [38] documented a greater DEH release (by 41% and 23%) from *E. coli* exposed to ZnO-NPs and TiO<sub>2</sub>-NPs due to loss of cell integrity. Similar findings were obtained by Korshed et al. [47] and El-Kaliuoby et al. [48], who confirmed a stimulated leakage of lactate dehydrogenases (LDH) from *E. coli* cells exposed to Ag-NPs and chitosan biopolymer NPs from *P. aeruginosa* and *S. aureus*, respectively. These studies indicate a targeted inactivation of metabolic activity of bacterial cells by a variety of different NPs.

Reduced glutathione plays an important role in the defence of bacterial cells, regulating the redox cycles of microbial cells. The measurement of GSH level is a valuable biomarker for determining the physiological status of a cell in various stress conditions, including oxidative stress [49,50]. A significant reduction in GSH level was observed in *E. coli* after exposure to Ag-NPs and ZnO-NPs and *S. epidermidis* treated with ZnO-NPs. GSH, apart from scavenging high levels of H<sub>2</sub>O<sub>2</sub>, can have a high affinity to released heavy metal ions from NPs, acting as a buffering agent against their excess concentration, which can further lead to the increase in its oxidised state (GSSG) [42,51]. Furthermore, NPs and released ions can interact with GSH thiol groups, depleting its concentration and reducing the defence mechanism of bacterial cells against generated ROS [9,23]. This finding and the potential agglomeration of NPs may explain the differences in obtained results. Additionally, each microorganism has a unique defence mechanism against oxidative stress, characterised by a different abundance of GSH and its divergent importance in protecting bacterial cells. For example, GSH is more abundant in gram-negative than gram-positive bacteria [52]. The results obtained in this work are in accordance with this statement because they clearly present a greater share of GSH in the protection of *E. coli* than *B. cereus* and *S. epidermidis*, producing a low concentration of GSH. Kumar et al. [38] found that GSH concentration in *E. coli* treated with ZnO-NPs and TiO<sub>2</sub>-NPs (80 µg mL<sup>-1</sup>) decreased by 53% and 60%, respectively. Referring to this study, an opposite trend was observed as a larger depletion of GSH by 15% in *E. coli* cells treated with ZnO-NPs than TiO<sub>2</sub>-NPs. This was correlated with small overall ROS concentration in *E. coli* cells detected after treatment with metal-oxide NPs, suggesting an active non-catalytic antioxidant defence system against the accumulation of intracellular ROS. In other studies, Korshed et al. [47] and Huang et al. [41] recorded a depletion of GSH in *E. coli* and *P. chrysosporium* treated with Ag-NPs, probably associated with detoxification of generated ROS. Similarly, Yuan et al. [43] reported a significant decrease in GSH levels by 80% and 70% in *P. aeruginosa* and *S. aureus* exposed to Ag-NPs, respectively. The lower bactericidal effect of Ag-NPs in this work may be related to the bigger size of commercial NPs and hence the smaller release of Ag<sup>+</sup> ions.

Disruption of redox homeostasis by ROS, released metal ions and oxidative activity of NPs may lead to the oxidative damage of proteins resulting from changes in their carbonyl and amine content [53,54]. Oxidation of proteins can result in the formation of carbonyls on protein side chains containing amino acids such as lysine, arginine, cysteine, or proline [55–58]. The formation of protein carbonyls causes significant structural changes in proteins, disrupting their functioning or even leading to their degradation [59]. In this study, Ag-NPs, Cu-NPs, ZnO-NPs and TiO<sub>2</sub>-NPs caused significant alternations in >C=O level in *E. coli*, *B. cereus* and *S. epidermidis*. In general, the most visible changes were observed in the presence of ZnO-NPs and TiO<sub>2</sub>-NPs. This is in accordance with high LPO levels in these bacteria as well as significant changes in CAT, PER, SOD and DEH activities. Moreover, further oxidation of protein side chains containing amine groups can also result in considerable changes in their overall content because these groups amongst sulphur-containing ones are the most susceptible to oxidative changes forced by ROS [58,60]. Here, it was also established that ZnO-NPs was characterised by the strongest stimulating effect

on -NH<sub>2</sub> content in bacterial cells. The knowledge concerning the impact of NPs on the content of carbonyl and amine groups in bacteria is very limited [53,54]; therefore, the obtained results can be considered innovative.

The formation of ROS, especially •OH and <sup>1</sup>O<sub>2</sub> can initiate lipid peroxidation, which is an oxidation process of unsaturated fatty acids and other lipids leading to severe structural changes in bacterial outer layers, including changes in its permeability, fluidity, and damage to the building components [53,61,62]. Herein, it was revealed that Ag-NPs, Cu-NPs and TiO<sub>2</sub>-NPs caused a significant increase in LPO level in *E. coli* and *S. epidermidis*; however, in *B. cereus* a visible increase in this parameter occurred only after exposure to Ag-NPs and Cu-NPs. The collected data further proved a strong oxidative stress generation by tested NPs in all tested strains. Interestingly, the addition of ZnO-NPs to the culture medium caused a decrease in LPO levels in *B. cereus* and *S. epidermidis*, which may suggest an adaptation of these bacteria to oxidative stress. In a similar study, Chatterjee et al. [53] documented a 35- and 50-fold increase in lipid peroxidation level in *E. coli* cells in the presence of Cu-NPs in concentrations of 3.0 and 7.5 µg mL<sup>-1</sup>, respectively. Analogously, Quinteros et al. [19] observed a 60% increase in the oxidation of lipids and proteins in *E. coli* after exposure to Ag-NPs. An increase in malondialdehyde (MDA) content in *E. coli* treated with TiO<sub>2</sub>-NPs was also positively correlated with ROS production [63]. In another study, Kumar et al. [38] found a dose-dependent increase in the formation of hydroperoxide ions and MDA levels in *E. coli* exposed to ZnO-NPs and TiO<sub>2</sub>-NPs, suggesting an increase in the lipid peroxidation. Those results indicated membrane damage in *E. coli*, further supported by an increased LDH release after treatment with NPs. Comparable results were obtained by Jain et al. [64], who recorded a greater MDA production in *E. coli* and *P. putida* in comparison with *B. cereus* and *S. aureus* strains. This may be attributed to greater activity of the *E. coli* enzymatic antioxidant system and additional protection of cells by GSH, which may prevent an increased production of MDA compared to *B. cereus* and *S. epidermidis* cells.

## 4. Materials and Methods

### 4.1. Bacterial Strains and Nanoparticles

In this study, three bacterial strains were tested for various responses to the exposure of selected metallic nanoparticles. They included gram-negative *Escherichia coli* (ATCC<sup>®</sup> 25922<sup>™</sup>) and gram-positive *Bacillus cereus* (ATCC<sup>®</sup> 11778<sup>™</sup>), and *Staphylococcus epidermidis* (ATCC<sup>®</sup> 12228<sup>™</sup>) strains purchased from the American Type Culture Collection (ATCC). *E. coli* was maintained using Bacto<sup>™</sup> Tryptic Soy Broth (cat. 211825; pancreatic digest of casein 17.0 g L<sup>-1</sup>, papaic digest of soybean 3.0 g L<sup>-1</sup>, dextrose 2.5 g L<sup>-1</sup>, sodium chloride 5.0 g L<sup>-1</sup>, dipotassium phosphate g L<sup>-1</sup>); however, *B. cereus* and *S. epidermidis* were passaged in Difco<sup>™</sup> Nutrient Broth (cat. 234000; beef extract 3.0 g L<sup>-1</sup>, peptone 5.0 g L<sup>-1</sup>).

All these strains were exposed to four types of nanoparticles (NPs): Ag-NPs (cat. 576832), Cu-NPs (cat. 774081), ZnO-NPs (cat. 677450) obtained from Sigma-Aldrich company and TiO<sub>2</sub>-NPs (cat. US1019F) acquired from US Research. The size of Ag-NPs, Cu-NPs and ZnO-NPs ranged in <100 nm, 25 nm and <50 nm, respectively, while TiO<sub>2</sub>-NPs were 20 nm in size. All NPs were characterised by 97–99.5% purity. Before starting the actual experiment, the stock solutions of NPs in sterile Millipore Water were sonicated (Vibra-Cell<sup>™</sup>, 20 kHz) for 10–20 min to avoid their aggregation/agglomeration.

### 4.2. Experimental Design

To determine toxicological parameters of NPs and assess their influence on antioxidant defence system and other accompanying processes, bacteria were grown in lysogeny broth medium (LB mix; NaCl 10 g L<sup>-1</sup>, tryptone 10 g L<sup>-1</sup>, yeast extract 5 g L<sup>-1</sup>) until they reached half of the logarithmic growth phase (4–5 h). Subsequently, bacterial suspension in 0.85% NaCl containing cells from this phase was used to inoculate sterile LB medium until OD<sub>600</sub> = 0.1 was achieved (~10<sup>7</sup> CFU mL<sup>-1</sup>), and the appropriate NPs were individually

added at a concentration corresponding to the IC<sub>50</sub> values (Table 1). Depending on the assay performed, the bacterial cultures were incubated for 1 to 24 h at 37 °C. The experimental design with multifaceted analyses of measured parameters is presented in Figure 8.

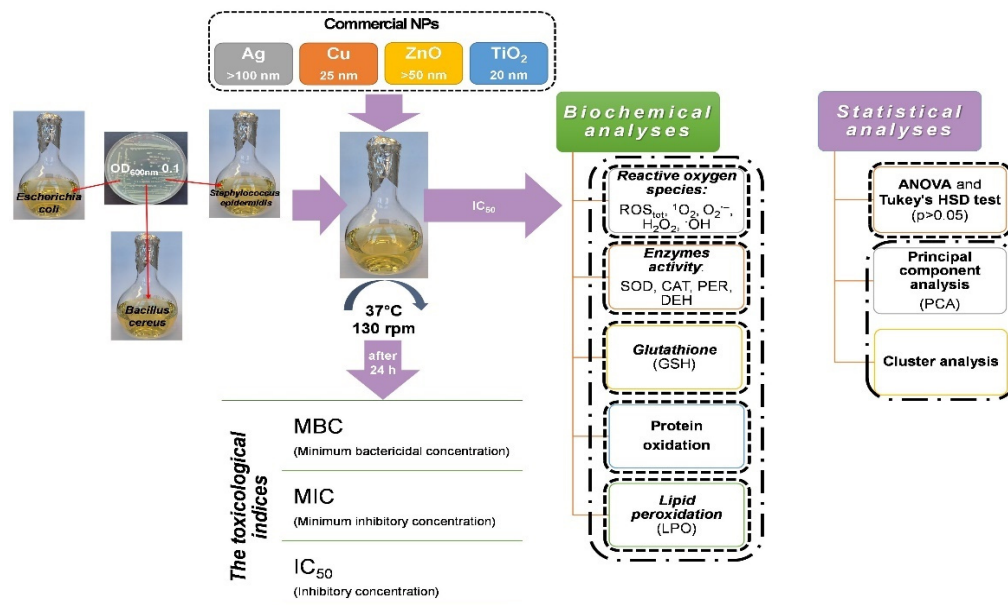


**Figure 8.** Scheme of experimental design.

#### 4.3. Evaluating the Toxicological Effect of NPs on Bacterial Strains

The broth dilution method was performed to study the potential toxicological effect of individual Ag-NPs, Cu-NPs, ZnO-NPs and TiO<sub>2</sub>-NPs on bacterial cell viability [65,66]. The determined toxicological parameters included: minimum bactericidal concentration (MBC), minimum inhibitory concentration (MIC), and the half-maximal inhibitory concentration (IC<sub>50</sub>). Before bacteria treatment, serial-fold dilutions of NPs were prepared in a sterile LB medium with final concentrations ranging between 0 and 1200 mg L<sup>-1</sup>. Next, increasing concentrations of NPs were added to the bacterial cultures, which were incubated for 24 h at 37 °C with shaking (140 rpm). After that, 10-fold dilution series of each culture were prepared in 0.85% NaCl, and 100 µL of each bacterial suspension were sub-cultured on LB agar plates and incubated for 24 h at 37 °C. Afterwards, bacterial colonies were counted, and the number of bacteria was expressed as colony-forming units—CFU mL<sup>-1</sup>. Inhibition of bacterial growth was established using a mortality rate formula with 99% and 100% inhibition accounted for MIC and MBC values, respectively [65,66]. Accordingly, toxicological IC<sub>50</sub> values of NPs were estimated with Prism 5 software (GraphPad Software, San Diego, CA, USA).

#### 4.4. Measuring the Concentration of Reactive Oxygen Species (ROS)

The total concentration of ROS and levels of singlet oxygen (<sup>1</sup>O<sub>2</sub>), superoxide radical anion (O<sub>2</sub><sup>•-</sup>), hydrogen peroxide (H<sub>2</sub>O<sub>2</sub>) and hydroxyl radical (•OH) were measured in biotic and abiotic samples treated with Ag-NPs, Cu-NPs, ZnO-NPs, and TiO<sub>2</sub>-NPs. Abiotic samples (research medium and NPs) were prepared to test the ability of NPs to spontaneously generate ROS, while the actual effect of NPs on ROS production in bacterial cells was assessed in the biotic trials. The final data concerning ROS production in the biotic samples are presented as the difference between biotic and abiotic samples for each NPs treatment. The total intracellular ROS concentration was evaluated using 2',7'-dichlorodihydrofluorescein diacetate (H<sub>2</sub>DCFDA) oxidised to 2',7'-dichlorofluorescein (DCF) by ROS [67]. First, bacterial cells from half of the log phase were suspended in phosphate-buffered saline (PBS) supplemented with individual NPs (IC<sub>50</sub>), and next, they were incubated for 1 h at 37 °C on a rotary shaker (140 rpm). Similarly, the appropriate

blank samples were prepared without bacterial cells. After adding 4 mM H<sub>2</sub>DCFDA, the samples were incubated for 30 min, and the fluorescence was measured at an excitation wavelength of 485 nm and an emission wavelength of 530 nm. Meanwhile, the tested samples were cultured on LB agar plates, and CFU was calculated after 24 h of incubation at 37 °C. The intracellular ROS concentration was calculated according to Alpaslan et al. [68] and expressed as AU·CFU mL<sup>-1</sup>, where AU means absorbance unit.

The level of <sup>1</sup>O<sub>2</sub> was measured using a modified method by Zhang et al. [69] based on quenching of the 1,3-diphenylisobenzofuran (DPBF) fluorescence. The fluorescence of the abiotic and biotic samples prepared in PBS with NPs (IC<sub>50</sub>) was measured after the addition of 3 mM DPBF at λ = 410 nm over a 5 min period. Unlike, the O<sub>2</sub><sup>•-</sup> level was estimated in compliance with a method by Horst et al. [70], involving the reduction of XTT tetrazolium salt to a colourful formazan. After the addition of 91.3 mg L<sup>-1</sup> XTT salt to the samples, the absorbance at λ = 490 nm was measured at 0 h and after 2 h of incubation with the reagent. Between the measurements, the samples were kept in the dark at 37 °C. The <sup>1</sup>O<sub>2</sub> and O<sub>2</sub><sup>•-</sup> level was expressed as AU. By comparison, H<sub>2</sub>O<sub>2</sub> level was identified through the use of Amplex Red (AR) reagent and horseradish peroxidase (HRP), which converts AR to fluorescent resorufin in the presence of H<sub>2</sub>O<sub>2</sub> measured at an excitation wavelength of 520 nm and an emission wavelength of 620 nm [71]. To measure the concentration of H<sub>2</sub>O<sub>2</sub>, 200 μM of AR reagent and 0.02 mg mL<sup>-1</sup> of HRP were added to the samples, and the fluorescence was detected at 0 and next after 5, 10, 15 and 20 min of incubation. The concentration of H<sub>2</sub>O<sub>2</sub> (μM) was estimated using a standard curve (y = 1592.9x) performed with concentrations ranging from 0.024 μM to 50 μM. The •OH content was established using the indirect method of deoxyribose degradation, which leads to the formation of degradation products reacting readily with thiobarbituric acid (TBA) measured spectrophotometrically at λ = 532 nm [72,73]. The cells in PBS with NPs (IC<sub>50</sub>) and 20 mmol L<sup>-1</sup> deoxyribose were incubated for 1 h at 37 °C and centrifuged (5000 rpm, 5 min, 4 °C). Next, 2.8% (m/v) trichloroacetic acid (TCA) and 1% (w/v) TBA were introduced to the supernatant and incubated for 15–20 min at 100 °C. After incubation, the absorbance of the sample was measured, and the concentration of •OH was calculated using a standard curve (y = 8.832x) performed with malondialdehyde (MDA) concentrations ranging from 0 μM to 0.1 μM.

#### 4.5. Measuring the Activity of Antioxidant Enzymes and Dehydrogenases

After exposure to NPs, the activities of three antioxidant enzymes: superoxide dismutase (SOD), catalase (CAT) and peroxidase (PER) in *E. coli*, *B. cereus* and *S. epidermidis* were assayed. The isolation of enzymes from bacterial cells was carried out in accordance with a method by Hegeman [74]. Bacteria were cultivated in LB medium with Ag-NPs, Cu-NPs, TiO<sub>2</sub>-NPs and ZnO-NPs (IC<sub>50</sub>) for 24 h at 37 °C and next, they were centrifuged (5000 rpm, 20 min, 4 °C). The resulting pellet was washed and suspended in 50 mM phosphate buffer (pH 7.0), and sonicated 6 times for 15 sec with 30-sec intervals (Vibra Cell™, 20 kHz) in the ice bath. The suspension was centrifuged (15,000 rpm, 20 min, 4 °C) and the obtained supernatant was subjected to the determination of the activity of enzymes. The activity of SOD was measured through an indirect method using a commercial reagent kit (cat. 19160; Sigma-Aldrich, St. Louis, MI, USA) based on the production of water-soluble colourful formazan dye and decrease in the colour intensity of the sample at λ = 450 nm. The specific activity of SOD was calculated using the formula described in the protocol by Zhang et al. [75]. The CAT activity was measured according to Banerjee et al. [76] and David et al. [77], based on the decomposition of H<sub>2</sub>O<sub>2</sub> in time. A decrease in the absorbance of the sample at λ = 240 nm was measured over 3 min, and specific CAT activity was determined with molar extinction coefficient ε = 36,000 dm<sup>3</sup>·mol<sup>-1</sup>·cm<sup>-1</sup>. The PER activity was assessed using colorimetric protocol by Sigma-Aldrich based on the purpurogallin production. An increase in the absorbance of the sample at λ = 420 nm was measured for 3 min. The total protein concentration in the sample was determined according to Bradford [78] with Coomassie Brilliant Blue G-250 reagent and lysozyme as a standard. The

activity of SOD, CAT, and PER was expressed as U mg<sup>-1</sup> protein. To determine dehydrogenases (DEH) activity in bacteria, the common colorimetric assay based on the reduction of 2,3,5-triphenyltetrazolium chloride (TTC) to the creaming red-coloured triphenylformazan (TPF) was applied [79]. The activity of DHA was expressed as mg TPF h<sup>-1</sup> mg<sup>-1</sup> protein.

#### 4.6. Measuring the Reduced Glutathione Concentration (GSH)

Glutathione is an important non-enzymatic component of the antioxidant system. The principal of the assay is based on the reaction between the sulfhydryl group of GSH with 5,5'-dithiobis(2-nitrobenzoic acid) (DTNB), known as Ellman's reagent, leading to the production of colourful 5-thio-2-nitrobenzoic acid (TNB) [38]. After adding 100% TCA to the bacterial cultures exposed to NPs (IC<sub>50</sub>) for 24 h, they were incubated for 10 min at 37 °C and centrifuged (10,000 rpm, 5 min, 4 °C). The samples were then neutralised with Tris-HCl buffer (pH 8.9), and 0.01% DTNB was added. After 15–20 min of incubation, the absorbance of the sample was measured at  $\lambda = 412$  nm. The concentration of GSH was estimated using a standard curve obtained for the concentrations ranging from 0.049 to 100  $\mu$ M.

#### 4.7. Determining Carbonyl and Amine Group Content in Oxidatively Modified Proteins

Determining the carbonyl (>C=O) and amine group (-NH<sub>2</sub>) content in proteins allows confirming protein oxidation in bacterial cells treated with NPs (IC<sub>50</sub>). The principal of the >C=O content assay is based on the reaction of protein carbonyl groups with 2,4-dinitrophenylhydrazine (DNPH), resulting in the formation of 2,4-dinitrophenylhydrazones measured calorimetrically [53,80,81]. Subsequently, -NH<sub>2</sub> content measurement is based on the reaction of fluorescamine with amine groups, which produces fluorescent product proportional to the amine content in a sample, whilst the unbound fluorescamine hydrolyses to non-fluorescent products [60,81]. The supernatant for analysis was obtained in a similar way to the procedure for isolating antioxidant enzymes. To determine >C=O content, the proteins in the supernatant were precipitated by adding 10% (*w/v*) TCA and centrifuged (12,000 rpm, 15 min, 4 °C). The obtained precipitate was treated with 0.2% (*m/v*) DNPH and the sample was incubated for 1 h at 37 °C in the darkness. Sequentially, the precipitate was dissolved in guanidine hydrochloride, incubated for 15 min, and centrifuged (5000 rpm, 2 min, 4 °C). The absorbance of the collected supernatant was measured at  $\lambda = 370$  nm, and the content of carbonyl groups was calculated using the molar extinction coefficient  $\epsilon = 21$  L·mmol<sup>-1</sup>·cm<sup>-1</sup> of the formed hydrazone. In turn, to determine -NH<sub>2</sub> content in proteins, 0.03% fluorescamine solution was added to the sample in a 3:1 ratio and then vortexed. After 30 min incubation in the dark, the fluorescence of a sample was measured at an excitation wavelength of 390 nm and an emission wavelength of 465 nm. The concentration of -NH<sub>2</sub> was estimated using a standard curve obtained for standardised albumin samples in concentrations ranging from 50 to 1000  $\mu$ g·mL<sup>-1</sup>.

#### 4.8. Assessing the Lipid Peroxidation Level in Bacterial Strains

In the process of lipid peroxidation, one of the most common products is malondialdehyde (MDA), which reacts with TBA generating spectrophotometrically measured chromophore [53,82]. The supernatant was obtained analogously to the antioxidant enzyme isolation. In the next stage, 15% (*w/v*) TCA and 0.37% (*w/v*) TBA were added to the supernatant in 1:1:1 ratio. Parallely, the control sample containing sterile H<sub>2</sub>O, instead of TBA, was prepared. The mixtures were incubated for 10 min at 100 °C and centrifuged (5000 rpm, 20 min, 4 °C). The absorbance of the solution was measured at  $\lambda = 535$  nm, and the concentration of MDA was calculated based on the molar extinction coefficient  $\epsilon = 156$  L·mmol<sup>-1</sup>·cm<sup>-1</sup>.

#### 4.9. Statistical Analysis

The assays were performed in three repeats for each sample set, and the final results were presented as the mean  $\pm$  the standard deviation (SD)/the standard error (SE). The statistical significance of data in tested samples was determined through one-way ANOVA,



followed by Tukey's Honest Significant Difference test (HSD). The substantial variations in obtained data are represented by annotated letters in the presented graphics for the  $p < 0.05$  statistical significance threshold. All statistical tests were carried out using STATISTICA 13.1 software package (Dell Inc., Austin, TE, USA).

## 5. Conclusions

This study revealed strong antimicrobial properties of Ag-NPs, Cu-NPs, ZnO-NPs and TiO<sub>2</sub>-NPs against *E. coli*, *B. cereus* and *S. epidermidis* strains and proved their antimicrobial effect depending on the species of bacteria and studied NPs. All NPs generated oxidative stress in the bacteria, which reflected in the production of different types of ROS in a wide range of concentrations. Disruption of bacterial redox homeostasis caused alterations in the activity of CAT, PER and SOD, depletion in GSH concentration and protein oxidation. Moreover, the research provided new insight into NPs effect on bacterial outer layers and respiratory metabolism through increased lipid peroxidation levels and alterations in DEH activity. Our ongoing research is focused on the expression of genes responsible for oxidative stress, redox homeostasis and antioxidant defence system, which will provide extra information on the genetic regulation of studied phenomena.

**Author Contributions:** Conceptualisation, O.M., D.W. and A.M.; methodology, O.M. and D.W.; validation, O.M. and D.W.; formal analysis, O.M., D.W. and A.M.; writing—original draft, O.M. and D.W.; writing—review and editing, A.M.; supervision, A.M. All authors have read and agreed to the published version of the manuscript.

**Funding:** This research was financed by the Doctoral School at the University of Silesia.

**Institutional Review Board Statement:** Not applicable.

**Informed Consent Statement:** Not applicable.

**Data Availability Statement:** All data that support the findings of this study are available from the corresponding authors upon reasonable request.

**Conflicts of Interest:** The authors declare no conflict of interest.

## References

1. Qayyum, S.; Khan, A.U. Nanoparticles vs. biofilms: A battle against another paradigm of antibiotic resistance. *Med. Chem. Commun.* **2016**, *7*, 1479–1498. [[CrossRef](#)]
2. Behera, N.; Arakha, M.; Priyadarshinee, M.; Pattanayak, B.S.; Soren, S.; Jha, S.; Mallick, B.C. Oxidative stress generated at nickel oxide nanoparticle interface results in bacterial membrane damage leading to cell death. *RSC Adv.* **2019**, *9*, 24888–24894. [[CrossRef](#)]
3. Ameen, F.; Alsamhary, K.; Alabdullatif, J.A.; AlNadhari, S. A review on metal-based nanoparticles and their toxicity to beneficial soil bacteria and fungi. *Ecotoxicol. Environ. Saf.* **2021**, *213*, 112027. [[CrossRef](#)]
4. Liu, J.; Liu, J.; Attarilar, S.; Wang, C.; Tamaddon, M.; Yang, C.; Xie, K.; Yao, J.; Wang, L.; Liu, C.; et al. Nano-modified titanium implant materials: A way toward improved antibacterial properties. *Front. Bioeng. Biotechnol.* **2020**, *8*, 576969. [[CrossRef](#)]
5. Wang, N.; Fuh, J.Y.H.; Dheen, S.T.; Senthil Kumar, A. Functions and applications of metallic and metallic oxide nanoparticles in orthopedic implants and scaffolds. *J. Biomed. Mater. Res.* **2021**, *109*, 160–179. [[CrossRef](#)] [[PubMed](#)]
6. Vergara-Llanos, D.; Koning, T.; Pavicic, M.F.; Bello-Toledo, H.; Díaz-Gómez, A.; Jaramillo, A.; Melendrez-Castro, M.; Ehrenfeld, P.; Sánchez-Sanhueza, G. Antibacterial and cytotoxic evaluation of copper and zinc oxide nanoparticles as a potential disinfectant material of connections in implant provisional abutments: An in-vitro study. *Arch. Oral Biol.* **2021**, *122*, 105031. [[CrossRef](#)] [[PubMed](#)]
7. Bundschuh, M.; Filser, J.; Lüderwald, S.; McKee, M.S.; Metreveli, G.; Schaumann, G.E.; Schulz, R.; Wagner, S. Nanoparticles in the environment: Where do we come from, where do we go to? *Environ. Sci. Eur.* **2018**, *30*, 6. [[CrossRef](#)] [[PubMed](#)]
8. Wang, L.; Hu, C.; Shao, L. The antimicrobial activity of nanoparticles: Present situation and prospects for the future. *Int. J. Nanomed.* **2017**, *12*, 1227–1249. [[CrossRef](#)]
9. Slavin, Y.N.; Asnis, J.; Häfeli, U.O.; Bach, H. Metal nanoparticles: Understanding the mechanisms behind antibacterial activity. *J. Nanobiotechnol.* **2017**, *15*, 65. [[CrossRef](#)] [[PubMed](#)]
10. Dayem, A.A.; Hossain, M.K.; Lee, S.B.; Kim, K.; Saha, S.K.; Yang, G.M.; Choi, H.Y.; Cho, S.G. The role of reactive oxygen species (ROS) in the biological activities of metallic nanoparticles. *Int. J. Mol. Sci.* **2017**, *18*, 120. [[CrossRef](#)]
11. Canaparo, R.; Foglietta, F.; Limongi, T.; Serpe, L. Biomedical applications of reactive oxygen species generation by metal nanoparticles. *Materials* **2020**, *14*, 53. [[CrossRef](#)] [[PubMed](#)]

12. Imlay, J.A. Pathways of oxidative damage. *Annu. Rev. Microbiol.* **2003**, *57*, 395–418. [[CrossRef](#)] [[PubMed](#)]
13. Collin, F. Chemical basis of reactive oxygen species reactivity and involvement in neurodegenerative diseases. *Int. J. Mol. Sci.* **2019**, *20*, 2407. [[CrossRef](#)]
14. Onyango, A.N. Endogenous generation of singlet oxygen and ozone in human and animal tissues: Mechanisms, biological significance, and influence of dietary components. *Oxidant Med. Cell Longev.* **2016**, *2016*, 2398573. [[CrossRef](#)]
15. Hubenko, K.; Yefimova, S.; Tkacheva, T.; Maksimchuk, P.; Borovoy, I.; Klochkov, V.; Kavok, N.; Opolonin, O.; Malyukin, Y. 2018. Reactive oxygen species generation in aqueous solutions containing GdVO<sub>4</sub>:Eu<sup>3+</sup> nanoparticles and their complexes with methylene blue. *Nanoscale Res. Lett.* **2018**, *13*, 100. [[CrossRef](#)]
16. Wang, D.; Zhao, L.; Ma, H.; Zhang, H.; Guo, L.H. Quantitative analysis of reactive oxygen species photogenerated on metal oxide nanoparticles and their bacteria toxicity: The role of superoxide radicals. *Environ. Sci. Technol.* **2017**, *51*, 10137–10145. [[CrossRef](#)] [[PubMed](#)]
17. Muñoz Diaz, R.; Cardoso-Avila, P.E.; Pérez Tavares, J.A.; Patakfalvi, R.; Villa Cruz, V.; Pérez Ladrón de Guevara, H.; Gutiérrez Coronado, O.; Arteaga Garibay, R.I.; Saavedra Arroyo, Q.E.; Marañón-Ruiz, V.F.; et al. Two-step triethylamine-based synthesis of MgO nanoparticles and their antibacterial effect against pathogenic bacteria. *Nanomaterials* **2021**, *11*, 410. [[CrossRef](#)]
18. Li, Y.; Zhang, W.; Niu, J.; Chen, Y. Mechanism of photogenerated reactive oxygen species and correlation with the antibacterial properties of engineered metal-oxide nanoparticles. *ACS Nano* **2012**, *6*, 5164–5173. [[CrossRef](#)]
19. Quinteros, M.A.; Aristizábal, V.C.; Dalmasso, P.R.; Paraje, M.G.; Páez, P.L. Oxidative stress generation of silver nanoparticles in three bacterial genera and its relationship with the antimicrobial activity. *Toxicol. In Vitro* **2016**, *36*, 216–223. [[CrossRef](#)]
20. Makhdoumi, P.; Karimi, H.; Khazaei, M. Review on metal-based nanoparticles: Role of reactive oxygen species in renal toxicity. *Chem. Res. Toxicol.* **2020**, *33*, 2503–2514. [[CrossRef](#)]
21. Fang, F.C. Antimicrobial actions of reactive oxygen species. *MBio* **2011**, *2*, e00141-11. [[CrossRef](#)] [[PubMed](#)]
22. Ezraty, B.; Gennaris, A.; Barras, F.; Collet, J.F. Oxidative stress, protein damage and repair in bacteria. *Nat. Rev. Microbiol.* **2017**, *15*, 385–396. [[CrossRef](#)]
23. Choi, Y.; Kim, H.A.; Kim, K.W.; Lee, B.T. Comparative toxicity of silver nanoparticles and silver ions to *Escherichia coli*. *J. Environ. Sci.* **2018**, *66*, 50–60. [[CrossRef](#)]
24. Yang, X.Y.; Chung, E.; Johnston, I.; Ren, G.; Cheong, Y.K. Exploitation of antimicrobial nanoparticles and their applications in biomedical engineering. *Appl. Sci.* **2021**, *11*, 4520. [[CrossRef](#)]
25. Zhao, J.; Lin, M.; Wang, Z.; Cao, X.; Xing, B. Engineered nanomaterials in the environment: Are they safe? *Crit. Rev. Environ. Sci. Technol.* **2021**, *51*, 1443–1478. [[CrossRef](#)]
26. Baptista, P.V.; McCusker, M.P.; Carvalho, A.; Ferreira, D.A.; Mohan, N.M.; Martins, M.; Fernandes, A.R. Nano-strategies to fight multidrug resistant bacteria—A battle of the titans. *Front. Microbiol.* **2018**, *9*, 1441. [[CrossRef](#)]
27. Kubo, A.L.; Capjak, I.; Vrček, I.V.; Bondarenko, O.M.; Kurvet, I.; Vija, H.; Ivask, A.; Kasemets, K.; Kahru, A. Antimicrobial potency of differently coated 10 and 50 nm silver nanoparticles against clinically relevant bacteria *Escherichia coli* and *Staphylococcus aureus*. *Colloids Surf. B* **2018**, *170*, 401–410. [[CrossRef](#)]
28. Ahmad, N.S.; Abdullah, N.; Yasin, F.M. Toxicity assessment of reduced graphene oxide and titanium dioxide nanomaterials on gram-positive and gram-negative bacteria under normal laboratory lighting condition. *Toxicol. Rep.* **2020**, *7*, 693–699. [[CrossRef](#)]
29. Bottone, E.J. *Bacillus cereus*, a volatile human pathogen. *Clin. Microbiol. Rev.* **2010**, *23*, 382–398. [[CrossRef](#)] [[PubMed](#)]
30. Foster, T.J. Surface proteins of *Staphylococcus epidermidis*. *Front. Microbiol.* **2020**, *11*, 1829. [[CrossRef](#)]
31. Odzak, N.; Kistler, D.; Behra, R.; Sigg, L. Dissolution of metal and metal oxide nanoparticles in aqueous media. *Environ. Pollut.* **2014**, *191*, 132–138. [[CrossRef](#)] [[PubMed](#)]
32. Wang, D.; Lin, Z.; Wang, T.; Yao, Z.; Qin, M.; Zheng, S.; Lu, W. Where does the toxicity of metal oxide nanoparticles come from: The nanoparticles, the ions, or a combination of both? *J. Hazard. Mater.* **2016**, *308*, 328–334. [[CrossRef](#)] [[PubMed](#)]
33. Ghorbani, R.; Biparva, P.; Moradian, F. Assessment of antibacterial activity and the effect of copper and iron zerovalent nanoparticles on gene expression DnaK in *Pseudomonas aeruginosa*. *BioNanoScience* **2020**, *10*, 204–211. [[CrossRef](#)]
34. Eckhardt, S.; Brunetto, P.S.; Gagnon, J.; Priebe, M.; Giese, B.; Fromm, K.M. Nanobio silver: Its interactions with peptides and bacteria, and its uses in medicine. *Chem. Rev.* **2013**, *113*, 4708–4754. [[CrossRef](#)] [[PubMed](#)]
35. Fasnacht, M.; Polacek, N. Oxidative stress in bacteria and the central dogma of molecular biology. *Front. Mol. Biosci.* **2021**, *8*, 671037. [[CrossRef](#)]
36. Bond, R.J.; Hansel, C.M.; Voelker, B.M. Heterotrophic bacteria exhibit a wide range of rates of extracellular production and decay of hydrogen peroxide. *Front. Mar. Sci.* **2020**, *7*, 72. [[CrossRef](#)]
37. Hong, R.; Kang, T.Y.; Michels, C.A.; Gadura, N. Membrane lipid peroxidation in copper alloy-mediated contact killing of *Escherichia coli*. *Appl. Environ. Microbiol.* **2012**, *78*, 1776–1784. [[CrossRef](#)]
38. Kumar, A.; Pandey, A.K.; Singh, S.S.; Shanker, R.; Dhawan, A. Engineered ZnO and TiO<sub>2</sub> nanoparticles induce oxidative stress and DNA damage leading to reduced viability of *Escherichia coli*. *Free Radic. Biol. Med.* **2011**, *51*, 1872–1881. [[CrossRef](#)] [[PubMed](#)]
39. Manke, A.; Wang, L.; Rojanasakul, Y. Mechanisms of nanoparticle-induced oxidative stress and toxicity. *Biomed. Res. Int.* **2013**, *2013*, 942916. [[CrossRef](#)] [[PubMed](#)]
40. Dwivedi, S.; Wahab, R.; Khan, F.; Mishra, Y.K.; Musarrat, J.; Al-Khedhairy, A.A. Reactive oxygen species mediated bacterial biofilm inhibition via zinc oxide nanoparticles and their statistical determination. *PLoS ONE* **2014**, *9*, e111289. [[CrossRef](#)] [[PubMed](#)]

41. Huang, Z.; He, K.; Song, Z.; Zeng, G.; Chen, A.; Yuan, L.; Li, H.; Hu, L.; Guo, Z.; Chen, G. Antioxidative response of *Phanerochaete chrysosporium* against silver nanoparticle- induced toxicity and its potential mechanism. *Chemosphere* **2018**, *211*, 573–583. [[CrossRef](#)] [[PubMed](#)]
42. Liao, S.; Zhang, Y.; Pan, X.; Zhu, F.; Jiang, C.; Liu, Q.; Cheng, Z.; Dai, G.; Wu, G.; Wang, L.; et al. Antibacterial activity and mechanism of silver nanoparticles against multidrug-resistant *Pseudomonas aeruginosa*. *Int. J. Nanomed.* **2019**, *14*, 1469–1487. [[CrossRef](#)] [[PubMed](#)]
43. Yuan, Y.G.; Peng, Q.L.; Gurunathan, S. Effects of silver nanoparticles on multiple drug- resistant strains of *Staphylococcus aureus* and *Pseudomonas aeruginosa* from mastitis-infected goats: An alternative approach for antimicrobial therapy. *Int. J. Mol. Sci.* **2017**, *18*, 569. [[CrossRef](#)]
44. Chowdhuri, A.R.; Tripathy, S.; Chandra, S.; Roy, S.; Sahu, S.K. A ZnO decorated chitosan–graphene oxide nanocomposite shows significantly enhanced antimicrobial activity with ROS generation. *RSC Adv.* **2015**, *5*, 49420–49428. [[CrossRef](#)]
45. Heikal, A.; Nakatani, Y.; Dunn, E.; Weimar, M.R.; Day, C.L.; Baker, E.N.; Lott, J.S.; Sazanov, L.A.; Cook, G.M. Structure of the bacterial type II NADH dehydrogenase: A monotopic membrane protein with an essential role in energy generation. *Mol. Microbiol.* **2014**, *91*, 950–964. [[CrossRef](#)]
46. Billenkamp, F.; Peng, T.; Berghoff, B.A.; Klug, G. A cluster of four homologous small RNAs modulates C1 metabolism and the pyruvate dehydrogenase complex in *Rhodobacter sphaeroides* under various stress conditions. *J. Bacteriol.* **2015**, *197*, 1839–1852. [[CrossRef](#)] [[PubMed](#)]
47. Korshed, P.; Li, L.; Liu, Z.; Wang, T. The molecular mechanisms of the antibacterial effect of picosecond laser generated silver nanoparticles and their toxicity to human cells. *PLoS ONE* **2016**, *11*, e0160078. [[CrossRef](#)] [[PubMed](#)]
48. El-Kaliuoby, M.I.; Amer, M.; Shehata, N. Enhancement of nano-biopolymer antibacterial activity by pulsed electric field. *Polymers* **2021**, *13*, 1869. [[CrossRef](#)]
49. Masip, L.; Veeravalli, K.; Georgiou, G. The many faces of glutathione in bacteria. *Antioxid. Redox Signal.* **2006**, *8*, 753–762. [[CrossRef](#)]
50. Smirnova, G.; Muzyka, N.; Oktyabrsky, O. Transmembrane glutathione cycling in growing *Escherichia coli* cells. *Mircobiol. Res.* **2012**, *167*, 166–172. [[CrossRef](#)]
51. Stewart, L.J.; Ong, C.L.Y.; Zhang, M.M.; Brouwer, S.; McIntrye, L.; Davies, M.R.; Walker, M.J.; McEwan, A.G.; Waldron, K.J.; Djoko, K.Y. A role for glutathione in buffering excess intracellular copper in *Streptococcus pyogenes*. *MBio* **2020**, *11*, e02804–e02820. [[CrossRef](#)] [[PubMed](#)]
52. Smirnova, G.V.; Oktyabrsky, O.N. Glutathione in bacteria. *Biochemistry* **2005**, *70*, 1199–1211. [[CrossRef](#)] [[PubMed](#)]
53. Chatterjee, A.K.; Chakraborty, R.; Basu, T. Mechanism of antibacterial activity of copper nanoparticles. *Nanotechnology* **2014**, *25*, 135101. [[CrossRef](#)]
54. Singh, R.; Cheng, S.; Singh, S. Oxidative stress-mediated genotoxic effect of zinc oxide nanoparticles on *Deinococcus radiodurans*. *3 Biotech* **2020**, *10*, 66. [[CrossRef](#)]
55. Dalle-Donne, I.; Rossi, R.; Giustarini, D.; Milzani, A.; Colombo, R. Protein carbonyl groups as biomarkers of oxidative stress. *Clin. Chim. Acta* **2003**, *329*, 23–38. [[CrossRef](#)]
56. Suzuki, Y.J.; Carini, M.; Butterfield, D.A. Protein carbonylation. *Antioxid. Redox Signal.* **2010**, *12*, 323–325. [[CrossRef](#)]
57. Nayak, J.; Jena, S.R.; Samanta, L. Oxidative stress and sperm dysfunction: An insight into dynamics of semen proteome. In *Oxidants, Antioxidants and Impact of the Oxidative Status in Male Reproduction*; Henkel, R., Samanta, L., Agarwal, A., Eds.; Academic Press: Cambridge, MA, USA, 2019; pp. 261–275.
58. Xiong, Y.L.; Guo, A. Animal and plant protein oxidation: Chemical and functional property significance. *Foods* **2021**, *10*, 40. [[CrossRef](#)]
59. Catalán, V.; Frühbeck, G.; Gómez-Ambrosi, J. Inflammatory and oxidative stress markers in skeletal muscle of obese subjects. In *Obesity, Oxidative Stress and Dietary Antioxidants*; Marti del Moral, A., Aguilera García, C.M., Eds.; Academic Press: Cambridge, MA, USA, 2018; pp. 163–189.
60. Wang, S.; Zhou, Q.; Chen, X.; Luo, R.H.; Li, Y.; Liu, X.; Yang, L.M.; Zheng, Y.T.; Wang, P. Modification of N-terminal  $\alpha$ -amine of proteins via biomimetic *ortho*-quinone-mediated oxidation. *Nat. Commun.* **2021**, *12*, 2257. [[CrossRef](#)]
61. Bhattacharya, P.; Dey, A.; Neogi, S. An insight into the mechanism of antibacterial activity by magnesium oxide nanoparticles. *J. Mater. Chem. B* **2021**, *9*, 5329–5339. [[CrossRef](#)]
62. Grotto, D.; Santa Maria, L.; Valentini, J.; Paniz, C.; Schmitt, G.; Garcia, S.C.; Pombalum, V.J.; Rocha, J.B.T.; Farina, M. Importance of the lipid peroxidation biomarkers and methodological aspects for malondialdehyde quantification. *Quím. Nova* **2009**, *32*, 169–174. [[CrossRef](#)]
63. Lin, X.; Li, J.; Ma, S.; Liu, G.; Yang, K.; Tong, M.; Lin, D. Toxicity of TiO<sub>2</sub> nanoparticles to *Escherichia coli*: Effects of particle size, crystal phase and water chemistry. *PLoS ONE* **2014**, *9*, e110247. [[CrossRef](#)]
64. Jain, N.; Bhargava, A.; Rathi, M.; Dilip, R.V.; Panwar, J. Removal of protein capping enhances the antibacterial efficiency of biosynthesized silver nanoparticles. *PLoS ONE* **2015**, *10*, e0134337. [[CrossRef](#)] [[PubMed](#)]
65. Wiegand, I.; Hilpert, K.; Hancock, R.E.W. Agar and broth dilution methods to determine the minimal inhibitory concentration (MIC) of antimicrobial substances. *Nat. Protoc.* **2008**, *3*, 163–175. [[CrossRef](#)]

66. Bagchi, B.; Kar, S.; Dey, S.K.; Bhandary, S.; Roy, D.; Mukhopadhyay, T.K.; Das, S.; Nandy, P. In situ synthesis and antibacterial activity of copper nanoparticle loaded natural montmorillonite clay based on contact inhibition and ion release. *Colloids Surf. B Biointerfaces* **2013**, *108*, 358–365. [[CrossRef](#)]
67. Yang, Y.; Wang, J.; Xiu, Z.; Alvarez, P.J.J. Impacts of silver nanoparticles on cellular and transcriptional activity of nitrogen-cycling bacteria. *Environ. Toxicol. Chem.* **2013**, *32*, 1488–1494. [[CrossRef](#)] [[PubMed](#)]
68. Alpaslan, E.; Geilich, B.M.; Yazici, H.; Webster, T.J. pH-controlled cerium oxide nanoparticle inhibition of both gram-positive and gram-negative bacteria growth. *Sci. Rep.* **2017**, *7*, 45859. [[CrossRef](#)]
69. Zhang, Y.; Huang, P.; Wang, D.; Chen, J.; Liu, W.; Hu, P.; Huang, M.; Chen, X.; Chen, Z. Near-infrared-triggered antibacterial and antifungal photodynamic therapy based on lanthanide-doped upconversion nanoparticles. *Nanoscale* **2018**, *10*, 15485–15495. [[CrossRef](#)] [[PubMed](#)]
70. Horst, A.M.; Vukanti, R.; Priester, J.H.; Holden, P.A. An assessment of fluorescence- and absorbance-based assays to study metal-oxide nanoparticle ROS production and effects on bacterial membranes. *Small* **2013**, *9*, 1753–1764. [[CrossRef](#)] [[PubMed](#)]
71. Seaver, L.C.; Imlay, J.A. Alkyl hydroperoxide reductase is the primary scavenger of endogenous hydrogen peroxide in *Escherichia coli*. *J. Bacteriol.* **2001**, *183*, 7173–7181. [[CrossRef](#)] [[PubMed](#)]
72. Rice-Evans, C.A.; Diplock, A.T.; Symons, M.C.R. The detection and characterization of free radical species. In *Laboratory Techniques in Biochemistry and Molecular Biology, Techniques in Free Radical Research*; Rice-Evans, C.A., Diplock, A.T., Symons, M.C.R., Eds.; Elsevier: Amsterdam, The Netherlands, 1991; Volume 22, pp. 51–100.
73. Meghana, S.; Kabra, P.; Chakraborty, S.; Padmavathy, N. Understanding the pathway of antibacterial activity of copper oxide nanoparticles. *RSC Adv.* **2015**, *5*, 12293–12299. [[CrossRef](#)]
74. Hegeman, G.D. Synthesis of the enzymes of the mandelate pathway by *Pseudomonas putida* I. Synthesis of enzymes by the wild type. *J. Bacteriol.* **1966**, *91*, 1140–1154. [[CrossRef](#)]
75. Zhang, C.; Bruins, M.E.; Yang, Z.Q.; Liu, S.T.; Rao, P.F. A new formula to calculate activity of superoxide dismutase in indirect assays. *Anal. Biochem.* **2016**, *503*, 65–67. [[CrossRef](#)] [[PubMed](#)]
76. Banerjee, G.; Pandey, S.; Ray, A.K.; Kumar, R. Bioremediation of heavy metals by a novel bacterial strain *Enterobacter cloacae* and its antioxidant enzyme activity, flocculant production and protein expression in presence of lead, cadmium and nickel. *Water Air Soil Pollut.* **2015**, *226*, 91. [[CrossRef](#)]
77. David, M.; Krishna, P.M.; Sangeetha, J. Elucidation of impact of heavy metal pollution on soil bacterial growth and extracellular polymeric substances flexibility. *3 Biotech* **2016**, *6*, 172. [[CrossRef](#)]
78. Bradford, M.M. A rapid and sensitive method for the quantitation of microgram quantities of protein utilizing the principle of protein-dye binding. *Anal. Biochem.* **1976**, *72*, 248–254. [[CrossRef](#)]
79. Nweke, C.O.; Alisi, C.S.; Okolo, J.C.; Nwanyanwu, C.E. Toxicity of zinc to heterotrophic bacteria from a tropical river sediment. *Appl. Ecol. Env. Res.* **2007**, *5*, 123–132. [[CrossRef](#)]
80. Levine, R.L.; Garland, D.; Oliver, C.N.; Amici, A.; Climent, I.; Lenz, A.G.; Ahn, B.W.; Shaltiel, S.; Stadtman, E.R. Determination of carbonyl content in oxidatively modified proteins. *Methods Enzymol.* **1990**, *186*, 464–478. [[PubMed](#)]
81. Rice-Evans, C.A.; Diplock, A.T.; Symons, M.C.R. Detection of protein structural modifications induced by free radicals. In *Laboratory Techniques in Biochemistry and Molecular Biology, Techniques in Free Radical Research*; Rice-Evans, C.A., Diplock, A.T., Symons, M.C.R., Eds.; Elsevier: Amsterdam, The Netherlands, 1991; Volume 22, pp. 207–235.
82. Rice-Evans, C.A.; Diplock, A.T.; Symons, M.C.R. Investigation of the consequences of free radical attack on lipids. In *Laboratory Techniques in Biochemistry and Molecular Biology, Techniques in Free Radical Research*; Rice-Evans, C.A., Diplock, A.T., Symons, M.C.R., Eds.; Elsevier: Amsterdam, The Netherlands, 1991; Volume 22, pp. 125–184.

## II.2

Metryka O., Wasilkowski D., Mrozik A. 2022. Evaluation of the effects of Ag, Cu, ZnO and TiO<sub>2</sub> nanoparticles on the expression level of oxidative stress-related genes and the activity of antioxidant enzymes in *Escherichia coli*, *Bacillus cereus* and *Staphylococcus epidermidis*. *International Journal of Molecular Sciences* 23(9): 4966



Article

# Evaluation of the Effects of Ag, Cu, ZnO and TiO<sub>2</sub> Nanoparticles on the Expression Level of Oxidative Stress-Related Genes and the Activity of Antioxidant Enzymes in *Escherichia coli*, *Bacillus cereus* and *Staphylococcus epidermidis*

Oliwia Metryka <sup>1,\*</sup> , Daniel Wasilkowski <sup>2,\*</sup> and Agnieszka Mrozik <sup>2</sup>

<sup>1</sup> Doctoral School, University of Silesia, Bankowa 14, 40-032 Katowice, Poland

<sup>2</sup> Institute of Biology, Biotechnology and Environmental Protection, Faculty of Natural Sciences, University of Silesia, Jagiellońska 28, 40-032 Katowice, Poland; agnieszka.mrozik@us.edu.pl

\* Correspondence: oliwia.metryka@us.edu.pl (O.M.); daniel.wasilkowski@us.edu.pl (D.W.)



Citation: Metryka, O.;

Wasilkowski, D.; Mrozik, A.

Evaluation of the Effects of Ag, Cu, ZnO and TiO<sub>2</sub> Nanoparticles on the Expression Level of Oxidative Stress-Related Genes and the Activity of Antioxidant Enzymes in *Escherichia coli*, *Bacillus cereus* and *Staphylococcus epidermidis*. *Int. J. Mol. Sci.* **2022**, *23*, 4966. <https://doi.org/10.3390/ijms23094966>

Academic Editor: Alexandru Mihai Grumezescu

Received: 29 March 2022

Accepted: 28 April 2022

Published: 29 April 2022

**Publisher's Note:** MDPI stays neutral with regard to jurisdictional claims in published maps and institutional affiliations.



**Copyright:** © 2022 by the authors. Licensee MDPI, Basel, Switzerland. This article is an open access article distributed under the terms and conditions of the Creative Commons Attribution (CC BY) license (<https://creativecommons.org/licenses/by/4.0/>).

**Abstract:** Although the molecular response of bacteria exposed to metal nanoparticles (NPs) is intensively studied, many phenomena related to their survival, metal uptake, gene expression and protein production are not fully understood. Therefore, this work aimed to study Ag-NPs, Cu-NPs, ZnO-NPs and TiO<sub>2</sub>-NPs-induced alterations in the expression level of selected oxidative stress-related genes in connection with the activity of antioxidant enzymes: catalase (CAT), peroxidase (PER) and superoxide dismutase (SOD) in *Escherichia coli*, *Bacillus cereus* and *Staphylococcus epidermidis*. The methodology used included: the extraction of total RNA and cDNA synthesis, the preparation of primers for selected housekeeping and oxidative stress genes, RT-qPCR reaction and the measurements of CAT, PER and SOD activities. It was established that the treatment of *E. coli* and *S. epidermidis* with NPs resulted mainly in the down-regulation of targeted genes, whilst the up-regulation of genes was confirmed in *B. cereus*. The greatest differences in the relative expression levels of tested genes occurred in *B. cereus* and *S. epidermidis* treated with TiO<sub>2</sub>-NPs, while in *E. coli*, they were observed under ZnO-NPs exposure. The changes found were mostly related to the expression of genes encoding proteins with PER and CAT-like activity. Among NPs, ZnO-NPs and Cu-NPs increased the activity of antioxidants in *E. coli* and *B. cereus*. In turn, TiO<sub>2</sub>-NPs had a major effect on enzymes activity in *S. epidermidis*. Considering all of the collected results for tested bacteria, it can be emphasised that the impact of NPs on the antioxidant system functioning was dependent on their type and concentration.

**Keywords:** *Escherichia coli*; *Bacillus cereus*; *Staphylococcus epidermidis*; metal nanoparticles; oxidative stress-related genes; catalase; peroxidase; superoxide dismutase

## 1. Introduction

The golden age of nanotechnology started in the 1980s, and its industrial breakthrough in the 21st century revolutionised the conventional approach to science and the production of various materials [1]. Nanoparticles (NPs) have gained particular recognition in medical applications due to their antimicrobial properties and the stability required for effective drug delivery systems; inter alia, such solutions are used as implant coatings. For example, the deposition of Ag-NPs on the surface of dental implants as a surface coating can improve the quality and biocompatibility of the implant and at the same time limit the use of conventional antibiotics [2,3].

The extensive use of NPs in many sectors of the economy and their release into various ecosystems have raised global concern about their adverse effects on living organisms, including microorganisms. Presently, intensive research is carried out on reference microbial strains as well as environmental microorganisms in order to understand the comprehensive impact of NPs on their physiological processes and the surrounding environment and

to determine the critical points of the observed effects [1,4,5]. According to the existing literature data, the major processes underlying the antibacterial effects of NPs include the disruption of the bacterial cell membrane, the generation of reactive oxygen species (ROS), the penetration of the bacterial cell membrane and the induction of intracellular antibacterial effects, including interactions with DNA and proteins [4–6]. Among these processes, the most significant attention has been paid to the generation of oxidative stress by NPs, as it has been proposed to be the leading mechanism of the biological activity of NPs. The catalytic oxidation of cellular components and building materials induced by ROS can disrupt fundamental metabolic processes and lead to cell death [4,6,7]. To mitigate the threat posed by NPs, bacteria have developed a variety of mechanisms to combat oxidative stress and balance ROS levels that lead to cellular toxicity. The literature data show that the presence of scavenging enzymes such as catalase (CAT), peroxidase (PER) and superoxide dismutase (SOD) that control and deplete ROS levels is of key importance in self-defence mechanisms against oxidative stress in bacteria [5,8,9]. However, under stressful conditions, the activity of antioxidants can be disturbed by the presence of NPs, releasing heavy metal ions and ROS and impairing the functioning of enzymes or their synthesis from the initial molecular stages. For example, in a study by Liao et al. [10], proteomic and biochemical analyses have shown that the exposure of *Pseudomonas aeruginosa* to Ag-NPs resulted in the alterations of CAT, PER and SOD activities, which was co-dependent on the generation of ROS and the up-regulation of these proteins. Additionally, such toxicological effects may depend not only on the unique characteristics of the materials tested but also on the standardised concentration. By way of illustration, in the experiment conducted by Choi et al. [11], an increase in CAT and SOD activities in *Escherichia coli* cells treated with Ag-NPs depended on the increase in the Ag-NPs concentration.

Moreover, the literature reports indicate that NPs may exhibit genotoxic properties and cause DNA and RNA damage and disrupt replication and the expression of genetic information in a cell, along with having a mutagenic effect. This mode of action can be attributed to the direct impact of NPs and the released metal ions as well as the indirect effect via the ROS-mediated and induced SOS responses in bacterial cells [6,12–15]. An interesting property of NPs is their influence on horizontal gene transfer between microorganisms, as they can facilitate this process, inter alia, through the induction of the formation of conjugation pairs or the stimulation of selected genes expression [16–18]. Furthermore, it was established that Au-NPs and Ag-NPs could damage DNA through the electrostatic interactions with phosphate groups in the polyanionic backbone of nucleic acids, in addition to the hydrophobic and van der Waals forces interactions of metal ions and to the oxygen and nitrogen atoms present in nucleic acids [13,19,20]. By contrast, RNA is more susceptible to oxidative damage caused by ROS than DNA, and, without RNA-repair mechanisms, important processes such as the regulation of transcriptional activity may be altered [9]. Additionally, despite research on gene expression and protein synthesis in microorganisms exposed to NPs, the greatest emphasis is put on stress-related, virulence and DNA-repair genes, alongside genes involved in the *quorum sensing* system, which play a vital role in the biofilm formation. Such NPs–microorganisms interactions can negatively impact the functioning of microorganisms, e.g., they can lead to disturbances in the biofilm formation and proper functioning of the *quorum sensing* system [19,21,22]. For example, the treatment of *Azotobacter vinelandii* with Ag-NPs resulted in the down-regulation of the *nifH* gene and decreased nitrogenase activity, leading to the inhibition of nitrogen fixation [23].

It is worth underlining that a limited number of studies consider the action of NPs on the gene expression, protein synthesis and metabolism of bacterial cells regarding the antioxidant defence system. The available information in this field shows the influence of various nanostructures regulating the expression of genes encoding individual antioxidants related to the effective utilisation of ROS and genes encoding proteins involved in oxidation-reduction processes. Yan et al. [24] demonstrated that the presence of Ag-NPs in *P. aeruginosa* culture induced oxidative stress and eventuated in the up-regulation of KatA and SodB ROS-related proteins. Similarly, Zhang et al. [17] reported that the relative expres-

sion of genes responsible for the ROS production in *Escherichia coli* and *Pseudomonas putida* exposed to CuO-NPs showed an up-regulation of the *sodA*, *sodB* and *katE* genes. In turn, de Celis et al. [25] only observed a significant up-regulation of *sodM* in *P. aeruginosa* under Ag-NPs and ZnO-NPs treatment compared to other oxidative stress genes. Correspondingly, an up-regulation of genes encoding SOD and a down-regulation of CAT-related genes were revealed in *Deinococcus radiodurans* cells exposed to ZnO-NPs [26].

Due to the scarce information on the direct relationship between the expression level of oxidative stress genes and the activity of the corresponding antioxidant-like proteins in bacteria under NPs stress, it seemed worthwhile to investigate this dependence thoroughly. Therefore, in this experimental study, the intended goals included: (1) assessing and comparing the transcriptional response of model *Escherichia coli*, *Bacillus cereus* and *Staphylococcus epidermidis* to the exposure of Ag-NPs, Cu-NPs, ZnO-NPs and TiO<sub>2</sub>-NPs at a half-maximal inhibitory concentration (IC<sub>50</sub>) and ½IC<sub>50</sub>; (2) measuring the activity of the antioxidant enzymes CAT, PER and SOD and (3) establishing the statistical similarities and differences between measured parameters. An experimental set-up presenting all of the issues to be tested is illustrated in Figure 1.

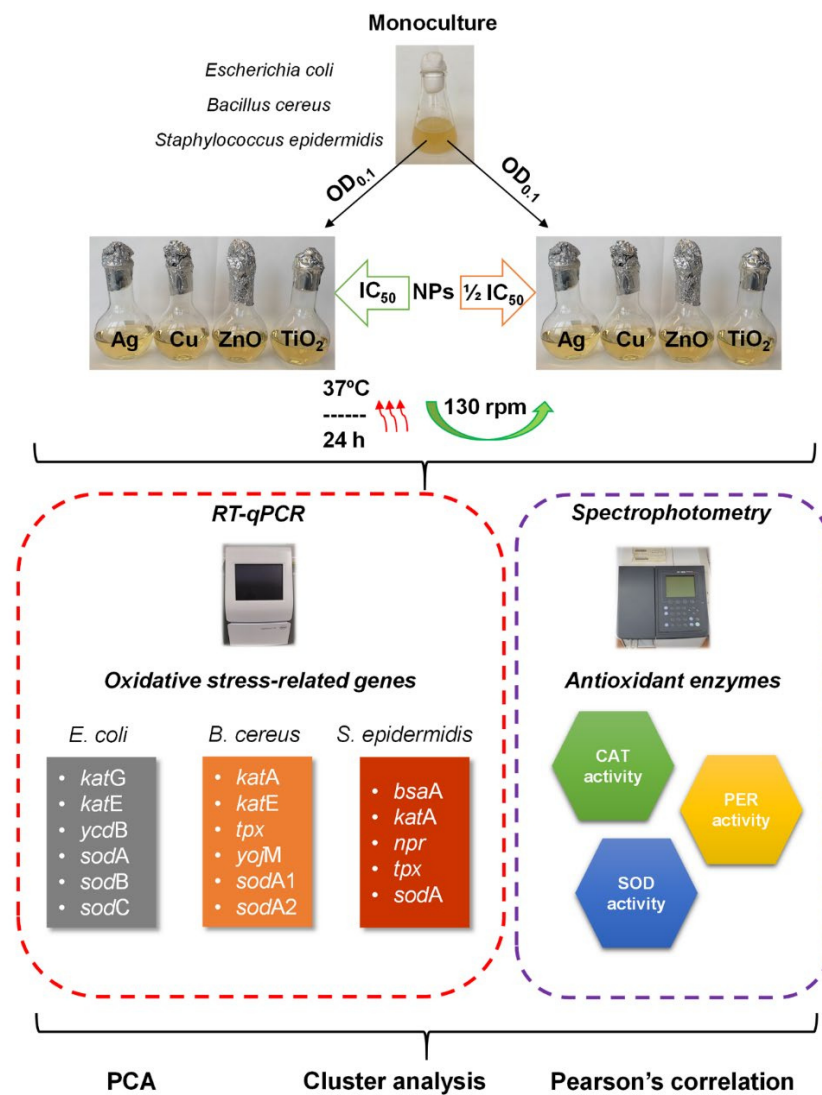


Figure 1. Diagram of experimental set-up.



## 2. Results

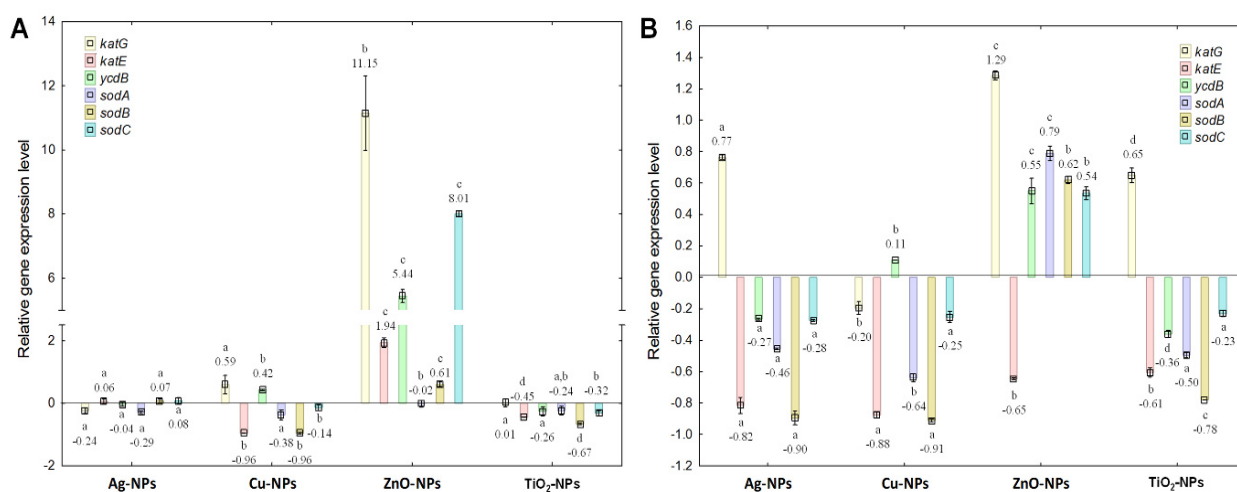
### 2.1. Analysis of the Expression Level of Tested Genes in Bacteria under NPs Exposure

Table 1 presents genes encoding antioxidant enzymes in tested bacterial strains chosen for the absolute quantification reaction against selected housekeeping genes used as internal controls. These particular genes were selected by analysing the *E. coli*, *B. cereus* and *S. epidermidis* genomes, as they all encode proteins with CAT, PER and SOD-like activity.

**Table 1.** Primer sequences for selected housekeeping and oxidative stress genes in *E. coli*, *B. cereus* and *S. epidermidis* used in the RT-qPCR reaction.

Gene/Product	Sequence of Primer		Product Length [bp]
	Forward (5'-3')	Reverse (5'-3')	
<i>E. coli</i>			
<b>Housekeeping genes</b>			
<i>gyrA</i> (DNA gyrase subunit A)	CTTCATCGAATAGACGCGG	TCTGCCGCACGTATTAAG	108
<i>gyrB</i> (DNA gyrase subunit B)	GCAAAGAAGACCACTTCCAC	AAGATATTCGGGTGGATCGG	91
<i>rpoE</i> (RNA polymerase sigma-E factor)	TACAGCAATCCGATACAGCC	TCCCGATGTGGTACAAGAAG	100
<b>Oxidative stress genes</b>			
<i>katE</i> (CAT HP11)	CATTCGGGAGTAGAGCAGTT	ATGATGAAGTGAGATCGGCA	89
<i>katG</i> (bifunctional CAT-PER)	ACGTAAATCAGGCCATCTC	TCTGGATGTTAACTGGGGTG	105
<i>ycdB</i> (heme-containing PER)	CGTAATCGGGAACATCATGC	TGAAAGAGCAGCAGACGATA	87
<i>sodA</i> (manganese SOD)	TTATCGCCTTTTTGCACCAG	GCTATCGAACGTGATTTCCGG	110
<i>sodB</i> (cytosolic iron-containing SOD)	CTTCAGCGACTTTTCCAGTC	TCTGAAGGTGGCGTATTCAA	109
<i>sodC</i> (copper-zinc SOD)	AAGCTGCCAGTGAAAAAGTC	GTTTCAGTAATGGTGACGCT	88
<i>B. cereus</i>			
<b>Housekeeping genes</b>			
<i>gyrA</i> (DNA gyrase subunit A)	TACGTTGGGCGATGAAGACC	AATCGGTGTACGCTTTCCGT	103
<i>gyrB</i> (DNA gyrase subunit B)	GCGTGGTATTCCGGTTGGTA	TATAACCGCCACCGCCAAAT	104
<i>rpoB</i> (RNA polymerase subunit beta)	ACCAGAGGGACCAAACATCG	CTGGGTCAACACGACGGTAT	101
<b>Oxidative stress genes</b>			
<i>katA</i> (main CAT)	CAACAACGTGATGGTGCGAT	GTTGAATCGCGTAAGCTGG	110
<i>katE</i> (CAT HP11)	GGCCCAACCTTAATGGAGGA	TAACCATGTACGCCAACCCC	110
<i>tpx</i> (thiol PER)	GCGCTGATTTACCATTGCTC	GAATGAAAGGTGCGGTGGT	92
<i>yojM</i> (zinc SOD-like protein)	GAAGGGTGCAGAAAACGGTG	TCAAGTGTGATGTGTGGGGC	93
<i>sodA1</i> (manganese SOD)	CCAGAAGCAATCCGTACAGC	CTCCGCCGTTTGGAGATAGG	91
<i>sodA2</i> (manganese SOD)	CGAAATAACGGTGGTGGTCA	TGCAACGTCTCCATTAGGCT	90
<i>S. epidermidis</i>			
<b>Housekeeping genes</b>			
<i>gyrB</i> (DNA gyrase subunit B)	GACAATGGCCGTGGTATTCTT	CCGAATTTACCTCCAGCGTG	98
<i>rpoB</i> (RNA polymerase subunit beta)	GGGAGCAAACATGCAACGTC	TCTCTTGGCGCTACGTGTTT	90
<i>pyk</i> (pyruvate kinase)	ACTGCTGGTGTACTACTGGA	CCTTACCAACACCTTGACCT	98
<b>Oxidative stress genes</b>			
<i>bsaA</i> (glutathione peroxidase homolog)	CGCTGCTAAAGGTATGTAACGA	TCCGGTTTCTTTGAGGGGAG	108
<i>katA</i> (CAT)	AGTCGTGATGGACAAATGCG	GTGGCTTCTTGTGTTTCAGGC	109
<i>npr</i> (NADH peroxidase)	CCAGCTACCGAGTGGCTAAA	GCCACCCGCATAGACATCTT	105
<i>tpx</i> (thiol PER)	ACGCTTACTTGCACGTTCCGG	CAGGGTAATTTCGTACCTTCGCT	89
<i>sodA</i> (SOD Mn/Fe)	TCAGCAGTGAAGGGACAGATT	CCACCGCCATTATTAGAACAG	110

To thoroughly examine the influence of NPs on the antioxidant profile, the transcriptional response of bacterial cells to NPs was assessed by comparing the relative expression level of selected genes, encoding proteins with CAT, PER and SOD-like activities. Moreover, this study allowed for the determination of correlations between product formation at the expression level of selected genes and the activity of encoded proteins. The obtained results confirmed a significant impact of NPs at  $IC_{50}$  and  $\frac{1}{2}IC_{50}$  on the relative expression level of *katE*, *katG*, *ycdB*, *sodA*, *sodB* and *sodC* genes in *E. coli* cells (Figure 2A,B). For example, ZnO-NPs at  $IC_{50}$  caused an 11-fold up-regulation of *katG* and an 8-fold up-regulation of *sodC*. By contrast, when Cu-NPs were added at  $IC_{50}$  to *E. coli* culture, there was a 1-fold reduction in the expression level of the *katE* and *sodB* genes, respectively (Figure 2A). Subsequently, the use of NPs at  $\frac{1}{2}IC_{50}$  had a divergent effect on the gene expression level compared to their expression induced by  $IC_{50}$  (Figure 2B). Overall, the findings showed that Ag-NPs, Cu-NPs and  $TiO_2$ -NPs at  $\frac{1}{2}IC_{50}$  decreased the expression level of the studied genes, while ZnO-NPs had the opposite effect. The highest 1.3-fold up-regulation was observed for *katG* in *E. coli* treated with ZnO-NPs. Interestingly, Ag-NPs and Cu-NPs at  $\frac{1}{2}IC_{50}$  down-regulated the expression of *katE* and *sodB* (about 1-fold). The statistical analysis uncovered significant differences ( $p < 0.05$ ) for the relative expression levels of *E. coli* genes between NPs treatments at different concentrations. The greatest variation between the results was noted in the data obtained for *katE*, *katG* and *sodA*. In turn, ZnO-NPs were found to be the most influential on the transcriptional response of *E. coli* cells. Nevertheless, Ag-NPs, Cu-NPs and  $TiO_2$ -NPs induced considerable but different changes in the expression levels of selected genes. Moreover, changes within the transcriptional response of *E. coli* depended on the concentration and type of NPs used and the kind of gene analysed.



**Figure 2.** The relative expression levels of *katE*, *katG*, *ycdB*, *sodA*, *sodB* and *sodC* genes in *E. coli* exposed to NPs at  $IC_{50}$  (A) and  $\frac{1}{2}IC_{50}$  (B), measured against *rpoE* as the reference gene (mean  $\pm$  SD;  $n = 4$ ). Significant statistical differences ( $p < 0.05$ ) between control and NPs treated cells ( $n = 4$ ) are represented by different letters by a two-way ANOVA test and followed by a *post-hoc* Tukey's HSD (honestly significant difference) test.

In the case of *B. cereus*, diverse and unique links were noted between the different treatments of cells with individual NPs and the expression levels of *katA*, *katE*, *tpx*, *yofM*, *sodA1* and *sodA2* genes (Figure 3A,B). It is worth underlining that the exposure of *B. cereus* to NPs induced a transcriptional response of bacterial cells consisting in up-regulating the expression of the studied genes in most samples. For example, the highest around 159-fold up-regulation of *katE* was recorded for Cu-NPs and  $TiO_2$ -NPs at  $IC_{50}$  (Figure 3A). It is also worth pointing out that ZnO-NPs and Cu-NPs at  $IC_{50}$  caused a 40- and 50-fold increase in the expression level of *yofM*, respectively. Interestingly, the exposure of *B. cereus* to Ag-NPs

at  $\frac{1}{2}IC_{50}$  caused a significant increase (165-fold) in the expression level of *katE* (Figure 3B). However, a notable decrease (about 0.5-fold) in the expression of all tested genes was confirmed after applying ZnO-NPs to bacterial culture. The results from the statistical analysis proved that all NPs at  $IC_{50}$  and  $\frac{1}{2}IC_{50}$  had a significant and differentiating effect ( $p < 0.05$ ) on the obtained data. The tested NPs mainly exhibited a strong influence on *katA* and *katE* genes ( $p = 0.000000$ ). Moreover, it was established that  $TiO_2$ -NPs had the most substantial effect on the expression of all selected genes ( $p = 0.000000$ ). Conclusively, the obtained findings demonstrated varying effects of applied NPs concentrations on the transcriptional response of *B. cereus*. The genes most susceptible to the effects of NPs were related to proteins revealing CAT and PER-like activities.

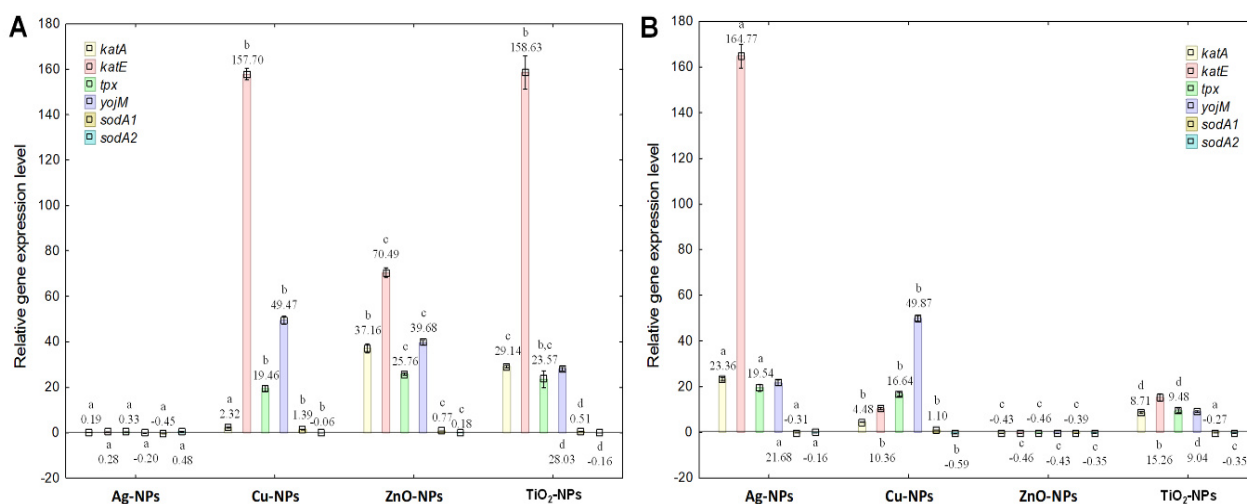


**Figure 3.** The relative expression levels of *katA*, *katE*, *tpx*, *yojM*, *sodA1* and *sodA2* genes in *B. cereus* exposed to NPs at  $IC_{50}$  (A) and  $\frac{1}{2}IC_{50}$  (B), measured against *rpoB* as the reference gene (mean  $\pm$  SD; n = 4). Significant statistical differences ( $p < 0.05$ ) between control and NPs treated cells (n = 4) are represented by different letters by a two-way ANOVA test and followed by a *post-hoc* Tukey's HSD (honestly significant difference) test.

In a parallel set of experiments, it was established that the treatment of *S. epidermidis* with NPs at both concentrations significantly altered the transcriptional response of bacterial cells, affecting the expression of *bsaA*, *katA*, *npr*, *tpx* and *sodA* genes (Figure 4A,B). Predominantly, Ag-NPs, Cu-NPs and  $TiO_2$ -NPs at  $IC_{50}$  showed a down-regulation of the tested genes, whereas adding ZnO-NPs caused their up-regulation (Figure 4A). The highest 0.6-fold decrease in the expression level was recorded for the *katA* gene in the cells exposed to Ag-NPs; however, ZnO-NPs resulted in the most distinctive increase (about 4-fold) in the expression of *bsaA*, *npr* and *sodA*. Compared to the  $IC_{50}$  dose, the application of Ag-NPs and Cu-NPs at  $\frac{1}{2}IC_{50}$  to bacterial culture caused prominent down-regulation of the tested genes, whereas ZnO-NPs and  $TiO_2$ -NPs reflected in their up-regulation. The greatest decrease in the expression of *sodA* (0.5-fold) was confirmed in the cells under Cu-NPs exposure, whereas the greatest increase (2.3-fold) in the expression of this gene occurred in the presence of ZnO-NPs. Statistical analysis revealed significant differences between the treatments of bacterial cells with both NPs concentrations ( $p < 0.05$ ). Furthermore, the highest statistical differences were calculated for the expression of *sodA* after treatment of the bacteria with Ag-NPs ( $p = 0.00027$ ), Cu-NPs ( $p = 0.000001$ ), ZnO-NPs ( $p = 0.000045$ ) and  $TiO_2$ -NPs ( $p = 0.000000$ ). It is worth underlining that  $TiO_2$ -NPs were the most impactful on the tested genes' expression levels.

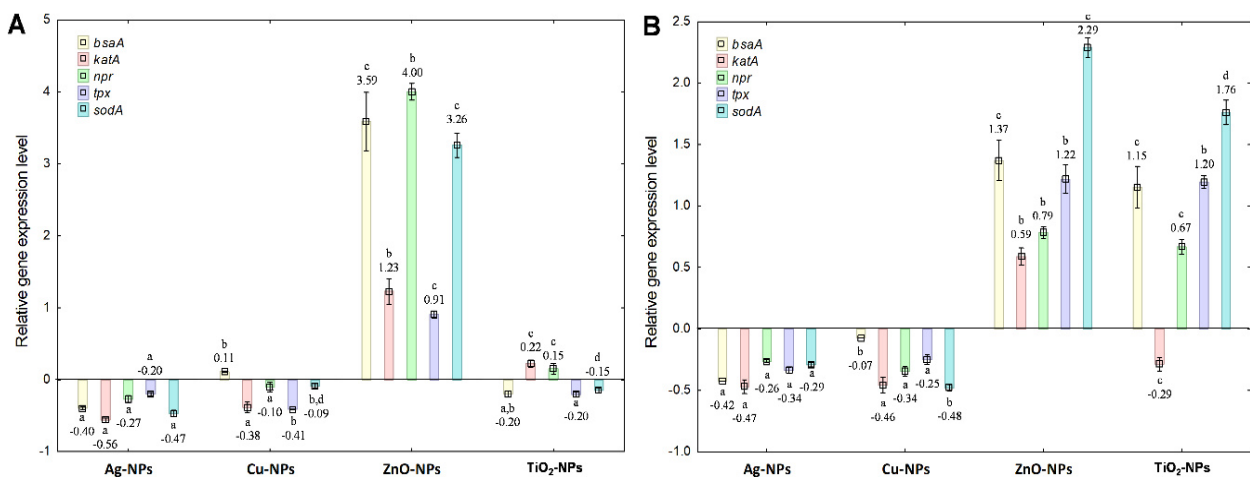


**Figure 4.** The relative expression levels of *bsaA*, *katA*, *npr*, *tpx* and *sodA* genes in *S. epidermidis* exposed to NPs at IC<sub>50</sub> (A) and 1/2 IC<sub>50</sub> (B), measured against *rpoB* as the reference gene (mean ± SD; n = 4). Significant statistical differences ( $p < 0.05$ ) between control and NPs treated cells (n = 4) are represented by different letters by a two-way ANOVA test and followed by a *post-hoc* Tukey's HSD (honestly significant difference) test.

Conclusively, significant and different changes in the genes' expression levels in each bacterial strain under NPs exposure indicate alterations in the product development at the genetic level. It was established that the treatment of *E. coli* and *S. epidermidis* resulted mainly in the down-regulation of tested genes, whilst the up-regulation of targeted genes was observed in *B. cereus* cells. Considering all of the collected data, TiO<sub>2</sub>-NPs caused the greatest differences in the transcriptional response of *B. cereus* and *S. epidermidis*, while in *E. coli*, most significant differences in the relative expression levels of tested genes occurred in the presence of ZnO-NPs. Overall, the conducted analyses confirmed most significant influence of NPs on the expression of genes encoding proteins with PER and CAT-like activity in all strains.

## 2.2. Activity of CAT, PER and SOD in Bacteria Exposed to NPs

In order to examine the functioning of the catalytic antioxidant system in bacteria cells, the activity of the primary antioxidant enzymes, including CAT, PER and SOD, was evaluated. The results obtained for *E. coli* showed a clear dependence of enzymes activity on the concentration of NPs (Figure 5A,B). The treatment of *E. coli* with ZnO-NPs and Cu-NPs at IC<sub>50</sub> resulted in the highest increase in CAT activity (Figure 5A). A similar increase in CAT activity was observed in bacteria exposed to NPs at 1/2 IC<sub>50</sub>, with ZnO-NPs and Ag-NPs having the most substantial impact on its catalytic activity (Figure 5B). Interestingly, the exposure of *E. coli* to Ag-NPs and TiO<sub>2</sub>-NPs at 1/2 IC<sub>50</sub> caused a higher (about 44% and 16%) increase in CAT activity compared to its activity at IC<sub>50</sub>. Furthermore, analysis of the variance of changes in CAT activity between individual treatments revealed significant statistical differences for Ag-NPs, Cu-NPs, ZnO-NPs and TiO<sub>2</sub>-NPs at IC<sub>50</sub> and 1/2 IC<sub>50</sub> since  $p$ -values (0.0029, 0.00026, 0.036 and 0.045, respectively) did not exceed the significance level of  $\alpha = 0.05$ . By comparison, the stimulating effect of individual NPs at IC<sub>50</sub> on PER activity in *E. coli* can be illustrated as follows: Ag-NPs < TiO<sub>2</sub>-NPs < Cu-NPs < ZnO-NPs (Figure 5A). The highest increase in PER activity occurred in the presence of ZnO-NPs at IC<sub>50</sub>. Intriguingly, Cu-NPs, ZnO-NPs and TiO<sub>2</sub>-NPs at 1/2 IC<sub>50</sub> caused a smaller increase in PER activity than these NPs at IC<sub>50</sub> (Figure 5B). It is worth noting that all NPs except for Ag-NPs resulted in significant differences between dosage treatments ( $p < 0.05$ ). In corresponding experiments relating to the measurements of SOD activity in *E. coli* exposed to NPs, a stimulating trend of individual NPs at both concentrations was established (Figure 5A,B). The highest increase in SOD activity was documented in the presence of ZnO-NPs at IC<sub>50</sub> (Figure 5A). An equally high increase in its activity was also established

for ZnO-NPs at  $\frac{1}{2}$ IC<sub>50</sub> (Figure 5B). Regarding the statistical significance between SOD functioning in *E. coli* cells under different experimental conditions, it was confirmed that only TiO<sub>2</sub>-NPs did not result in significant differences ( $p > 0.05$ ). Summarising this series of studies, it can be concluded that, among the studied NPs, the most substantial impact on the activity of antioxidant enzymes in *E. coli* showed ZnO-NPs and Cu-NPs.

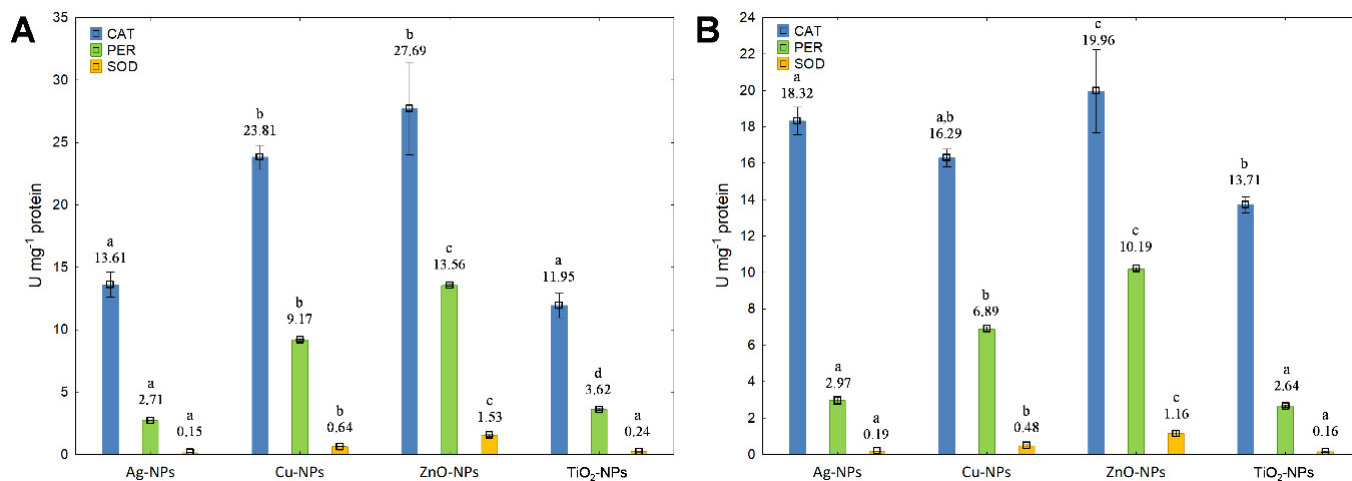


**Figure 5.** The activity of CAT, PER and SOD in *E. coli* exposed to NPs at IC<sub>50</sub> (A) and  $\frac{1}{2}$ IC<sub>50</sub> (B) (mean  $\pm$  SD; n = 3). Significant statistical differences ( $p < 0.05$ ) between control and NPs treated cells (n = 3) are represented by different letters by a two-way ANOVA test and followed by a *post-hoc* Tukey's HSD (honestly significant difference) test.

In a parallel experiment, the activity of antioxidant enzymes in *B. cereus* exposed to NPs was measured. The effect of individual NPs at IC<sub>50</sub> on the increase in CAT activity may be illustrated as follows: Ag-NPs < TiO<sub>2</sub>-NPs < Cu-NPs < ZnO-NPs (Figure 6A). A relatively high stimulation of CAT activity was recorded for Cu-NPs and ZnO-NPs. Interestingly, the activity of CAT also increased after treatment with Ag-NPs (by 192%), TiO<sub>2</sub>-NPs (by 51%) and ZnO-NPs (by 104%) at  $\frac{1}{2}$ IC<sub>50</sub>, whilst Cu-NPs caused its decrease (by 60%) compared to its activity at IC<sub>50</sub> (Figure 6B). Similar to CAT, PER of *B. cereus* was most affected by Cu-NPs and ZnO-NPs at IC<sub>50</sub>, reflecting in the increase in its activity (Figure 6A). Furthermore, Cu-NPs at IC<sub>50</sub> proved to have a greater impact on the activity of PER than Ag-NPs and TiO<sub>2</sub>-NPs. Predictably, Ag-NPs, Cu-NPs and TiO<sub>2</sub>-NPs added to the bacteria cultures at  $\frac{1}{2}$ IC<sub>50</sub> had a lower stimulating effect on PER activity than these NPs at IC<sub>50</sub> (Figure 6A,B). Based on the measurements of SOD activity, it can be concluded that Cu-NPs and ZnO-NPs at IC<sub>50</sub> had the greatest impact on the stimulation of this enzyme activity (Figure 6A). Interestingly, the treatment of *B. cereus* with ZnO-NPs at  $\frac{1}{2}$ IC<sub>50</sub> in contrast to IC<sub>50</sub> resulted in a higher increase in SOD activity by 249% (Figure 6B). It is worth underlining that the obtained findings for CAT, PER and SOD activities in *B. cereus* proved to be statistically significant for both concentrations of all NPs ( $p < 0.05$ ). Overall, the greatest changes in the activity of assayed enzymes in cells treated with NPs at IC<sub>50</sub> and  $\frac{1}{2}$ IC<sub>50</sub> were observed for CAT and SOD. On the other hand, the greatest differentiation of the overall enzymatic activity in bacterial cells exposed to NPs at IC<sub>50</sub> and  $\frac{1}{2}$ IC<sub>50</sub> was observed in the presence of Cu-NPs and ZnO-NPs.

In the case of *S. epidermidis*, it is difficult to indicate the similarities in the influence of individual NPs on the activity of CAT, SOD and PER due to their very diverse and often contradictory effect on the activity of tested enzymes. Since each NPs had a different effect on the antioxidant activity profile, it was found that the presence of Cu-NPs (IC<sub>50</sub>) caused a decrease in CAT activity, whilst other treatments resulted in the stimulation of CAT functioning (Figure 7A). The greatest increase in CAT activity was recorded for TiO<sub>2</sub>-NPs at IC<sub>50</sub>. Comparatively, TiO<sub>2</sub>-NPs at  $\frac{1}{2}$ IC<sub>50</sub> had a smaller stimulating effect on CAT activity by 87% than at IC<sub>50</sub> (Figure 7B). In turn, an opposite effect of Cu-NPs and ZnO-NPs at both

concentrations on CAT activity was documented. Moreover, significant differences in CAT activity at  $IC_{50}$  and  $\frac{1}{2}IC_{50}$  were established for Cu-NPs ( $p = 0.00011$ ), ZnO-NPs ( $p = 0.028$ ) and  $TiO_2$ -NPs ( $p = 0.000003$ ), except for Ag-NPs ( $p = 0.058$ ). Simultaneously, the exposure of *S. epidermidis* to NPs at both concentrations reduced PER activity, except for  $TiO_2$ -NPs at  $IC_{50}$  generating the increase in its activity (Figure 7A,B). The high decrease in PER activity occurred in the cells exposed to ZnO-NPs at  $IC_{50}$  and  $\frac{1}{2}IC_{50}$ . Statistical analysis revealed significant differences in the activity of PER treated with Ag-NPs ( $p = 0.0046$ ), ZnO-NPs ( $p = 0.014$ ) and  $TiO_2$ -NPs ( $p = 0.000001$ ), except for Cu-NPs ( $p = 0.088$ ). The conducted research also confirmed an enhancing impact of NPs on SOD activity in *S. epidermidis* (Figure 7A,B). The highest increase in SOD activity was ascertained for Ag-NPs and  $TiO_2$ -NPs at  $IC_{50}$ . Interestingly, the treatment of bacteria with  $TiO_2$ -NPs at  $\frac{1}{2}IC_{50}$  caused a significant decrease in SOD activity by 103% (Figure 7B). It is worth pointing out that both Ag-NPs and Cu-NPs exhibited a smaller inhibiting effect on SOD activity at  $\frac{1}{2}IC_{50}$  than at  $IC_{50}$ . Moreover, the obtained findings for SOD activities were demonstrated to be statistically significant for both concentrations of all NPs ( $p < 0.05$ ).

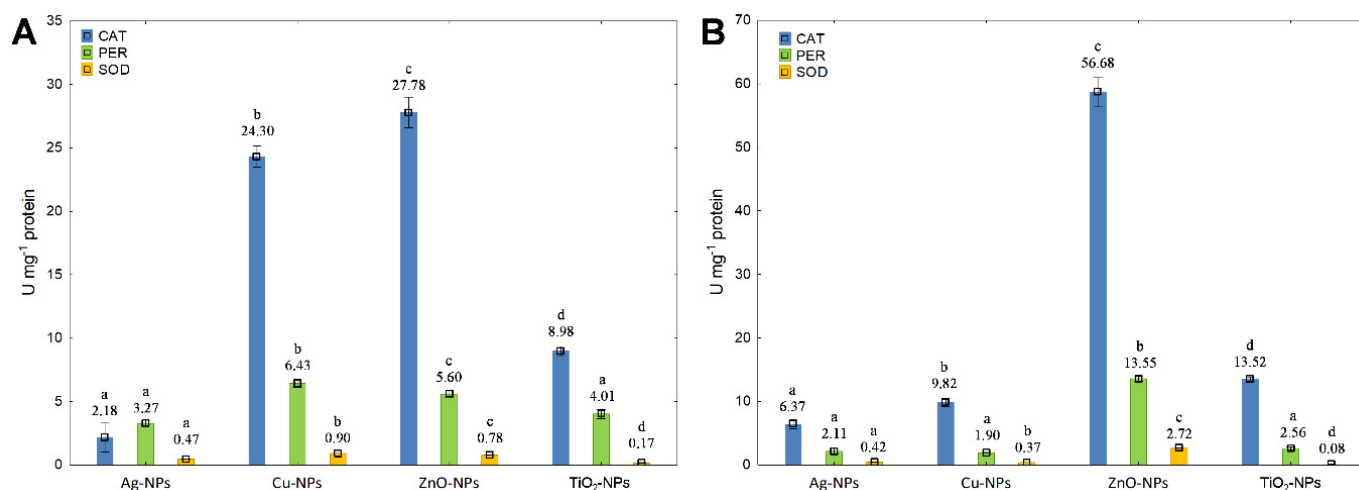


**Figure 6.** The activity of CAT, PER and SOD in *B. cereus* exposed to NPs at  $IC_{50}$  (A) and  $\frac{1}{2}IC_{50}$  (B) (mean  $\pm$  SD;  $n = 3$ ). Significant statistical differences ( $p < 0.05$ ) between control and NPs treated cells ( $n = 3$ ) are represented by different letters by a two-way ANOVA test and followed by a *post-hoc* Tukey's HSD (honestly significant difference) test.

Conclusively, considering all of the collected results for *E. coli*, *B. cereus* and *S. epidermidis*, it can be emphasised that the impact of NPs on the antioxidant system functioning was dependent on their type and concentration. Furthermore, *E. coli* and *B. cereus* under NPs exposure were characterised by increased activity of antioxidants, mainly affected by ZnO-NPs and Cu-NPs. In turn,  $TiO_2$ -NPs had a major effect on enzymes activity in *S. epidermidis*. More significant differences in enzymes activity were found for *B. cereus* and *S. epidermidis* than for *E. coli*. The obtained findings indicated different degrees of sensitivity and susceptibility of the tested strains to varying concentrations of NPs.

### 2.3. Statistical Data Exploration

Statistical analyses including PCA and cluster analysis were performed to evaluate the NPs treatment variability and variance between the whole set of data. At the same time, a cluster analysis of all variables was carried out in order to check whether the examined variables are statistically related to each other and whether there are correlations in the collected data. Additionally, the interdependence of the tested components and the NPs-concentration was included. PCA analyses and a coordination biplot for *E. coli* distinguished two clusters along PC1, separating ZnO-NPs as the most differentiating NPs (Figure 8B,D). Two clusters along PC1 were also created for *B. cereus*, including Cu-NPs

with ZnO-NPs, Ag-NPs with control and separate for TiO<sub>2</sub>-NPs (Figure 9B,D). Similar results to *E. coli* were obtained for *S. epidermidis* (Figure 10B,D).

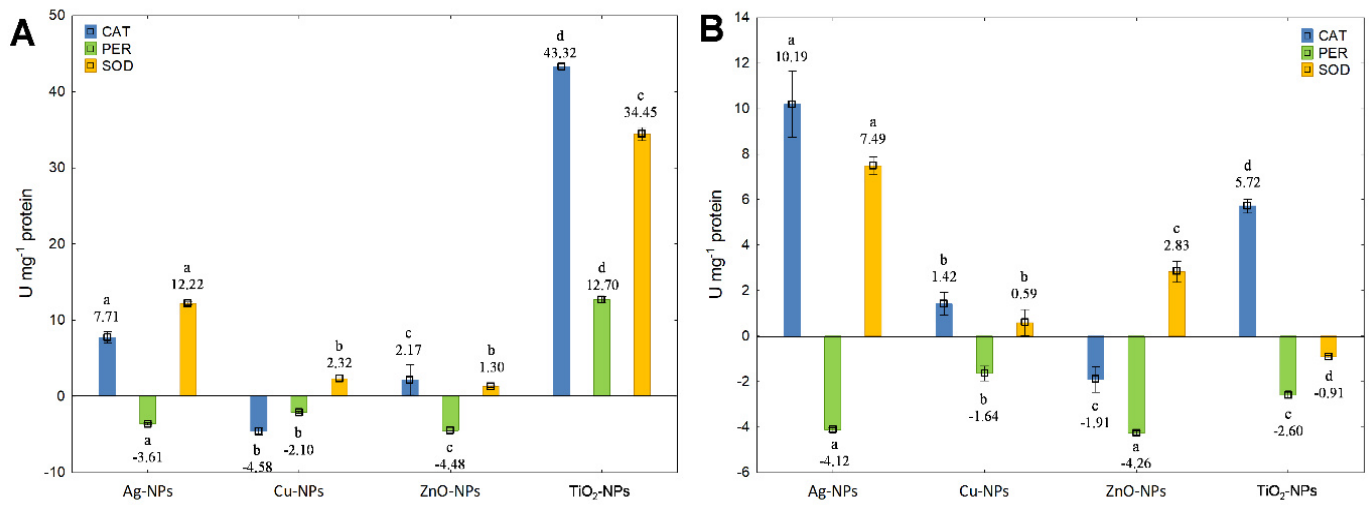


**Figure 7.** The activity of CAT, PER and SOD in *S. epidermidis* exposed to NPs at IC<sub>50</sub> (A) and 1/2 IC<sub>50</sub> (B) (mean ± SD; n = 3). Significant statistical differences ( $p < 0.05$ ) between control and NPs treated cells (n = 3) are represented by different letters by a two-way ANOVA test and followed by a *post-hoc* Tukey's HSD (honestly significant difference) test.

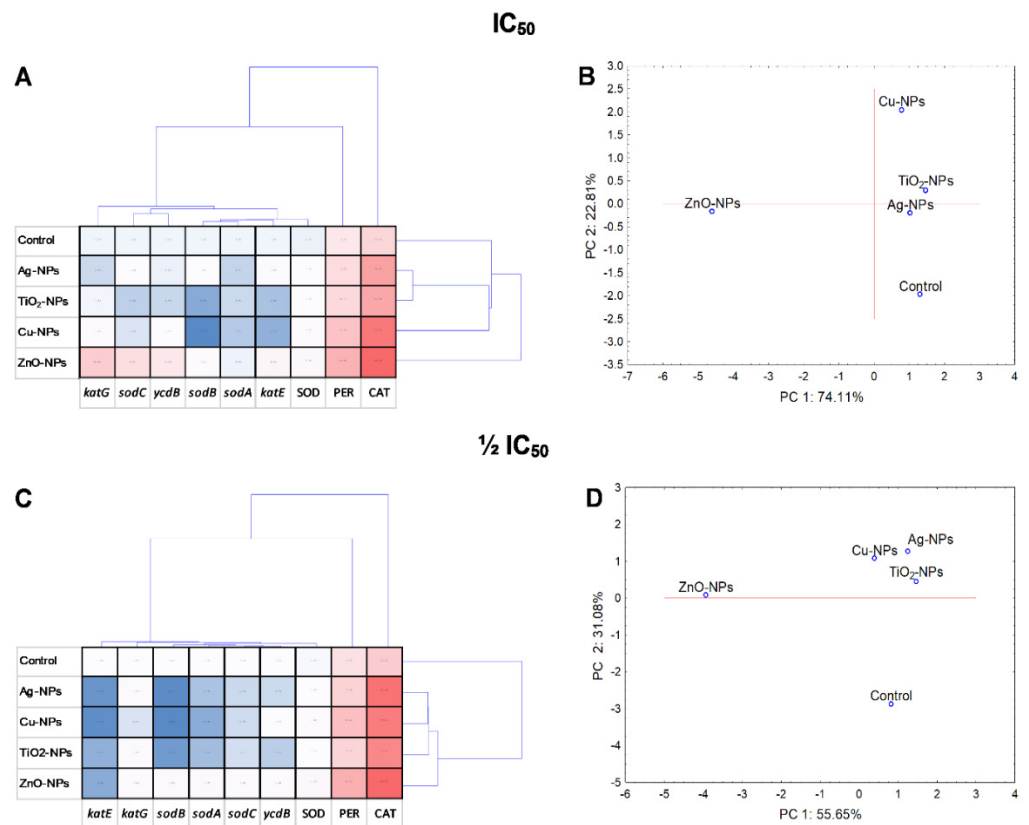


**Figure 8.** Projection of cluster analysis dendrograms (A,C) and PCA analysis biplots (B,D) for *E. coli* exposed to NPs at IC<sub>50</sub> and 1/2 IC<sub>50</sub>.

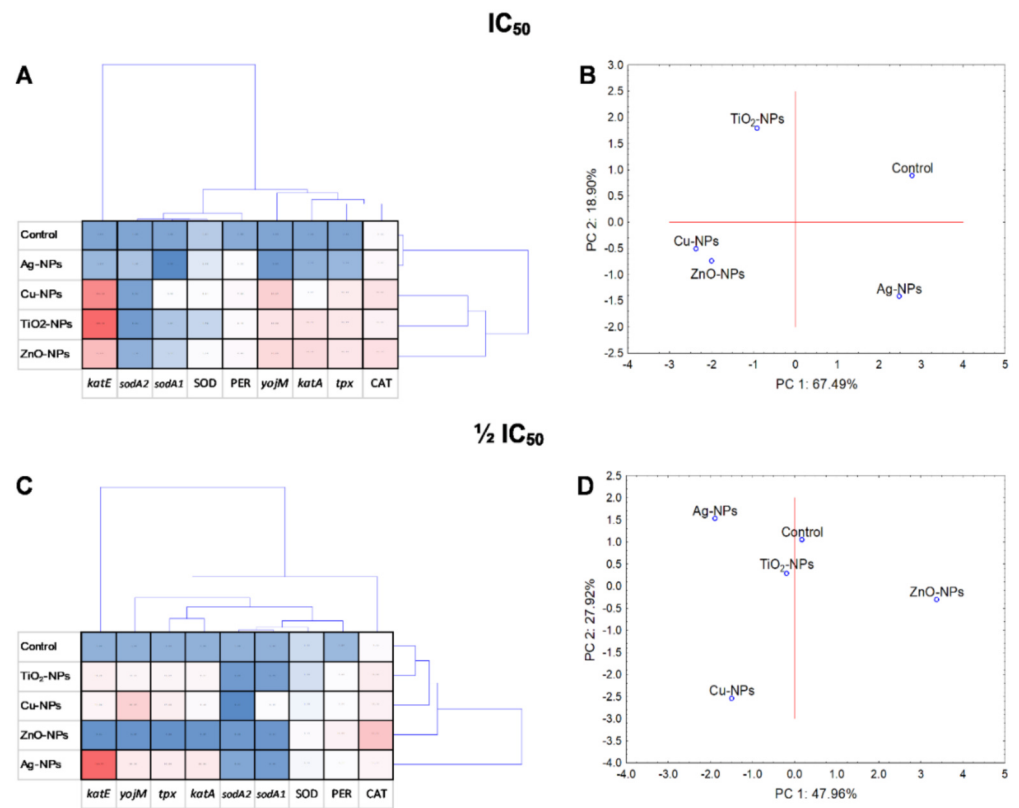


**Figure 9.** Projection of cluster analysis dendrograms (A,C) and PCA analysis biplots (B,D) for *B. cereus* exposed to NPs at IC<sub>50</sub> and 1/2 IC<sub>50</sub>.

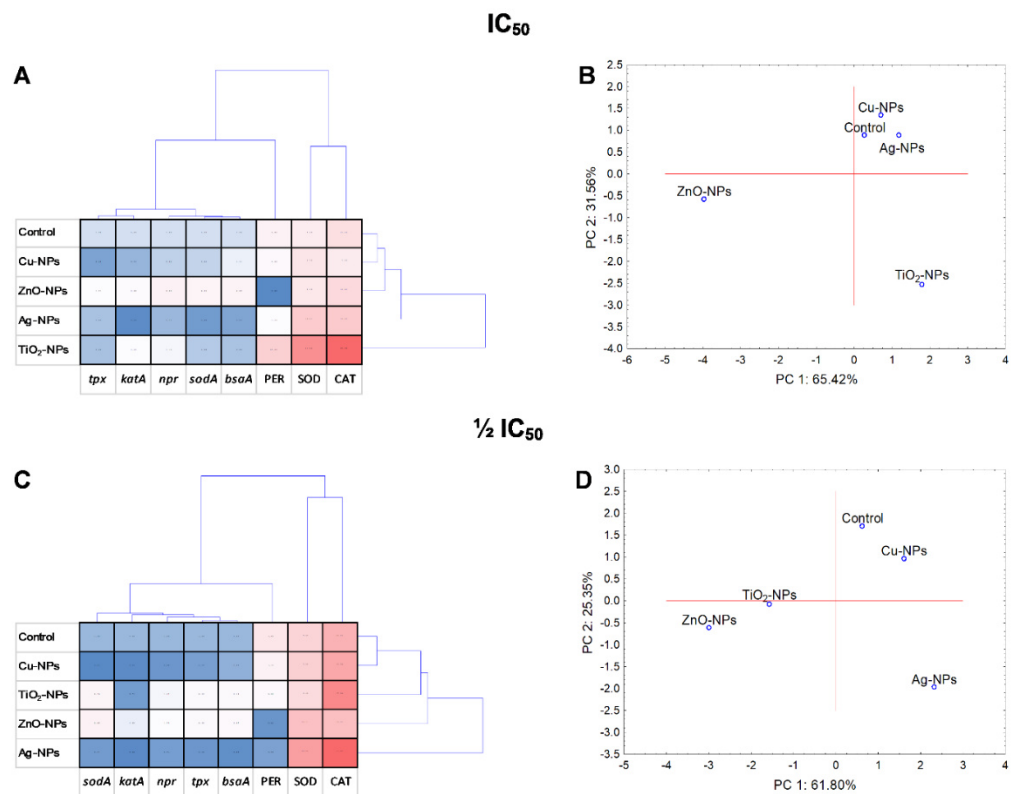


**Figure 10.** Projection of cluster analysis dendrograms (A,C) and PCA analysis biplots (B,D) for *S. epidermidis* exposed to NPs at IC<sub>50</sub> and 1/2 IC<sub>50</sub>.



The performed cluster analysis displayed a correlation of results specific for each strain. For example, the diagram generated for *E. coli* exposed to NPs revealed that the most differentiating were ZnO-NPs, while Ag-NPs and TiO<sub>2</sub>-NPs had a comparable impact on bacteria (Figure 8A,C). Additionally, it was demonstrated that PER and CAT activity and the expression level of *katG* in *E. coli* had a major discriminating influence on the obtained data. It is worth pointing out that a strong positive correlation ( $p < 0.05$ ) was validated for PER with CAT ( $r = 0.950$ ) and *katG* with SOD ( $r = 0.941$ ), *katE* ( $r = 0.945$ ), *ycdB* ( $r = 0.998$ ) and *sodC* ( $r = 0.997$ ) (Table S1). Regarding *B. cereus*, the obtained dendrogram projection revealed two separate groups for IC<sub>50</sub>. The first included the control and Ag-NPs, while the second consisted of other NPs treatments (Figure 9A). It was documented that ZnO-NPs along with *katE*, PER and *yojM* had the most differentiating influence on the data set. Additionally, notable positive relationships ( $p < 0.05$ ) were only observed for *yojM* with CAT ( $r = 0.929$ ), PER ( $r = 0.882$ ), *tpx* ( $r = 0.892$ ) and *sodA1* ( $r = 0.96$ ) and for PER with SOD ( $r = 0.888$ ) (Table S2). The dendrogram created for *S. epidermidis* showed the formation of two groups, one dedicated to TiO<sub>2</sub>-NPs and the other containing other treatments (Figure 10A). It was proved that all analysed enzymes were the most differentiating variables, without correlation ( $p < 0.05$ ) with the relative genes' expression levels (Table S3).

The PCA and cluster analyses revealed that the dose of NPs had a significant impact on the oxidative system of *B. cereus* and *S. epidermidis*, especially in the case of TiO<sub>2</sub>-NPs, Ag-NPs and ZnO-NPs. Conversely, the results from PCA for *E. coli* showed that IC<sub>50</sub> and  $\frac{1}{2}$ IC<sub>50</sub> NPs concentration had a slight effect on the enzymes activity and genes expression.

### 3. Discussion

In recent years, advances in nanotoxicological studies show that both the intentional and unintentional exposure of living organisms to NPs force them to overcome toxicological effects and thus precisely model biological activity profiles. The often diverse experimental data on the cytotoxicity of various NPs present a challenge to the scientific community due to the complexity and difficulty of verifying the extremely complex microorganism–NPs interactions. As each type of NPs causes a different cellular bacterial response, various assays and research methods are critical in tracking NPs-induced changes at the molecular level. Understanding these changes is essential to ensuring their safe application and to defining their impact when released into various ecosystems [27–29].

In the conducted studies, the combination of transcription and enzymatic analyses allowed for a new and in-depth assessment of the expression level of genes encoding antioxidant enzymes and other related products, together with the precise determination of the correlation and relationship between these intracellular processes in model *E. coli*, *B. cereus* and *S. epidermidis* strains. Such an approach to the studied topic revealed that the influence of NPs on the analysed phenomena depended on their type and current concentration in the bacterial culture. It is worth underlining that the concentration of NPs was not always associated with the higher impact of NPs on the tested processes. For example, Ag-NPs, Cu-NPs and TiO<sub>2</sub> at  $\frac{1}{2}$ IC<sub>50</sub> appear to be more toxic to tested bacteria than at IC<sub>50</sub>. Such a dose-dependency was also documented by Leung et al. [30], who established that TiO<sub>2</sub>-NPs at a lower concentration had greater influence on the expression of ROS-related proteins than at a higher concentration. The divergent effects of NPs at different concentrations on bacterial cells may be related to their bioavailability depending on the ability of these structures to agglomerate/aggregate, changing their direct contact with the cell. In this work, this is clearly shown by the opposite results obtained in the same analyses for selected strains and NPs. For example, an up-regulation of *katE* and *katA* genes in *E. coli* and *S. epidermidis* occurred after exposure to ZnO-NPs and TiO<sub>2</sub>-NPs at IC<sub>50</sub>, respectively; however, an opposite effect was observed at  $\frac{1}{2}$ IC<sub>50</sub>. NPs have different and more effective properties than their larger counterparts. It is worth emphasising that there are no identical NPs at the atomic level [31,32]. Furthermore, it has been observed that the size of NPs affects their various properties, including toxicity, which causes various functional changes in the cell [31]. Here, no size-toxicity of NPs was observed, while

the main factors influencing the variability of the obtained results could be the rather different atomic structures, composition and dosage of the tested NPs. This is justified by the toxicity of the heavy metals themselves, because, for example, Cu and Ag have been used since ancient times as antibacterial agents [33,34]. However, they may show different toxicological properties as NPs compared to their ionised form. Confirming this possibility, Peszke et al. [35] reported that Cu as Cu/SiO<sub>2</sub> nanocomposite (NCs) was more toxic to *E. coli*, *Pseudomonas putida* and *Arthrobacter globiformis* than Cu ions; however, an opposite effect was observed for Ag ions and Ag/SiO<sub>2</sub>-NCs. These results further confirm that the toxicity of NPs depends on their aggregation/agglomeration and the release of bioavailable metal ions.

Previous studies have suggested that the presence of NPs in bacterial cultures may influence their antioxidant activity and the transcription of stress-related genes responsible for protecting bacterial cells from oxidative stress [30,36]. Herein, the presented results confirmed the diversified changes in these cellular processes, depending on the strain tested. In the case of *E. coli*, it was established that the transcriptional activity of *katG* and *katE* genes encoding CAT and PER-like proteins was affected by different NPs treatments. The changes in the transcriptional activity of these genes were directly proportional to the overall activity of CAT and PER enzymes, especially in the presence of ZnO-NPs and Cu-NPs at IC<sub>50</sub>. It should be emphasised that the activity of CAT in *E. coli* was higher in all samples than PER activity, even in the control conditions. This phenomenon may be explained by the fact that in *E. coli* are present two types of CAT: hydroperoxidase I (HPI) and hydroperoxidase II (HPII), with bifunctional CAT-PER and monofunctional CAT-like activities, respectively [37,38]. The level of HPI is regulated by the expression of *katG*, which is induced by H<sub>2</sub>O<sub>2</sub>. By contrast, *katE* encoding stable HPII is constitutively expressed, independently of H<sub>2</sub>O<sub>2</sub> [37–39]. Considering this, the increase in CAT activity in *E. coli* cells treated with NPs may result from stimulated HPI activity dependent on the presence of H<sub>2</sub>O<sub>2</sub>. This is in agreement with our previous findings, which revealed that the tested NPs, especially ZnO-NPs and Cu-NPs, induced the formation of H<sub>2</sub>O<sub>2</sub> along with other types of ROS in bacterial cells [40]. Additionally, a positive correlation between CAT and PER activity along with the expression of *katG* and *katE* genes was confirmed by statistical analysis. Moreover, a lower stimulation of SOD activity compared to the CAT and PER activity can be attributed to the down-regulation of genes encoding corresponding proteins. On the contrary, the considerable up-regulation of *sodC* in *E. coli* treated with ZnO-NPs at IC<sub>50</sub> correlated with greater activity of SOD. This may be explained by the relatively high concentration of Zn<sup>2+</sup> ions in the cells, this being one of the cofactors of the encoded enzyme. This association was further explained by the positive correlation between SOD general activity and the expression of *sodC*. Although many tested genes in *E. coli* cells were down-regulated, it was established that this did not affect the activity of the antioxidant defence system under NPs stress. It is worth pointing out that mRNA abundance present in a cell at a given time is not always complementary to protein quantity [41]. Considering other mechanisms of the biological activity of NPs, it can be hypothesised that the observed down-regulation of genes encoding antioxidants may be attributed to the increased regulation of genes related to the repair of bacterial outer layers or nucleic acids, as well as genes necessary to maintain cell homeostasis [41].

Conversely, the exposure of *B. cereus* cells to NPs resulted in the up-regulation of most examined genes, corresponding with increased overall activity of CAT, PER and SOD. This may suggest the rapid response of bacterial cells to the stressful conditions caused by the presence of NPs. For example, a relatively high up-regulation of *yojM* was correlated with elevated SOD activity. This is particularly true for ZnO-NPs and Cu-NPs treatments, because the SOD-like protein encoded by *yojM* uses Zn<sup>2+</sup> as a cofactor and can bind Cu<sup>2+</sup>, which in high concentrations enhances the enzyme activity. Furthermore, *sodA1* in *B. cereus* is constitutively expressed, whilst *sodA2* expression depends on the growth stages of bacteria together with intracellular O<sub>2</sub><sup>·−</sup> concentration [42–44]. This explanation is consistent with our previous study because it links the up-regulation of *sodA2*

by Ag-NPs and ZnO-NPs at IC<sub>50</sub> with the formation of O<sub>2</sub><sup>·-</sup> [40]. Similarly, the increased relative expression level of *katE* in *B. cereus* under Cu-NPs exposure was associated with a stimulation of CAT activity. The *katA* gene encodes vegetative CAT and *katE* encodes σ<sup>B</sup>-dependent CAT characterised by different transcriptional activity under stress conditions. In a study by Ganesh Babu et al. [45], the expression of *katE* in *B. cereus* exposed to AgNO<sub>3</sub> was directly induced by Ag<sup>+</sup> ions. This may also be the reason why Ag-NPs at ½IC<sub>50</sub> caused a high up-regulation of *katE*. Interestingly, the transcriptional activity of this gene was not reflected in accelerated CAT activity. The reason may be the inactivation of the protein or the inhibition of its synthesis at the translation level through the prevention of tRNA binding to a small ribosome subunit [6,46]. The obtained findings for *B. cereus* revealed that an increase in the transcriptional response of bacterial cells was associated with increased antioxidant function.

Contrary to the strains described above, the experimental data collected for *S. epidermidis* showed significant discrepancies between the expression levels of the studied genes and the activity of their molecular counterparts. Despite these differences, statistical analyses showed a positive correlation between all of the results. Generally, the increase in the expression of selected genes was positively correlated with the activity of the antioxidant enzymes, while a down-regulation usually had the opposite effect. For example, a relatively high up-regulation of *katA* in the cells treated with ZnO-NPs at ½IC<sub>50</sub> was not reflected in the stimulation of CAT activity. Gene *katA* encodes CAT and is regulated by Fe<sup>2+</sup> [47]. Zn<sup>2+</sup> and Cu<sup>2+</sup> cations can form very stable structures with proteins and bind to protein sites that are not their characteristic binding sites, such as Fe-S clusters [48]. Therefore, it can be assumed that the free metal ions may interact with protein groups (-SH, -NH<sub>2</sub>, -COOH) and Fe-S centres, causing their inactivation [6,49]. Additionally, disturbances in metal homeostasis and H<sub>2</sub>O<sub>2</sub> detoxification can lead to the inactivation of Fe-dependent enzymes through the oxidation of Fe<sup>2+</sup> to Fe<sup>3+</sup> and its dissociation, leaving an open site for Zn<sup>2+</sup> attachment [50]. It is worth underlining that, generally, the down-regulation of *bsaA*, *npr* and *tpx* in *S. epidermidis* was correlated with relatively low overall activity of PER-like proteins; however, the opposite dependency was documented for ZnO-NPs. A PER-like protein encoded by *tpx* contains a disulphide bond in the structure, which may be a target for the negative effect of ZnO-NPs. Previous studies have shown that metal oxide NPs such as Fe<sub>3</sub>O<sub>4</sub>@Au-NPs had a strong affinity to the protein's disulphide bonds, altering the functioning of the bacterial redox system [51]. In turn, the expression of *sodA* in *S. epidermidis* is regulated by intracellular and extracellular levels of O<sub>2</sub><sup>·-</sup> [52]. In this study, the high SOD activity and the high expression of the corresponding gene in the cells cultured with TiO<sub>2</sub>-NPs (IC<sub>50</sub>) were closely related to the high intracellular concentration of O<sub>2</sub><sup>·-</sup> documented in our previous study [40].

The number of works linking the antioxidant activity of bacteria with the expression of the relevant genes is almost invisible. This is because most research focuses on analysing gene expression and the accompanying desired cytotoxic changes in microbial cells. The research findings published so far concerned the changes in the expression level of selected genes belonging to designated categories, including biological processes (e.g., fatty acid metabolic processes), stress responses (e.g., oxidative stress, osmotic stress) and genetic information processing (e.g., DNA repair) [30,36,41,53]. Since no direct correlation between the expression of genes related to oxidative stress and changes in the antioxidant defence system has been experimentally confirmed, comparing studies at the molecular level is a big challenge. Notwithstanding this, Sohm et al. [41] performed a global transcriptomic and proteomic analysis combined with chemical and biochemical analyses for *E. coli* exposed to TiO<sub>2</sub>-NPs. Among 1702 analysed genes, 152 were found to be differentially expressed, with 68 up-regulated and 84 down-regulated. Interestingly, the transcript level of *sodC* encoding SOD (Cu-Zn) was increased by 1.5-fold. In another study by Moore et al. [36], the treatment of *E. coli* with CuO-NPs resulted in a significant 3.4-fold increase in *sodA* expression and other oxidative stress genes. Similarly, the exposure of *Campylobacter jejuni* to ZnO-NPs had a stimulating effect on *katA* and *sodB* expression, causing their 6-fold

and 2-fold increase, respectively [54]. By comparison, in this study, a down-regulation of *sodA* and *sodC* was revealed in *E. coli* treated with Cu-NPs and TiO<sub>2</sub>-NPs at IC<sub>50</sub> and  $\frac{1}{2}$ IC<sub>50</sub>. In studies on the effects of ZnO-NPs and TiO<sub>2</sub>-NPs on *E. coli*, Leung et al. [30] found that although ZnO-NPs up-regulated genes associated with ROS-related proteins, they had lower antimicrobial activity compared to TiO<sub>2</sub>-NPs, indicating their opposite effect on gene transcription activity. Additionally, the authors observed a dose-dependent effect, similar to that presented in this paper. For example, ZnO-NPs and TiO<sub>2</sub>-NPs at a higher concentration decreased the expression level of the thiol peroxidase gene, while a lower dose increased its expression.

#### 4. Materials and Methods

##### 4.1. Bacterial Strains, Nanoparticles and Culture Conditions

This study was conducted using three model bacteria strains, *Escherichia coli* (ATCC<sup>®</sup> 25922<sup>™</sup>), *Bacillus cereus* (ATCC<sup>®</sup> 11778<sup>™</sup>) and *Staphylococcus epidermidis* (ATCC<sup>®</sup> 12228<sup>™</sup>), equipped from American Type Culture Collection (ATCC). The microorganisms were cultured in lysogeny broth (LB mix; tryptone 10 g L<sup>-1</sup>, NaCl 10 g L<sup>-1</sup>, yeast extract 5 g L<sup>-1</sup>) under exposure to four types of nanoparticles, Ag-NPs (cat. 576832, Sigma-Aldrich, <100 nm), Cu-NPs (cat. 774081, Sigma-Aldrich, 25 nm), TiO<sub>2</sub>-NPs (cat. US1019F, US Research, 20 nm) and ZnO-NPs (cat. 677450, Sigma-Aldrich, <50 nm), at a half-maximal inhibitory concentration (IC<sub>50</sub>) and at a concentration equal to half IC<sub>50</sub> ( $\frac{1}{2}$ IC<sub>50</sub>) (Table 2). The controls were bacterial cells not treated with NPs. Prior to genetic analysis, the bacteria were grown for 4–5 h at 37 °C and under shaking conditions (140 rpm) until they reached the logarithmic growth phase; however, in biochemical tests aimed at measuring the activity of the antioxidant enzymes catalase (CAT), peroxidase (PER) and superoxide dismutase (SOD), the bacteria were cultivated for 24 h to achieve substantial enzyme production.

**Table 2.** The IC<sub>50</sub> and  $\frac{1}{2}$ IC<sub>50</sub> values of tested NPs against bacterial strains [40].

Type of NPs (Size, nm)	<i>E. coli</i>		<i>B. cereus</i>		<i>S. epidermidis</i>	
	Toxicological Parameters [mg L <sup>-1</sup> ]					
	IC <sub>50</sub>	$\frac{1}{2}$ IC <sub>50</sub>	IC <sub>50</sub>	$\frac{1}{2}$ IC <sub>50</sub>	IC <sub>50</sub>	$\frac{1}{2}$ IC <sub>50</sub>
Ag-NPs (<100)	7.84	3.92	480.10	240.05	442.20	221.10
Cu-NPs (25)	180.80	90.40	52.15	26.075	112.00	56.00
TiO <sub>2</sub> -NPs (20)	43.40	21.70	50.30	25.15	703.40	351.70
ZnO-NPs (<50)	176.10	88.05	319.10	159.55	201.70	100.85

##### 4.2. Extraction of Total RNA and cDNA Synthesis

To isolate the total RNA, the bacterial cultures treated with NPs were centrifuged at 5000 rpm and 4 °C for 25 min. The supernatant was suspended, and the remaining precipitate was washed three times with sterile Millipore water, each time centrifuging the probe content at 14,000 rpm and 4 °C for 10 min. The precipitate after the final wash was used for the extraction of total RNA from the bacterial cells using a GeneMATRIX Universal RNA Purification Kit (cat. E3598, EURx, Gdańsk, Poland). For Gram-positive bacteria, an additional incubation with lysosome at 37 °C for 1 h was performed in order to disintegrate the double-layer of peptidoglycan of the cell wall. The extracted total RNA was subjected to additional purification with RNase-free DNase (Invitrogen, ThermoFisher Scientific, Waltham, MA, USA) to digest the residual genomic DNA present in the samples [55]. The concentration and purity of collected RNA were assessed using an ND-1000 NanoDrop spectrophotometer (ThermoFisher Scientific, Waltham, MA, USA) through the measurement of the absorbance of acquired samples at 230, 260 and 280 nm and the calculating of 260/280 and 260/230 optical density (OD) ratios [36,41,55]. Moreover, the quality and integrity of the obtained RNA samples were examined through agarose gel electrophoresis [55].

The synthesis of cDNA templates was carried out in triplicates using the RevertAid First Strand cDNA Synthesis Kit (cat. K1621, ThermoFisher Scientific, Waltham, MA, USA). For this purpose, 1 µg of total RNA from each sample was used [55]. Aliquots of cDNA were stored at −21 °C for further experiments.

#### 4.3. Preparation of Primers

The specific primers for the tested genes were designed using the Primer-BLAST designing tool (<https://www.ncbi.nlm.nih.gov/tools/primer-blast/> accessed on 25 March 2022), and genome nucleotide sequences are available for each strain at the ATCC site (<https://genomes.atcc.org/genomes/> accessed on 25 March 2022) (Table 1). Each primer pair was designed to have the optimal sequence of 20 nucleotides with ≥50% of GC pairs and ≥60 °C melting temperature ( $T_m$ ) to provide the high specificity of starter annealing to the cDNA template in the mainstream reaction [56]. The specificity of the designed primers was initially tested using control reaction with Color Taq PCR Master Mix (2x) (cat. E2525, EURx, Gdańsk, Poland) to eliminate incorrectly matched primers to the generated cDNA template.

#### 4.4. Study of the Expression Level of Genes Encoding Antioxidant Proteins

The expression of oxidative stress genes was assessed through the RT-qPCR reaction using a LightCycler® 480 SYBR Green I Master (cat. 04707516001, Roche, Basel, Switzerland). The analysis was carried out in 96-well Multiwell plates in two biological and three technical replicates [55]. The fluorescence signal from the tested samples was measured using a LightCycler® 96 Real-Time PCR System (Roche, Basel, Switzerland) under the following experiment set-up: preincubation at 95 °C for 10 min, 3 step amplification in 45 cycles consisting of 95 °C—10 s, 60 °C—10 s and 72 °C—10 s, melting at 97 °C—1 s, 65 °C—60 s and 95 °C—10 s and cooling at 40 °C for 10 s [55]. The results from the melting curve assays were used as supplementary data for checking the specificity of the amplification reactions [36,41]. Furthermore, RT-qPCR's efficiency was examined by preparing standard curve quantification of the serial dilution of the cDNA control template and each primer pair. The efficiency of the RT-qPCR reaction was calculated by a qPCR Efficiency Calculator provided by ThermoFisher Scientific (<https://www.thermofisher.com/pl/en/home/brands/thermo-scientific/molecular-biology/molecular-biology-learning-center/molecular-biology-resource-library/thermo-scientific-web-tools/qpcr-efficiency-calculator.html/> accessed on 25 March 2022). To determine the level of relative expression of the studied genes, the method employed by Livak and Schmittgen [57] was used. The reference genes used as an internal control for *E. coli* included: *gyrA*, *gyrB* and *rpoE* [53,58]. A similar set of primary metabolic genes was chosen for *B. cereus* strains except for *rpoE*, replaced by *rpoB* [59]. Contrarily, the housekeeping genes of *S. epidermidis* comprised *gyrB*, *pyk* and *rpoB* genes [60]. These genes were used for normalisation against target genes due to a similar level of expression in both treated and untreated bacterial cells [36,41].

#### 4.5. Determining the Activity of CAT, PER and SOD

To compare the changes in the product formation at the expression level of selected genes, the activity of their secondary molecular equivalents, CAT, PER and SOD, was assessed. The activity of all enzymes was measured in crude enzyme fraction obtained from bacterial cells exposed to NPs using Hegeman's method [61]. The CAT activity was measured by observing a decrease in the absorbance at  $\lambda = 240$  nm in time, equivalent to the  $H_2O_2$  degradation by an active enzyme [62,63]. The activity of PER was determined by the enzyme assay provided by Sigma-Aldrich, where an increase of absorbance at  $\lambda = 420$  nm, specific to an increase in the colourful purpurogallin product in time, was recorded. To assess SOD activity, a commercial kit with xanthine oxidase and tetrazolium salt as reagents (cat. 19160, Sigma-Aldrich, St. Louis, MI, USA) was used. The absorbances measured at  $\lambda = 450$  nm were used in the SOD activity calculations according to Zhang et al. [64]. The

protein concentrations in the isolated protein fractions were determined by the Bradford method [65], and, finally, CAT, PER and SOD activities were presented as  $U \cdot mg^{-1}$  of protein.

#### 4.6. Statistical Analysis

All of the experimental data were presented as the mean  $\pm$  the standard deviation (SD) of four replicates. Grubbs' outlier test was applied to all experimental data to verify and exclude any significant outliers from the results. The statistical significance between studied NPs, their effect on enzymes activities and the relative expression levels of the selected genes was followed up using a one-way ANOVA. The experimental groups were separated by applying the post-hoc Tukey's honest significant difference test ( $p \leq 0.05$ ) and are represented on figures by annotated letters. Additionally, to compare the effect of tested NPs at the concentrations of  $IC_{50}$  and  $\frac{1}{2}IC_{50}$ , the independent Student's *t*-test for the  $p < 0.05$  was used. Furthermore, cluster analysis was applied to evaluate how closely associated NPs treatments are over the whole set of data. Principal component analysis (PCA) and the Pearson correlation coefficient (Pearson's *r*;  $p \leq 0.05$ ) were calculated to determine the linear dependence of all variable values. All of the statistical studies were conducted using MS Office 2019 (Microsoft Inc., Redmond, WA, USA) and the STATISTICA 13.1 software package (TIBCO Software Inc., Palo Alto, CA, USA).

## 5. Conclusions

The results presented in this study confirmed the diverse influence of Ag-NPs, Cu-NPs, ZnO-NPs and TiO<sub>2</sub>-NPs on the expression level of selected genes and the activity of their secondary molecular counterparts in *E. coli*, *B. cereus* and *S. epidermidis* cells. The effect of NPs on the gene expression level depended on the type and concentration of NPs and the species of bacteria. Despite the considerable diversity of the results, it turned out that, in most cases, the regulation of the expression of selected genes was correlated with the activity of the encoded proteins, especially those with CAT and PER-type activities. Moreover, the obtained results confirmed the ability of bacterial cells to respond to stress caused by NPs, providing protection against oxidative stress. Undeniably, the conducted study is innovative, as it provides direct evidence in the explanation of the biological action of metal and metal oxide NPs at the molecular level. The presented results are valuable, as they confirm the ability of the tested bacterial strains to activate sophisticated and diverse strategies of defence against ROS in order to minimise oxidative damage.

**Supplementary Materials:** The following supporting information can be downloaded at: <https://www.mdpi.com/article/10.3390/ijms23094966/s1>.

**Author Contributions:** Conceptualisation, O.M., D.W. and A.M.; methodology, O.M. and D.W.; software, O.M. and D.W.; validation, O.M. and D.W.; formal analysis, O.M., D.W. and A.M.; investigation, O.M. and D.W.; resources, O.M., D.W. and A.M.; data curation, O.M., D.W. and A.M.; writing—original draft preparation, O.M. and D.W.; writing—review and editing, A.M.; visualisation, O.M., D.W. and A.M.; supervision, A.M.; project administration, O.M.; funding acquisition, O.M. and A.M. All authors have read and agreed to the published version of the manuscript.

**Funding:** This research was funded in whole by the National Science Centre, Poland, grant number 2021/41/N/NZ9/02506. The APC was funded by the National Science Centre, Poland. For the purpose of Open Access, the author has applied a CC-BY public copyright licence to any Author Accepted Manuscript (AAM) version arising from this submission.

**Institutional Review Board Statement:** Not applicable.

**Informed Consent Statement:** Not applicable.

**Data Availability Statement:** Not applicable.

**Conflicts of Interest:** The authors declare no conflict of interest.

## References

1. Martínez, G.; Merinero, M.; Pérez-Aranda, M.; Pérez-Soriano, E.M.; Ortiz, T.; Villamor, E.; Begines, B.; Alcudia, A. Environmental impact of nanoparticles' application as an emerging technology: A review. *Materials* **2020**, *14*, 166. [[CrossRef](#)]
2. Gaviria, J.; Alcudia, A.; Begines, B.; Beltrán, A.M.; Rodríguez-Ortiz, J.A.; Trueba, P.; Villarraga, J.; Torres, Y. Biofunctionalization of porous Ti substrates coated with Ag nanoparticles for potential antibacterial behavior. *Metals* **2021**, *11*, 692. [[CrossRef](#)]
3. Alcudia, A.; Begines, B.; Rodríguez-Lejarraga, P.; Greyer, V.; Godinho, V.C.F.; Pajuelo, E.; Torres, Y. Development of porous silver nanoparticle/polycaprolactone/polyvinyl alcohol coatings for prophylaxis in titanium interconnected samples for dental implants. *Colloids Interface Sci. Commun.* **2022**, *48*, 100621. [[CrossRef](#)]
4. Khanna, K.; Kohli, S.K.; Handa, N.; Kaur, H.; Ohri, P.; Bhardwaj, R.; Yousaf, B.; Rinklebe, J.; Ahmad, P. Enthralling the impact of engineered nanoparticles on soil microbiome: A concentric approach towards environmental risks and cogitation. *Ecotoxicol. Environ. Saf.* **2021**, *222*, 112459. [[CrossRef](#)] [[PubMed](#)]
5. Mammari, N.; Lamouroux, E.; Boudier, A.; Duval, R.E. Current knowledge on the oxidative-stress-mediated antimicrobial properties of metal-based nanoparticles. *Microorganisms* **2022**, *10*, 437. [[CrossRef](#)] [[PubMed](#)]
6. Wang, L.; Hu, C.; Shao, L. The antimicrobial activity of nanoparticles: Present situation and prospects for the future. *Int. J. Nanomed.* **2017**, *12*, 1227–1249. [[CrossRef](#)] [[PubMed](#)]
7. Singh, J.; Vishwakarma, K.; Ramawat, N.; Rai, P.; Singh, V.K.; Mishra, R.K.; Kumar, V.; Tripathi, D.K.; Sharma, S. Nanomaterials and microbes' interactions: A contemporary overview. *3 Biotech* **2019**, *9*, 68. [[CrossRef](#)]
8. Borisov, V.B.; Siletsky, S.A.; Nastasi, M.R.; Forte, E. ROS defense systems and terminal oxidases in bacteria. *Antioxidants* **2021**, *10*, 839. [[CrossRef](#)]
9. Seixas, A.F.; Quendera, A.P.; Sousa, J.P.; Silva, A.F.Q.; Arraiano, C.M.; Andrade, J.M. Bacterial response to oxidative stress and RNA oxidation. *Front. Genet.* **2022**, *12*, 821535. [[CrossRef](#)]
10. Liao, S.; Zhang, Y.; Pan, X.; Zhu, F.; Jiang, C.; Liu, Q.; Cheng, Z.; Dai, G.; Wang, L.; et al. Antibacterial activity and mechanism of silver nanoparticles against multidrug-resistant *Pseudomonas aeruginosa*. *Int. J. Nanomed.* **2019**, *14*, 1469–1487. [[CrossRef](#)]
11. Choi, Y.; Kim, H.-A.; Kim, K.-W.; Lee, B.-T. Comparative toxicity of silver nanoparticles and silver ions to *Escherichia coli*. *J. Environ. Sci.* **2018**, *66*, 50–60. [[CrossRef](#)] [[PubMed](#)]
12. Simonin, M.; Richaume, A. Impact of engineered nanoparticles on the activity, abundance, and diversity of soil microbial communities: A review. *Environ. Sci. Pollut. Res.* **2015**, *22*, 13710–13723. [[CrossRef](#)] [[PubMed](#)]
13. Karimi, E.; Mohseni Fard, E. Nanomaterial effects on soil microorganisms. In *Nanoscience and Plant-Soil Systems. Soil Biology*; Ghorbanpour, M., Khanuja, M., Varma, A., Eds.; Springer: Cham, Switzerland, 2017; Volume 48, pp. 137–200.
14. Zhang, Y.; Gu, A.Z.; Xie, S.; Li, X.; Cen, T.; Li, D.; Chen, J. Nano-metal oxides induce antimicrobial resistance via radical-mediated mutagenesis. *Environ. Int.* **2018**, *121*, 1162–1171. [[CrossRef](#)] [[PubMed](#)]
15. Brandelli, A. The interaction of nanostructured antimicrobials with biological systems: Cellular uptake, trafficking and potential toxicity. *Food Sci. Hum. Wellness* **2020**, *9*, 8–20. [[CrossRef](#)]
16. Wang, X.; Yang, F.; Zhao, J.; Xu, Y.; Mao, D.; Zhu, X.; Luo, Y.; Alvarez, P.J.J. Bacterial exposure to ZnO nanoparticles facilitates horizontal transfer of antibiotic resistance genes. *NanoImpact* **2018**, *10*, 61–67. [[CrossRef](#)]
17. Zhang, S.; Wang, Y.; Song, H.; Lu, J.; Yuan, Z.; Guo, J. Copper nanoparticles and copper ions promote horizontal transfer of plasmid-mediated multi-antibiotic resistance genes across bacterial genera. *Environ. Int.* **2019**, *129*, 478–487. [[CrossRef](#)]
18. Lu, J.; Wang, Y.; Jin, M.; Yuan, Z.; Bond, P.; Guo, J. Both silver ions and silver nanoparticles facilitate the horizontal transfer of plasmid-mediated antibiotic resistance genes. *Water Res.* **2020**, *169*, 115229. [[CrossRef](#)]
19. Joshi, A.S.; Singh, P.; Mijakovic, I. Interactions of gold and silver nanoparticles with bacterial biofilms: Molecular interactions behind inhibition and resistance. *Int. J. Mol. Sci.* **2020**, *21*, 7658. [[CrossRef](#)]
20. Abarca-Cabrera, L.; Fraga-García, P.; Berensmeier, S. Bio-nano interactions: Binding proteins, polysaccharides, lipids and nucleic acids onto magnetic nanoparticles. *Biomater. Res.* **2021**, *25*, 12. [[CrossRef](#)]
21. Singh, B.R.; Singh, B.N.; Singh, A.; Khan, W.; Naqvi, A.H.; Singh, H.B. Mycofabricated biosilver nanoparticles interrupt *Pseudomonas aeruginosa* quorum sensing systems. *Sci. Rep.* **2015**, *5*, 13719. [[CrossRef](#)]
22. Ouyang, K.; Mortimer, M.; Holden, P.A.; Cai, P.; Wu, Y.; Gao, C.; Huang, Q. Towards a better understanding of *Pseudomonas putida* biofilm formation in the presence of ZnO nanoparticles (NPs): Role of NP concentration. *Environ. Int.* **2020**, *137*, 105485. [[CrossRef](#)] [[PubMed](#)]
23. Zhang, L.; Wu, L.; Si, Y.; Shu, K. Size-dependent cytotoxicity of silver nanoparticles to *Azotobacter vinelandii*: Growth inhibition, cell injury, oxidative stress and internalization. *PLoS ONE* **2018**, *13*, e0209020. [[CrossRef](#)]
24. Yan, X.; He, B.; Liu, L.; Qu, G.; Shi, J.; Hu, L.; Jiang, G. Antibacterial mechanism of silver nanoparticles in *Pseudomonas aeruginosa*: Proteomics approach. *Metallomics* **2018**, *10*, 557–564. [[CrossRef](#)] [[PubMed](#)]
25. de Celis, M.; Belda, I.; Marquina, D.; Santos, A. Phenotypic and transcriptional study of the antimicrobial activity of silver and zinc oxide nanoparticles on a wastewater biofilm-forming *Pseudomonas aeruginosa* strain. *Sci. Total Environ.* **2022**, *826*, 153915. [[CrossRef](#)] [[PubMed](#)]
26. Singh, R.; Cheng, S.; Singh, S. Oxidative stress-mediated genotoxic effect of zinc oxide nanoparticles on *Deinococcus radiodurans*. *3 Biotech* **2020**, *10*, 66. [[CrossRef](#)] [[PubMed](#)]

27. Reimhult, E. Nanoparticle risks and identification in a world where small things do not survive. *Nanoethics* **2017**, *11*, 283–290. [[CrossRef](#)] [[PubMed](#)]
28. Ameen, F.; Alsamhary, K.; Alabdullatif, J.A.; AlNadhari, S. A review on metal-based nanoparticles and their toxicity to beneficial soil bacteria and fungi. *Ecotoxicol. Environ. Saf.* **2021**, *213*, 112027. [[CrossRef](#)] [[PubMed](#)]
29. Mortimer, M.; Wang, Y.; Holden, P.A. Molecular mechanisms of nanomaterial-bacterial interactions revealed by omics—the role of nanomaterial effect level. *Front. Bioeng. Biotechnol.* **2021**, *9*, 683520. [[CrossRef](#)]
30. Leung, Y.H.; Xu, X.; Ma, A.P.; Liu, F.; Ng, A.M.; Shen, Z.; Gethings, L.A.; Guo, M.Y.; Djurišić, A.B.; Lee, P.K.; et al. Toxicity of ZnO and TiO<sub>2</sub> to *Escherichia coli* cells. *Sci. Rep.* **2016**, *6*, 35243. [[CrossRef](#)]
31. Khan, I.; Saeed, K.; Khan, I. Nanoparticles: Properties, applications and toxicities. *Arab. J. Chem.* **2019**, *12*, 908–931. [[CrossRef](#)]
32. Jin, R.; Higaki, T. Open questions on the transition between nanoscale and bulk properties of metals. *Commun. Chem.* **2021**, *4*, 28. [[CrossRef](#)]
33. Arendsen, L.P.; Thakar, R.; Sultan, A.H. The use of copper as an antimicrobial agent in health care, including obstetrics and gynecology. *Clin. Microbiol. Rev.* **2019**, *32*, e00125-18. [[CrossRef](#)] [[PubMed](#)]
34. Fan, X.; Yahia, L.; Sacher, E. Antimicrobial properties of the Ag, Cu nanoparticle system. *Biology* **2021**, *10*, 137. [[CrossRef](#)] [[PubMed](#)]
35. Peszke, J.; Dulski, M.; Nowak, A.; Balin, K.; Zubko, M.; Sułowicz, S.; Nowak, B.; Piotrowska-Seget, Z.; Talik, E.; Wojtyniak, M.; et al. Unique properties of silver and copper silica-based nanocomposites as antimicrobial agents. *RSC Adv.* **2017**, *7*, 28092–28104. [[CrossRef](#)]
36. Moore, J.D.; Avellan, A.; Noack, C.W.; Guo, Y.; Lowry, G.V.; Gregory, K.B. Time-dependent bacterial transcriptional response to CuO nanoparticles differs from that of Cu<sup>2+</sup> and provides insights into CuO nanoparticle toxicity mechanisms. *Environ. Sci. Nano* **2017**, *4*, 2321–2335. [[CrossRef](#)]
37. Schellhorn, H.E. Regulation of hydroperoxidase (catalase) expression in *Escherichia coli*. *FEMS Microbiol. Lett.* **1995**, *131*, 113–119. [[CrossRef](#)]
38. Loewen, P. Probing the structure of catalase HPII of *Escherichia coli*—A review. *Gene* **1996**, *179*, 39–44. [[CrossRef](#)]
39. Switala, J.; O'Neil, J.O.; Loewen, P.C. Catalase HPII from *Escherichia coli* exhibits enhanced resistance to denaturation. *Biochemistry* **1999**, *38*, 3895–3901. [[CrossRef](#)]
40. Metryka, O.; Wasilkowski, D.; Mroziak, A. Insight into the antibacterial activity of selected metal nanoparticles and alterations within the antioxidant defence system in *Escherichia coli*, *Bacillus cereus* and *Staphylococcus epidermidis*. *Int. J. Mol. Sci.* **2021**, *22*, 11811. [[CrossRef](#)]
41. Sohm, B.; Immel, F.; Bauda, P.; Pagnout, C. Insight into the primary mode of action of TiO<sub>2</sub> nanoparticles on *Escherichia coli* in the dark. *Proteomics* **2015**, *15*, 98–113. [[CrossRef](#)]
42. Wang, Y.; Wang, H.; Yang, C.-H.; Wang, Q.; Mei, R. Two distinct manganese-containing superoxide dismutase genes in *Bacillus cereus*: Their physiological characterizations and roles in surviving in wheat rhizosphere. *FEMS Microbiol. Lett.* **2007**, *272*, 206–213. [[CrossRef](#)]
43. Wang, Y.; Mo, X.; Zhang, L.; Wang, Q. Four superoxide dismutase (isozymes) genes of *Bacillus cereus*. *Ann. Microbiol.* **2011**, *61*, 355–360. [[CrossRef](#)]
44. Gao, T.-T.; Ding, M.-Z.; Li, Y.; Zeng, Q.-C.; Wang, Q. Identification of genes involved in regulating MnSOD2 production and root colonization in *Bacillus cereus* 905. *J. Integr. Agric.* **2021**, *20*, 1570–1584. [[CrossRef](#)]
45. Ganesh Babu, M.M.; Sridhar, J.; Gunasekaran, P. Global transcriptome analysis of *Bacillus cereus* ATCC 14579 in response to silver nitrate stress. *J. Nanobiotechnology* **2011**, *9*, 49. [[CrossRef](#)] [[PubMed](#)]
46. Kumar, M.; Curtis, A.; Hoskins, C. Application of nanoparticle technologies in the combat against anti-microbial resistance. *Pharmaceutics* **2018**, *10*, 11. [[CrossRef](#)] [[PubMed](#)]
47. Cosgrove, K.; Coutts, G.; Jonsson, I.M.; Tarkowski, A.; Kokai-Kun, J.F.; Mond, J.J.; Foster, S.J. Catalase (KatA) and alkyl hydroperoxide reductase (AhpC) have compensatory roles in peroxide stress resistance and are required for survival, persistence, and nasal colonization in *Staphylococcus aureus*. *J. Bacteriol.* **2007**, *189*, 1025–1035. [[CrossRef](#)] [[PubMed](#)]
48. Hassan, K.A.; Pederick, V.G.; Elbourne, L.D.; Paulsen, I.T.; Paton, J.C.; McDevitt, C.A.; Eijkelkamp, B.A. Zinc stress induces copper depletion in *Acinetobacter baumannii*. *BMC Microbiol.* **2017**, *17*, 59. [[CrossRef](#)]
49. Raghunath, A.; Perumal, E. Metal oxide nanoparticles as antimicrobial agents: A promise for the future. *Int. J. Antimicrob. Agents* **2017**, *49*, 137–152. [[CrossRef](#)]
50. Chandransu, P.; Rensing, C.; Helmann, J.D. Metal homeostasis and resistance in bacteria. *Nat. Rev. Microbiol.* **2017**, *15*, 338–350. [[CrossRef](#)]
51. Niemirowicz, K.; Swiecicka, I.; Wilczewska, A.Z.; Misztalewska, I.; Kalska-Szostko, B.; Bienias, K.; Bucki, R.; Car, H. Gold-functionalized magnetic nanoparticles restrict growth of *Pseudomonas aeruginosa*. *Int. J. Nanomed.* **2014**, *9*, 2217–2224.
52. Karavolos, M.H.; Horsburgh, M.J.; Ingham, E.; Foster, S.J. Role and regulation of the superoxide dismutases of *Staphylococcus aureus*. *Microbiology* **2003**, *149*, 2749–2758. [[CrossRef](#)]
53. Osonga, F.J.; Akgul, A.; Yazgan, I.; Akgul, A.; Ontman, R.; Kariuki, V.M.; Eshun, G.B.; Sadik, O.A. Flavonoid-derived anisotropic silver nanoparticles inhibit growth and change the expression of virulence genes in *Escherichia coli* SM10. *RSC Adv.* **2018**, *8*, 4649–4661. [[CrossRef](#)]



54. Xie, Y.; He, Y.; Irwin, P.L.; Jin, T.; Shi, X. Antibacterial activity and mechanism of action of zinc oxide nanoparticles against *Campylobacter jejuni*. *Appl. Environ. Microbiol.* **2011**, *77*, 2325–2331. [[CrossRef](#)] [[PubMed](#)]
55. Zur, J.; Piński, A.; Wojcieszynska, D.; Smulek, W.; Guzik, U. Diclofenac degradation—Enzymes, genetic background and cellular alterations triggered in diclofenac-metabolizing strain *Pseudomonas moorei* KB4. *Int. J. Mol. Sci.* **2020**, *21*, 6786. [[CrossRef](#)] [[PubMed](#)]
56. Bustin, S.A.; Mueller, R.; Nolan, T. Parameters for successful PCR primer design. In *Quantitative Real-Time PCR. Methods in Molecular Biology*; Biassoni, R., Raso, A., Eds.; Humana: New York, NY, USA, 2020; Volume 2065. [[CrossRef](#)]
57. Livak, K.J.; Schmittgen, T.D. Analysis of relative gene expression data using real-time quantitative PCR and the  $2^{-\Delta\Delta CT}$  method. *Methods* **2001**, *25*, 402–408. [[CrossRef](#)] [[PubMed](#)]
58. Hou, Z.; Fink, R.C.; Black, E.P.; Sugawara, M.; Zhang, Z.; Diez-Gonzalez, F.; Sadowsky, M.J. Gene expression profiling of *Escherichia coli* in response to interactions with the lettuce rhizosphere. *J. Appl. Microbiol.* **2012**, *113*, 1076–1086. [[CrossRef](#)]
59. Ko, K.S.; Kim, J.W.; Kim, J.M.; Kim, W.; Chung, S.I.; Kim, I.J.; Kook, Y.H. Population structure of the *Bacillus cereus* group as determined by sequence analysis of six housekeeping genes and the *plcR* gene. *Infect. Immun.* **2004**, *72*, 5253–5261. [[CrossRef](#)]
60. Sihto, H.M.; Tasara, T.; Stephan, R.; Jöhler, S. Validation of reference genes for normalization of qPCR mRNA expression levels in *Staphylococcus aureus* exposed to osmotic and lactic acid stress conditions encountered during food production and preservation. *FEMS Microbiol. Lett.* **2014**, *356*, 134–140. [[CrossRef](#)]
61. Hegeman, G.D. Synthesis of the enzymes of the mandelate pathway by *Pseudomonas putida* I. Synthesis of enzymes by the wild type. *J. Bacteriol.* **1966**, *91*, 1140–1154. [[CrossRef](#)]
62. Banerjee, G.; Pandey, S.; Ray, A.K.; Kumar, R. Bioremediation of heavy metals by a novel bacterial strain *Enterobacter cloacae* and its antioxidant enzyme activity, flocculant production and protein expression in presence of lead, cadmium and nickel. *Water Air Soil Pollut.* **2015**, *226*, 91. [[CrossRef](#)]
63. David, M.; Krishna, P.M.; Sangeetha, J. Elucidation of impact of heavy metal pollution on soil bacterial growth and extracellular polymeric substances flexibility. *3 Biotech* **2016**, *6*, 172. [[CrossRef](#)] [[PubMed](#)]
64. Zhang, C.; Bruins, M.E.; Yang, Z.Q.; Liu, S.T.; Rao, P.F. A new formula to calculate activity of superoxide dismutase in indirect assays. *Anal. Biochem.* **2016**, *503*, 65–67. [[CrossRef](#)] [[PubMed](#)]
65. Bradford, M.M. A rapid and sensitive method for the quantitation of microgram quantities of proteins utilizing the principle of protein-dye binding. *Anal. Biochem.* **1976**, *72*, 248–254. [[CrossRef](#)]

### II.3

Metryka O., Wasilkowski D., Adamczyk-Habrajska M., Mroziak A. 2023. Undesirable consequences of the metallic nanoparticles action on the properties and functioning of *Escherichia coli*, *Bacillus cereus* and *Staphylococcus epidermidis* membranes. *Journal of Hazardous Materials* 446: 130728



## Research Article

# Undesirable consequences of the metallic nanoparticles action on the properties and functioning of *Escherichia coli*, *Bacillus cereus* and *Staphylococcus epidermidis* membranes

Oliwia Metryka<sup>a,\*</sup>, Daniel Wasilkowski<sup>b</sup>, Małgorzata Adamczyk-Habrajska<sup>c</sup>, Agnieszka Mrozik<sup>b,\*</sup>

<sup>a</sup> Doctoral School, University of Silesia, Bankowa 14, Katowice 40-032, Poland

<sup>b</sup> Institute of Biology, Biotechnology and Environmental Protection, Faculty of Natural Sciences, University of Silesia, Jagiellońska 29, Katowice 40-032, Poland

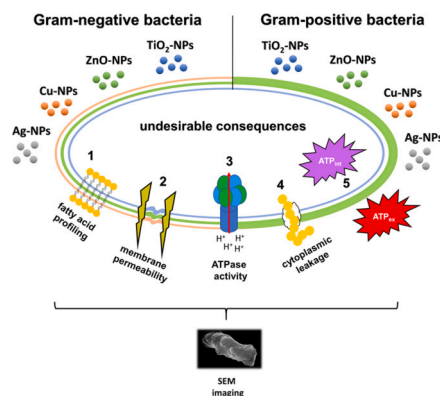
<sup>c</sup> Institute of Materials Engineering, Faculty of Science and Technology, University of Silesia, Żytnia 12, Sosnowiec 41-200, Poland



## HIGHLIGHTS

- Metal nanoparticles induced dose-dependent effects on bacterial outer layers.
- Nanoparticles reduced membrane permeability and altered fatty acid composition.
- Nanoparticles affected ATP depletion and decreased ATPase activity.
- ZnO-NPs and Cu-NPs most greatly impacted bacterial membrane properties.

## GRAPHICAL ABSTRACT



## ARTICLE INFO

Editor: Karina S. B. Miglioranza

## Keywords:

Bacteria  
Nanoparticles  
Membrane properties  
ATP level  
Fatty acid profiling

## ABSTRACT

Controversial and inconsistent findings on the toxicity of metallic nanoparticles (NPs) against many bacteria are common in recorded studies; therefore, further advanced experimental work is needed to elucidate the mechanisms underlying nanotoxicity. This study deciphered the direct effects of Ag-NPs, Cu-NPs, ZnO-NPs and TiO<sub>2</sub>-NPs on membrane permeability, cytoplasmic leakage, ATP level, ATPase activity and fatty acid profiling of *Escherichia coli*, *Bacillus cereus* and *Staphylococcus epidermidis* as model microorganisms. A multifaceted analysis of all collected results indicated the different influences of individual NPs on the measured parameters depending on their type and concentration. Predominantly, membrane permeability was correlated with increased cytoplasmic leakage, reduced total ATP levels and ATPase activity. The established fatty acid profiles were unique and concerned various changes in the percentages of hydroxyl, cyclopropane, branched and unsaturated fatty acids. Decisively, *E. coli* was more susceptible to changes in measured parameters than *B. cereus* and *S. epidermidis*. Also, it was established that ZnO-NPs and Cu-NPs had a major differentiating impact on studied

\* Corresponding authors.

E-mail addresses: [oliwia.metryka@us.edu.pl](mailto:oliwia.metryka@us.edu.pl) (O. Metryka), [agnieszka.mrozik@us.edu.pl](mailto:agnieszka.mrozik@us.edu.pl) (A. Mrozik).

<https://doi.org/10.1016/j.jhazmat.2023.130728>

Received 14 November 2022; Received in revised form 3 January 2023; Accepted 3 January 2023

Available online 4 January 2023

0304-3894/© 2023 The Authors. Published by Elsevier B.V. This is an open access article under the CC BY license (<http://creativecommons.org/licenses/by/4.0/>).

parameters. Additionally, bacterial cell imaging using scanning electron microscopy elucidated different NPs distributions on the cell surface. The presented results are believed to provide novel, valuable and accumulated knowledge in the understanding of NPs action on bacterial membranes.

## 1. Introduction

Due to the wide range of applications and the increase in production, nanotechnology materials are currently the subject of extensive investigation [12,13,8]. A spectacular breakthrough has been made in research on the antimicrobial properties of nanomaterials, including inorganic nanoparticles (NPs), used to produce innovative nanotechnology products with practical applications in medicine, agriculture, food production, construction and environmental protection [4,35]. The exploited bactericidal mode of action of NPs is significant progress in the fight against the multi-drug resistance (MDR) of microorganisms [52]. The well-known properties of NPs, including their high surface-to-volume ratio, quantum confinement and surface energy, make them highly desirable materials in many areas of life due to their high reactivity and stability [3,12]. However, it is challenging to predict the fate and effects of NPs actions in environmental conditions that may threaten organisms inhabiting various ecosystems through direct and experimental methods [52]. Therefore, in future studies, protocols should combine selected techniques, allowing the quantification and characterisation of NM fate in biological matrices [1]. Nevertheless, promising bioinformatics and data modelling approaches take into account various NM fate factors that could contribute to producing environmentally safe materials and predict interactions of such structures with living organisms in nature [55]. The main routes of NPs action have been reported in the literature; however, the effects and risks that may arise from introducing such materials into worldwide product circulation are still unidentified. Therefore, controlled and sustainable applications of nano-derived products should be maintained. One of the mechanisms of NPs action and the released metal ions is their direct or indirect interaction with bacterial outer layers [5–7]. Such interactions, along with other bactericidal effects including generation of reactive oxygen species (ROS), damage to cellular macromolecules, inhibition of cell metabolism or genotoxicity, can have a destructive and irreversible impact on microorganisms [35,40]. The outcomes of NPs-bacteria interactions can lead to the disruption of the integrity and structure of cells envelopes, decoupling of cellular respiration, cytoplasmic leakage and eventually, cell death [40,48,56]. The decisive factor determining the characteristic and specific interactions between bacteria and NPs is the different organisation of the outer layers. Gram-negative bacteria are surrounded by an inner and outer phospholipid membrane separated by a periplasm with a thin peptidoglycan layer [15]. Furthermore, Gram-negative bacteria contain lipopolysaccharides with phosphate groups that bind divalent cations and control the rigidity of the membrane [40,50]. However, Gram-positive bacteria do not have an outer membrane, but they are covered by thick layers of peptidoglycan with teichoic, lipoteichoic and teichuronic acids providing additional protection against NPs stress [15,41,48]. Many studies have indicated that NPs adhere to the cell membrane through electrostatic interactions, hydrophobicity interactions, hydrogen bonding and van der Waals forces [29,40]. The deposition of NPs on the bacterial surface can result in membrane fluidisation, changes in its hydrophobicity, loss of amphiphilic properties of phospholipids, impairment of ion exchange, and damage to structural and enzyme proteins [10,29]. In addition, the induction of ROS by NPs can increase membrane fluidity and induce cell wall and cytoplasmic membrane degradation through the oxidation of lipids and proteins [2,29,58]. Impairment of outer layers can disrupt the functioning of vital enzymes of respiration metabolism of the cells, including dehydrogenases and ATPase activities [20,24,35,53]. NPs can also modify the transport of electrons, diminish proton motive force, impair the transport of  $K^+$  and hence hinder adenosine triphosphate

(ATP) production [20,53]. These metabolic parameters can be used as vital bioindicators in NPs toxicological studies.

The cell membrane is a dynamic structure that undergoes different changes under certain environmental circumstances. During stress conditions, bacteria can trigger SOS response and remodel the membrane structure and permeability, thus enhancing the resistance against external factors [48,54]. For example, bacteria under chemical stress can adjust the lipid content or modify the branching and saturation of fatty acids' acyl chains. Since the binding of NPs on bacterial membranes depends on the electrostatic interactions, some bacteria can attain resistance mechanisms that alter the overall surface charge, lessening such interactions [9]. Therefore, adaptive processes should be identified when considering the vast impact of NPs. These kinds of coping mechanisms could protect microorganisms from NPs stress.

Despite ongoing advanced research on the toxicity of NPs against microorganisms, some aspects of their effects on the membrane properties and functioning remain unanswered. Therefore, it was worth investigating these issues comprehensively to gain new knowledge about bacteria cell response to NPs. Accordingly, the main goals of this work included: (1) studying and comparing the membrane permeability and cytoplasmic leakage from the cells of *E. coli*, *B. cereus* and *S. epidermidis* exposed to AgNPs, Cu-NPs, ZnO-NPs and TiO<sub>2</sub>-NPs, (2) measuring the total ATP concentration and adenosine 5'-triphosphatase (ATPase) activity; (3) evaluating the changes in fatty acid profiles; (4) establishing statistical dependencies between measured parameters, and (5) visualising NPs distribution on the bacterial surface.

## 2. Materials and methods

### 2.1. Bacterial strains, inorganic nanoparticles, and culture conditions

This study was performed using the following bacterial strains: *Escherichia coli* (ATCC® 25922™), *Bacillus cereus* (ATCC® 11778™) and *Staphylococcus epidermidis* (ATCC® 12228™), purchased from the American Type Culture Collection (ATCC). All strains were grown overnight in lysogeny broth (LB mix; tryptone 10 g L<sup>-1</sup>, NaCl 10 g L<sup>-1</sup>, yeast extract 5 g L<sup>-1</sup>) at 37 °C, under shaking conditions (140 rpm) in the presence of four types of inorganic NPs, including Ag-NPs (cat. 576832, Sigma-Aldrich, <100 nm), Cu-NPs (cat. 774081, Sigma-Aldrich, 25 nm), ZnO-NPs (cat. 677450, Sigma-Aldrich, <50 nm) and TiO<sub>2</sub>-NPs (cat. US1019F, US Research, 20 nm). The concentrations of individual NPs added to the bacterial cultures were equal to the half-maximal inhibitory concentrations (IC<sub>50</sub>) and their corresponding half concentrations (½IC<sub>50</sub>) (Table 1) [39]. Control samples in the conducted research were bacterial cells cultured without NPs. All bacterial cultures

**Table 1**  
The IC<sub>50</sub> and ½IC<sub>50</sub> (mg L<sup>-1</sup>) of NPs against *E. coli*, *B. cereus* and *S. epidermidis*.

Bacterial strain	NPs	IC <sub>50</sub>	½IC <sub>50</sub>
<i>Escherichia coli</i> ATCC® 25922™	Ag-NPs	7.84	3.92
	Cu-NPs	180.80	90.40
	ZnO-NPs	176.10	88.05
	TiO <sub>2</sub> -NPs	43.40	21.70
<i>Bacillus cereus</i> ATCC® 11778™	Ag-NPs	480.10	240.05
	Cu-NPs	52.15	26.08
	ZnO-NPs	319.10	159.55
	TiO <sub>2</sub> -NPs	50.30	25.15
<i>Staphylococcus epidermidis</i> ATCC® 12228™	Ag-NPs	422.20	211.10
	Cu-NPs	112.00	56.00
	ZnO-NPs	201.70	100.85
	TiO <sub>2</sub> -NPs	703.40	351.70

were subjected to a multifaceted analysis covering various aspects of the influence of NPs on membrane properties, functioning and direct interactions with the cell wall. The experimental set-up with all performed studies is presented in Fig. 1.

## 2.2. Measuring membrane permeability

The cell membrane permeability was measured using a crystal violet assay developed by [18] and [21]. The 24-hour bacterial cultures treated with individual NPs, and the control samples were centrifuged at 5 000 rpm, 4 °C for 20 min. The residue was washed twice and resuspended in phosphate-buffered saline (PBS) (pH 7.4) to obtain optical density  $OD_{600} = 0.1$  of the solution containing the mixture of bacterial cells and NPs. Subsequently, crystal violet solution ( $0.1 \text{ mg mL}^{-1}$ ) was added to the samples and incubated at 37 °C for 10 min. Then, the bacterial-dye suspensions were centrifuged at 13,000 rpm, 4 °C for 15 min. Afterwards, the absorbance of the samples at  $\lambda = 590 \text{ nm}$  was measured. The membrane permeability equivalent to the percentage of crystal violet uptake by bacterial cells was calculated according to the following equation:

$$\text{Membrane permeability}[\%] = \frac{OD_{\text{sample}}}{OD_{\text{CV}}} \cdot 100\%$$

where:  $OD_{\text{CV}}$  – optical density of crystal violet ( $0.1 \text{ mg mL}^{-1}$ ) in PBS solution (1:20 ratio);  $OD_{\text{sample}}$  – optical density of a sample treated with individual NPs or a control sample.

The final membrane permeability of the NPs-treated cells was expressed as the percentage difference in membrane permeability between the treated and control cells.

## 2.3. Measuring cytoplasmic leakage

The protocols described by [33] and [45] were applied to examine the cytoplasmic leakage from bacterial cells. The principle of this method focuses on the changes in the content of nucleic acids and

proteins released from microbial cells after the disruption of bacterial outer layers. Firstly, bacterial suspensions in 0.85% NaCl with  $OD_{600} = 0.5$  were prepared. Next, the appropriate concentrations of individual NPs were added. In parallel, the control samples without NPs were prepared. All samples were incubated within 4 h at 37 °C under shaking conditions (140 rpm). At hour intervals, appropriate 2 mL aliquots were collected from the samples and centrifuged at 10,000 rpm, 4 °C for 10 min. Alternately, the absorbance of the supernatants was measured at  $\lambda = 260 \text{ nm}$ , corresponding to the amount of released nucleic acids. Finally, the differences in the absorbances for each treated and untreated strain were calculated.

## 2.4. Measuring intracellular and extracellular ATP concentration

The total cellular and dissolved ATP concentrations were quantified using a commercial Molecular Probes™ ATP Determination Kit by ThermoFisher Scientific (cat. No. A22066) according to the manufacturer's instructions. It is a bioluminescence assay based on the oxidation of D-luciferin by firefly luciferase, which uses ATP,  $\text{Mg}^{2+}$  and  $\text{O}_2$ , resulting in its conversion to the excited oxyluciferin molecule, which emits visible light (emission maximum  $\sim 560 \text{ nm}$  at pH 7.8) proportionally to the amount of ATP in a sample. Firstly, 24-hour bacterial culture was filtered through 0.22  $\mu\text{m}$  to eliminate the cells. Next, the filtered supernatant was used to determine the dissolved ATP concentration. Subsequently, the levels of cellular ATP were assayed in the cell-free extracts obtained from each culture using Hegeman's method [23]. A standard curve with a 0 – 5  $\mu\text{M}$  ATP concentration range was prepared to convert the sample luminescence reading into ATP concentration. The final data concerning intracellular and extracellular ATP levels in a sample was presented as the difference between their concentrations in the treated and control cells.

## 2.5. Measuring ATPase activity

As a part of a complementary study to quantify ATP concentration in

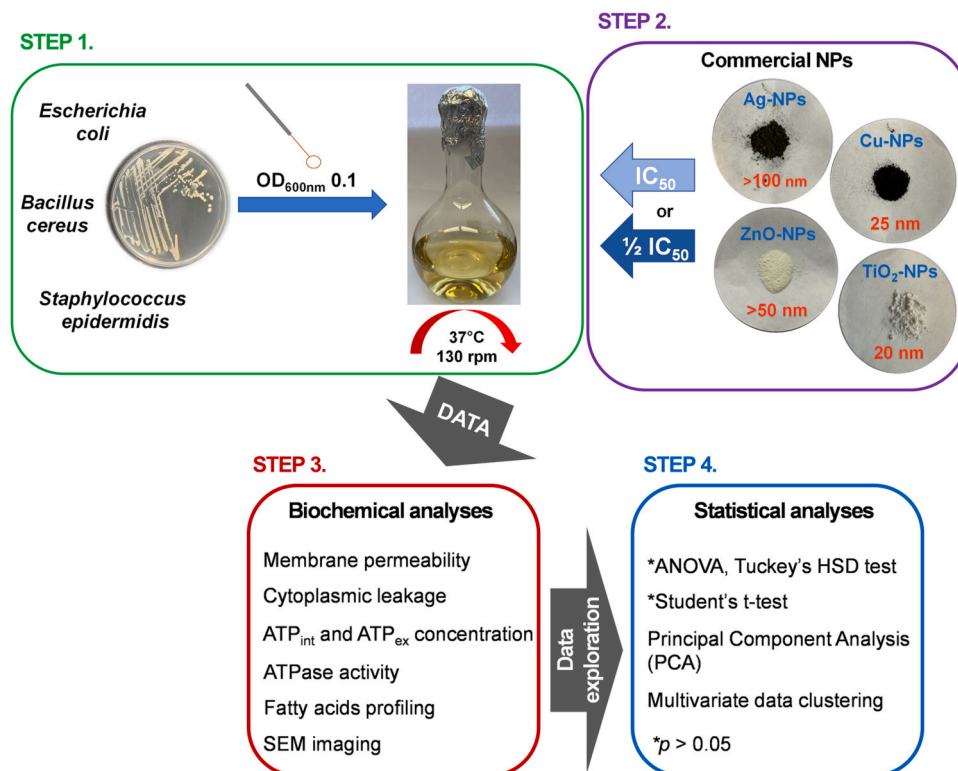


Fig. 1. Scheme of experimental design.

bacterial cells, ATPase activity was measured. For this purpose, a commercial ATPase/GTPase Activity Assay Kit by Sigma Aldrich (cat. No. MAK113) was used. ATPase catalyses the breakdown of ATP into ADP and free phosphate. This procedure enables the measurement of the concentration of free phosphate released during the enzyme reaction with the malachite green reagent. The dye reacts with free phosphate forming a colourful product proportionally to ATPase activity measured at  $\lambda = 620$  nm. One unit of ATPase activity is the amount of enzyme that catalyses the production of 1  $\mu\text{mol}$  of free phosphate per minute under assay conditions. Herein, bacteria incubated with NPs for 24 h were used directly in the assay. Pigmented samples were subjected to prior centrifugation at 14,000 rpm for 5 min. The concentration of free phosphate in the supernatant was calculated from a standard curve prepared in the concentration range of 0–50  $\mu\text{M}$ . The final ATPase activity in a sample was presented as the difference between enzyme activity in the treated and untreated cells.

## 2.6. Evaluating bacterial fatty acid composition

The fatty acids were isolated from bacteria exposed to NPs and the control cells according to the procedure by [46]. Initially, the bacterial cultures were centrifuged at 5,000 rpm, 4 °C for 20 min. The collected biomass was subjected to four-steps in fatty acid isolation, including saponification (5 g NaOH, 150 mL  $\text{CH}_3\text{OH}$ , 150 mL  $\text{H}_2\text{O}$ ), methylation (325 mL 6 N HCl, 275 mL  $\text{CH}_3\text{OH}$ ), extraction (200 mL  $\text{C}_6\text{H}_{14}$ , 200 mL  $(\text{CH}_3)_3\text{COCH}_3$ ) and a base wash (0.8 g NaOH in 900 mL distilled  $\text{H}_2\text{O}$ ). Finally, fatty acid methyl esters (FAMES) were analysed using a gas chromatograph (Agilent 7820 A, USA) equipped with a phenyl (5%)-methyl-silica capillary column (diameter 0.22 mm, length 25 m, 0.33  $\mu\text{m}$  film thickness) and a flame ionisation detector (FID). Hydrogen was exploited as a carrier gas with the following technical settings: 71.33 kPa inlet pressure and 0.54 mL  $\text{min}^{-1}$  flow velocity. The separated FAMES were identified using MIDI Microbial Identification System Sherlock software (version 6.2B) and the TSBA 6 library from MIDI Inc. For a comprehensive and comparative analysis, all the detected FAMES were sorted into two groups: saturated and unsaturated fatty acids.

## 2.7. Visualisation of bacterial cells with scanning electron microscopy

Bacteria treated with NPs were imaged using scanning electron microscopy (SEM) in compliance with a protocol by [30] to recognise the impact of NPs as an external stress factor on bacterial outer layers responsible for maintaining cell shape and structural integrity. Firstly, the bacterial cultures exposed to NPs at  $\frac{1}{2}\text{IC}_{50}$  were centrifuged (5,000 rpm, 4 °C, 20 min), and the remaining bacterial pellet was washed thrice with water. Next, three following steps were successively carried out to prepare the material for SEM imaging: fixing of bacterial cells with 3% glutaraldehyde at 4 °C, dehydration in the alcohol series (30%, 50%, 70%, 80%, 90%, 95% and 100%) and chemical drying using 100% hexamethyldisilazane [22]. After all, the samples were transferred onto the carbon tape, coated with technical gold and observed using SEM with field emission (JEOL JSM-7100 F, Japan) at an accelerating voltage of 15 kV and a vacuum of  $9.6 \cdot 10^{-5}$  Pa.

## 2.8. Statistical analysis

All results were subjected to statistical significance tests and presented as mean values with standard deviation ( $\pm$  SD) of three replicates obtained from each NPs treatment. The statistical differences between the results obtained for the samples supplemented with NPs and control samples were determined using one-way analysis of variance (ANOVA), followed by Tukey's Honest Significant Difference test (HSD) for  $p < 0.05$ . In the presented graphics, the significant variations in obtained data were presented by annotated letters for the  $p$ -value of 5%. Moreover, the independent Student's  $t$ -test ( $p < 0.05$ ) was used to verify NPs influence/or its lack on evaluated biochemical parameters

between  $\text{IC}_{50}$  and  $\frac{1}{2}\text{IC}_{50}$ . The principal component analysis (PCA) of the FAME profiles with a relative contribution of  $> 1.5\%$  of fatty acids ( $p < 0.05$ ) was used to identify any shift in the composition of fatty acids. In order to find similar groups of objects forming clusters, a projection of the topographic map of the entire set of variable values for NPs in both doses was used. All the statistical and graphical analyses were carried out using the STATISTICA 13.3 software package (TIBCO Software Inc., Palo Alto, CA, USA) and MS Office 2019 (Microsoft Inc., Redmond, WA, USA).

## 3. Results

### 3.1. Bacterial membrane permeability under NPs stress

Changes in membrane permeability of bacterial cells exposed to individual NPs were analysed based on alternations in crystal violet dye uptake. In the case of *E. coli*, individual NPs generally resulted in increased membrane permeability (Fig. 2A). The most significant increase by 134.7% and 80.5% compared to the untreated cells (10%) was established for ZnO-NPs at  $\text{IC}_{50}$  and  $\frac{1}{2}\text{IC}_{50}$ , respectively. Significant increases in membrane permeability by 48.4% also occurred after bacteria treatment with  $\text{TiO}_2$ -NPs at  $\frac{1}{2}\text{IC}_{50}$ . Interestingly, Ag-NPs at  $\frac{1}{2}\text{IC}_{50}$  increased membrane permeability, while the same NPs at  $\text{IC}_{50}$  caused the opposite effect. The statistical analysis revealed significant differences ( $p > 0.05$ ) in membrane permeability of *E. coli* exposed to different concentrations of NPs except for Cu-NPs ( $p < 0.05$ ). Treatment of *E. coli* with metal oxide NPs compared with the unoxidised forms generated the most considerable modifications in the uptake of crystal violet dye.

A parallel experiment with *B. cereus* showed that individual NPs at  $\text{IC}_{50}$  and  $\frac{1}{2}\text{IC}_{50}$  had different and often opposite effects on the membrane permeability. Still, the dominating trend was a decrease in crystal violet uptake (Fig. 2B). The highest reduction in membrane permeability by 9.6% was recorded for Cu-NPs at  $\text{IC}_{50}$ . Contrarily, the application of NPs at  $\frac{1}{2}\text{IC}_{50}$  did not have a notable statistical outcome on the gathered findings. Nevertheless, it is worth underlining that  $\text{TiO}_2$ -NPs at  $\frac{1}{2}\text{IC}_{50}$  reduced the most membrane permeability compared to other NPs (Fig. 2B). However, statistical analysis disclosed that Ag-NPs, ZnO-NPs and  $\text{TiO}_2$ -NPs at  $\text{IC}_{50}$  and  $\frac{1}{2}\text{IC}_{50}$  had a significant and differentiating effect ( $p < 0.05$ ) on the collected data. Regardless of the NPs concentrations, Ag-NPs ( $p = 0.015$ ) and  $\text{TiO}_2$ -NPs ( $p = 0.0018$ ) proved to have the most pronounced effect on the membrane permeability.

As with previous strains, separate NPs also generated different alterations in the membrane permeability of *S. epidermidis*. Ag-NPs and ZnO-NPs at  $\text{IC}_{50}$  and  $\frac{1}{2}\text{IC}_{50}$  acted similarly. Only ZnO-NPs at  $\frac{1}{2}\text{IC}_{50}$  slightly decreased membrane permeability compared to the control cells. However,  $\text{TiO}_2$ -NPs showed the opposite effect leading to a significant increase in membrane permeability by 88.5% (Fig. 2C). It is also worth emphasising that Ag-NPs, Cu-NPs and  $\text{TiO}_2$ -NPs at  $\frac{1}{2}\text{IC}_{50}$  had a lower impact on the membrane permeability than at  $\text{IC}_{50}$ . Statistical analysis showed that almost all NPs at both concentrations, except for Ag-NPs, induced significant changes in membrane permeability ( $p < 0.05$ ). The most distinguishable differences between the samples treated with both concentrations of NPs were established for Cu-NPs ( $p = 0.00000$ ) and  $\text{TiO}_2$ -NPs ( $p = 0.00002$ ).

Conclusively, the uptake of crystal violet by tested microorganisms depended on the type and concentration of individual NPs. The obtained findings also evidenced that the extent of crystal violet uptake was more remarkable in *E. coli* than in *B. cereus* and *S. epidermidis*, suggesting more prominent alterations in membrane permeability of *E. coli* cells under NPs stress. Moreover, it is essential to underline that *S. epidermidis* was more susceptible to changes in membrane permeability caused by NPs than *B. cereus*.

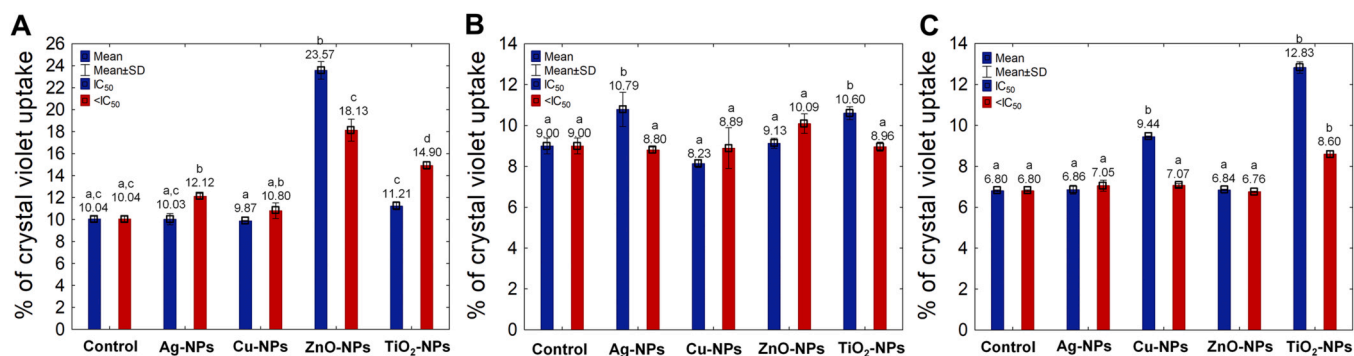


Fig. 2. Changes in membrane permeability of *E. coli* (A), *B. cereus* (B) and *S. epidermidis* (C) exposed to NPs at IC<sub>50</sub> and 1/2IC<sub>50</sub> (mean ± SD; n = 3).

### 3.2. Cytoplasmic leakage from bacteria exposed to NPs

The disruption of the outer layers and cytoplasmic leakage from bacterial cells exposed to NPs at IC<sub>50</sub> and 1/2IC<sub>50</sub> were monitored over 24 h. However, the presented results refer only to the sampling times when changes in the outflow of extracellular content occurred, preceding the rupture of the outer cell layers. It was found that all strains increased the release of cellular content under NPs stress (Fig. 3). In *E. coli* cells, the most noticeable increase in cytoplasmic leakage by 2276.8% was established in the presence of Cu-NPs at IC<sub>50</sub> (Fig. 3A). Similarly, all NPs at 1/2IC<sub>50</sub> stimulated release of cellular content from these bacteria. However, treatment of *E. coli* with NPs at IC<sub>50</sub> and 1/2IC<sub>50</sub> caused considerable modifications in released intracellular content ( $p < 0.05$ ), the most prominent changes emerged under Cu-NPs ( $p = 0.0019$ ) and TiO<sub>2</sub>-NPs ( $p = 0.0023$ ) exposure.

Intriguingly, the data set obtained for *B. cereus* revealed a similar impact of all NPs on the cytoplasmic leakage from bacterial cells (Fig. 3B). A noteworthy increase by 401.2% and 511.6% in the released cellular content appeared under ZnO-NPs at IC<sub>50</sub> and TiO<sub>2</sub>-NPs at 1/2IC<sub>50</sub> treatments, respectively. Simultaneously, the bacteria cultured with Cu-NPs and ZnO-NPs at 1/2IC<sub>50</sub> were characterised by reduced cytoplasmic leakage compared to NPs at IC<sub>50</sub>; however, Ag-NPs and TiO<sub>2</sub>-NPs at 1/2IC<sub>50</sub> caused the opposite effect. Interestingly, significant changes in cytoplasmic leakage from bacterial cells treated with both concentrations of NPs occurred only in the presence of ZnO-NPs ( $p = 0.026$ ) and TiO<sub>2</sub>-NPs ( $p = 0.021$ ). Finally, it was established that *B. cereus* was most sensitive to metal oxide NPs.

Significant changes in the cytoplasmic leakage from *S. epidermidis* cells were also displayed compared to the untreated cells (Fig. 3C). The highest increase in the release of cellular content by 1640.6% from these bacteria occurred after exposure to Cu-NPs at IC<sub>50</sub>. Interestingly, NPs at 1/2IC<sub>50</sub> showed a similar effect on the cytoplasmic leakage, with a clear predominance of Ag-NPs affecting the most the increase in the outflow of cellular content (by 1275.1%). Statistical analysis revealed that solely the presence of Ag-NPs and Cu-NPs at IC<sub>50</sub> and 1/2IC<sub>50</sub> significantly altered the release of cytoplasmic content from *S. epidermidis* cells ( $p < 0.05$ ). Furthermore, it was established that *S. epidermidis* was most sensitive to Cu-NPs and TiO<sub>2</sub>-NPs treatment which may result from a comparable mode of action.

To conclude, *E. coli* was more susceptible to NPs treatment than *B. cereus* and *S. epidermidis*. Correspondingly, *B. cereus* and *S. epidermidis* were most affected by different NPs concentrations than *E. coli*.

### 3.3. Intracellular and extracellular content of ATP under NPs stress

The findings confirmed significant differences in total ATP concentrations after exposure of *E. coli*, *B. cereus* and *S. epidermidis* to NPs stress (Fig. 4). Regarding *E. coli* cells, treatment with Ag-NPs at IC<sub>50</sub> caused the highest increase by 198.8% in ATP intracellular level. It is worth underlining that other NPs at IC<sub>50</sub> had the opposite effect (Fig. 4A). By

contrast, an overall increase in the extracellular ATP concentration occurred under Ag-NPs and Cu-NPs at 1/2IC<sub>50</sub> treatments, while an opposite outcome was observed in the presence of ZnO-NPs and TiO<sub>2</sub>-NPs (Fig. 4B). Interestingly, the only significant differences in ATP contents were established for two concentrations of ZnO-NPs ( $p = 0.0015$ ). The greatest repletion by 515.6% was recorded for Cu-NPs at 1/2IC<sub>50</sub> compared to the untreated cells. To conclude, treating *E. coli* cells with NPs resulted in various modifications in total ATP content. A similar mode of action was exhibited by ZnO-NPs and TiO<sub>2</sub>-NPs, which caused comparable depletion in the intracellular and extracellular ATP contents.

The results for *B. cereus* showed that all NPs, except for Ag-NPs at 1/2IC<sub>50</sub>, caused a decrease in the intracellular ATP level (Fig. 4C). Significant differences between different dosage treatments were established for Ag-NPs ( $p = 0.000023$ ), Cu-NPs ( $p = 0.00020$ ) and ZnO-NPs ( $p = 0.045$ ). The most significant depletion and repletion in the extracellular ATP concentrations, by 213.3% and 432%, were recorded for ZnO-NPs and Ag-NPs at IC<sub>50</sub>, respectively (Fig. 4D). Interestingly, treatment of these bacteria with NPs at IC<sub>50</sub> and 1/2IC<sub>50</sub> caused significant ( $p < 0.05$ ) alternations in the extracellular ATP concentrations. To summarise, each NPs showed a characteristic effect on the total ATP concentration in *B. cereus* cells. Among NPs used, only ZnO-NPs and TiO<sub>2</sub>-NPs had a comparable impact on the total ATP concentrations.

Simultaneously, the data for *S. epidermidis* displayed a decrease in the intracellular and extracellular ATP concentrations under NPs stress. Taking into account both doses of NPs, the following order of NPs: TiO<sub>2</sub>-NPs < Cu-NPs < Ag-NPs < ZnO-NP shows a downward trend in the concentrations of both types of ATP (Fig. 4E, F). It is worth noting that the presence of ZnO-NPs at IC<sub>50</sub> in bacteria culture resulted in the greatest reduction in the intracellular and extracellular ATP contents by 89.9% and 95.2% compared to the untreated cells, respectively. The statistical analysis demonstrated a significant impact of Cu-NPs ( $p = 0.00026$ ) and TiO<sub>2</sub>-NPs ( $p = 0.000002$ ) at different dosages on the intracellular ATP content in *S. epidermidis*. Contrarily, only Cu-NPs ( $p = 0.00049$ ) and ZnO-NPs ( $p = 0.034$ ) caused significant changes in the extracellular ATP concentration. In conclusion, *S. epidermidis* was less sensitive to NPs at 1/2IC<sub>50</sub> than at IC<sub>50</sub>. Additionally, NPs influenced changes in the extracellular content of ATP to a lesser extent than the intracellular concentration.

Summarising this research series, the alterations in the intracellular and extracellular ATP contents were fundamentally different and depended solely on the strain, type of NPs and their concentrations. Moreover, bacteria exposure to NPs exhibited more significant variations in the intracellular ATP levels than external ones. A similar effect of NPs on total ATP content was observed for *B. cereus* and *S. epidermidis*. Moreover, these strains were more susceptible to different dosage treatments than *E. coli*. The conclusion is also that ZnO-NPs were common NPs for all strains causing significant differences in the measured ATP values.

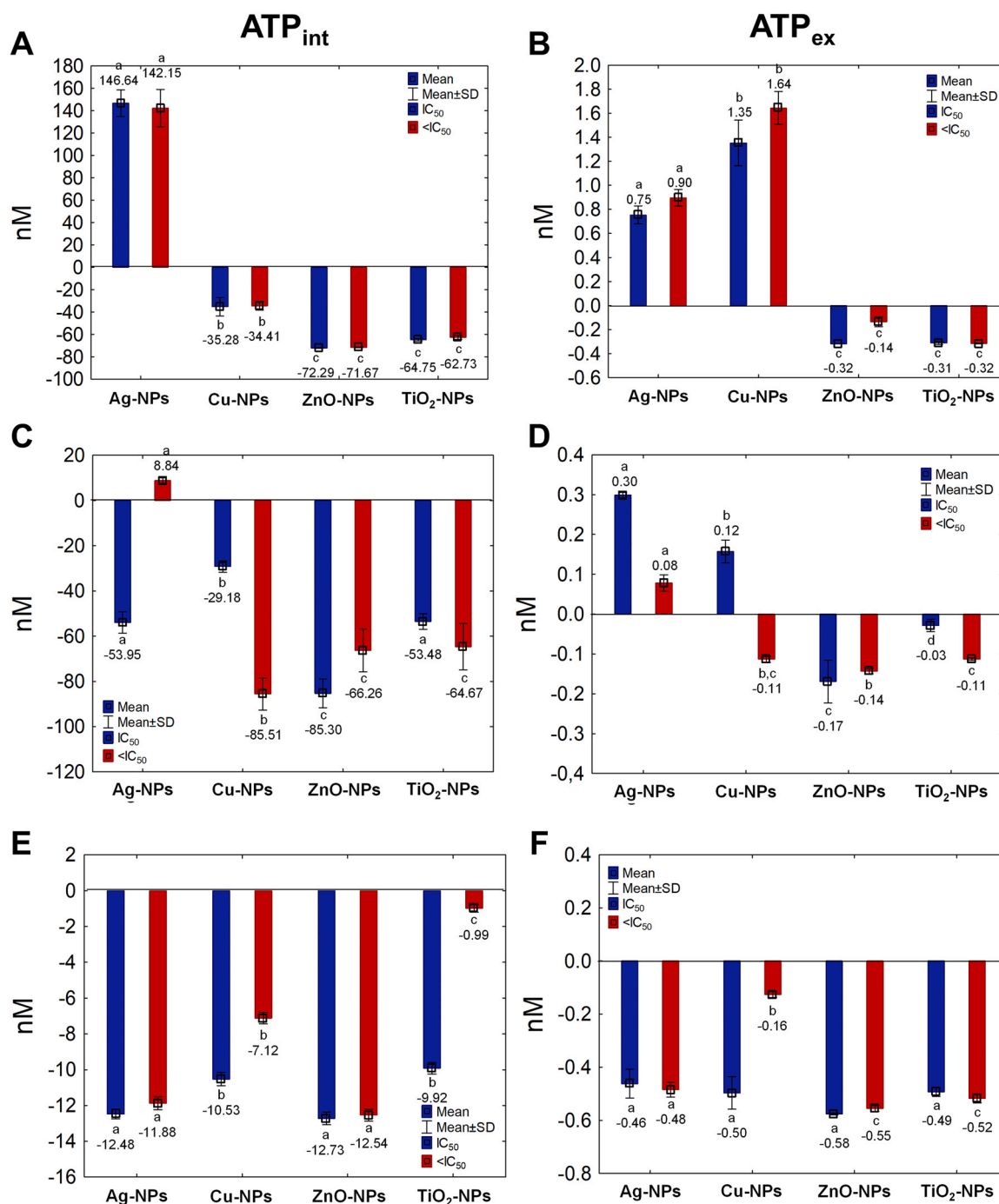


Fig. 3. Changes in cytoplasmic leakage from *E. coli* (A), *B. cereus* (B) and *S. epidermidis* (C) cells exposed to NPs at IC<sub>50</sub> and 1/2IC<sub>50</sub> at λ = 260 nm (mean ± SD; n = 3).

3.4. ATPase activity in bacteria exposed to NPs

ATPase activity was measured to extend the research concerning the changes in total ATP concentration in bacteria under NPs stress. In *E. coli*, the most remarkable increase in ATPase activity by 28.2% appeared in the presence of ZnO at IC<sub>50</sub>; however, the highest reduction in its activity by 19.9% occurred under exposure to Cu-NPs at 1/2IC<sub>50</sub> (Fig. 5A). Although there was a significant variability in ATPase activity between different dosage treatments (p < 0.05), the most visible differences were found for *E. coli* exposed to Ag-NPs (p = 0.000042) and TiO<sub>2</sub>-NPs (p = 0.00058). To summarise, ATPase in *E. coli* was more sensitive to Cu-NPs and ZnO-NPs than other NPs.

In *B. cereus*, only TiO<sub>2</sub>-NPs at IC<sub>50</sub> and 1/2IC<sub>50</sub> caused an increase in

ATPase activity by around 5.4%. By contrast, the remaining NPs inhibited its activity (Fig. 5B). The highest decrease in ATPase activity by 25.9% compared to its activity in the untreated cells occurred in the presence of Ag-NPs at IC<sub>50</sub>. Furthermore, the most significant and differentiating alterations in ATPase activity were documented for Ag-NPs and Cu-NPs (p < 0.05). Intriguingly, this bacterium was less susceptible to NPs at 1/2IC<sub>50</sub> than at IC<sub>50</sub>.

Conversely, the measurements of ATPase activity in *S. epidermidis* exposed to NPs confirmed a downward trend under Ag-NPs, Cu-NPs and TiO<sub>2</sub>-NPs at IC<sub>50</sub> and 1/2IC<sub>50</sub> treatments compared to the control cells (Fig. 5C). A substantial decrease in its activity by 27% and 28.7% was recorded for Ag-NPs and TiO<sub>2</sub>-NPs at IC<sub>50</sub>, respectively. The only NPs that enhanced the ATPase activity were ZnO-NPs. Correspondingly,



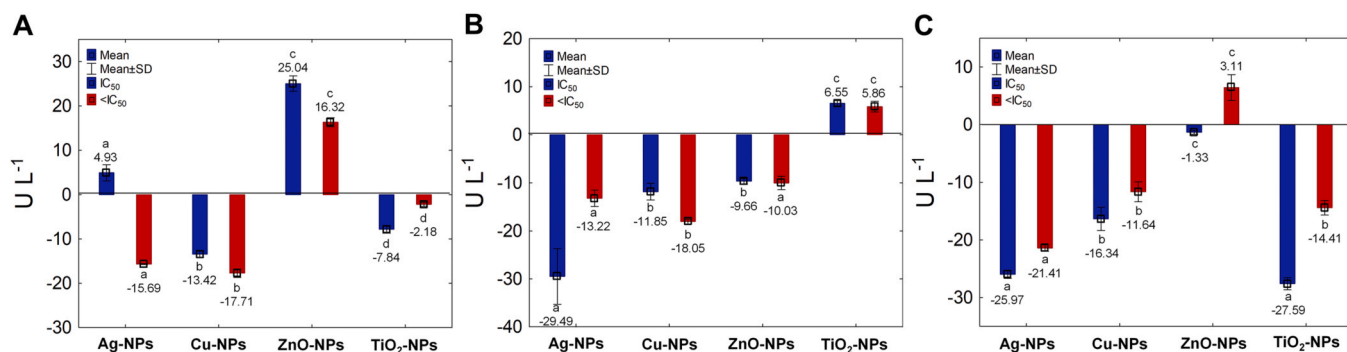


Fig. 4. Changes in the intracellular and extracellular content of ATP under exposure of *E. coli* (A, B), *B. cereus* (C, D) and *S. epidermidis* (E, F) to NPs at  $IC_{50}$  and  $\frac{1}{2}IC_{50}$  (mean  $\pm$  SD;  $n = 3$ ).

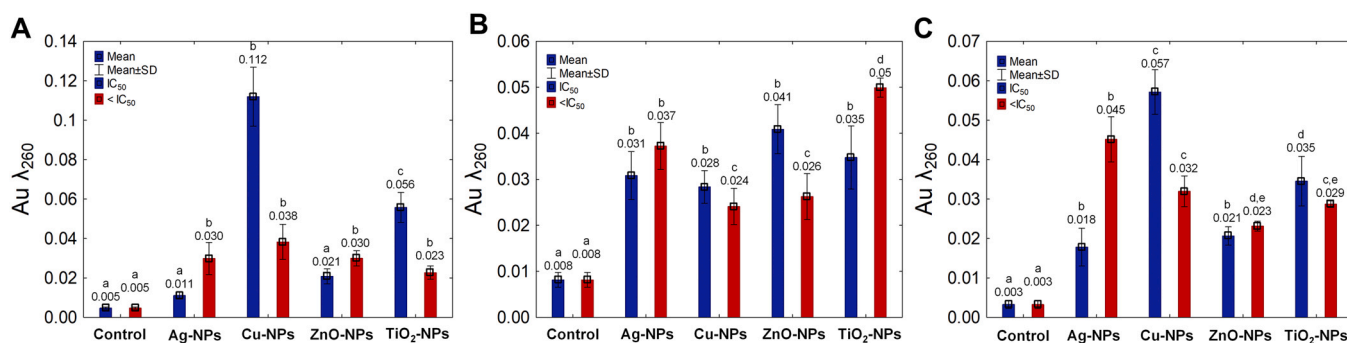


Fig. 5. ATPase activity in *E. coli* (A), *B. cereus* (B) and *S. epidermidis* (C) exposed to NPs at  $IC_{50}$  and  $\frac{1}{2}IC_{50}$  (mean  $\pm$  SD;  $n = 3$ ).

statistical data analysis confirmed the most significant differences between NPs treatments for Ag-NPs ( $p = 0.001$ ) and  $TiO_2$ -NPs ( $p = 0.00015$ ). It is worth pointing out that *S. epidermidis* was generally characterised by similar susceptibility to metal NPs.

Ultimately, individual NPs similarly affected ATPase activity in *B. cereus* and *S. epidermidis*; however, more divergent modulations were documented for *E. coli*. It is worth underlining that both *E. coli* and *S. epidermidis* were more sensitive to NPs at  $IC_{50}$  than  $\frac{1}{2}IC_{50}$  compared to *B. cereus*. In analogy to the conclusions of previous studies, the recorded ATPase activity varied depending on the type and concentrations of tested NPs.

### 3.5. Fatty acid composition of bacteria exposed to NPs

FAME profiles were analysed to investigate how individual NPs affect the composition of bacterial cell membranes. The FAME profiles generated for *E. coli*, *B. cereus* and *S. epidermidis* treated with NPs showed significant alternations in the percentages of relevant saturated and unsaturated fatty acids compared to the control cells (Fig. 6). For instance, the exposure of *E. coli* to Ag-NPs at  $IC_{50}$  resulted in a substantial increase by 29.9% in the straight-chain fatty acid abundance along with a notable decrease in the contents of hydroxylated and cyclopropane fatty acid by 38.9% and 47.1%, respectively (Fig. 6A). It is also worth emphasising that treatment of *E. coli* with Cu-NPs at  $\frac{1}{2}IC_{50}$  caused a prominent decrease in the hydroxylated and cyclopropane fatty acid percentages by 28.5% and 51.9%, respectively. This phenomenon was accompanied by a simultaneous reduction in the content of branched fatty acids by 37.6%. The PCA analysis explained 96.03% and 96.57% of the variance for the data concerning *E. coli* exposed to NPs at  $IC_{50}$  and  $\frac{1}{2}IC_{50}$ , respectively (Fig. 7A, B). Furthermore, the most significant influence of Ag-NPs at  $IC_{50}$  and Cu-NPs  $\frac{1}{2}IC_{50}$  on the composition of FAME profiles was confirmed. To summarise, both metal NPs resulted in the most remarkable modifications in the fatty acid composition of *E. coli*.

In FAME profiles of *B. cereus*, significant changes were related to the decrease in the content of branched fatty acids after exposure to NPs (Fig. 6B). The highest decline in their percentages by 83.7% and 81.4% were recorded in the presence of Cu-NPs and ZnO-NPs at  $\frac{1}{2}IC_{50}$ , respectively. On the other hand, exposure of *B. cereus* to NPs increased cyclopropane fatty acid abundance, especially in the presence of  $TiO_2$ -NPs. A significant decrease accompanied these changes by 19.7% and an increase by 22.7% in the unsaturated fatty acid levels under exposure to Ag-NPs at  $\frac{1}{2}IC_{50}$  and ZnO-NPs at  $IC_{50}$ , respectively. It is worth pointing out that PCA analysis for *B. cereus* treated with NPs at  $IC_{50}$  and  $\frac{1}{2}IC_{50}$  was represented by 89.43% and 83.29% of the variance (Fig. 7C, D). Moreover, it indicated that *B. cereus* was predominantly affected by ZnO-NPs. Nevertheless, treatment of this bacterium with Cu-NPs and  $TiO_2$ -NPs at  $\frac{1}{2}IC_{50}$  caused significant changes in FAME profiles.

Simultaneously, the data for *S. epidermidis* revealed significant alterations in the hydroxylated and cyclopropane fatty acid contents (Fig. 6C). For instance, the highest decrease by 55.4% and 23.3% in hydroxylated fatty acid participation occurred under exposure of Cu-NPs at  $IC_{50}$  and Ag-NPs at  $IC_{50}$ . In parallel, adding Cu-NPs at  $IC_{50}$  and  $\frac{1}{2}IC_{50}$  to *S. epidermidis* culture decreased the percentages of cyclopropane fatty acids by 47.6% and 49.1% compared to the untreated cells, respectively. Interestingly, the presence of Ag-NPs at  $IC_{50}$  caused a notable increase by 32.9% in the unsaturated fatty acid level. The PCA projection for FAME profiles showed 81.14% and 98.98% divergence (Fig. 7E, F). Major dissimilarities for the control and NPs treated samples were discovered for ZnO-NPs at  $IC_{50}$ , and Cu-NPs and  $TiO_2$ -NPs at a lower dose. Considering the FAME results for *S. epidermidis*, there was a unique and extraordinary effect of two doses of NPs on the proportions of selected fatty acids. The stress induced in the cells by Cu-NPs resulted in the most remarkable changes in the percentages of analysed fatty acid groups.

The FAME comprehensive analysis indicated the diverse and significant effects of NPs at  $IC_{50}$  and  $\frac{1}{2}IC_{50}$  on the participation of distinguished fatty acid groups in *E. coli*, *B. cereus* and *S. epidermidis*. The

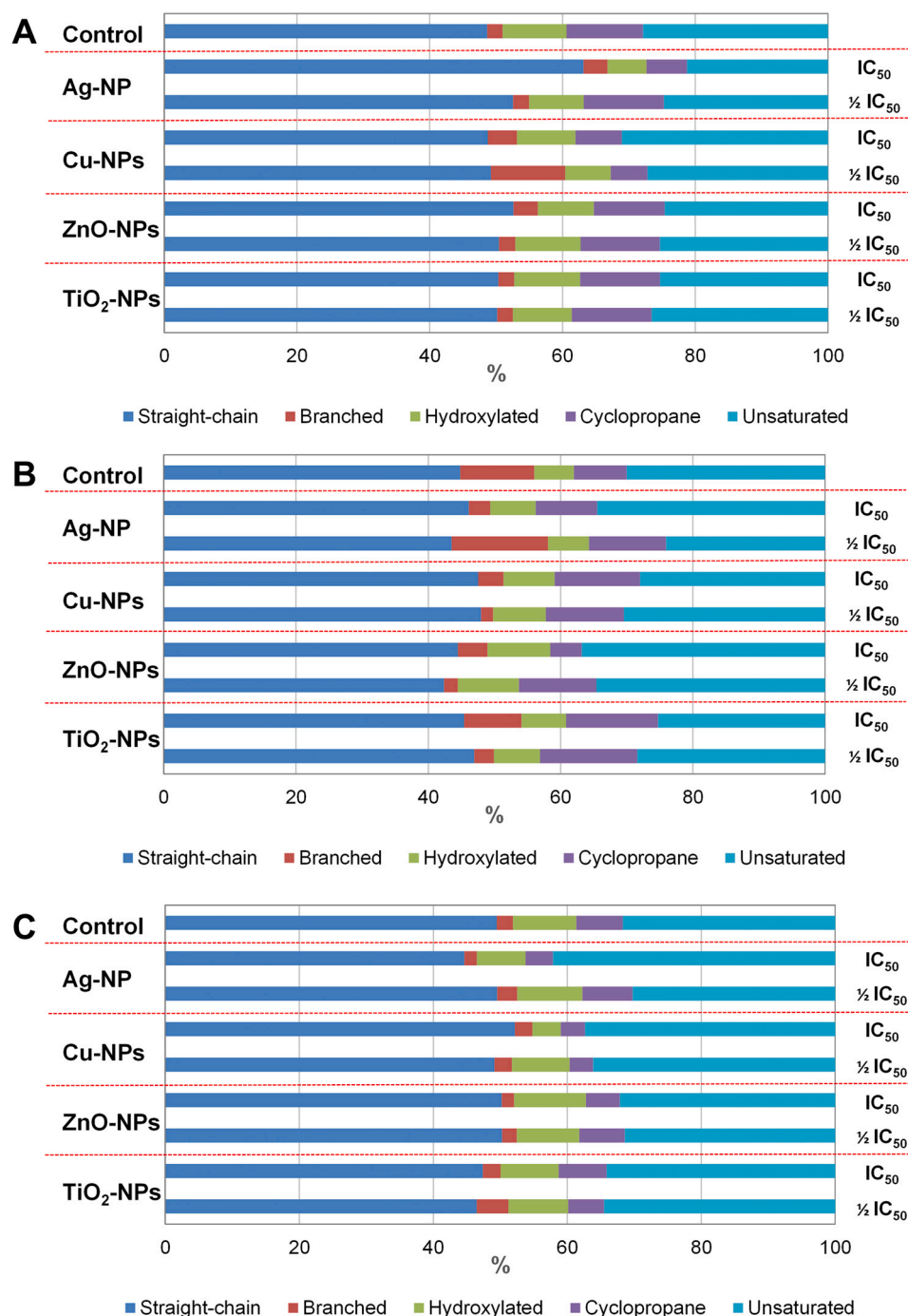


**Fig. 6.** Percentages of straight-chain, branched, hydroxylated, cyclopropane and unsaturated fatty acids in FAME profiles of *E. coli* (A), *B. cereus* (B) and *S. epidermidis* (C) exposed to NPs at IC<sub>50</sub> and ½IC<sub>50</sub>.

uncovered changes were characteristic for each strain and tested NPs. The acids most prone to NPs stress turned out to be cyclopropane fatty acids. Furthermore, it was established that metal NPs changed FAME profiles to a greater extent than metal oxide NPs. Correspondingly, *B. cereus* and *S. epidermidis* were more sensitive to NPs at a lower concentration than *E. coli*.

### 3.6. Statistical data exploration

The cluster analysis with a tree diagram showed that all attributes present a unique pattern for each strain (Fig. 8). Overall, the cluster visualisation revealed no differences between the NPs concentrations.

Cluster analysis dendrograms for *E. coli* demonstrated that only Ag-NPs had the most differentiating impact on bacteria, with intracellular ATP concentration (ATP<sub>int</sub>) as a major discriminating factor in the obtained data (Fig. 8A, B). By comparison, the diagrams generated for *B. cereus* formed hierarchical clusters with the most significant changes in the samples with ZnO-NPs at IC<sub>50</sub> and Cu-NPs, ZnO-NPs, and TiO<sub>2</sub>-NPs at ½IC<sub>50</sub> (Fig. 8C, D). However, clustering showed identical dendrogram for conducted analysis independently of NPs concentrations. Similarly to *B. cereus*, the dendrogram created for *S. epidermidis* separated two groups for both NPs doses and demonstrated that Ag-NPs, Cu-NPs and TiO<sub>2</sub>-NPs at IC<sub>50</sub> and ½IC<sub>50</sub> had the most divergent effect on the collected results (Fig. 8E, F). It is worth pointing out that ATPase activity and FAME

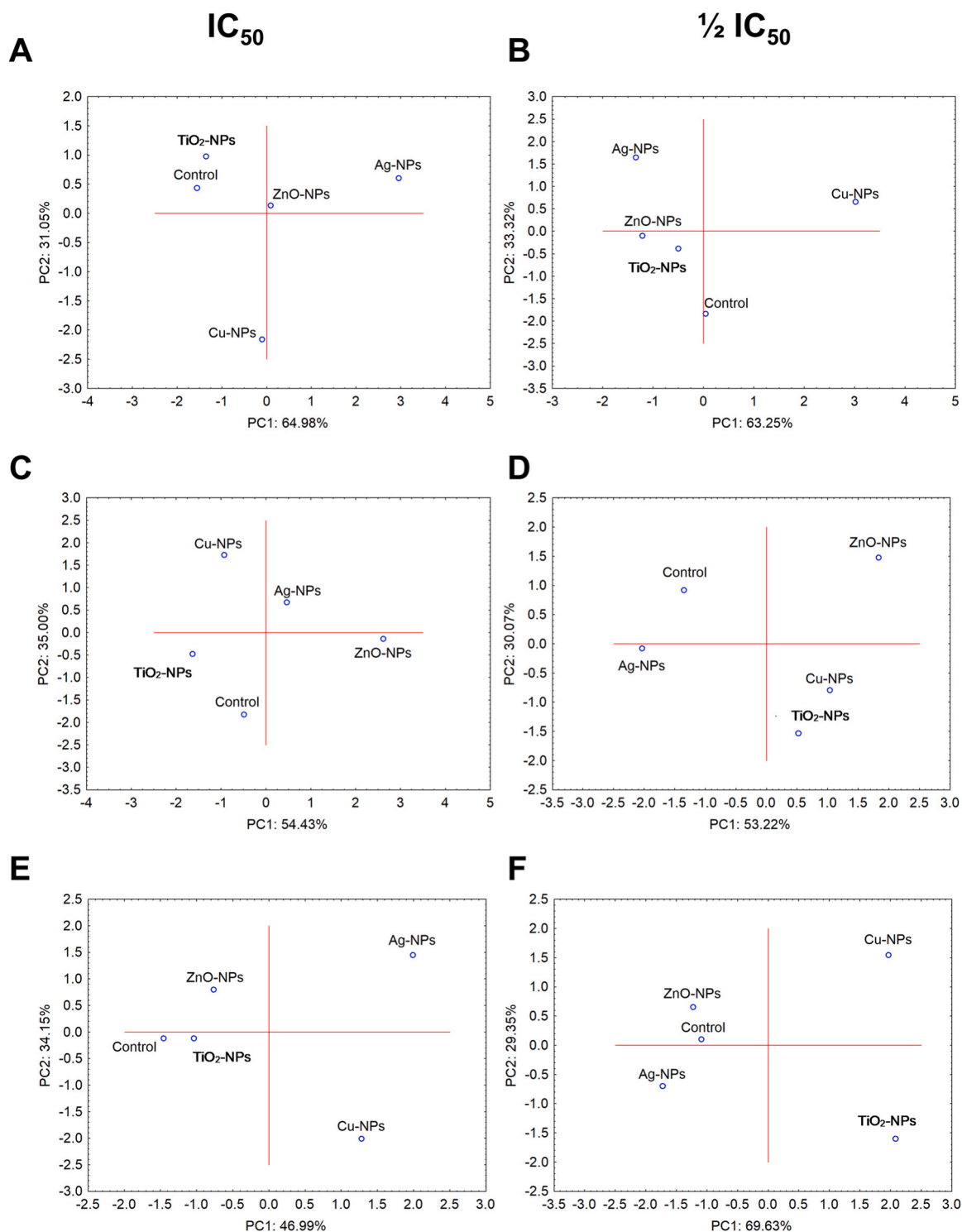


**Fig. 7.** Projection of PCA analysis of FAME profiles for *E. coli* (A, B), *B. cereus* (C, D), and *S. epidermidis* (E, F) exposed to NPs at  $IC_{50}$  and  $\frac{1}{2}IC_{50}$ .

composition (Sat and Unsat) were the most distinguished analyses.

### 3.7. Scanning electron micrographs of bacteria exposed to NPs

SEM analysis was performed to study the distribution and interactions of individual NPs with the bacteria surface and determine possible damage in their outer layers. Comparative analysis was only carried out for NPs at  $\frac{1}{2}IC_{50}$ , as NPs at  $IC_{50}$  created an intense background preventing image exploration. The collected SEM micrographs illustrate the diversified distribution and various NPs interactions with

*E. coli*, *B. cereus* and *S. epidermidis* cells compared to the intact control cells (Fig. 9). For example, Ag-NPs and  $TiO_2$ -NPs were characterised by slight affinity to the surface of *E. coli* cells, resulting in no changes in the cell morphology and damage to the cell wall (Fig. 9A). On the other hand, Cu-NPs accumulated on the entire surface of *E. coli*, but most often in peripheral places where large agglomerates were observed. Similarly, ZnO-NPs were dispersed evenly over the whole surface of this bacterium.

Interestingly, Ag-NPs, Cu-NPs and  $TiO_2$ -NPs showed less affinity to the surface of *B. cereus* than *E. coli* (Fig. 9B). Nevertheless, large clusters

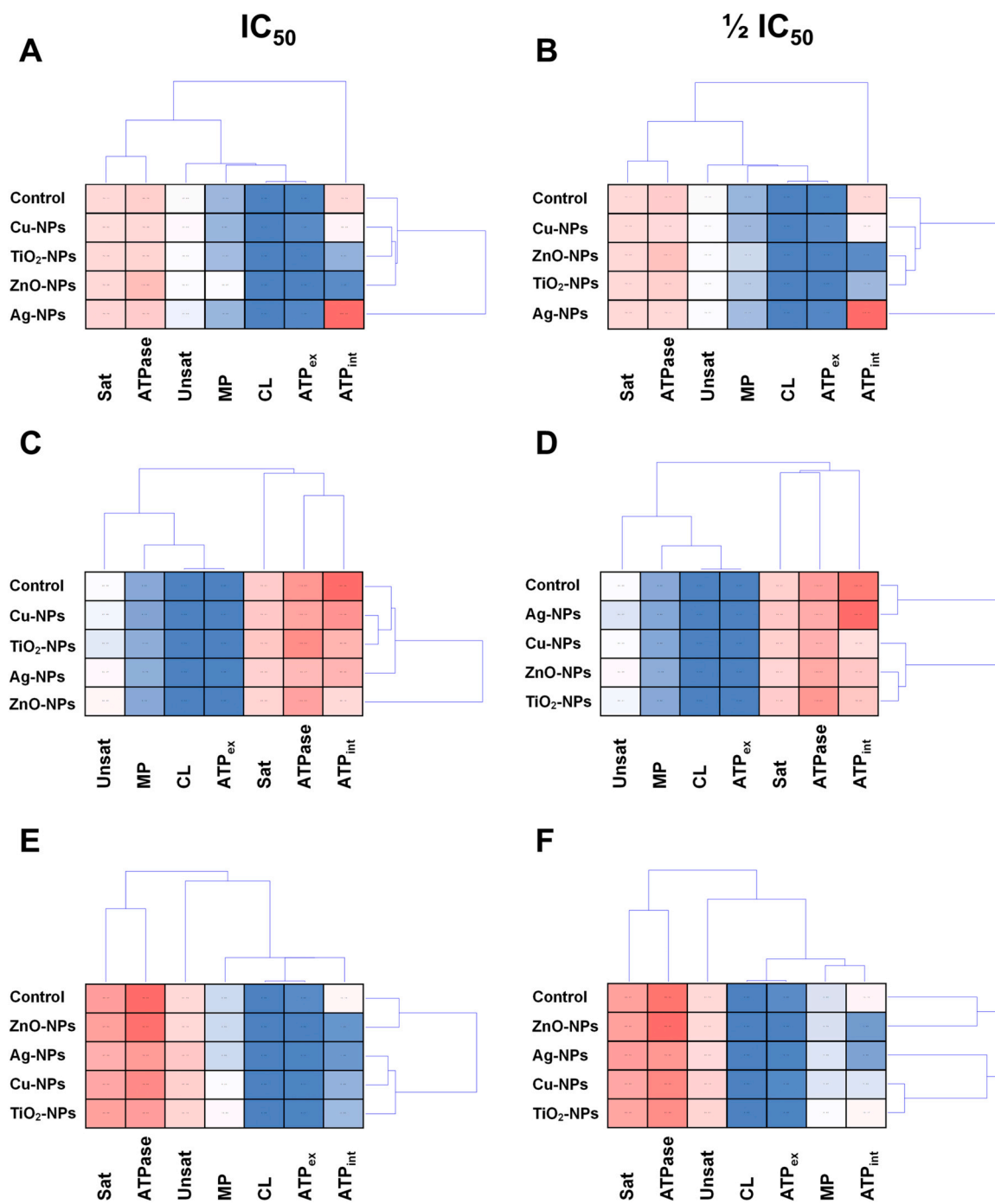


**Fig. 8.** Visualisation of multivariate data clustering for *E. coli* (A, B), *B. cereus* (C, D), and *S. epidermidis* (E, F) exposed to NPs at  $IC_{50}$  and  $\frac{1}{2}IC_{50}$ . Notes: ATPase - ATPase activity; ATP<sub>ex</sub> - extracellular ATP concentration; ATP<sub>int</sub> - intracellular ATP concentration; MP - membrane permeability; CL - cytoplasmic leakage; Sat - saturated fatty acids; Unsats - unsaturated fatty acids.

of Cu-NPs and TiO<sub>2</sub>-NPs were discerned in many places of the irregularly shaped outer layers. Intriguing observations were made for the cells treated with ZnO-NPs as they formed agglomerates and aggregates of various shapes and dimensions over the entire cell surface. The large quantity of ZnO-NPs attached to *B. cereus* cell displayed a tough outer shell formed by several rows of NPs clusters (Fig. 9B). The cell shape remained unchanged despite forming such a structure.

Similarly, most NPs did not change the shape of *S. epidermidis* cells compared to the untreated cells (Fig. 9C). Only Cu-NPs treatment resulted in slight morphological changes and the appearance of large NPs agglomerates with non-characteristic distribution on the bacteria

surface. In turn, TiO<sub>2</sub>-NPs covered the whole cell regularly, forming a uniform monolayer with the occasional appearance of larger NPs clusters.

In summary, ZnO-NPs were found to have the highest affinity to *E. coli* and *B. cereus* cells, while TiO<sub>2</sub>-NPs were most closely related to the surface of *S. epidermidis*. Moreover, Cu-NPs formed large clusters with no specific localisation on the surface of all tested cells. It can also be concluded that *E. coli* showed stronger interactions with NPs than *B. cereus* and *S. epidermidis*.

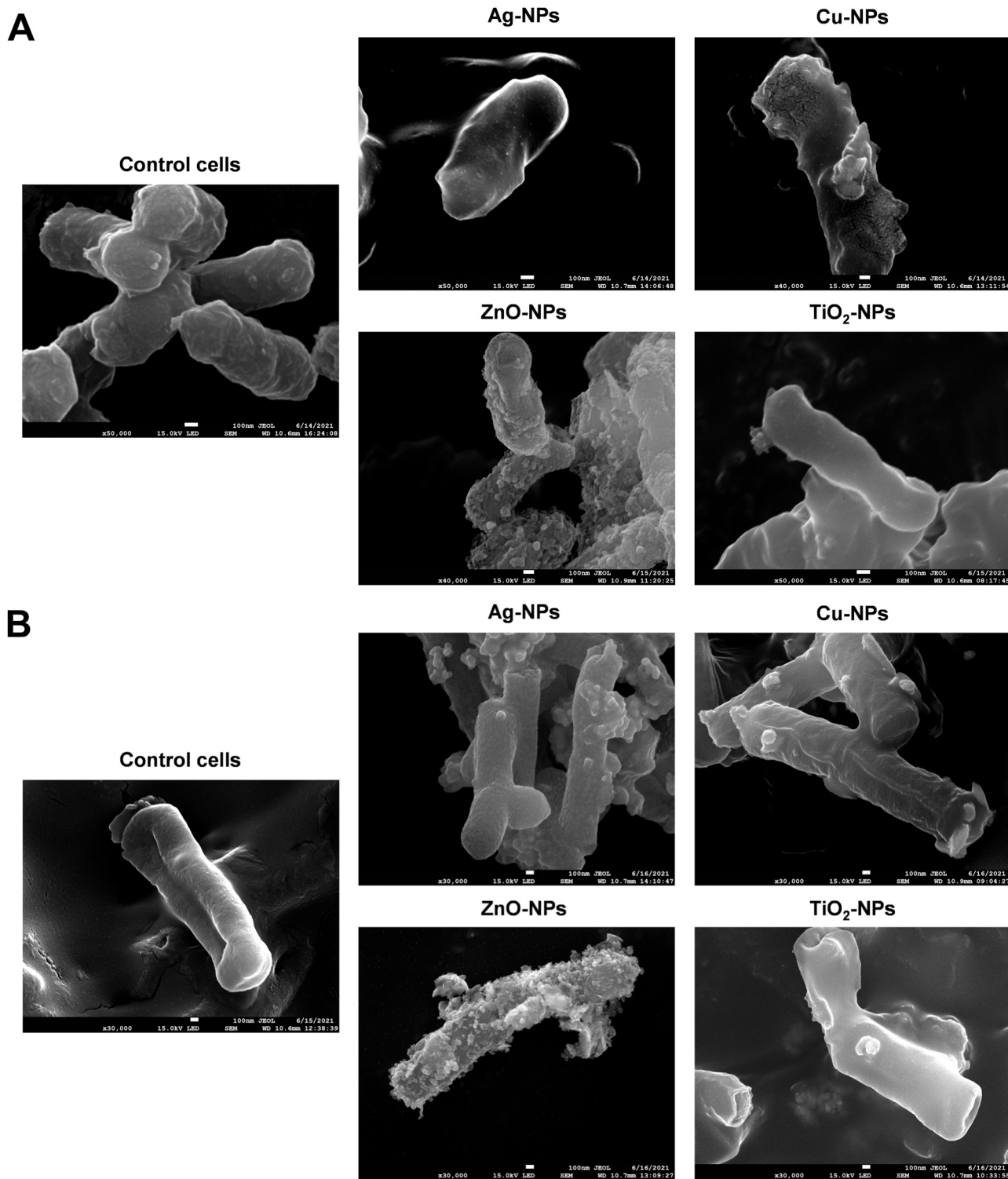


Fig. 9. SEM micrographs of *E. coli* (A), *B. cereus* (B) and *S. epidermidis* (C) exposed to NPs at  $\frac{1}{2}IC_{50}$ .

#### 4. Discussion

Microbial outer layers are the first line of defence systems against different external factors and potentially toxic substances. They are dynamic structures and simultaneously create an effective barrier for the strictly controlled transport of various substances, including NPs. It has been reported that NPs in size range up to 12 nm can pass through the bacterial cell membrane or get trapped within the lipid bilayer.

However, the disruptive effect of larger NPs (> 10 nm) on outer layer integrity is solely dependent on their adhesion and specific binding to the bacterial surface [37,48]. Research undertaken in this work confirmed the distinctive and idiosyncratic impact of differently sized NPs on the functioning of *E. coli*, *B. cereus* and *S. epidermidis* membranes. Regardless of the differences in the membrane permeability of the tested strains in the presence of NPs, increased cytoplasmic leakage was observed. Additionally, the cluster analysis confirmed the correlation

C

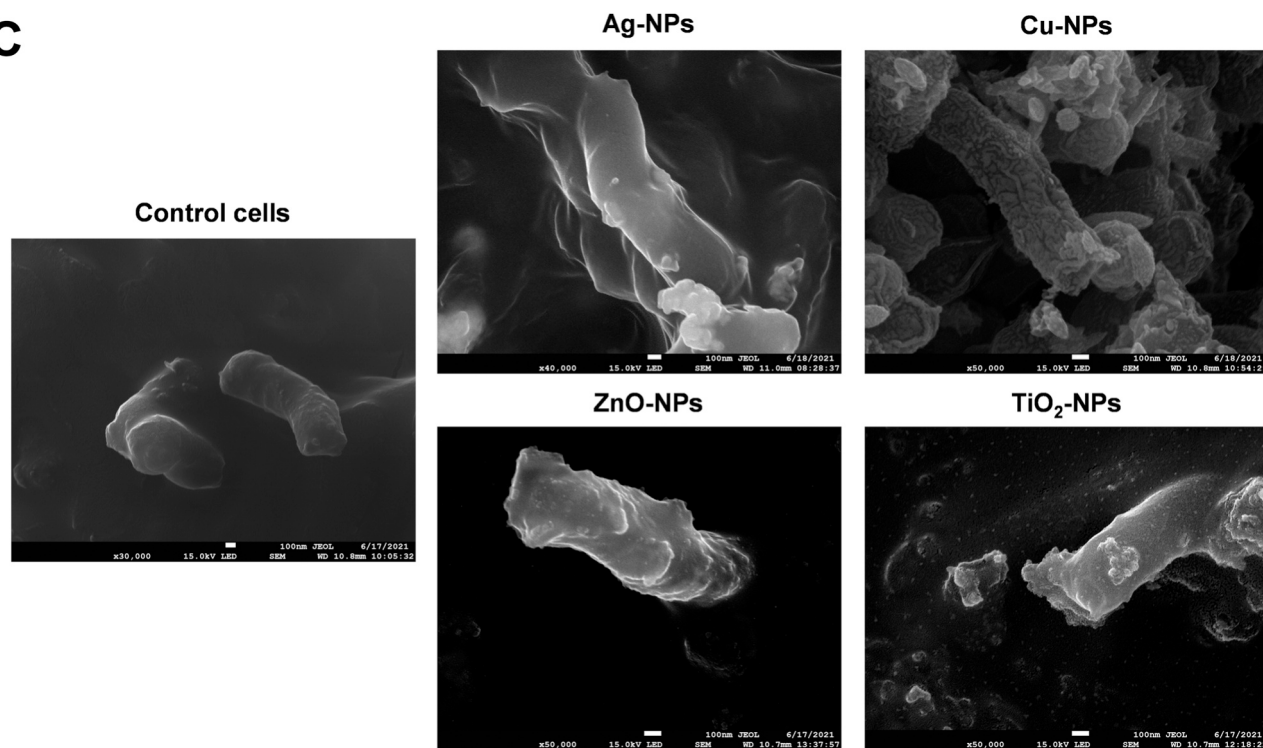


Fig. 9. (continued).

between membrane permeability and cytoplasmic leakage. It was also demonstrated that *E. coli* was characterised by more significant changes in membrane permeability than *B. cereus* and *S. epidermidis*. These changes could have resulted from the different organisation of the cell wall of the bacteria tested. Such an explanation is in accordance with the results by [31], who confirmed that both the membrane permeability and the value of the membrane potential of *E. coli* after exposure to  $\text{TiO}_2$ -NPs differed significantly from the corresponding values obtained for *Staphylococcus aureus*. By comparison, [28] observed membrane rupture of *E. coli*, *Pseudomonas putida*, *B. cereus* and *S. aureus* in the presence of Ag-NPs, which was accompanied by a distinctly different leakage of cytoplasmic protein, carbohydrates, and nucleic acids from individual strains. Herein, *B. cereus* was more resistant to membrane permeability changes and cytoplasmic leakage than *S. epidermidis*. It has been ascertained that *B. cereus* strains produce siderophores, which can chelate iron and other metals, providing independent metal tolerance mechanisms [47,57]. There is a possibility that these siderophores could inhibit the uptake and diffusion of released metal ions from NPs, diminishing their effect on membrane functioning. It is worth noting that a correlation between increased membrane permeability and cytoplasmic leakage was established for *S. epidermidis* after treatment with  $\text{TiO}_2$ -NPs. It could be due to the evenly distributed clusters of  $\text{TiO}_2$ -NPs on the surface of this bacterium compared to other bacterial cells with a different NPs localisation. Such adsorption of  $\text{TiO}_2$ -NPs onto the surface of *S. epidermidis* could cause membrane tension dependent on the contact area with the phospholipid bilayer resulting in its stretching and mechanical deformation. Overall, the increased interactive affinity and the higher density of surface-attached NPs clusters lead to more significant membrane breakage due to the higher concentration of NPs [37].

The direct and indirect interactions of NPs with bacterial cell envelopes can lead to disturbances in cellular respiration, electron transport, and, thus, in the level of total ATP. Considering that ATP is an important metabolite and the primary energy source in various cellular chemical reactions, alterations in its concentration can be used as a beneficial stress indicator in cells exposed to toxicological substances. The

obtained findings proved that the exposure of *E. coli*, *B. cereus* and *S. epidermidis* to metallic NPs significantly altered the total ATP concentrations. Moreover, the decrease in the whole ATP level was correlated with reduced ATPase activity. A similar dependence was found in the case of the action of metal oxide NPs, with ZnO-NPs having the most significant impact on ATP level and ATPase activity. Furthermore, it is essential to underline that the extracellular concentration of ATP as a signalling molecule fluctuates during the growth stages of bacterial cells, despite its level rising when the cell membrane ruptures [26]. Corresponding observations were acknowledged by [42], who reported that treatment of *E. coli* with  $\text{TiO}_2$ -NPs resulted in the depletion of intracellular ATP whilst increasing its content in extracellular solution. An opposite effect was disclosed in this study, as a general decrease in overall ATP in all bacterial strains. Such a conclusion can be attributed to the inhibition of ATPase functioning. The investigated inorganic NPs can generate various ROS and increase the concentration of protein carbonyls through their oxidation, which was revealed in our previous research [38]. Accordingly, disturbances in the cell membrane and the stimulated cascade mechanism of ROS-induced oxidation and reduction reactions can inactivate the action of ATPase. Moreover, induced oxidative stress and the release of metal ions by NPs can lead to enzymes' mismetallation, resulting in their inactivation [27]. Our previous work indicated that the presence of NPs in *E. coli*, *B. cereus* and *S. epidermidis* culture also resulted in the inhibition of overall dehydrogenase activity [38]. Decreased activity of this enzyme playing an essential role in the respiratory system of the bacterial cell could also contribute to the overall depletion of ATP. Likewise, the changes in ATP concentration and ATPase activity caused by Ag-NPs and  $\text{Fe}_3\text{O}_4$ -NPs in *E. coli* cells were associated with inhibiting the  $\text{H}^+$ -translocating system [19]. Additionally, the concentration of ATP changes dynamically under stressful conditions because it is used in various cellular processes, including protein synthesis [17]. Therefore, it could be used as a driving force for redox protein synthesis as a defence mechanism against NPs stress. Interestingly,  $\text{Zn}^{2+}$  ions can mediate an increase in ATP production through enhanced protein synthesis with ATP synthase function [58]. Such a phenomenon would explain the stimulating effect of

ZnO-NPs at IC<sub>50</sub> and 1/2IC<sub>50</sub> on *E. coli* ATPase activity. According to literature data, NPs can alter protein synthesis through changes in the expression level of selected bacterial genes and denaturation of the ribosome [48,49]. For example, treating *E. coli* with TiO<sub>2</sub>-NPs resulted in the down-regulation of genes encoding components of ATPase protein, which was reflected in a reduced concentration of ATP and proton export [49]. The heavy metal ions released from NPs and generated ROS could have contributed to changes in the transcriptional activity of tested microorganisms, additionally influencing the synthesis of proteins of respiratory metabolism. The differential effect of metallic NPs on cells presented in this work may relate to their dimensions and, thus, different interactions and reactivity with the bacterial cell surface. In addition, some metals are necessary and essential for microbial cell growth and metabolic functions [36]. Therefore, the very adaptations of bacteria to specific heavy metals may result in a differentiated response to their presence.

Despite the emergence of new knowledge concerning the effects of NPs on bacterial cells, little is still known about the impact of NPs on bacterial fatty acid composition and the associated fluctuations in the permeability of the cell membranes. It is a crucial issue because the fatty acid composition determines the dynamic nature of membranes and can provide additional resistance against toxic factors [34]. Here, the recorded alterations in FAME profiles were unique for each strain and type of tested NPs. Nevertheless, both *E. coli* and *B. cereus* were characterised by a significant decrease in the percentages of cyclopropane and hydroxyl fatty acid, especially in the presence of Cu-NPs and ZnO-NPs, respectively. According to [43], cyclopropane fatty acids stabilise membranes through induction of a greater degree of order than their unsaturated precursors and limit the rotation of the bonds surrounding the cyclopropane ring. They also disrupt lipid packing, favour the occurrence of "gauche" defects in the chains and increase the lateral lipid diffusion, enhancing membrane fluidity. Here, cyclopropane fatty acids are more likely to decrease the membrane order and seal cytoplasmic leakage. Reducing the percentages of hydroxyl and branched fatty acids makes the phospholipid bilayer more rigid [34]. Branched-chain fatty acids display a lower melting point temperature than their equivalent straight-chain fatty acids. Hence, their decreased content in the membrane is expected to reduce its fluidity. Similarly, lower content of hydroxylated fatty acids in *S. epidermidis* exposed to NPs could potentially contribute to the rigidity of the cell membrane. Furthermore, the increased ratio of saturated to unsaturated fatty acids calculated for all strains indicates a decrease in membrane fluidity, making it less permeable. Our recent research showed that NPs and generated ROS induced lipid peroxidation and altered the composition of certain groups of fatty acids [38]. In general, lipid peroxidation can enhance membrane fluidity making them more susceptible to NPs damage [32]. The obtained changes in the content of the analysed fatty acid groups can be attributed to the resistance mechanism of the tested bacterial cells. However, considering the differences in membrane permeability and cytoplasmic leakage, it can be argued that NPs could cause holes in outer layers through the interaction with bacterial surfaces or through accumulation in the cell membrane, causing intense cellular leakage [16]. [14] stated that Ag-NPs acted upon the plasma membrane in *E. coli* and *P. aeruginosa* cells resulting in the release of intracellular K<sup>+</sup> and internalisation of NPs through the formation of pits on the bacterial surfaces.

SEM analysis provided valuable information on bacteria-NPs interactions and allowed imaging of NPs distribution on the cell surface. All NPs adhered to a different extent to the surface of *E. coli*, *B. cereus* and *S. epidermidis*, depending on the type of NPs and the microorganism. For example, Cu-NPs exhibited a strong affinity to peripheral sites of *E. coli*. This may suggest that there could be more binding sites, such as lipopolysaccharides favouring hydrogen bonding and hydrophobic interactions at these sites [44]. On the other hand, ZnO-NPs had a powerful affinity to the whole surface of *B. cereus*, forming large and layered NPs clusters. This indicates eminent sequestration and anionic

binding of ZnO-NPs by peptidoglycan and teichoic acids of *B. cereus* cells. Specifically, divalent metal ions are bound by the phosphate groups of teichoic acids [51]. Here, both Cu-NPs (Cu<sup>2+</sup>) and ZnO-NPs (Zn<sup>2+</sup>) were attached similarly to the surface of *B. cereus* cells. Analogously, [15] confirmed the importance of teichoic acids and negatively charged moieties in *Bacillus subtilis* cells in Au-NPs binding. By comparison, *S. epidermidis* cells were fully covered by large agglomerates of TiO<sub>2</sub>-NPs. It was reported that TiO<sub>2</sub>-NPs adhere strongly to COO<sup>-</sup> groups in the cell membrane [25]. Intriguingly, both ZnO-NPs and TiO<sub>2</sub>-NPs formed large aggregates and agglomerates on bacterial surfaces with high concentrations of NPs. In addition, the micrographs showed the released metal ions in the closest vicinity of the cell. It is worth emphasising that Ag-NPs did not adhere to the surface of *E. coli*, *B. cereus* and *S. epidermidis* compared to the other NPs. This might be due to the potential lower overall positive charge of Ag-NPs, and, thus, less attraction to the negatively charged outer layers of microbial cells. Furthermore, no morphological alterations or visible damages to the bacterial envelopes were discovered compared to the published data indicating evident cell damage [11]. In order to explain in detail the mechanisms of NPs interactions with the surface of bacterial cells, we have just started new research at the molecular level aimed at determining the distribution of atoms on the cell surface and the interaction of NPs with the functional groups of phospholipids and surface proteins using advanced attenuated total reflection Fourier transform infrared spectroscopy (ATR-FTIR).

## 5. Conclusions

The presented results provided new knowledge in understanding the complex processes induced by NPs in bacterial cells, underlying the disturbance and functioning of the cell envelope structure. The tested NPs were characterised by a specific mechanism of action and an individual, unique way of interacting with the tested bacteria. Interestingly, metal oxide NPs exhibited a similar effect on the studied microorganisms. On the other hand, the most visible changes in the values of the measured parameters occurred in *E. coli*, *B. cereus* and *S. epidermidis* cells exposed to ZnO-NPs and Cu-NPs. The research also documented that NPs attenuate on the surface of bacterial cells, which results in increased membrane permeability, positively correlated with cytoplasmic leakage. Surprisingly, NPs inhibited the respiratory metabolism of the tested strains, which was reflected in a decrease in total ATP concentration and low ATPase activity. Moreover, all NPs significantly, but in different ways, modified the content of the bacterial fatty acid composition. In general, *E. coli* proved to be more sensitive to the presence of NPs, resulting in their distinct impact on the increase of membrane permeability and cytoplasmic leakage, as well as alterations in ATP level compared to Gram-positive strains. However, Gram-positive strains, especially *B. cereus*, were characterised by distinguishable changes in ATPase activity and fatty acid composition. All the observed changes implied that bacteria activate various defence mechanisms that protect them against NPs stress.

## CRedit authorship contribution statement

**Oliwia Metryka:** Conceptualisation, Methodology, Investigation, Resources, Formal analysis, Visualisation, Writing – original draft, Project administration, Funding acquisition. **Daniel Wasilkowski:** Conceptualisation, Methodology, Resources, Software, Validation, Visualisation, Formal analysis, Writing – original draft. **Małgorzata Adamczyk-Habrajska:** SEM analysis. **Agnieszka Mroziak:** Conceptualisation, Methodology, Resources, Formal analysis, Writing – review & editing, Funding acquisition, Supervision.

## Declaration of Competing Interest

The authors declare the following financial interests/personal

relationships which may be considered as potential competing interests: Oliwia Metyka reports financial support was provided by National Science Centre Poland.

## Data Availability

Data will be made available on request.

## Acknowledgments

This research was entirely funded by the National Science Centre, Poland, grant number 2021/41/N/NZ9/02506. For Open Access, the author has applied a CC-BY public copyright licence to any Author Accepted Manuscript (AAM) version arising from this submission. The research activities was co-financed by the funds granted under the Research Excellence Initiative of the University of Silesia in Katowice.

## Environmental Implication

Due to their unique antimicrobial properties, nanomaterials, including inorganic NPs, have been identified as potential threats to the environment and related microorganisms. The complete lack of standardised methods to assess the risk of the widespread use of NPs as well as the complex nature of nanomaterials, make tracking changes in microbial populations under NPs exposure difficult and currently unattainable. For this reason, it is necessary to understand the biological activity of NPs using model microorganisms thoroughly. Knowledge of NPs activity in biological matrices used in various market products will allow for future intended and safe use of these materials. Undoubtedly, the experimental data obtained in this study provided new and solid evidence of the undesirable effect of NPs on the structure and function of bacterial cell envelopes. In particular, the complex information on total ATP concentration, ATPase activity, and changes in the bacterial fatty acid composition is unprecedented and of high cognitive importance. Moreover, the presented results may contribute to a better understanding of the effects of inorganic NPs on various species of bacteria, concerning Gram-negative and Gram-positive bacteria. The proposed biomarkers and the methodology used may constitute the basis for standardising the methods in future studies on the toxicity of nanomaterials.

## References

- [1] Abdolapur Monikh, F., Guo, Z., Zhang, P., Vijver, M.G., Lynch, I., Valsami-Jones, E., et al., 2022. An analytical workflow for dynamic characterisation and quantification of metal-bearing nanomaterials in biological matrices. *Nat Protoc* 17, 1926–1952. <https://doi.org/10.1038/s41596-022-00701-x>.
- [2] Ahmed, B., Ameen, F., Rizvi, A., Ali, K., Sonbol, H., Zaidi, A., et al., 2020. Destruction of cell topography, morphology, membrane, inhibition of respiration, biofilm formation, and bioactive molecule production by nanoparticles of Ag, ZnO, CuO, TiO<sub>2</sub>, and Al<sub>2</sub>O<sub>3</sub> toward beneficial soil bacteria. *ACS Omega* 5, 7861–7876. <https://doi.org/10.1021/acsomega.9b04084>.
- [3] Ahmed, B., Hashmi, A., Khan, M.S., Musarrat, J., 2018. ROS mediated destruction of cell membrane, growth and biofilms of human bacterial pathogens by stable metallic AgNPs functionalised from bell pepper extract and quercetin. *Adv Powder Technol* 29, 1601–1616. <https://doi.org/10.1016/j.apt.2018.03.025>.
- [4] Ahmed, B., Rizvi, A., Ali, K., Lee, J., Zaidi, A., Khan, M.S., et al., 2021. Nanoparticles in the soil–plant system: a review. *Environ Chem Lett* 19, 1545–1609. <https://doi.org/10.1007/s10311-020-01138-y>.
- [5] Ahmed, B., Solanki, B., Zaidi, A., Khan, M.S., Musarrat, J., 2019. Bacterial toxicity of biomimetic green zinc oxide nanoantibiotic: insights into ZnONP uptake and nanocolloid–bacteria interface. *Toxicol Res* 8, 246–261. <https://doi.org/10.1039/C8TX00267C>.
- [6] Ali, K., Ahmed, B., Ansari, S.M., Saquib, Q., Al-Khedhairi, A.A., Dwivedi, S., et al., 2019. Comparative in situ ROS mediated killing of bacteria with bulk analogue, Eucalyptus leaf extract (ELE)-capped and bare surface copper oxide nanoparticles. *Mater Sci Eng C Mater Biol Appl* 100, 747–758. <https://doi.org/10.1016/j.msec.2019.03.012>.
- [7] Ali, K., Ahmed, B., Khan, M.S., Musarrat, J., 2018. Differential surface contact killing of pristine and low EPS *Pseudomonas aeruginosa* with *Aloe vera* capped hematite ( $\alpha$ -Fe<sub>2</sub>O<sub>3</sub>) nanoparticles. *J Photochem Photobiol B Biol* 188, 146–158. <https://doi.org/10.1016/j.jphotobiol.2018.09.017>.
- [8] Ameen, F., Alsamhary, K., Alabdullatif, J.A., AlNadhari, S., 2021. A review on metal-based nanoparticles and their toxicity to beneficial soil bacteria and fungi. *Ecotoxicol Environ Saf* 213, 112027. <https://doi.org/10.1016/j.ecoenv.2021.112027>.
- [9] Ammendolia, M.G., De Berardis, B., 2022. Nanoparticle impact on the bacterial adaptation: focus on nano-titania. *Nanomater (Basel)* 12, 3616. <https://doi.org/10.3390/nano12203616>.
- [10] Ansari, M.A., Khan, H.M., Khan, A.A., Cameotra, S.S., Saquib, Q., Musarrat, J., 2014. Interaction of Al<sub>2</sub>O<sub>3</sub> nanoparticles with *Escherichia coli* and their cell envelope biomolecules. *J Appl Microbiol* 116, 772–783. <https://doi.org/10.1111/jam.12423>.
- [11] Anuj, S.A., Gajera, H.P., Hirpara, D.G., Golakiya, B.A., 2019. Bacterial membrane destabilisation with cationic particles of nano-silver to combat efflux-mediated antibiotic resistance in Gram-negative bacteria. *Life Sci* 230, 178–187. <https://doi.org/10.1016/j.lfs.2019.05.072>.
- [12] Athie-García, M.S., Piñón-Castillo, H.A., Muñoz-Castellanos, L.N., Ulloa-Ogaz, A.L., Martínez-Varela, P.I., Quintero-Ramos, A., et al., 2018. Cell wall damage and oxidative stress in *Candida albicans* ATCC10231 and *Aspergillus niger* caused by palladium nanoparticles. *Toxicol Vitro* 48, 111–120. <https://doi.org/10.1016/j.tiv.2018.01.006>.
- [13] Bayda, S., Adeel, M., Tuccinardi, T., Cordani, M., Rizzolio, F., 2020. The history of nanoscience and nanotechnology: from chemical-physical applications to nanomedicine. *Molecules* 25, 112. <https://doi.org/10.3390/molecules25010112>.
- [14] Bondarenko, O.M., Sihtmäe, M., Kuzmičiová, J., Ragelienė, L., Kahru, A., Daugelavičius, R., 2018. Plasma membrane is the target of rapid antibacterial action of silver nanoparticles in *Escherichia coli* and *Pseudomonas aeruginosa*. *Int J Nanomed* 13, 6779–6790. <https://doi.org/10.2147/IJN.S177163>.
- [15] Caudill, E.R., Hernandez, R.T., Johnson, K.P., O'Rourke, J.T., Zhu, L., Haynes, C.L., et al., 2020. Wall teichoic acids govern cationic gold nanoparticle interaction with Gram-positive bacterial cell walls. *Chem Sci* 11, 4106–4118. <https://doi.org/10.1039/C9SC05436G>.
- [16] Chen, K.L., Bothun, G.D., 2014. Nanoparticles meet cell membranes: probing nonspecific interactions using model membranes. *Environ Sci Technol* 48, 873–880. <https://doi.org/10.1021/es403864v>.
- [17] Deng, Y., Beahm, D.R., Ionov, S., Sarpeshkar, R., 2021. Measuring and modeling energy and power consumption in living microbial cells with a synthetic ATP reporter. *BMC Biol* 19, 101. <https://doi.org/10.1186/s12915-021-01023-2>.
- [18] Devi, K.P., Sakthivel, R., Nisha, S.A., Suganthi, N., Pandian, S.K., 2013. Euthenol alters the integrity of cell membrane and acts against the nosocomial pathogen *Proteus mirabilis*. *Arch Pharm Res* 36, 282–292. <https://doi.org/10.1007/s12272-013-0028-3>.
- [19] Gabrielyan, L., Badalyan, H., Gevorgyan, V., Trchounian, A., 2020. Comparable antibacterial effects and action mechanisms of silver and iron oxide nanoparticles on *Escherichia coli* and *Salmonella typhimurium*. *Sci Rep* 10, 13145. <https://doi.org/10.1038/s41598-020-70211-x>.
- [20] Gómez-Núñez, M.F., Castillo-López, M., Sevilla-Castillo, F., Roque-Reyes, O.J., Romero-Lechuga, F., Medina-Santos, D.I., et al., 2020. Nanoparticle-based devices in the control of antibiotic resistant bacteria. *Front Microbiol* 11, 563821. <https://doi.org/10.3389/fmicb.2020.563821>.
- [21] Halder, S., Yadav, K.K., Sarkar, R., Mukherjee, S., Saha, P., Haldar, S., et al., 2015. Alteration of Zeta potential and membrane permeability in bacteria: a study with cationic agents. *Springerplus* 4, 672. <https://doi.org/10.1186/s40064-015-1476-7>.
- [22] Hazrin-Chong, N.H., Manfield, M., 2012. An alternative SEM drying method using hexamethyldisilazane (HMDS) for microbial cell attachment studies on sub-bituminous coal. *J Microbiol Methods* 90, 96–99. <https://doi.org/10.1016/j.mimet.2012.04.014>.
- [23] Hegeman, G.D., 1966. Synthesis of the enzymes of the mandelate pathway by *Pseudomonas putida* I. Synthesis of enzymes by the wild type. *J Bacteriol* 91, 1140–1154. <https://doi.org/10.1128/jb.91.3.1140-1154.1966>.
- [24] Hegem, H.A., 2017. Nanomaterials for alternative antibacterial therapy. *Int J Nanomed* 12, 8211–8225. <https://doi.org/10.2147/IJN.S132163>.
- [25] Huang, G., Ng, T.W., An, T., Li, G., Wang, B., Wu, D., et al., 2017. Interaction between bacterial cell membranes and nano-TiO<sub>2</sub> revealed by two-dimensional FTIR correlation spectroscopy using bacterial ghost as a model cell envelope. *Water Res* 118, 104–113. <https://doi.org/10.1016/j.watres.2017.04.023>.
- [26] Ihssen, J., Jovanovic, N., Sirec, T., Spitz, U., 2021. Real-time monitoring of extracellular ATP in bacterial cultures using thermostable luciferase. *PLoS One* 16, e0244200. <https://doi.org/10.1371/journal.pone.0244200>.
- [27] Imlay, J.A., 2014. The metallation of enzymes during oxidative stress. *J Biol Chem* 289, 28121–28128. <https://doi.org/10.1074/jbc.R114.588814>.
- [28] Jain, N., Bhargava, A., Rathi, M., Dilip, R.V., Panwar, J., 2015. Removal of protein capping enhances the antibacterial efficiency of biosynthesised silver nanoparticles. *PLoS One* 10, e0134337. <https://doi.org/10.1371/journal.pone.0134337>.
- [29] Joshi, A.S., Singh, P., Mijakovic, I., 2020. Interactions of gold and silver nanoparticles with bacterial biofilms: molecular interactions behind inhibition and resistance. *Int J Mol Sci* 21, 7658. <https://doi.org/10.3390/ijms21207658>.
- [30] Karcz, J., Woznica, A., Binkowski, M., Klonowska-Olejnik, M., Bernas, T., Karczewski, J., et al., 2015. SEM-EDS and X-ray micro computed tomography studies of skeletal surface pattern and body structure in the freshwater sponge *Spongilla lacustris* collected from Goczałkowski reservoir habit (Southern Poland). In: *Folia Histochem. Cytobiol*, 53, pp. 88–95. <https://doi.org/10.5603/FHC.a2015.0002>.
- [31] Khater, M.S., Kulkarni, G.R., Khater, S.S., Gholap, H., Patil, R., 2020. Study to elucidate effect of titanium dioxide nanoparticles on bacterial membrane potential



- and membrane permeability. *Mater Res Express* 7, 035005. <https://doi.org/10.1088/2053-1591/ab731a>.
- [32] Khezerlou, A., Alizadeh-Sani, M., Azizi-Lalabadi, M., Ehsani, A., 2018. Nanoparticles and their antimicrobial properties against pathogens including bacteria, fungi, parasites and viruses. *Microb Pathog* 123, 505–526. <https://doi.org/10.1016/j.micpath.2018.08.008>.
- [33] Kora, A., Sashidhar, R., 2015. Antibacterial activity of biogenic silver nanoparticles synthesised with gum ghatti and gum olibanum: a comparative study. *J Antibiot* 68, 88–97. <https://doi.org/10.1038/ja.2014.114>.
- [34] Kumariya, R., Sood, S.K., Rajput, Y.S., Saini, N., Garsa, A.K., 2015. Increased membrane surface positive charge and altered membrane fluidity leads to cationic antimicrobial peptide resistance in *Enterococcus faecalis*. *Biochim Biophys Acta Biomembr* 1848, 1367–1375. <https://doi.org/10.1016/j.bbmem.2015.03.007>.
- [35] Lange, A., Sawosz, E., Daniluk, K., Wierzbecki, M., Małolepszy, A., Gotębiewski, M., et al., 2022. Bacterial surface disturbances affecting cell function during exposure to three-compound nanocomposites based on graphene materials. *Nanomater (Basel)* 12, 3058. <https://doi.org/10.3390/nano12173058>.
- [36] Lima de Silva, A.A., de Carvalho, M.A., de Souza, S.A., Dias, P.M., da Silva Filho, R. G., de Meirelles Saramago, C.S., et al., 2012. Heavy metal tolerance (Cr, Ag and Hg) in bacteria isolated from sewage. *Braz J Microbiol* 43, 1620–1631. <https://doi.org/10.1590/S1517-838220120004000047>.
- [37] Linklater, D.P., Baulin, V.A., Le Guével, X., Fleury, J.B., Hanssen, E., Nguyen, T.H. P., et al., 2020. Antibacterial action of nanoparticles by lethal stretching of bacterial cell membranes. *Adv Mater* 32, e2005679. <https://doi.org/10.1002/adma.202005679>.
- [38] Metryka, O., Wasilkowski, D., Mroziak, A., 2021. Insight into the antibacterial activity of selected metal nanoparticles and alterations within the antioxidant defence system in *Escherichia coli*, *Bacillus cereus* and *Staphylococcus epidermidis*. *Int J Mol Sci* 22, 11811. <https://doi.org/10.3390/ijms222111811>.
- [39] Metryka, O., Wasilkowski, D., Mroziak, A., 2022. Evaluation of the effects of Ag, Cu, ZnO and TiO<sub>2</sub> nanoparticles on the expression level of oxidative stress-related genes and the activity of antioxidant enzymes in *Escherichia coli*, *Bacillus cereus* and *Staphylococcus epidermidis*. *Int J Mol Sci* 23, 4966. <https://doi.org/10.3390/ijms23094966>.
- [40] Munir, M.U., Ahmad, M.M., 2022. Nanomaterials aiming to tackle antibiotic-resistant bacteria. *Pharmaceutics* 14, 582. <https://doi.org/10.3390/pharmaceutics14030582>.
- [41] Ozdal, M., Gurkok, S., 2022. Recent advances in nanoparticles as antibacterial agent. *ADMET DMPK* 10, 115–129. <https://doi.org/10.5599/admet.1172>.
- [42] Planchon, M., Léger, T., Spalla, O., Huber, G., Ferrari, R., 2017. Metabolomic and proteomic investigations of impacts of titanium dioxide nanoparticles on *Escherichia coli*. *PLoS One* 12, e0178437. <https://doi.org/10.1371/journal.pone.0178437>.
- [43] Poger, D., Mark, A.E., 2015. A ring to rule them all: the effect of cyclopropane fatty acids on the fluidity of lipid bilayers. *J Phys Chem B* 119, 5487–5495. <https://doi.org/10.1021/acs.jpcc.5b00958>.
- [44] Poh, T.Y., Ali, N.A.B.M., Mac Aogáin, M., Kathawala, M.H., Setyawati, M.I., Ng, K. W., et al., 2018. Inhaled nanomaterials and the respiratory microbiome: clinical, immunological and toxicological perspectives. *Part Fibre Toxicol* 15, 46. <https://doi.org/10.1186/s12989-018-0282-0>.
- [45] Ranjan, S., Ramalingam, C., 2016. Titanium dioxide nanoparticles induce bacterial membrane rupture by reactive oxygen species generation. *Environ Chem Lett* 14, 487–494. <https://doi.org/10.1007/s10311-016-0586-y>.
- [46] Sasser, M., 1990. Bacterial identification by gas chromatographic analysis of fatty acid methyl esters (GC-FAME); Technical Note #101; MIDI: Newark, DE, USA, 1990; revised 2006.
- [47] Schalk, I.J., Hannauer, M., Braud, A., 2011. New roles for bacterial siderophores in metal transport and tolerance. *Environ Microbiol* 13, 2844–2854. <https://doi.org/10.1111/j.1462-2920.2011.02556.x>.
- [48] Slavina, Y.N., Asnis, J., Häfeli, U.O., Bach, H., 2017. Metal nanoparticles: understanding the mechanisms behind antibacterial activity. *J Nanobiotechnol* 15, 65. <https://doi.org/10.1186/s12951-017-0308-z>.
- [49] Sohm, B., Immel, F., Bauda, P., Pagnout, C., 2015. Insight into the primary mode of action of TiO<sub>2</sub> nanoparticles on *Escherichia coli* in the dark. *Proteomics* 15, 98–113. <https://doi.org/10.1002/pmic.201400101>.
- [50] Steimle, A., Autenrieth, I.B., Frick, J.S., 2016. Structure and function: lipid A modifications in commensals and pathogens. *Int J Med Microbiol* 306, 290–301. <https://doi.org/10.1016/j.ijmm.2016.03.001>.
- [51] Thomas 3rd, K.J., Rice, C.V., 2015. Equilibrium binding behavior of magnesium to wall teichoic acid. *Biochim Biophys Acta* 1848, 1981–1987. <https://doi.org/10.1016/j.bbmem.2015.05.003>.
- [52] Tyagi, N., Kumar, A., 2020. Understanding effect of interaction of nanoparticles and antibiotics on bacteria survival under aquatic conditions: knowns and unknowns. *Environ Res* 181, 108945. <https://doi.org/10.1016/j.envres.2019.108945>.
- [53] Vardanyan, Z., Gevorgyan, V., Ananyan, M., Vardapetyan, H., Trchounian, A., 2015. Effects of various heavy metal nanoparticles on *Enterococcus hirae* and *Escherichia coli* growth and proton-coupled membrane transport. *J Nanobiotechnol* 13, 69. <https://doi.org/10.1186/s12951-015-0131-3>.
- [54] Willdigg, J.R., Helmann, J.D., 2021. Mini review: bacterial membrane composition and its modulation in response to stress. *Front Mol Biosci* 8, 634438. <https://doi.org/10.3389/fmolb.2021.634438>.
- [55] Wyrzykowska, E., Mikołajczyk, A., Lynch, I., Jeliakova, N., Kochev, N., Sarimveis, H., et al., 2022. Representing and describing nanomaterials in predictive nanoinformatics. *Nat Nanotechnol* 17, 924–932. <https://doi.org/10.1038/s41565-022-01173-6>.
- [56] Yeh, Y.C., Huang, T.H., Yang, S.C., Chen, C.C., Fang, J.Y., 2020. Nano-based drug delivery or targeting to eradicate bacteria for infection mitigation: a review of recent advances. *Front Chem* 8, 286. <https://doi.org/10.3389/fchem.2020.00286>.
- [57] Zawadzka, A.M., Abergel, R.J., Nichiporuk, R., Andersen, U.N., Raymond, K.N., 2009. Siderophore-mediated iron acquisition systems in *Bacillus cereus*: Identification of receptors for anthrax virulence-associated petrobactin. *Biochemistry* 48, 3645–3657. <https://doi.org/10.1021/bi801867a>.
- [58] Zhang, S., Lu, J., Wang, Y., Verstraete, W., Yuan, Z., Guo, J., 2022. Insights of metallic nanoparticles and ions in accelerating the bacterial uptake of antibiotic resistance genes. *J Hazard Mater* 421, 126728. <https://doi.org/10.1016/j.jhazmat.2021.126728>.

### III. Wnioski

1. Wartości parametrów toksykologicznych (MIC, MBC i IC<sub>50</sub>) wskazały na zróżnicowany wpływ nanocząstek Ag, Cu, ZnO i TiO<sub>2</sub> na wzrost szczepów *E. coli*, *B. cereus* i *S. epidermidis*. Badane szczepy były bardziej wrażliwe na toksyczne działanie nanocząstek metali niż tlenków metali.
2. Wszystkie nanocząstki generowały różne formy reaktywnych form tlenu (O<sub>2</sub><sup>•-</sup>, H<sub>2</sub>O<sub>2</sub> i •OH) w komórkach bakterii.
3. Zmiany aktywności enzymów systemu antyoksydacyjnego, tj. katalazy, peroksydazy i dysmutazy ponadtlenkowej oraz poziomu zredukowanego glutationu były skutkiem zakłóconej równowagi redoks w komórkach bakterii traktowanych nanocząstkami.
4. Skutki stresu oksydacyjnego prowadziły do wzrostu poziomu peroksydacji lipidów i utleniania białek, szczególnie w komórkach bakterii Gram-dodatnich.
5. Wszystkie nanocząstki miały istotny wpływ na zmiany ekspresji analizowanych genów obrony antyoksydacyjnej, co było skorelowane z zakłóconym działaniem enzymów antyoksydacyjnych. Największe różnice między profilami transkrypcyjnymi i antyoksydacyjnymi ustalono dla białek o aktywności podobnej do katalazy i peroksydazy.
6. Zmiany aktywności dehydrogenaz i ATPazy oraz całkowitego stężenia ATP potwierdziły istotny wpływ nanocząstek na metabolizm oddechowy komórek bakterii.
7. Nanocząstki miały zróżnicowany wpływ na zmiany przepuszczalności błony komórkowej bakterii i wyciek zawartości wewnątrzkomórkowej.
8. Konsekwencją działania nanocząstek na komórki bakterii były zmiany składów i udziałów procentowych analizowanych grup kwasów tłuszczowych. U wszystkich bakterii najbardziej podatnymi na zmiany były cyklopropanowe i/lub hydroksylowe kwasy tłuszczowe.
9. Nanocząstki wykazywały silne powinowactwo i zróżnicowany rozkład na powierzchni komórek bakterii, prowadzące niejednokrotnie do zmian ich morfologii.
10. Zmiany w analizowanych procesach metabolicznych i strukturze komórek bakterii były specyficzne gatunkowo i zależały od stężenia oraz rodzaju nanocząstek.

#### IV. Streszczenie

Dotychczas prowadzone prace eksperymentalne nad bakteriobójczymi właściwościami nanocząstek (NPs) koncentrowały się głównie na fragmentarycznej analizie ich wpływu na wybrane procesy metaboliczne i nie w pełni odzwierciedlają ich wielopoziomowej presji na funkcjonowanie mikroorganizmów. Mimo wielu prac dotyczących indukcji stresu oksydacyjnego w komórkach bakterii przez NPs, tylko niewielka ich część dotyczy identyfikacji generowanych reaktywnych form tlenu (RFT) bez ich uprzedniej fotoaktywacji oraz zdefiniowania towarzyszących temu procesowi zmian patologicznych, w tym peroksydacji lipidów i utleniania białek. Ograniczona jest również wiedza w zakresie połączonej analizy zmian na poziomie ekspresji genów obrony antyoksydacyjnej z aktywnością ich białkowych odpowiedników molekularnych. Niewiele także wiadomo na temat interakcji NPs z osłonami zewnętrznymi bakterii oraz wpływu NPs na profile kwasów tłuszczowych. Powyższe względy uzasadniają wybór tematyki badawczej i konsekwentne dążenie do wyjaśnienia mechanizmów leżących u podstaw biologicznej aktywności i toksyczności NPs.

Celem rozprawy doktorskiej była wieloaspektowa analiza mechanizmów stresu oksydacyjnego w komórkach bakterii: *Escherichia coli* (ATCC® 25922™), *Bacillus cereus* (ATCC® 11778™) i *Staphylococcus epidermidis* (ATCC® 12228™), eksponowanych na działanie nanocząstek nieorganicznych: Ag-NPs, Cu-NPs, ZnO-NPs i TiO<sub>2</sub>-NPs. W ramach przeprowadzonych badań zweryfikowano następujące hipotezy: (1) NPs wpływają na działanie bakteryjnych antyoksydantów; (2) NPs wpływają na poziom ekspresji genów stresu oksydacyjnego; (3) NPs modyfikują aktywność oddechową komórek bakteryjnych i (4) NPs oddziałują z osłonami zewnętrznymi bakterii oraz powodują zmiany morfologiczne komórek.

Istotną kwestią w badaniach toksyczności środków przeciwdrobnoustrojowych jest precyzyjne zdefiniowanie ich bakteriobójczego i bakteriostatycznego działania na konkretne mikroorganizmy. Analiza wartości wskaźników toksykologicznych MIC, MBC i IC<sub>50</sub> potwierdziła przeciwbakteryjne działanie wszystkich NPs względem *E. coli*, *B. cereus* i *S. epidermidis*. Jednocześnie stwierdzono zróżnicowaną wrażliwość badanych szczepów na stres wywołany ekspozycją na poszczególne rodzaje NPs. Udokumentowano, że badane szczepy były bardziej wrażliwe na toksyczne działanie nanocząstek metali niż tlenków metali. Wyniki badań mikrobiologicznych potwierdziły wysoki stopień śmiertelności komórek *E. coli* po traktowaniu Ag-NPs, ZnO-NPs i TiO<sub>2</sub>-NPs w porównaniu do *B. cereus* i *S. epidermidis*.

Szczegółowa analiza indukcji stresu oksydacyjnego i generacji RFT w komórkach bakterii *E. coli*, *B. cereus* i *S. epidermidis* przez NPs wskazała, że jest to jeden z podstawowych mechanizmów ich przeciwdrobnoustrojowego działania. Poszczególne NPs generowały różne rodzaje RFT oraz podwyższały ogólny poziom RFT w komórkach bakterii. Największy wzrost całkowitego stężenia RFT w komórkach *E. coli* i *B. cereus* nastąpił po ekspozycji na Cu-NPs. Z kolei ZnO-NPs i TiO<sub>2</sub>-NPs miały znaczący wpływ na produkcję RFT w komórkach *S. epidermidis*. Ustalono, że NPs w największym stopniu indukowały tworzenie RFT w komórkach *B. cereus* i *S. epidermidis*, natomiast w mniejszym stopniu w komórkach *E. coli*. Odnosząc się do poziomu poszczególnych form RFT, zasadniczy udział w całkowitym stężeniu RFT w komórkach *E. coli* traktowanych Cu-NPs miały O<sub>2</sub><sup>•-</sup>, H<sub>2</sub>O<sub>2</sub> i •OH, w komórkach *S. epidermidis* traktowanych TiO<sub>2</sub>-NPs - O<sub>2</sub><sup>•-</sup> i •OH, a w komórkach *B. cereus* eksponowanych na Cu-NPs i ZnO-NPs - O<sub>2</sub><sup>•-</sup> i H<sub>2</sub>O<sub>2</sub>. Wyniki przedstawione w niniejszej rozprawie potwierdziły również fundamentalne znaczenie GSH w ochronie komórek *E. coli* i *S.*

*epidermidis* przed stresem oksydacyjnym. Dowodem na to był spadek stężenia GSH w komórkach *E. coli* eksponowanych na ZnO-NPs i Ag-NPs oraz w komórkach *S. epidermidis* traktowanych ZnO-NPs. Dla porównania stężenie GSH w komórkach *B. cereus* nie zmieniło się istotnie, co wskazuje na niewielki jego udział w ochronie tego szczepu przed stresem oksydacyjnym. Warto podkreślić, że każdy mikroorganizm posiadał unikalny i swoisty mechanizm obrony, charakteryzujący się odmienną zawartością i udziałem przeciwutleniaczy w mechanizmach ochronnych.

Produkcja RFT w komórkach bakterii wiąże się nierozdzielnie z utlenianiem różnych biomolekuł, w tym przede wszystkim lipidów i białek. Stwierdzono, że traktowanie komórek *E. coli*, *B. cereus* i *S. epidermidis* Ag-NPs, Cu-NPs i TiO<sub>2</sub>-NPs skutkowało istotnym wzrostem poziomu peroksydacji lipidów, natomiast w obecności ZnO-NPs nie obserwowano tego zjawiska. Największy wzrost poziomu peroksydacji lipidów w odniesieniu do kontroli nastąpił w komórkach *B. cereus* i *S. epidermidis* traktowanych Cu-NPs. Dla porównania w komórkach *E. coli* wzrost ten był największy w obecności TiO<sub>2</sub>-NPs. Wzrost peroksydacji lipidów w komórkach bakterii po ekspozycji na NPs był dodatnio skorelowany ze wzrostem poziomu RFT. Na przykład znaczny wzrost stężenia <sup>•</sup>OH w komórkach *B. cereus* i *S. epidermidis* był dodatnio skorelowany ze wzrostem peroksydacji lipidów. Natomiast wysoki poziom <sup>1</sup>O<sub>2</sub> w komórkach *E. coli* traktowanych TiO<sub>2</sub>-NPs może wyjaśniać wpływ tej formy RFT na proces peroksydacji lipidów. Najczęściej przypisywaną modyfikacją białek indukowaną przez RFT jest karbonylacja białek i zmiany w zawartości grup aminowych. Analiza zawartości grup karbonylowych potwierdziła znaczny ich wzrost w strukturze białek szczepów *E. coli*, *B. cereus* i *S. epidermidis* eksponowanych na wszystkie rodzaje NPs. Największy wzrost zawartości grup karbonylowych białek nastąpił u bakterii *E. coli* traktowanych Ag-NPs, ZnO-NPs i TiO<sub>2</sub>-NPs. Z kolei u bakterii *B. cereus* i *S. epidermidis* największy wzrost zawartości tych grup wywołał kontakt komórek z tlenkami metali. W przypadku grup aminowych, największy wzrost ich zawartości u wszystkich szczepów stwierdzono po ekspozycji na ZnO-NPs.

Ochrona komórek bakterii przed stresem oksydacyjnym wymaga prawidłowego funkcjonowania katalitycznego układu antyoksydacyjnego. Aktywność podstawowych enzymów antyoksydacyjnych, tj. CAT, PER i SOD jest powszechnie wykorzystywana jako biomarker stresu oksydacyjnego. Wszystkie NPs stymulowały aktywność CAT, PER i SOD w komórkach *E. coli* i *B. cereus*, przy czym największy wzrost aktywności dotyczył CAT i PER. Największy wpływ na aktywność enzymów antyoksydacyjnych *E. coli* i *B. cereus* wykazały Cu-NPs i ZnO-NPs. Zmiany aktywności CAT, PER i SOD w komórkach *S. epidermidis* traktowanych NPs były trudne do interpretacji, ponieważ każdy rodzaj NPs w odmienny i często przeciwstawny sposób wpływał na profil katalityczny tych enzymów. Zaburzenia w funkcjonowaniu enzymów przeciwutleniających były powiązane ze zmianami w poziomie RFT oraz utlenianiem białek. Na podstawie otrzymanych wyników stwierdzono także, że wszystkie NPs zmieniały ekspresję wybranych genów, co było skorelowane z zaburzonym działaniem enzymów antyoksydacyjnych. Najbardziej znaczące różnice między profilami transkrypcyjnymi i antyoksydacyjnymi ustalono dla białek o aktywności podobnej do CAT i PER. Analiza zjawiska stresu oksydacyjnego oraz właściwości genotoksycznych nanocząstek potwierdziła również zależność pomiędzy generacją RFT, a regulacją ekspresji wybranych genów szoku oksydacyjnego bakterii. Na przykład stwierdzono dodatnią korelację pomiędzy regulacją transkrypcji genu *sodA2* i *sodA* w komórkach odpowiednio *B. cereus* i *S. epidermidis* a podwyższonym poziomem rodnika O<sub>2</sub><sup>•-</sup>.

Jedną z konsekwencji oddziaływania NPs z powierzchnią komórek bakterii były zmiany w metabolizmie oddechowym. Na podstawie uzyskanych wyników stwierdzono zróżnicowane aktywności DEH i ATPazy oraz zmiany w całkowitym stężeniu ATP w komórkach *E. coli*, *B. cereus* i *S. epidermidis* traktowanych NPs. Obserwowany spadek aktywności ATPazy był dodatnio skorelowany ze spadkiem ogólnego stężenia ATP we wszystkich szczepach bakterii oraz zmianami w zawartości grup karbonylowych białek. Co więcej, analiza aktywności oddechowej komórek bakterii potwierdziła także zależność pomiędzy aktywnością DEH a ogólnym poziomem ATP. Warto podkreślić, że zasadnicze zmiany dotyczyły głównie stężenia wewnątrzkomórkowego ATP. Stężenie to zmienia się dynamicznie w warunkach stresowych, ponieważ ATP wykorzystywany jest w różnych procesach komórkowych, w tym w syntezie białek redoks.

Pośrednie i bezpośrednie oddziaływanie NPs z błonami komórkowymi bakterii może prowadzić do nieodwracalnych zmian w ich strukturze i funkcjonowaniu. Najbardziej znaczące zmiany w przepuszczalności błony komórkowej i wycieku cytoplazmy stwierdzono u szczepu *E. coli* traktowanego ZnO-NPs i TiO<sub>2</sub>-NPs. W przypadku szczepów *B. cereus* i *S. epidermidis*, analiza statystyczna wykazała brak istotnych różnic w przepuszczalności błony pomiędzy komórkami traktowanymi NPs a komórkami kontrolnymi. Zidentyfikowano również istotne zmiany w procentowych zawartościach nasyconych i nienasyconych kwasów tłuszczowych w profilach FAME bakterii traktowanych NPs. Analiza profili FAME wykazała zróżnicowany i zależny od stężenia wpływ NPs na udział procentowy kwasów tłuszczowych *E. coli*, *B. cereus* i *S. epidermidis*. Grupami kwasów tłuszczowych najbardziej podatnymi na działanie NPs były u wszystkich bakterii cyklopropanowe i/lub hydroksylowe kwasy tłuszczowe. Bakterie Gram-dodatnie okazały się bardziej wrażliwe na działanie NPs w tym zakresie niż *E. coli*.

Analizę SEM przeprowadzono w celu zbadania rozmieszczenia i interakcji poszczególnych NPs z powierzchnią bakterii oraz określenia potencjalnych uszkodzeń w ich osłonach zewnętrznych. Stwierdzono, że poszczególne NPs charakteryzowały się różnym stopniem powinowactwa do powierzchni *E. coli*, *B. cereus* i *S. epidermidis* i ulegały różnej dystrybucji na powierzchni komórek. Na przykład ZnO-NPs były równomiernie rozproszone na całej powierzchni komórek *E. coli*, natomiast na powierzchni komórek *B. cereus* tworzyły warstwowe skupiska w postaci aglomeratów i agregatów o różnych kształtach. Warto podkreślić, że Ag-NPs w najmniejszym stopniu ulegały adhezji do powierzchni *E. coli*, *B. cereus* i *S. epidermidis* w porównaniu z pozostałymi NPs.

Podsumowując, przeprowadzone badania dostarczyły nowych i solidnych dowodów na negatywny wpływ NPs na mikroorganizmy. Zmiany w metabolizmie i strukturze komórek bakterii zależały od rodzaju NPs i były specyficzne gatunkowo. Szczep *E. coli* charakteryzował się wzmożonym funkcjonowaniem układu antyoksydacyjnego oraz zasadniczymi zmianami w przepuszczalności błon komórkowych. Natomiast ekspozycja szczepów *B. cereus* i *S. epidermidis* skutkowałą głównie upośledzeniem metabolizmu oddechowego. Użyte w pracy biomarkery stresu oksydacyjnego oraz zaproponowana i zoptymalizowana metodologia mogą stanowić podstawę do standaryzacji metod empiryczno-analitycznych w przyszłych badaniach toksyczności nanomateriałów.

## V. Summary

Experimental works on the bactericidal properties of nanoparticles (NPs) focused mainly on a partial analysis of their impact on selected metabolic processes, therefore, do not fully reflect their multi-level pressure on the functioning of microorganisms. Although current research on the induction of oxidative stress in bacterial cells by NPs is extensively conducted, it includes, in many cases, the production and identification of generated reactive oxygen species (ROS) after NPs photoactivation and rarely connect them with accompanying pathological changes such as lipid peroxidation and protein oxidation. Moreover, the available knowledge on the combined analysis of the expression level of antioxidant defense genes with the activity of their molecular counterparts is severely limited. Little is also known about the interaction of NPs with the outer layers of bacteria and the effect of NPs on fatty acid profiles. The above considerations justify the choice of the research topic and the consistent pursuit of elucidating the mechanisms underlying the biological activity and toxicity of NPs.

The aim of the doctoral dissertation was a multifaceted analysis of the mechanisms of oxidative stress in *Escherichia coli* (ATCC<sup>®</sup> 25922<sup>™</sup>), *Bacillus cereus* (ATCC<sup>®</sup> 11778<sup>™</sup>) and *Staphylococcus epidermidis* (ATCC<sup>®</sup> 12228<sup>™</sup>), exposed to inorganic nanoparticles: Ag-NPs, Cu-NPs, ZnO-NPs and TiO<sub>2</sub>-NPs. As part of the conducted research, the following hypotheses were verified: (1) NPs affect the action of bacterial antioxidants; (2) NPs affect the expression level of oxidative stress genes; (3) NPs modify the respiratory activity of bacterial cells and (4) NPs interact with the outer layers of bacteria and cause cell morphological changes.

The primary issue in studying the antibacterial agents' toxicity is the precise explanation of their bactericidal and bacteriostatic effects on specific microorganisms. Herein, the analysis of the MIC, MBC and IC<sub>50</sub> toxicological indices confirmed the antibacterial activity of all NPs against *E. coli*, *B. cereus* and *S. epidermidis*. Simultaneously, the tested strains exhibited varying sensitivity to particular types of NPs. Moreover, they were more susceptible to metal nanoparticles than metal oxides. The results of microbiological tests confirmed higher mortality of *E. coli* cells after treatment with Ag-NPs, ZnO-NPs and TiO<sub>2</sub>-NPs compared to *B. cereus* and *S. epidermidis*.

A detailed analysis of oxidative stress induction and ROS generation in *E. coli*, *B. cereus* and *S. epidermidis* by NPs indicated that this is one of the basic mechanisms of their antimicrobial activity. Individual NPs generated different types of ROS and increased the overall level of ROS in bacterial cells. The most significant increase in the total concentration of ROS in *E. coli* and *B. cereus* cells occurred after exposure to Cu-NPs. In turn, ZnO-NPs and TiO<sub>2</sub>-NPs had a considerable effect on the production of ROS in *S. epidermidis*. It was found that NPs induced ROS formation to a greater extent in *B. cereus* and *S. epidermidis* cells than in *E. coli*. Referring to the level of individual forms of ROS, the principal share in the total concentration of ROS in *E. coli* cells treated with Cu-NPs were O<sub>2</sub><sup>•-</sup>, H<sub>2</sub>O<sub>2</sub> and •OH, in *S. epidermidis* cells treated with TiO<sub>2</sub>-NPs were O<sub>2</sub><sup>•-</sup> and •OH, and in *B. cereus* cells exposed to Cu-NPs and ZnO-NPs turned out to have O<sub>2</sub><sup>•-</sup> and H<sub>2</sub>O<sub>2</sub>. The results presented in this dissertation also confirmed the fundamental importance of GSH in protecting *E. coli* and *S. epidermidis* cells against oxidative stress. This was evidenced by decreased GSH concentration in *E. coli* cells exposed to ZnO-NPs and Ag-NPs, and in *S. epidermidis* cells treated with ZnO-NPs. By comparison, the concentration of GSH in *B. cereus* cells did not change significantly, which indicates its small contribution to the protection against oxidative stress. It is worth emphasising that each

microorganism had a unique and specific defense mechanism, characterised by different content and participation of antioxidants in the protective mechanisms.

The production of ROS in bacterial cells is inextricably linked to the oxidation of various biomolecules, primarily lipids and proteins. The treatment of *E. coli*, *B. cereus* and *S. epidermidis* cells with Ag-NPs, Cu-NPs and TiO<sub>2</sub>-NPs resulted in a significant increase in lipid peroxidation; however, ZnO-NPs did not cause this phenomenon. The most significant increase in lipid peroxidation in *B. cereus* and *S. epidermidis* cells compared to the control cells occurred after treatment with Cu-NPs. By comparison, this increase in *E. coli* cells was the highest in the presence of TiO<sub>2</sub>-NPs. Statistical analysis confirmed the positive correlation between lipid peroxidation and ROS formation. For example, a significant increase in  $\cdot\text{OH}$  concentration in *B. cereus* and *S. epidermidis* cells was positively correlated with an increase in lipid peroxidation. However, the high level of <sup>1</sup>O<sub>2</sub> in *E. coli* cells treated with TiO<sub>2</sub>-NPs may explain the influence of this ROS on lipid peroxidation. The most commonly attributed modification of proteins induced by ROS is protein carbonylation and changes in the content of amino groups. The detailed analysis confirmed a significant increase in the content of carbonyl groups in the protein of *E. coli*, *B. cereus* and *S. epidermidis* exposed to all types of NPs. The highest increase in the content of protein carbonyl groups occurred in *E. coli* treated with Ag-NPs, ZnO-NPs and TiO<sub>2</sub>-NPs. In turn, the greatest increase in the content of these groups in *B. cereus* and *S. epidermidis* appeared after contact of the cells with metal oxides. In the case of amino groups, the most significant increase in their content in all strains was found after exposure to ZnO-NPs.

The protection of bacterial cells against oxidative stress requires the proper functioning of the catalytic antioxidant system. The activity of antioxidant enzymes, i.e. CAT, PER and SOD, is commonly used as a biomarker of oxidative stress. All NPs stimulated CAT, PER and SOD activity in *E. coli* and *B. cereus* cells, with the greatest increase in CAT and PER activity. The most significant influence on the activity of antioxidant enzymes in *E. coli* and *B. cereus* was established after treatment with Cu-NPs and ZnO-NPs. Changes in the CAT, PER and SOD activities in *S. epidermidis* exposed to NPs were difficult to interpret because each type of NPs affected the catalytic profile of these enzymes in a different and often opposite way. Disturbances in the functioning of antioxidant enzymes were associated with ROS levels and protein oxidation. The obtained results also indicated that all NPs changed the expression level of selected genes, which was correlated with impaired activity of antioxidant enzymes. The most significant differences between transcriptional and antioxidant profiles were found for proteins with CAT and PER-like activity. The analysis of the oxidative stress induction and the genotoxic properties of NPs also confirmed the relationship between ROS generation and the expression level of selected oxidative stress-related genes. For example, a positive correlation was found between the expression level of *sodA2* and *sodA* genes in *B. cereus* and *S. epidermidis* cells, respectively, and increased levels of the O<sub>2</sub><sup>•-</sup> radical.

A severe consequence of NPs interaction with the surface of bacterial cells was altered respiratory metabolism. Based on the obtained results, different DEH and ATPase activities and changes in total ATP concentration in *E. coli*, *B. cereus* and *S. epidermidis* cells treated with NPs were evidenced. The decrease in ATPase activity was positively correlated with a reduction in the total ATP concentration in all bacterial strains and changes in carbonyl group content. Interestingly, the analysis of the respiratory activity of bacterial cells also confirmed the relationship between DEH activity and general ATP levels. It is worth emphasising that the alternations mainly concerned intracellular ATP

concentration. It dynamically changes under stress conditions due to ATP utilisation in various cellular processes, including the synthesis of redox proteins.

Direct and indirect interaction of NPs with bacterial cell membranes can lead to irreversible changes in their structure and functioning. The most significant changes in cell membrane permeability and cytoplasm leakage were found in *E. coli* treated with ZnO-NPs and TiO<sub>2</sub>-NPs. By comparison, statistical analysis showed no significant differences in membrane permeability between treated and untreated *B. cereus* and *S. epidermidis* cells. Substantial changes in the percentages of saturated and unsaturated fatty acids in the FAME profiles of all bacteria treated with NPs were also identified. The detailed analysis of the FAME profiles showed a differential and concentration-dependent effect of NPs on the percentages of *E. coli*, *B. cereus* and *S. epidermidis* fatty acids. In all bacteria, the most susceptible to NPs action were cyclopropane and/or hydroxyl fatty acids. Gram-positive bacteria turned out to be more sensitive to NPs than *E. coli*.

SEM analysis was performed to study the distribution and interaction of individual NPs with the bacterial surface and to identify potential damage to their outer layers. It was evidenced that individual NPs had a differential affinity to the surface of *E. coli*, *B. cereus* and *S. epidermidis* and were distributed on the bacteria's surface depending on their type. For example, ZnO-NPs were evenly dispersed over the entire surface of *E. coli* cells. Contrarily, they formed layered clusters in the form of agglomerates and aggregates of various shapes on the surface of *B. cereus* cells. It is worth emphasising that Ag-NPs slightly adhered to the surface of *E. coli*, *B. cereus* and *S. epidermidis* compared to the remaining NPs.

In conclusion, the conducted research provided new and solid evidence of the negative impact of NPs on microorganisms. Changes in the metabolism and structure of bacterial cells depended on the type of NPs and were species-specific. *E. coli* strain was characterised by an increased functioning of the antioxidant defense system and noteworthy changes in the permeability of cell membranes. On the other hand, the exposure of *B. cereus* and *S. epidermidis* to NPs resulted mainly in impaired respiratory metabolism. The biomarkers of oxidative stress and the proposed and optimised methodology may help standardise empirical and analytical methods in future studies of nanomaterial toxicity.



## **VI. Oświadczenia doktoranta i współautorów**

OŚWIADCZENIE KANDYDATA/WSPÓŁAUTORA  
O WKŁADZIE PRACY

Katowice, 10.05.2023 r.  
miejsowość, data

Oliwia Metryka  
imię i nazwisko

ul. Brzozowa 9, 43-600 Jaworzno  
adres do korespondencji

791 308 621  
nr telefonu

oliwia.metryka@us.edu.pl  
adres e-mail

Insight into the antibacterial activity of selected metal nanoparticles and alterations within the antioxidant defence system in *Escherichia coli*, *Bacillus cereus* and *Staphylococcus epidermidis*. International Journal of Molecular Sciences, 2021, 22(21): 11811  
tytuł publikacji, czasopismo, rok wydania, strony

Oliwia Metryka, Daniel Wasilkowski, Agnieszka Mroziak  
imiona i nazwiska autorów publikacji

Niniejszym oświadczam, że mój udział w w/w. pracy polegał na:

konceptualizacji pracy, opracowaniu metodologii, zbieraniu/analizie danych, walidacji danych, wykonaniu analiz laboratoryjnych, przygotowaniu manuskryptu

szczegółowy opis wkładu współautora w powstaniu pracy (np. koncepcja pracy, zbieranie/analiza danych, wykonanie analiz laboratoryjnych, przygotowanie publikacji, korekta manuskryptu etc.)



podpis

OŚWIADCZENIE KANDYDATA/WSPÓŁAUTORA  
O WKŁADZIE PRACY

Katowice, 10.05.2023 r.  
miejsowość, data

Daniel Wasilkowski  
imię i nazwisko

ul. Jagiellońska 28, 40-032 Katowice  
adres do korespondencji

32 2009 576  
nr telefonu

daniel.wasilkowski@us.edu.pl  
adres e-mail

Insight into the antibacterial activity of selected metal nanoparticles and alterations within the antioxidant defence system in *Escherichia coli*, *Bacillus cereus* and *Staphylococcus epidermidis*. International Journal of Molecular Sciences, 2021, 22(21): 11811  
tytuł publikacji, czasopismo, rok wydania, strony

Oliwia Metryka, Daniel Wasilkowski, Agnieszka Mroziak  
imiona i nazwiska autorów publikacji

Niniejszym oświadczam, że mój udział w w/w. pracy polegał na:

konceptualizacji pracy, opracowaniu metodologii, zbieraniu/analizie danych, walidacji danych, wykonaniu analiz laboratoryjnych, przygotowaniu manuskryptu

szczegółowy opis wkładu współautora w powstaniu pracy (np. koncepcja pracy, zbieranie/analiza danych, wykonanie analiz laboratoryjnych, przygotowanie publikacji, korekta manuskryptu etc.)



podpis

# OŚWIADCZENIE KANDYDATA/WSPÓŁAUTORA

## O WKŁADZIE PRACY

Katowice, 10.05.2023 r.  
miejsowość, data

Agnieszka Mrozik  
imię i nazwisko

ul. Jagiellońska 28, 40-032 Katowice  
adres do korespondencji

32 2009 555  
nr telefonu

agnieszka.mrozik@us.edu.pl  
adres e-mail

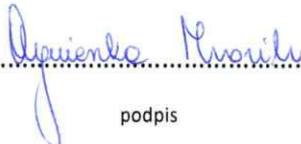
Insight into the antibacterial activity of selected metal nanoparticles and alterations within the antioxidant defence system in *Escherichia coli*, *Bacillus cereus* and *Staphylococcus epidermidis*. International Journal of Molecular Sciences, 2021, 22(21): 11811  
tytuł publikacji, czasopismo, rok wydania, strony

Oliwia Metryka, Daniel Wasilkowski, Agnieszka Mrozik  
imiona i nazwiska autorów publikacji

Niniejszym oświadczam, że mój udział w w/w. pracy polegał na:

nadzorze merytorycznym nad badaniami, opracowaniu koncepcji pracy, analizie danych, korekcie manuskryptu.

szczegółowy opis wkładu współautora w powstaniu pracy (np. koncepcja pracy, zbieranie/analiza danych, wykonanie analiz laboratoryjnych, przygotowanie publikacji, korekta manuskryptu etc.)

  
.....  
podpis

# OŚWIADCZENIE KANDYDATA/WSPÓŁAUTORA

## O WKŁADZIE PRACY

Katowice, 10.05.2023 r.  
miejsowość, data

Oliwia Metryka  
imię i nazwisko

ul. Brzozowa 9, 43-600 Jaworzno  
adres do korespondencji

791 308 621  
nr telefonu

oliwia.metryka@us.edu.pl  
adres e-mail

Evaluation of the effects of Ag, Cu, ZnO and TiO<sub>2</sub> nanoparticles on the expression level of oxidative stress-related genes and the activity of antioxidant enzymes in *Escherichia coli*, *Bacillus cereus* and *Staphylococcus epidermidis*.

International Journal of Molecular Sciences, 2022, 23(9): 4966

tytuł publikacji, czasopismo, rok wydania, strony

Oliwia Metryka, Daniel Wasilkowski, Agnieszka Mrozik

imiona i nazwiska autorów publikacji

Niniejszym oświadczam, że mój udział w w/w. pracy polegał na:

konceptualizacji pracy, opracowaniu metodologii, zbieraniu/analizie danych, walidacji danych, wykonaniu analiz laboratoryjnych, wizualizacji wyników, przygotowaniu manuskryptu

szczegółowy opis wkładu współautora w powstaniu pracy (np. koncepcja pracy, zbieranie/analiza danych, wykonanie analiz laboratoryjnych, przygotowanie publikacji, korekta manuskryptu etc.)



.....  
podpis

OŚWIADCZENIE KANDYDATA/WSPÓŁAUTORA  
O WKŁADZIE PRACY

Katowice, 10.05.2023 r.  
miejsowość, data

Daniel Wasilkowski  
imię i nazwisko

ul. Jagiellońska 28, 40-032 Katowice  
adres do korespondencji

32 2009 576  
nr telefonu

daniel.wasilkowski@us.edu.pl  
adres e-mail

Evaluation of the effects of Ag, Cu, ZnO and TiO<sub>2</sub> nanoparticles on the expression level of oxidative stress-related genes and the activity of antioxidant enzymes in *Escherichia coli*, *Bacillus cereus* and *Staphylococcus epidermidis*.  
International Journal of Molecular Sciences, 2022, 23(9): 4966  
tytuł publikacji, czasopismo, rok wydania, strony

Oliwia Metryka, Daniel Wasilkowski, Agnieszka Mrozik  
imiona i nazwiska autorów publikacji

Niniejszym oświadczam, że mój udział w w/w. pracy polegał na:

konceptualizacji pracy, opracowaniu metodologii, zbieraniu/analizie danych, walidacji danych, wykonaniu analiz laboratoryjnych, wizualizacji wyników, przygotowaniu manuskryptu

szczegółowy opis wkładu współautora w powstaniu pracy (np. koncepcja pracy, zbieranie/analiza danych, wykonanie analiz laboratoryjnych, przygotowanie publikacji, korekta manuskryptu etc.)



podpis

OŚWIADCZENIE KANDYDATA/WSPÓŁAUTORA  
O WKŁADZIE PRACY

Katowice, 10.05.2023 r.  
miejsowość, data

Agnieszka Mrozik  
imię i nazwisko

ul. Jagiellońska 28, 40-032 Katowice  
adres do korespondencji

32 2009 555  
nr telefonu

agnieszka.mrozik@us.edu.pl  
adres e-mail

Evaluation of the effects of Ag, Cu, ZnO and TiO<sub>2</sub> nanoparticles on the expression level of oxidative stress-related genes and the activity of antioxidant enzymes in *Escherichia coli*, *Bacillus cereus* and *Staphylococcus epidermidis*.

International Journal of Molecular Sciences, 2022, 23(9): 4966

tytuł publikacji, czasopismo, rok wydania, strony

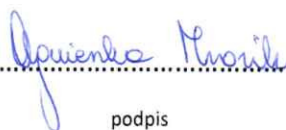
Oliwia Metryka, Daniel Wasilkowski, Agnieszka Mrozik

imiona i nazwiska autorów publikacji

Niniejszym oświadczam, że mój udział w w/w. pracy polegał na:

nadzorze merytorycznym nad badaniami, opracowaniu koncepcji pracy, analizie danych, korekcie manuskryptu.

szczegółowy opis wkładu współautora w powstaniu pracy (np. koncepcja pracy, zbieranie/analiza danych, wykonanie analiz laboratoryjnych, przygotowanie publikacji, korekta manuskryptu etc.)

  
.....  
podpis

OŚWIADCZENIE KANDYDATA/WSPÓŁAUTORA  
O WKŁADZIE PRACY

Katowice, 10.05.2023 r.  
miejsowość, data

Oliwia Metryka  
imię i nazwisko

ul. Brzozowa 9, 43-600 Jaworzno  
adres do korespondencji

791 308 621  
nr telefonu

oliwia.metryka@us.edu.pl  
adres e-mail

Undesirable consequences of the metallic nanoparticles action on the properties and functioning of *Escherichia coli*,  
*Bacillus cereus* and *Staphylococcus epidermidis* membranes. Journal of Hazardous Materials, 2023, 446: 130728  
tytuł publikacji, czasopismo, rok wydania, strony

Oliwia Metryka, Daniel Wasilkowski, Małgorzata Adamczyk-Habrajska, Agnieszka Mrozik  
imiona i nazwiska autorów publikacji

Niniejszym oświadczam, że mój udział w w/w. pracy polegał na:

konceptualizacji pracy, opracowaniu metodologii, zbieraniu/analizie danych, walidacji danych, wykonaniu analiz laboratoryjnych, wizualizacji wyników, przygotowaniu manuskryptu

szczegółowy opis wkładu współautora w powstaniu pracy (np. koncepcja pracy, zbieranie/analiza danych, wykonanie analiz laboratoryjnych, przygotowanie publikacji, korekta manuskryptu etc.)



podpis



OŚWIADCZENIE KANDYDATA/WSPÓŁAUTORA  
O WKŁADZIE PRACY

Katowice, 10.05.2023 r.  
miejsowość, data

Daniel Wasilkowski  
imię i nazwisko

ul. Jagiellońska 28, 40-032 Katowice  
adres do korespondencji

32 2009 576  
nr telefonu

daniel.wasilkowski@us.edu.pl  
adres e-mail

Undesirable consequences of the metallic nanoparticles action on the properties and functioning of *Escherichia coli*,  
*Bacillus cereus* and *Staphylococcus epidermidis* membranes. Journal of Hazardous Materials, 2023, 446: 130728  
tytuł publikacji, czasopismo, rok wydania, strony

Oliwia Metryka, Daniel Wasilkowski, Małgorzata Adamczyk-Habrajska, Agnieszka Mrozik  
imiona i nazwiska autorów publikacji

Niniejszym oświadczam, że mój udział w w/w. pracy polegał na:

konceptualizacji pracy, opracowaniu metodologii, zbieraniu/analizie danych, walidacji danych, wykonaniu analiz laboratoryjnych, wizualizacji wyników, przygotowaniu manuskryptu

szczegółowy opis wkładu współautora w powstaniu pracy (np. koncepcja pracy, zbieranie/analiza danych, wykonanie analiz laboratoryjnych, przygotowanie publikacji, korekta manuskryptu etc.)



podpis

# OŚWIADCZENIE KANDYDATA/WSPÓŁAUTORA

## O WKŁADZIE PRACY

Katowice, 10.05.2023 r.  
miejsowość, data

Małgorzata Adamczyk-Habrajska  
imię i nazwisko

ul. Żytnia 12, 41-200 Sosnowiec  
adres do korespondencji

32 2691 848  
nr telefonu

malgorzata.adamczyk-habrajska@us.edu.pl  
adres e-mail

Undesirable consequences of the metallic nanoparticles action on the properties and functioning of *Escherichia coli*,  
*Bacillus cereus* and *Staphylococcus epidermidis* membranes. Journal of Hazardous Materials, 2023, 446: 130728  
tytuł publikacji, czasopismo, rok wydania, strony

Oliwia Metryka, Daniel Wasilkowski, Małgorzata Adamczyk-Habrajska, Agnieszka Mrozik  
imiona i nazwiska autorów publikacji

Niniejszym oświadczam, że mój udział w w/w. pracy polegał na:  
przeprowadzeniu mikroanalizy rentgenowskiej i badań SEM

szczegółowy opis wkładu współautora w powstaniu pracy (np. koncepcja pracy, zbieranie/analiza danych,  
wykonanie analiz laboratoryjnych, przygotowanie publikacji, korekta manuskryptu etc.)

  
.....  
podpis

OŚWIADCZENIE KANDYDATA/WSPÓŁAUTORA  
O WKŁADZIE PRACY

Katowice, 10.05.2023 r.  
miejsowość, data

Agnieszka Mrozik  
imię i nazwisko

ul. Jagiellońska 28, 40-032 Katowice  
adres do korespondencji

32 2009 555  
nr telefonu

agnieszka.mrozik@us.edu.pl  
adres e-mail

Undesirable consequences of the metallic nanoparticles action on the properties and functioning of *Escherichia coli*,  
*Bacillus cereus* and *Staphylococcus epidermidis* membranes. Journal of Hazardous Materials, 2023, 446: 130728

tytuł publikacji, czasopismo, rok wydania, strony

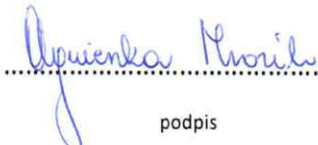
Oliwia Metryka, Daniel Wasilkowski, Małgorzata Adamczyk-Habrajska, Agnieszka Mrozik

imiona i nazwiska autorów publikacji

Niniejszym oświadczam, że mój udział w w/w. pracy polegał na:

nadzorze merytorycznym nad badaniami, opracowaniu koncepcji pracy, metodologii, analizie danych, korekcie  
manuskryptu.

szczegółowy opis wkładu współautora w powstaniu pracy (np. koncepcja pracy, zbieranie/analiza danych,  
wykonanie analiz laboratoryjnych, przygotowanie publikacji, korekta manuskryptu etc.)

  
.....  
podpis